Supporting Information for

Accessing Five- and Seven-Membered Phosphorus-Based Heterocycles via Cycloaddition Reactions of Azophosphines

Ethan D.E. Calder, Louise Male, Andrew R. Jupp

Contents

S1. Synthetic Details

S1.1. General Synthetic Information

Unless otherwise noted, all manipulations were carried out in an MBraun ECO glovebox under an inert atmosphere of dry, oxygen-free N_2, with water and oxygen levels maintained at < 0.1 ppm, or performed on the Schlenk line (using dry, oxygen-free N_2 as the inert gas) using standard Schlenk line procedures. All glassware and Teflon-coated stirrer bars were dried in a 180 °C oven overnight prior to use, unless otherwise stated. All molecular sieves are 3 angstrom and purchased from VWR chemicals, and were activated by heating at 400°C under vacuum prior to use. Unless otherwise stated, degassing refers to three freeze-pump-thaw cycles. Room temperature (RT) refers to reactions where no thermostatic control was applied and the temperature was recorded as 16–25◦C. Unless otherwise stated, overnight reactions refer to a period of 16 hours. Thin layer chromatography (TLC) analysis was performed using Machery-Nagel aluminium-backed silica plates. Spots were visualised by the quenching of ultraviolet light. All flash column chromatography was performed using Fluorochem 60 silica gel (particle size 40–63 μm) with a column of appropriate size.

Commercial reagents were purchased, suitably stored as specified by the supplier, and used as received, unless otherwise stated, from Sigma-Aldrich (*sec*-butyllithium, 1.42 M in cyclohexane; borane-di(tert-butyl)phosphine complex, 94%; pyrrolidine, anhydrous, > 99.5%, stored in an air-tight ampoule; borane dimethylsulfide complex; diisobutylaluminium hydride solution, 1.0M in toluene; diethyl acetylenedicarboxylate, 97%), Fisher Scientific (sodium hydroxide, white pellets; magnesium sulfate, dried), TCI Chemicals (tris(pentafluorophenyl)borane, > 98.0%), Acros Organics (chlorodiisopropylphosphine, 96%; chlorodicyclohexylphosphine, 97%), or Alfa Aesar (ethyl 2-butynoate, 98%). Solvents were purchased and used as received, unless otherwise stated, from Sigma-Aldrich (hexane, puriss, p.a., ACS reagent, reag. Ph. Eur., 99+ (GC), degassed and stored in air-tight ampoules over 3 Å molecular sieves; diethyl ether, ACS reagent, 99.8%; 2-propanol (isopropanol), ACS reagent, 99.8% (GC); chloroform-d_3, 99.8 atom % D, dried by overnight reaction with CaH_2, degassed and stored in an air-tight ampoule over 3 Å molecular sieves; toluene-d_8, 99.6 atom % D, dried by overnight reaction with CaH_2, degassed and stored in an air-tight ampoule over 3 Å molecular sieves), Fisher Scientific (dichloromethane (DCM), 99.8% HPLC grade), or VWR Chemicals (ethyl acetate, ≥99%, GPR RECTAPUR). Toluene was obtained from the laboratory solvent purification system, degassed, and stored in air-tight ampoules over 3 Å molecular sieves. THF was obtained from the laboratory solvent purification system,

degassed, dried over Na/benzophenone, and stored in air-tight ampoules over 3 Å molecular sieves. Deionised water was obtained from an Elga DV35 Purelab. Mesitylenediazonium tetrafluoroborate ([$MesN_2$][BF_4]) was synthesised in accordance with previously reported literature.[1]

Unless otherwise stated, all NMR spectra used for characterisation were collected at 298 K on a Bruker 500 MHz AV_NEO Advance NMR Spectrometer or a Bruker 400 MHz AV_NEO Advance NMR Spectrometer. Chemical shifts are reported in parts per million (ppm), coupling constants (J) are reported in Hz. ^{1}H and $^{13}C\{^{1}H\}$ NMR spectra were referenced internally to the most upfield solvent peak; ^{31}P and $^{31}P\{^{1}H\}$ NMR spectra are externally referenced to 85% H_3PO_4; $^{11}B\{^{1}H\}$ NMR spectra are externally referenced to $BF_3.OEt_2$; $^{19}F\{^{1}H\}$ NMR spectra are externally referenced to $CFCl_3$. All shifts and coupling constants are given to one or two decimal places.

All UV/Vis absorption spectra were collected on an Agilent Cary60 UV/Vis Spectrometer. The samples were prepared as 5 x 10^{-5} M solutions in toluene and irradiated in a quartz glass High Precision Cell cuvette (10 x 10 mm) from Hellma Analytics. Air-sensitive UV-Vis samples were collected using a sealable cuvette, with solutions made up in the glovebox. The wavelength of maximum absorption (λ_{max}) is reported in nm, along with the corresponding absorbance value, given in arbitrary units to four decimal places. Before running all samples, a background reading was run (with blank solvent, and no sample present), with the values from this background readings subsequently subtracted from the actual sample.

All IR spectra were collected on a Perkin Elmer Spectrum Two FT-IR spectrometer using attenuated total reflection (ATR) sampling technique. Absorption maxima are reported in wavenumbers (cm^{-1}), with no decimal places.

All mass spectra were collected on a Waters Xevo G2-XS TOF mass spectrometer using electrospray ionisation (ESI) positive ion mode. Samples were dissolved either in dry dichloromethane or acetonitrile, and directly injected into the ESI ionisation chamber via a 250 µL glass syringe. High resolution mass spectra were obtained using the same method, and are reported to four decimal places. All elemental analysis samples were collected on a CE Instruments EA1110 elemental analyser.

Unless otherwise stated, single-crystal X-ray diffraction data were collected at 100 K on a Rigaku SuperNova diffractometer using an Atlas detector, using Cu-Kα radiation (λ = 1.54184). The data collections were driven and processed, and absorption corrections were applied using face indexing with a Gaussian absorption correction, using CrysalisPro.[2] Using OLEX2,[3] the structures were solved using SHELXT,[4] and were refined by a full-matrix least-squares

procedure on F^2 using SHELX programmes.[5] All non-hydrogen atoms were refined with anisotropic displacement parameters. Further details relating to crystal structures can be found in section S3.

S1.2. Synthesis of phosphine-borane adducts (Method A)

This procedure is based on an adapted form of the procedure from Busacca et al.[6] A 100 mL Schlenk flask was charged with R_2PCl (1 equiv; R = iPr, Cy) in a nitrogen atmosphere, and toluene was added to create a 1 M solution of R_2PCl in toluene. The mixture was cooled to -78°C, and a 0.98 M solution of DIBALH in toluene (diisobutylaluminium hydride; 1.1 equiv) was added dropwise. The resulting colourless solution was stirred for two hours, before being allowed to warm temperature and stirred for another two hours. $BH_3.SMe_2$ (1.2 equiv) was then added at once to the reaction mixture, and the solution allowed to stir overnight (16 hours) at room temperature, with the mixture remaining a colourless solution. The reaction mixture was then cooled to -78°C, and 4M aqueous NaOH (4 equiv) added dropwise, yielding a white precipitate in the flask. The mixture was warmed to room temperature, and stirred for one hour. The following steps are now carried out using non-air-sensitive techniques in the open fume-hood, using non-dried, non-degassed solvents. The mixture was poured into a separatory funnel, giving a clear organic phase on top of an aqueous suspension. The organic phase was separated and saved, while the aqueous phase was washed with dichloromethane (2 x 10 mL). All organic phases were then combined and filtered through a Celite pad, washing with dichloromethane (2 x 20 mL). The filtered organic phase was dried over $MgSO_4$, and all volatiles removed in vacuo to yield the final products.

Synthesis of $H^iPr_2P.BH_3$

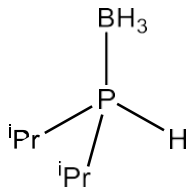

Phosphine-borane $H^iPr_2P.BH_3$ was synthesised from precursor iPr_2PCl (2.39 mL, 15 mmol) according to method A, with the product yielded as a colourless oil (1.307 g, 9.90 mmol, 66%). We observed that the product should be left drying *in vacuo* for no more than one hour, due to its volatility. ^1H (300.1 MHz, $CDCl_3$, 298 K): δ 4.09 (1H, doub. of sextets, $^1J_{H\text{-}P}$ = 350.5 Hz; PH), δ 2.05 (2H, m; $P(CH(CH_3)_2)_2$), δ 1.15 (6H, dd, $^3J_{H\text{-}P}$ = 15.2 Hz, $^3J_{H\text{-}H}$ = 7.1 Hz; $P(CH(CH_3)_2)$, δ 1.13 (6H, dd, $^3J_{H\text{-}P}$ = 15.2 Hz, $^3J_{H\text{-}H}$ = 7.0 Hz; $P(CH(CH_3)_2)$, δ 0.34 (3H, br. quart., $^1J_{B\text{-}H}$ = 97.2 Hz; BH_3). $^{31}P\{^1H\}$ (121.5 MHz, $CDCl_3$, 298 K): δ 27.2 (q, $^1J_{P\text{-}B}$ = 50.0 Hz). Obtained data in

accord with reported literature.[7]

Synthesis of $HCy_2P.BH_3$

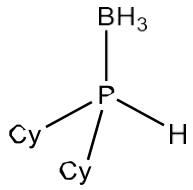

Phosphine-borane $HCy_2P.BH_3$ was synthesised from precursor Cy_2PCl (0.88 mL, 4 mmol) according to method A, with the product yielded as colourless crystals (0.754 g, 3.56 mmol, 89%). ^1H (300.1 MHz, $CDCl_3$, 298 K): δ 4.11 (1H, doub. of sextets, $^1J_{H\text{-}P}$ = 350.8 Hz; PH), δ 1.82 (11H, m), δ 1.27 (11H, m), δ 0.41 (3H, br. quart., $^1J_{B\text{-}H}$ = 96.5 Hz; B**H**$_3$). $^{31}P\{^1H\}$ (121.5 MHz, $CDCl_3$, 298 K): δ 17.4 (q, $^1J_{P\text{-}B}$ = 58.8 Hz). Obtained data in accord with reported literature.[6]

S1.3. Synthesis of azophosphine-borane adducts (Method B)

A 25 mL Schlenk flask was charged with $HR_2P.BH_3$ (1 equiv.), and freshly distilled THF was added to create a 0.7 M solution of $HR_2P.BH_3$ in THF. This solution is cooled to – 78 °C, and a 1.41 M cyclohexane solution of *sec*-butyllithium (1 equiv.) was added dropwise, resulting in a colour change from colourless to pale yellow. The solution was allowed to warm to room temperature over one hour, and then stirred for a further three hours at room temperature; after this time, a colour change back to a colourless solution was observed. This solution was then added dropwise to a separate 50 mL Schlenk flask containing a slurry of $[MesN_2]^+[BF_4]^-$ (1 equiv.) in freshly distilled THF (0.25 M) at –78°C, resulting in an immediate colour change to deep purple. The reaction was left to warm slowly to room temperature over the course of one hour. The volatiles were removed in vacuo, with the materials now being treated as air-stable. The product was then isolated by column chromatography. Removal of the volatiles in vacuo yielded the product as an intensely coloured solid or oil. The air-stable, solid products were stored in vials, away from direct light, in the freezer.

Synthesis of $MesN_2P(^iPr)_2.BH_3$ (1•BH_3)

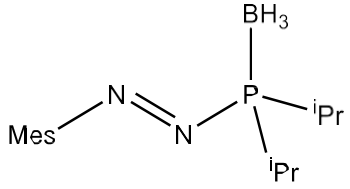

Azophosphine-borane **(1•BH_3)** was synthesised from precursor $H^iPr_2P.BH_3$ (0.502 g, 3.8 mmol) according to method B, with purification by column chromatography (eluent = 97:3 hexane:Et_2O, with the product appearing as a purple spot with R_f = 0.38 in this eluent system; the residual starting material ($H^iPr_2P.BH_3$) had an Rf = 0.30, and could be identified by TLC by staining in $KMnO_4$), with the product yielded as a purple oil (0.434 g, 1.56 mmol, 41 % yield). ^{1}H (500.1 MHz, $CDCl_3$, 298 K): δ 6.95 (2H, br. doub., $^6J_{H\text{-}P}$ = 0.6 Hz; *m*-ArH), δ 2.52 (2H, m; P(CH(CH_3)$_2$)$_2$), δ 2.40 (6H, s; *o*-CH_3), δ 2.33 (3H, s; *p*-CH_3), δ 1.32 (12H, m; CH(C*H*$_3$)$_2$), δ 0.53 (3H, br. quart., $^1J_{B\text{-}H}$ = 95.4 Hz; BH_3). ^{13}C{^{1}H} (125.7 MHz, $CDCl_3$, 298 K): δ 150.8 (d, $^3J_{C\text{-}P}$ = 34.1 Hz; *i*-C_{Ar}(Mes)), δ 141.8 (s; *p*-C_{Ar} (Mes)), δ 133.0 (d, $^4J_{C\text{-}P}$ = 1.4 Hz; *o*-C_{Ar}(Mes)), δ 130.6 (d, $^5J_{C\text{-}P}$ = 1.0 Hz; *m*-C_{Ar}(Mes)), δ 23.3 (d, $^1J_{C\text{-}P}$ = 30.6 Hz; *C*H(CH_3)$_2$), δ 21.4 (s; *p*-CH_3(Mes)), δ 20.1 (s; *o*-CH_3(Mes)), δ 16.7-16.8 (m; CH(*C*H$_3$)$_2$). ^{31}P{^{1}H} (202.4 MHz, $CDCl_3$, 298 K): δ 102.4 (br. quart). ^{31}P (162.0 MHz, $CDCl_3$, 298 K): δ 102.4 (br. s). ^{11}B{^{1}H} (128.4 MHz, $CDCl_3$, 298 K): δ -43.6 (d, $^1J_{B\text{-}P}$ = 51.3 Hz). UV-Vis Spectroscopy: (5 x 10^{-5}M in toluene): 312 nm, 0.4829 absorption; 508 nm, 0.0074 absorption. ESI-HRMS m/z for $C_{15}H_{28}N_2PB$ [*M* — H] + : calcd. 276.2041, 277.2008, 278.2038; found 276.2044, 277.2014, 278.2043 Additional peaks: [$MesN_2P^iPr_2$]$^+$: found 265.18; [$MesN_2P^iPr_2$ + H]$^+$: found 266.19;; [$MesN_2P^iPr_2.BH_3$ + H]$^+$: found 279.2. IR: ν_{max} (cm^{-1}) 2964 (m), 2930 (m), 2874 (m), 2381 (m; B-H), 2339 (m; B-H), 1607 (m; N=N).

Synthesis of $MesN_2P(Cy)_2.BH_3$ (2•BH_3)

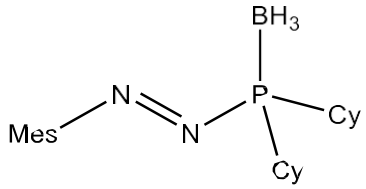

Azophosphine-borane **2•BH_3** was synthesised from precursor $HCy_2P.BH_3$ (0.487 g, 2.3 mmol) according to method B, with purification by column chromatography (eluent = 98:2 hexane:Et_2O, with the product appearing as a purple spot with R_f = 0.32 in this eluent system; the residual starting material ($HCy_2P.BH_3$) had an R_f = 0.27, and could be identified by TLC by staining in $KMnO_4$), with the product yielded as a purple oil; after being left overnight sat in the flask under static N_2 at room temperature, this oil hardened into an air-stable purple solid, the final product (0.365 g, 1.02 mmol, 44 %). ^{1}H (500.1 MHz, $CDCl_3$, 298 K): δ 6.95 (2H, s; *m*-ArH), δ 2.40 (6H, s; *o*-CH_3), δ 2.33 (3H, s; *p*-CH_3), δ 2.28 (2H, m; Cy-H), δ 2.00 (4H, m; Cy-H), δ 1.86 (4H, m; Cy-H), δ 1.74 (2H, m; Cy-H), δ 1.54 (4H, m; Cy-H), δ 1.30 (6H, m; Cy-H), δ 0.53 (3H, br. quart., $^1J_{B\text{-}H}$ = 112.9 Hz; BH_3). ^{13}C{^{1}H} (125.7 MHz, $CDCl_3$, 298 K): δ 150.6 (d, $^3J_{C\text{-}P}$ = 33.9 Hz; *i*-C_{Ar}(Mes)), δ 141.6 (s; *p*-C_{Ar} (Mes)), δ 132.8 (d, $^4J_{C\text{-}P}$ = 1.5 Hz; *o*-C_{Ar} (Mes)),

δ 130.5 (d, $^{5}J_{C\text{-}P}$ = 1.0 Hz; *m*-C_{Ar}(Mes)), δ 32.9 (d, $^{1}J_{C\text{-}P}$ = 29.8 Hz; *i*-C_{Cy}), δ 27.0 (d, $^{2}J_{C\text{-}P}$ = 11.4 Hz; *o*-C_{Cy}), δ 26.9 (d, $^{2}J_{C\text{-}P}$ = 10.5 Hz; *o*-C_{Cy}), δ 26.42 (s; *p*-C_{Cy}), δ 26.37 (d, $^{3}J_{C\text{-}P}$ = 2.3 Hz; *m*-C_{Cy}), δ 26.1 (br. doub., $^{4}J_{C\text{-}P}$ = 1.1 Hz; *m*-C_{Cy}), δ 21.4 (s; *p*-CH_3(Mes)), δ 20.1 (s; *o*-CH_3(Mes)). $^{31}P\{1H\}$ (202.4 MHz, $CDCl_3$, 298 K): δ 96.0 (br. quart). ^{31}P (162.0 MHz, $CDCl_3$, 298 K): δ 96.0 (br. s). $^{11}B\{^{1}H\}$ (160.4 MHz, $CDCl_3$, 298 K): δ -42.9 (br. doub.). UV-Vis Spectroscopy: (5 x 10^{-5} M in toluene): 313 nm, 0.7118 absorption; 514 nm, 0.0111 absorption. ESI-HRMS m/z for $C_{21}H_{36}N_2PB$ [*M* + Na]$^+$: calcd. 380.2643, 381.2611, 382.2641; found 380.2640, 381.2615, 382.2644 Additional peaks: [$MesN_2PCy_2$ + H]$^+$: found 345.25; [$MesN_2PCy_2.BH_2$]$^+$: found 357.27; [$MesN_2PCy_2$ + Na]$^+$: found 367.23. IR: ν_{max} (cm^{-1}) 2928 (s), 2852 (s), 2369 (m; B-H), 2345 (m; B-H), 1607 (m; N=N).

Synthesis of $MesN_2P(^tBu)_2.BH_3$ 3•BH_3

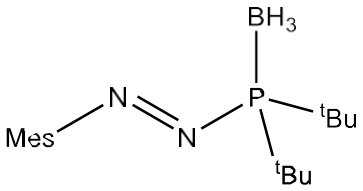

Azophosphine-borane **3•BH_3** was synthesised from commercially available precursor $H^tBu_2P.BH_3$ (2.68 mL, 0.67 mmol) according to method B, with purification by column chromatography (eluent = 95:5 hexane:Et_2O, with the product appearing as a purple spot with Rf = 0.35 in this eluent system), and the product yielded as a purple powder (112.2 mg, 0.37 mmol, 55% yield). ^{1}H (400.1 MHz, $CDCl_3$, 298 K): δ 6.96 (s, 2H; H_{Ar} (Mes)), δ 2.47 (s, 6H; *o*-CH_3 (Mes)), δ 2.34 (s, 3H; *p*-CH_3 (Mes)), δ 1.41 (d, $^{3}J_{H-P}$ = 12 Hz, 18H; ^{t}Bu), δ 0.56 (br. quart., 3H; BH_3). $^{31}P\{^{1}H\}$ (162.0 MHz, $CDCl_3$): δ 108.5 (br. quart.). $^{11}B\{^{1}H\}$ (128.4 MHz, $CDCl_3$): δ -42.5 (d, $^{1}J_{B-P}$ = 51 Hz). Obtained data in accord with reported literature (E.J. Jordan et al., *Chem. Eur. J.*, **2024**, e202401358).

S1.3. Synthesis of azophosphines (Method C)

The relevant azophosphine-borane $MesN_2PR_2.BH_3$ (R = ^{t}Bu, ^{i}Pr, Cy; 1 equiv.) was added to a 50 mL Schlenk flask and dissolved in toluene, creating a 0.05 M solution of azophosphine-borane in toluene. To this, pyrrolidine was added (10 equiv.), and the mixture stirred at room temperature overnight (16 hours), which gave 100% conversion to $MesN_2PR_2$ by crude $^{31}P\{^{1}H\}$ NMR spectroscopy. Excess pyrrolidine was removed in vacuo and the resulting oil filtered

through a short silica plug in the glovebox (eluent = 90:10 hexane:Et_2O) to remove the pyrrolidine.BH_3 adduct. Removal of the eluent in vacuo obtained the target deprotected $MesN_2PR_2$ product as an intensely-coloured solid or oil. The air-sensitive products were stored in vials in the glovebox freezer.

Synthesis of $MesN_2P(^iPr)_2$ (1)

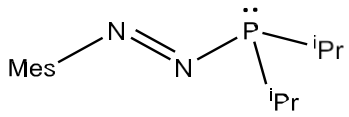

Azophosphine **1** was synthesised from precursor $MesN_2P(^iPr)_2.BH_3$ (145 mg, 0.52 mmol) according to method C. After overnight stirring, a colour change from purple to red was observed. The product was isolated as a red oil (107 mg, 0.41 mmol, 78 % yield). Removal of the residual pyrrolidine-borane adduct was determined by $^{11}B\{^1H\}$ NMR spectroscopy, which showed no peaks. ^1H (500.1 MHz, tol-d_8, 298 K): δ 6.69 (2H, s; *m*-Ar*H*), δ 2.33 (6H, s; *o*-CH_3), δ 2.19 (2H, septet of doublets, $^3J_{H\text{-}H}$ = 7.1 Hz, $^2J_{H\text{-}P}$ = 1.2 Hz; P(C*H*$(CH_3)_2)_2$), δ 2.10 (3H, s; *p*-CH_3), δ 1.22 (12H, m; CH(C$H_3)_2$). $^{13}C\{^1H\}$ (125.7 MHz, tol-d_8, 298 K): δ 152.1 (d, $^3J_{C\text{-}P}$ = 20.7 Hz; *i*-C_{Ar}(Mes)), δ 138.0 (d, $^4J_{C\text{-}P}$ = 0.8 Hz; *o*-C_{Ar} (Mes)), δ 130.5 (s; *p*-C_{Ar} (Mes)), δ 130.4 (s; *m*-C_{Ar} (Mes)), δ 26.2 (d, $^1J_{C\text{-}P}$ = 18.0 Hz; *C*H$(CH_3)_2$), δ 21.0 (s; *p*-CH_3 (Mes)), δ 19.6 (s; *o*-CH_3 (Mes)), δ 18.8-19.1 (m; CH(*C*$H_3)_2$). $^{31}P\{^1H\}$ (202.4 MHz, tol-d_8, 298 K): δ 106.9 (m). ^{31}P (162.0 MHz, tol-d_8, 298 K): δ 106.9 (m). UV-Vis Spectroscopy: (5 x 10^{-5} M in toluene): 333 nm, 0.7503 absorption; 500 nm, 0.0239 absorption. ESI-HRMS m/z for $C_{15}H_{25}N_2P$ $[M + H]^+$: calcd. 265.1833, 266.1833; found 265.1839, 266.1848. IR: ν_{max} (cm^{-1}) 2953 (s), 2924 (s), 2866 (s), 1607 (m; N=N).

Synthesis of $MesN_2P(Cy)_2$ (2)

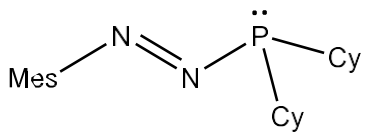

Azophosphine **2** was synthesised from precursor $MesN_2P(Cy)_2.BH_3$ (91 mg, 0.25 mmol) according to method C. After overnight stirring, a colour change from purple to red was observed. The product was isolated as a red oil (62 mg, 0.18 mmol, 71 % yield). Removal of the residual pyrrolidine-borane adduct was determined by $^{11}B\{^1H\}$ NMR spectroscopy, which showed no peaks. ^1H (500.1 MHz, tol-d_8, 298 K): δ 6.71 (2H, s; *m*-ArH), δ 2.37 (6H, s; *o*-CH_3),

δ 2.17 (3H, m; Cy-H), δ 2.10 (3H, s; *p*-CH_3), δ 1.91 (2H, m; Cy-H), δ 1.74 (4H, m; Cy-H), δ 1.63 (3H, m; Cy-H), δ 1.55 (4H, m; Cy-H), δ 1.24 (6H, m; Cy-H). $^{13}C\{^1H\}$ (125.7 MHz, tol-d_8, 298 K): δ 152.1 (d, $^3J_{C\text{-}P}$ = 20.4 Hz; *i*-C_{Ar}(Mes)), δ 137.9 (d, $^5J_{C\text{-}P}$ = 0.7 Hz; *m*-C_{Ar}(Mes)), δ 130.5 (d, $^4J_{C\text{-}P}$ = 1.5 Hz; *o*-C_{Ar}(Mes)), δ 130.4 (s; *p*-C_{Ar}(Mes)), δ 36.2 (d, $^1J_{C\text{-}P}$ = 18.6 Hz; *i*-C_{Cy}), δ 29.6 (d, $^2J_{C\text{-}P}$ = 9.8 Hz; *o*-C_{Cy}), δ 29.2 (d, $^2J_{C\text{-}P}$ = 10.3 Hz; *o*-C_{Cy}), δ 27.7 (d, $^3J_{C\text{-}P}$ = 9.5 Hz; *m*-C_{Cy}), δ 27.5 (d, $^3J_{C\text{-}P}$ = 8.6 Hz; *m*-C_{Cy}), δ 26.9 (br. doub., $^4J_{C\text{-}P}$ = 0.8 Hz; *p*-C_{Cy}), δ 21.0 (s; *p*-CH_3 (Mes)), δ 19.7 (s; *o*-CH_3 (Mes)). $^{31}P\{^1H\}$ (202.4 MHz, tol-d_8, 298 K): δ 100.5 (s). ^{31}P (162.0 MHz, tol-d_8, 298 K): δ 100.5 (br. s). UV-Vis Spectroscopy: (5 x 10^{-5} M in toluene): 315 nm, 1.3298 absorption; 499 nm, 0.0061 absorption. ESI-HRMS m/z for $C_{21}H_{33}N_2P$ [*M* + H]$^+$: calcd. 345.2460, 346.2460; found 345.2453, 346.2500. IR: ν_{max} (cm^{-1}) 2921 (s), 2849 (s), 1607 (m; N=N).

Synthesis of $MesN_2P(^tBu)_2$ (3)

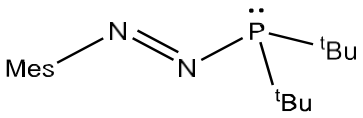

Azophosphine **3** was synthesised from precursor $MesN_2P(^tBu)_2.BH_3$ (123 mg, 0.40 mmol) according to method C. The product was isolated as a purple oil, which hardened into a purple solid after being left in the freezer overnight (99 mg, 0.34 mmol, 85 % yield). Removal of the residual pyrrolidine-borane adduct was determined by $^{11}B\{^1H\}$ NMR spectroscopy, which showed no peaks. ^1H (400.1 MHz, tol-d_8, 298 K): δ 6.71 (m, 2H; *m*-H_{Ar} (Mes)), δ 2.38 (s, 6H; *o*-CH_3 (Mes)), δ 2.10 (s, 3H; *p*-CH_3(Mes)), δ 1.32 (d, $^3J_{H\text{–}P}$ = 11 Hz, 18H; ^{t}Bu). $^{13}C\{^1H\}$ (125.8 MHz, tol-d_8): δ 152.17 (d, $^3J_{C\text{–}P}$ = 21 Hz; *i*-C_{Ar} (Mes)), δ 138.11 (s; *p*-C_{Ar} (Mes)), δ 130.67 (d, $^4J_{C\text{–}P}$ = 2 Hz; *o*-C_{Ar} (Mes)), δ 130.50 (s; *m*-C_{Ar} (Mes)), δ 35.75 (d, $^1J_{C\text{–}P}$ = 27 Hz; $C(CH_3)_3$), δ 29.20 (d, $^2J_{C\text{–}P}$ = 12 Hz; $C(CH_3)_3$), δ 20.94 (s; *p*-CH_3 (Mes)), δ 20.22 (s; *o*-CH_3 (Mes)). $^{31}P\{^1H\}$ (162.0 MHz, tol-d_8): δ 118.3 (s). Obtained data in accord with reported literature (E.J. Jordan et al., *Chem. Eur. J.*, **2024**, e202401358).

S1.4. Synthesis of five-membered heterocycles (Method D)

In the glovebox, the relevant azophosphine ($MesN_2PR_2$; R = ^{t}Bu, ^{i}Pr, Cy; 1 equiv.) was added to a 25 mL Schlenk flask and dissolved in toluene, creating a 0.05 M solution of azophosphine in toluene. Diethyl acetylenedicarboxylate ($C_2(CO_2Et)_2$; 1 equiv)) was then added to this

solution, giving an immediate colour change to pale yellow and 100% conversion of the azophosphine by crude $^{31}P\{^{1}H\}$ NMR spectroscopy. Removal of the solvent *in vacuo* yielded the heterocyclic products as beige/pale yellow coloured solids.

Synthesis of $MesN_2P(^{i}Pr)_2C_2(CO_2Et)_2$ (4)

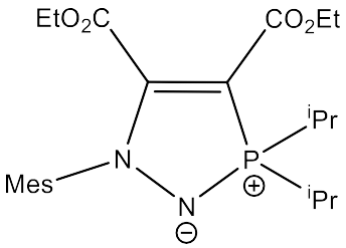

Five-membered heterocycle **4** was synthesised from precursor $MesN_2P(^{i}Pr)_2$ (30 mg, 0.11 mmol) according to method D. The product was isolated as an air-sensitive beige/pale-yellow coloured solid (42 mg, 0.10 mmol, 85 % yield). Colourless single crystals of **4** suitable for X-ray diffraction were grown by slow evaporation of a concentrated hexane solution of **4**. ^{1}H (400.1 MHz, tol-d_8, 298 K): δ 6.62 (2H, s; m-Ar*H*), δ 4.09 (2H, q, $^{3}J_{H\text{-}H}$ = 7.01 Hz; $CO_2CH_2CH_3$), δ 3.85 (2H, q, $^{3}J_{H\text{-}H}$ = 7.08 Hz; $CO_2CH_2CH_3$), δ 2.40 (6H, s; o-CH_3), δ 2.22 (2H, m; $CH(CH_3)_2$), δ 2.02 (3H, s; p-CH_3), δ 1.19 (6H; dd, $^{3}J_{H\text{-}P}$ = 17.6 Hz, $^{3}J_{H\text{-}H}$ = 7.23 Hz; $CH(CH_3)_2$), δ 1.12 (6H; dd, $^{3}J_{H\text{-}P}$ = 16.1 Hz, $^{3}J_{H\text{-}H}$ = 7.18 Hz; $CH(CH_3)_2$), δ 1.03 (3H, t, $^{3}J_{H\text{-}H}$ = 7.17 Hz; $CO_2CH_2CH_3$), δ 0.75 (3H, t, $^{3}J_{H\text{-}H}$ = 7.23 Hz; $CO_2CH_2CH_3$). $^{13}C\{^{1}H\}$ (100.6 MHz, tol-d_8, 298 K): δ 165.3 (d, $^{3}J_{C\text{-}P}$ = 10.5 Hz; *C*(=O)CC(CO_2Et)P), δ 161.9 (d, $^{2}J_{C\text{-}P}$ = 15.1 Hz; *C*(=O)CP), δ 149.4 (d, $^{3}J_{C\text{-}P}$ = 19.7 Hz; *i*-C_{Ar}(Mes)), δ 138.4 (s; *p*-C_{Ar}(Mes)), δ 138.1 (d; $^{2}J_{C\text{-}P}$ = 12.0 Hz; *C*=C-P), δ 136.6 (s; *o*-C_{Ar} (Mes)), δ 128.8 (s; *m*-C_{Ar} (Mes)), δ 66.9 (d, $^{1}J_{C\text{-}P}$ = 75.5 Hz; C=*C*-P), δ 61.4 (s; $CO_2CH_2CH_3$), δ 59.0 (s; $CO_2CH_2CH_3$), δ 27.7 (d, P*C*$(CH_3)_2$; $^{1}J_{C\text{-}P}$ = 58.9 Hz), δ 20.9 (s; *p*-CH_3 (Mes)), δ 18.0 (s; *o*-CH_3 (Mes)), δ 17.3 (d, $^{2}J_{C\text{-}P}$ = 1.80 Hz; PC(CH_3)$_2$), δ 15.6 (d, $^{2}J_{C\text{-}P}$ = 3.01 Hz; PC(CH_3)$_2$), δ 14.7 (s; $CO_2CH_2CH_3$), δ 13.6 (s; $CO_2CH_2CH_3$). $^{31}P\{^{1}H\}$ (162.0 MHz, tol-d_8, 298 K): δ 74.9 (s). ^{31}P (162.0 MHz, tol-d_8, 298 K): δ 74.9 (m). UV-Vis Spectroscopy: (5 x 10^{-5} M in toluene): 353 nm, 0.4385 absorption. ESI-HRMS m/z for $C_{23}H_{35}O_4N_2P$ $[M+H]^+$: calcd. 435.2413, 436.2445, 437.2473; found 435.2413, 436.2445, 437.2471. IR: ν_{max} (cm^{-1}) 2924 (m), 1735 (s; C=O), 1678 (s; C=O).

Synthesis of $MesN_2P(Cy)_2C_2(CO_2Et)_2$ (5)

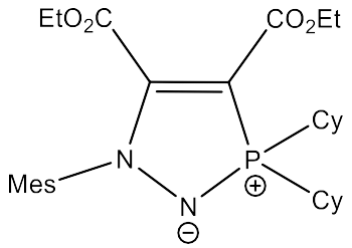

Five-membered heterocycle **5** was synthesised from precursor $MesN_2P(Cy)_2$ (27 mg, 0.077 mmol) according to method D. The product was isolated as an air-sensitive beige/pale-yellow coloured solid (22 mg, 0.062 mmol, 80 % yield). ^{1}H (500.1 MHz, tol-d_8, 298 K): δ 6.64 (2H, s; *m*-Ar*H*), δ 4.13 (2H, q, $^3J_{H\text{-}H}$ = 7.2 Hz; $CO_2CH_2CH_3$), δ 3.87 (2H, q, $^3J_{H\text{-}H}$ = 7.2 Hz; $CO_2CH_2CH_3$), δ 2.45 (6H, s; *o*-CH_3), δ 2.19 (2H, m; Cy-*H*), δ 2.03 (3H, s; *p*-CH_3), δ 1.99 (4H, m; Cy-*H*), δ 1.51-1.75 (10H, m; Cy-*H*), δ 1.09-1.19 (6H, m; Cy-*H*), δ 1.06 (3H, t, $^3J_{H\text{-}H}$ = 7.2 Hz; $CO_2CH_2CH_3$), δ 0.77 (3H, t, $^3J_{H\text{-}H}$ = 7.2 Hz; $CO_2CH_2CH_3$). $^{13}C\{^1H\}$ (125.7 MHz, tol-d_8, 298 K): δ 165.4 (d, $^3J_{C\text{-}P}$ = 8.4 Hz; *C*(=O)CC(CO_2Et)P), δ 162.1 (d, $^2J_{C\text{-}P}$ = 14.2 Hz; *C*(=O)CP), δ 149.1 (d, $^3J_{C\text{-}P}$ = 20.6 Hz; *i*-C_{Ar}(Mes)), δ 138.5 (s; *p*-C_{Ar}(Mes)), δ 138.3 (d, $^2J_{C\text{-}P}$ = 12.2 Hz; *C*=C-P), δ 136.7 (s; *o*-C_{Ar} (Mes)), δ 128.3 (s; *m*-C_{Ar} (Mes)), δ 66.6 (d, $^1J_{C\text{-}P}$ = 74.8 Hz; C=*C*-P), δ 61.4 (s; $CO_2CH_2CH_3$), δ 59.0 (s; $CO_2CH_2CH_3$), δ 37.6 (d, $^1J_{C\text{-}P}$ = 57.4 Hz; P-C_{Cy}), δ 27.3 (d, $J_{C\text{-}P}$ = 2.2 Hz; C_{Cy}), δ 26.91 (d, $^2J_{C\text{-}P}$ = 14.5 Hz; P-C_{Cy}-C_{Cy}), δ 26.87 (d, $^2J_{C\text{-}P}$ = 12.5 Hz; P-C_{Cy}-C_{Cy}), δ 26.4 (d, $J_{C\text{-}P}$ = 1.4 Hz; C_{Cy}), δ 25.8 (d, $J_{C\text{-}P}$ = 2.8 Hz; C_{Cy}), δ 21.0 (s; *p*-CH_3 (Mes)), δ 18.2 (s; *o*-CH_3 (Mes)), δ 14.7 (s; $CO_2CH_2CH_3$), δ 13.7 (s; $CO_2CH_2CH_3$). $^{31}P\{^1H\}$ (202.4 MHz, tol-d_8, 298 K): δ 68.9 (s). ^{31}P (202.4 MHz, tol-d_8, 298 K): δ 68.9 (m). UV-Vis Spectroscopy: (5 x 10^{-5} M in toluene): 356 nm, 0.3111 absorption. ESI-HRMS m/z for $C_{29}H_{43}O_4N_2P$ $[M+\mathrm{H}]^+$: calcd. 515.3039, 516.3071, 517.3101; found 515.3043, 516.3069, 517.3121. IR: ν_{max} (cm^{-1}) 2978 (w), 2929 (w), 2853 (w), 1738 (m; C=O),1689 (m; C=O).

Synthesis of $MesN_2P(^tBu_2)_2C_2(CO_2Et)_2$ (6)

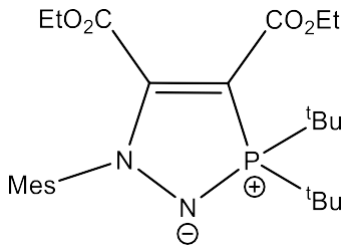

Five-membered heterocycle **6** was synthesised from precursor $MesN_2P(^tBu)_2$ (44 mg, 0.15 mmol) according to method D. The product was isolated as an air-stable beige/pale-yellow

coloured solid (58 mg, 0.13 mmol, 83 % yield). Colourless single crystals of **6** suitable for X-ray diffraction were grown by slow evaporation of a mixed THF/hexane (approximately 1:10 ratio of THF:hexane) solution of **6**. ^{1}H (500.1 MHz, d_8-toluene, 298 K): δ 6.62 (2H, br. doub., $^{6}J_{H\text{-}P}$ = 0.6 Hz; *m*-Ar*H*), δ 4.10 (2H, q, $^{3}J_{H\text{-}H}$ = 7.1 Hz; $CO_2CH_2CH_3$), δ 3.83 (2H, q, $^{3}J_{H\text{-}H}$ = 7.1 Hz; $CO_2CH_2CH_3$), δ 2.42 (6H, s; *o*-CH_3), δ 2.02 (3H, s; *p*-CH_3), δ 1.34 (18H, d, $^{3}J_{H\text{-}P}$ = 15.0 Hz; $P(C(CH_3)_3)_2$), δ 1.04 (3H, t, $^{3}J_{H\text{-}H}$ = 7.1 Hz; $CO_2CH_2CH_3$), δ 0.73 (3H, t, $^{3}J_{H\text{-}H}$ = 7.1 Hz; $CO_2CH_2CH_3$). ^{13}C{^{1}H} (125.7 MHz, d_8-toluene, 298 K): δ 166.1 (d, $^{3}J_{C\text{-}P}$ = 10.8 Hz; *C*(=O)CC(CO_2Et)P), δ 162.1 (d, $^{2}J_{C\text{-}P}$ = 14.9 Hz; *C*(=O)CP), δ 149.5 (d, $^{3}J_{C\text{-}P}$ = 19.3 Hz; *i*-C_{Ar}(Mes)), δ 138.4 (s; *p*-C_{Ar}(Mes)), δ 138.2 (d, $^{2}J_{C\text{-}P}$ = 10.5 Hz; *C*=C-P), δ 136.6 (s; *o*-C_{Ar} (Mes)), δ 129.0 (s; *m*-C_{Ar} (Mes)), δ 69.9 (d, $^{1}J_{C\text{-}P}$ = 70.6 Hz; C=*C*-P), δ 61.3 (s; $CO_2CH_2CH_3$), δ 59.1 (s; $CO_2CH_2CH_3$), δ 40.3 (d, $^{1}J_{C\text{-}P}$ = 49.8 Hz; *C*$(CH_3)_3$), δ 27.3 (s; C(CH_3)$_3$), δ 20.9 (s; *p*-CH_3 (Mes)), δ 18.6 (s; *o*-CH_3 (Mes)), δ 14.7 (s; $CO_2CH_2CH_3$), δ 13.6 (s; $CO_2CH_2CH_3$). ^{31}P{^{1}H} (202.4 MHz, d_8-toluene, 298 K): δ 77.5 (s). ^{31}P (202.4 MHz, d_8-toluene, 298 K): δ 77.5 (m). UV-Vis Spectroscopy: (5 x 10-5 M in toluene): 358 nm, 0.4202 absorption. ESI-HRMS m/z for $C_{25}H_{39}O_4N_2P$ $[M + H]^+$: calcd. 463.2726, 464.2758, 465.2787; found 463.2726, 464.2755, 465.2780. Additional peaks: $[C_{33}H_{49}O_8N_2P + H]^+$: found 633.33, 634.33, 635.33. These peaks likely correspond to a 1:2 equivalence of $MesN_2P^iPr_2$ and $C_8H_{10}O_4$, presumably a similar seven-membered ring structure to that of **7** or **8**, although this species was not observed via any other technique. IR: ν_{max} (cm^{-1}) 2969 (m), 2921 (m), 2870 (m), 1735 (s; C=O), 1678 (s; C=O). Elemental Analysis Found (Calculated) for $C_{25}H_{39}O_4N_2P$: C, 64.27(64.91); H, 8.30(8.50); N, 5.73(6.06).

S1.5. Synthesis of seven-membered heterocycles (Method E)

In the glovebox, the relevant azophosphine ($MesN_2PR_2$; R = ^{i}Pr, Cy; 1 equiv.) was added to a 25 mL Schlenk flask and dissolved in toluene, creating a 0.05 M solution of azophosphine in toluene. Diethyl acetylenedicarboxylate ($C_2(CO_2Et)_2$; 4 equiv)) was then added to this solution, giving an immediate colour change to pale yellow. This solution was then left stirring in the glovebox at room temperature for 2 days, after which time complete conversion had been observed by crude ^{31}P{^{1}H} NMR spectroscopy, and the solution had become a visibly brighter yellow colour. The volatiles were removed *in vacuo*, with further drying overnight to remove all excess alkyne; the material is then treated as air-stable. The product can then be isolated by column chromatography. Removal of the volatiles in vacuo yielded the product as a bright yellow solid. The air-stable, solid products were stored in vials in the freezer.

The same procedure could also be achieved by starting with the relevant five-membered heterocycle (**4** or **6**; 1 equiv.)., rather than azophosphine, with spectroscopically pure seven-membered heterocycles still obtained. The same conditions and reagents are used regardless

of whether the azophosphine or five-membered ring is used as the starting material. For clarity, the procedures below detail preparation from the azophosphine starting material.

Synthesis of $MesN_2C_2(CO_2Et)_2P(^iPr)_2C_2(CO_2Et)_2$ (7)

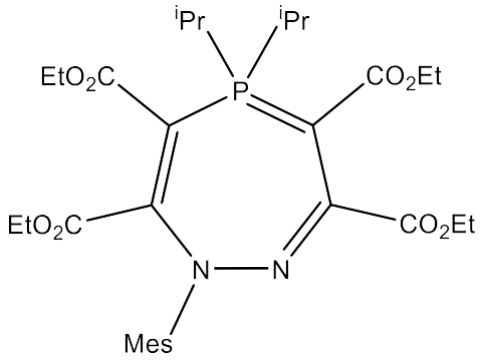

Seven-membered heterocycle **7** was synthesised from precursor $MesN_2P(^iPr)_2$ (52 mg, 0.20 mmol) according to method E, with purification by column chromatography (eluent = 3:1 hexane:EtOAc, with the product appearing as a yellow spot with R_f = 0.26 in this eluent system). The product was isolated as an air-stable, yellow coloured solid (104 mg, 0.17 mmol, 88 % yield). Yellow single crystals of **7** suitable for X-ray diffraction were grown by slow diffusion of hexane into a concentrated THF solution of **7**. We observed **7** to slowly degrade over the course of weeks at room temperature, in both air and inert atmosphere, thus **7** is best stored in a freezer. ^{1}H (400.1 MHz, tol-d_8, 298 K): δ 6.48 (2H, s; m-Ar*H*), δ 4.09 (2H, q, $^3J_{H\text{-}H}$ = 7.0 Hz; $CO_2CH_2CH_3$), δ 4.03 (2H, q, $^3J_{H\text{-}H}$ = 7.0 Hz; $CO_2CH_2CH_3$), δ 3.86 (2H, q, $^3J_{H\text{-}H}$ = 7.1 Hz; $CO_2CH_2CH_3$), δ 3.66 (2H, q, $^3J_{H\text{-}H}$ = 7.0 Hz; $CO_2CH_2CH_3$), δ 3.63 (2H, m; $CH(CH_3)_2$), δ 2.49 (6H, s; o-CH_3), δ 1.95 (3H, s; p-CH_3), δ 1.61 (6H; dd, $^3J_{H\text{-}P}$ = 18.1 Hz, $^3J_{H\text{-}H}$ = 7.1 Hz; $CH(CH_3)_2$), δ 1.37 (6H; dd, $^3J_{H\text{-}P}$ = 17.9 Hz, $^3J_{H\text{-}H}$ = 7.3 Hz; $CH(CH_3)_2$), δ 1.07 (3H, t, $^3J_{H\text{-}H}$ = 7.1 Hz; $CO_2CH_2CH_3$), δ 0.96 (3H, t, $^3J_{H\text{-}H}$ = 7.1 Hz; $CO_2CH_2CH_3$), δ 0.88 (3H, t, $^3J_{H\text{-}H}$ = 7.0 Hz; $CO_2CH_2CH_3$), δ 0.68 (3H, t, $^3J_{H\text{-}H}$ = 7.0 Hz; $CO_2CH_2CH_3$). $^{13}C\{^1H\}$ (100.6 MHz, tol-d_8, 298 K): δ 168.0 (d, $J_{C\text{-}P}$ = 15.6 Hz; *C*=O), δ 167.1 (d, $J_{C\text{-}P}$ = 6.6 Hz; *C*=O), δ 166.5 (d, $J_{C\text{-}P}$ = 11.9 Hz; *C*=O), δ 166.1 (br. s; P-C(CO_2Et)-*C*(CO_2Et)), δ 163.6 (d, $J_{C\text{-}P}$ = 11.9 Hz; *C*=O), δ 161.8 (s; P-C(CO_2Et)-*C*(CO_2Et)), δ 139.9 (s; *i*-C_{Ar}(Mes)), δ 138.7 (s; *p*-C_{Ar}(Mes)), δ 137.1 (s; *o*-C_{Ar} (Mes)), δ 129.3 (s; *m*-C_{Ar} (Mes)), δ 67.3 (d, $^1J_{C\text{-}P}$ = 95.6 Hz; P-*C*(CO_2Et)), δ 61.8 (s; $CO_2CH_2CH_3$), δ 61.3 (s; $CO_2CH_2CH_3$), δ 60.2 (s; $CO_2CH_2CH_3$), δ 58.8 (s; $CO_2CH_2CH_3$), δ 43.4 (d, $^1J_{C\text{-}P}$ = 106.2 Hz; P-*C*(CO_2Et)), δ 27.7 (d, P*C*H(CH_3)$_2$; $^1J_{C\text{-}P}$ = 51.6 Hz), δ 20.9 (s; *p*-CH_3 (Mes)), δ 19.2 (s; *o*-CH_3 (Mes)), δ 17.9 (d, $^2J_{C\text{-}P}$ = 2.6 Hz; PCH(*C*H_3)$_2$), δ 17.0 (d, $^2J_{C\text{-}P}$ = 1.0 Hz; PCH(*C*H_3)$_2$), δ 14.8 (s; $CO_2CH_2CH_3$), δ 14.14 (s; $CO_2CH_2CH_3$), δ 14.08 (s; $CO_2CH_2CH_3$), δ 13.2 (s; $CO_2CH_2CH_3$). $^{31}P\{^1H\}$ (162.0 MHz, tol-d_8, 298 K): δ 60.4 (s). ^{31}P (162.0 MHz, tol-d_8, 298 K): δ

60.4 (m). UV-Vis Spectroscopy: (5 x 10^{-5} M in toluene): 319 nm, 0.8932 absorption; 411 nm, 0.2454 absorption. ESI-HRMS m/z for $C_{31}H_{45}O_8N_2P$ $[M + H]^+$: calcd. 605.2992, 606.3024, 607.3052, 608.3079; found 605.2997, 606.3022, 607.3045, 608.3068. Elemental Analysis Found (Calculated) for $C_{31}H_{45}O_8N_2P$: C, 61.29(61.58); H, 7.40(7.50); N, 5.02(4.63). IR: ν_{max} (cm^{-1}) 2926 (w), 1735 (m; C=O), 1724 (m; C=O), 1687 (m; C=O), 1652 (m; C=O).

$MesN_2C_2(CO_2Et)P^iPr_2C_2(CO_2Et)_2B(C_6F_5)_3$ (7·BCF)

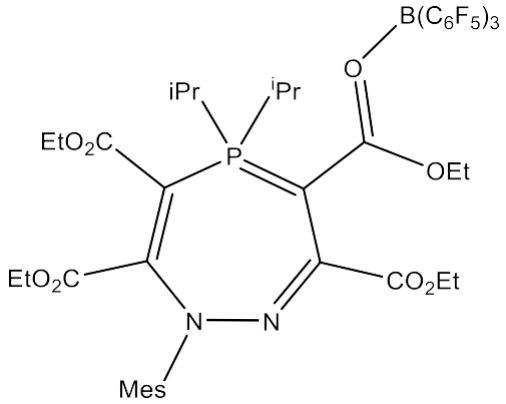

In the glovebox, 17.0 mg of **7** ($MesN_2C_2(CO_2Et)_2P(^iPr)_2C_2(CO_2Et)_2$; 0.028 mmol, 1 equiv) was dissolved in 0.6 mL of d_8-toluene in a glass vial. 14.4 mg of tris(pentafluorophenyl)borane ($B(C_6F_5)_3$; 0.028 mmol, 1 equiv) was then added to this solution; no noticeable colour changes were observed after addition of $B(C_6F_5)_3$, with the sample remaining bright yellow. To obtain NMR spectroscopy data, this sample was then immediately analysed in an airtight J-Young NMR tube. Repeating the same reaction in hexane, followed by slow evaporation of the corresponding hexane solution, allowed for growth of yellow single crystals of **7** suitable for X-ray diffraction. These crystals were also used for UVVis and IR measurements. ^{1}H (500.1 MHz, tol-d_8, 298 K): δ 6.51 (1H, s; m-Ar*H*), δ 6.42 (1H, s; m-Ar*H*), δ 4.09 (1H, br. m; C*H*$(CH_3)_2$), δ 3.52 - 4.00 (8H, m; $CO_2CH_2CH_3$), δ 3.02 (1H, br. m; C*H*$(CH_3)_2$), δ 2.41 (6H, s; o-CH_3), δ 1.87 (3H, s; p-CH_3), δ 1.56 (3H; m; CH(CH_3)$_2$), δ 1.39 (3H; m; CH(CH_3)$_2$), δ 1.30 (3H; m; CH(CH_3)$_2$), δ 1.04 (3H; m; CH(CH_3)$_2$), δ 0.87 (3H, t, $^3J_{H\text{-}H}$ = 7.1 Hz; $CO_2CH_2CH_3$), δ 0.82 (3H, t, $^3J_{H\text{-}H}$ = 7.1 Hz; $CO_2CH_2CH_3$), δ 0.62 (3H, t, $^3J_{H\text{-}H}$ = 7.1 Hz; $CO_2CH_2CH_3$), δ 0.55 (3H, t, $^3J_{H\text{-}H}$ = 7.1 Hz; $CO_2CH_2CH_3$). ^{13}C{^{1}H} (125.8 MHz, tol-d_8, 298 K): δ 175.3 (d, $^2J_{C\text{-}P}$ = 10.1 Hz; P-C-*C*(=O)), δ 165.9 (d, $^2J_{C\text{-}P}$ = 13.6 Hz; P-C-*C*(=O)), δ 164.3 (d, $^3J_{C\text{-}P}$ = 4.8 Hz; P-C-C-*C*(=O)), δ 162.1 (d, $^3J_{C\text{-}P}$ = 8.4 Hz; P-C-C-*C*(=O)), δ 159.8 (s; N-*C*(CO_2Et)), δ 159.2 (s; N-*C*(CO_2Et)), δ 148.6 (d, $^1J_{C\text{-}F}$ = 242.0 Hz; C_{BCF}), δ 140.2 (d, $^1J_{C\text{-}F}$ = 249.7 Hz; C_{BCF}), δ 140.1 (s; *p*-C_{Ar}(Mes)), δ 137.9 (s; *o*-C_{Ar}(Mes)), δ 137.5 (d, $^1J_{C\text{-}F}$ = 251.0 Hz; C_{BCF}), δ 135.4 (br. s; *i*-C_{Ar}(Mes)), δ 130.5 (s; *m*-C_{Ar}(Mes)), δ 129.4 (s; *m*-C_{Ar}(Mes)), δ 120.4 (br. m; *i*-C_{BCF}), δ 73.8 (d, $^1J_{C\text{-}P}$ = 89.3 Hz; P-*C*(CO_2Et)), δ 70.8 (s; $CO_2CH_2CH_3$), δ 63.1 (s; $CO_2CH_2CH_3$), δ 62.6 (s; $CO_2CH_2CH_3$), δ 61.7 (s; $CO_2CH_2CH_3$), δ 56.8 (d, $^1J_{C\text{-}P}$ = 94.5 Hz; P-*C*(CO_2Et)), δ 26.8 (d, $^1J_{C\text{-}P}$ = 44.0 Hz; P*C*H$(CH_3)_2$),

δ 24.8 (d, $^{1}J_{C\text{-}P}$ = 53.1 Hz; P*C*H(CH$_3$)$_2$), δ 19.3 (s; *p*-*C*H$_3$ (Mes)), δ 18.8 (s; *o*-*C*H$_3$ (Mes)), δ 18.4 (s; PCH(*C*H$_3$)$_2$), δ 17.5 (s; PCH(*C*H$_3$)$_2$), δ 17.3 (s; PCH(*C*H$_3$)$_2$), δ 15.0 (s; PCH(*C*H$_3$)$_2$), δ 13.9 (s; CO$_2$CH$_2$*C*H$_3$), δ 13.7 (s; CO$_2$CH$_2$*C*H$_3$), δ 13.6 (s; CO$_2$CH$_2$*C*H$_3$), δ 13.0 (s; CO$_2$CH$_2$*C*H$_3$). ^{31}P{^{1}H} (162.0 MHz, tol-d$_8$, 298 K): δ 60.0 (s). ^{31}P (202.4 MHz, tol-d$_8$, 298 K): δ 60.0 (br. m). ^{19}F{^{1}H} (376.5 MHz, tol-d$_8$, 298 K): δ -132.8 (m), -158.7 (m), -164.9 (m). ^{11}B{^{1}H} (160.4 MHz, tol-d$_8$, 298 K): δ -1.7 (br. s). UV-Vis Spectroscopy*:* (5 x 10^{-5} M in toluene): 408 nm, 0.1222 absorption; 321 nm, 0.3880 absorption. IR: ν_{max} (cm^{-1}) 2984 (w), 2158 (m; C=O), 1742 (m; C=O), 1679 (m; C=O), 1644 (m; C=O).

Synthesis of MesN$_2$C$_2$(CO$_2$Et)$_2$P(Cy)$_2$C$_2$(CO$_2$Et)$_2$ (8)

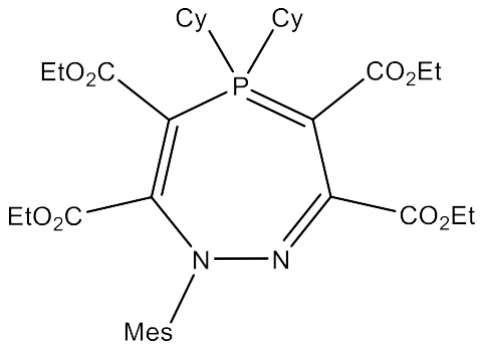

Seven-membered heterocycle **8** was synthesised from precursor MesN$_2$P(Cy)$_2$ (23 mg, 0.065 mmol) according to method E, with purification by column chromatography (eluent = 3:1 hexane:EtOAc, with the product appearing as a yellow spot with R$_f$ = 0.60 in this eluent system). The product was isolated as an air-stable, yellow coloured solid (41 mg, 0.060 mmol, 92 % yield). Yellow single crystals of **8** suitable for X-ray diffraction were grown by slow evaporation of a concentrated hexane solution of **8**. We observed **8** to slowly degrade over the course of weeks at room temperature, in both air and inert atmosphere, thus **8** is best stored in a freezer. ^{1}H (400.1 MHz, tol-d$_8$, 298 K): δ 6.50 (2H, s; m-Ar*H*), δ 4.10 (2H, q, $^{3}J_{H\text{-}H}$ = 7.1 Hz; CO$_2$C*H*$_2$CH$_3$), δ 4.05 (2H, q, $^{3}J_{H\text{-}H}$ = 7.1 Hz; CO$_2$C*H*$_2$CH$_3$), δ 3.90 (2H, q, $^{3}J_{H\text{-}H}$ = 7.1 Hz; CO$_2$C*H*$_2$CH$_3$), δ 3.70 (2H, q, $^{3}J_{H\text{-}H}$ = 7.1 Hz; CO$_2$C*H*$_2$CH$_3$), δ 3.47 (2H, m; P-C$_{Cy}$*H*), δ 2.51 (6H, s; o-C*H*$_3$), δ 2.18-2.42 (4H, m; Cy-*H*), δ 1.96 (3H, s; p-C*H*$_3$), δ 1.56-1.90 (8H; m; Cy-*H*), δ 1.24-1.41 (10H; m; Cy-*H*), δ 1.07 (3H, t, $^{3}J_{H\text{-}H}$ = 7.1 Hz; CO$_2$CH$_2$C*H*$_3$), δ 0.98 (3H, t, $^{3}J_{H\text{-}H}$ = 7.1 Hz; CO$_2$CH$_2$C*H*$_3$), δ 0.93 (3H, t, $^{3}J_{H\text{-}H}$ = 7.0 Hz; CO$_2$CH$_2$C*H*$_3$), δ 0.71 (3H, t, $^{3}J_{H\text{-}H}$ = 7.0 Hz; CO$_2$CH$_2$C*H*$_3$). ^{13}C{^{1}H} (100.6 MHz, tol-d$_8$, 298 K): δ 168.0 (d, $J_{C\text{-}P}$ = 14.9 Hz; *C*=O), δ 167.3 (d, $J_{C\text{-}P}$ = 7.2 Hz; *C*=O), δ 166.5 (d, $J_{C\text{-}P}$ = 11.9 Hz; *C*=O), δ 166.1 (br. s; P-C(CO$_2$Et)-*C*(CO$_2$Et)), δ 163.6 (d, $J_{C\text{-}P}$ = 9.8 Hz; *C*=O), δ 162.1 (s; P-C(CO$_2$Et)-*C*(CO$_2$Et)), δ 140.0 (s; *i*-*C*$_{Ar}$(Mes)), δ 138.7 (s; *p*-*C*$_{Ar}$(Mes)), δ 137.2 (s; *o*-*C*$_{Ar}$(Mes)), δ 129.3 (s; *m*-*C*$_{Ar}$(Mes)), δ 62.2 (d, $^{1}J_{C\text{-}P}$ = 77.1 Hz; P-*C*(CO$_2$Et)), δ 61.8 (s; CO$_2$CH$_2$CH$_3$), δ 61.3 (s; CO$_2$CH$_2$CH$_3$), δ 60.1 (s; CO$_2$CH$_2$CH$_3$), δ

58.8 (s; $CO_2CH_2CH_3$), δ 43.8 (d, $^1J_{C\text{-}P}$ = 107.1 Hz; P-*C*(CO_2Et)), δ 37.3 (d, $^1J_{C\text{-}P}$ = 51.1 Hz; P-C_{Cy}), δ 27.9 (d, $J_{C\text{-}P}$ = 13.8 Hz; C_{Cy}), δ 27.6 (d, $J_{C\text{-}P}$ = 3.6 Hz; C_{Cy}), δ 27.5 (d, $J_{C\text{-}P}$ = 7.3 Hz; C_{Cy}), δ 27.0 (d, $J_{C\text{-}P}$ = 1.7 Hz; C_{Cy}), δ 26.3 (d, $J_{C\text{-}P}$ = 1.4 Hz; C_{Cy}), δ 20.9 (s; *p*-CH_3 (Mes)), δ 19.3 (s; *o*-CH_3 (Mes)), δ 14.8 (s; $CO_2CH_2CH_3$), δ 14.21 (s; $CO_2CH_2CH_3$), δ 14.20 (s; $CO_2CH_2CH_3$), δ 13.2 (s; $CO_2CH_2CH_3$). $^{31}P\{^1H\}$ (162.0 MHz, tol-d_8, 298 K): δ 54.0 (s). ^{31}P (162.0 MHz, tol-d_8, 298 K): δ 54.0 (m). UV-Vis Spectroscopy: (5 x 10^{-5} M in toluene): 319 nm, 0.4573 absorption; 412 nm, 0.1252 absorption. ESI-HRMS m/z for $C_{37}H_{53}O_8N_2P$ $[M+H]^+$: calcd. 685.3618, 686.3651, 687.3680, 688.3708; found 685.3630, 686.3655, 687.3682, 688.3700. IR: ν_{max} (cm^{-1}) 2923 (m), 2853 (m), 1743 (m; C=O), 1724 (m; C=O), 1697 (m; C=O), 1655 (m; C=O).

S1.6. Synthesis of five- and seven-membered heterocycles using ethyl 2-butynoate

Synthesis of $MesN_2P(^tBu)_2C(CH_3)C(CO_2Et)$ (9)

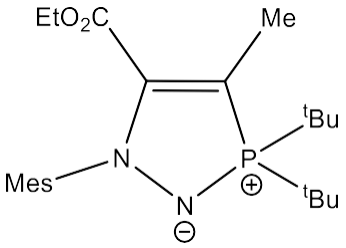

In the glovebox, 50 mg of $MesN_2P^tBu_2$ (0.17 mmol, 1 equiv) is dissolved in 2.5 mL of toluene in a Schlenk flask. To this solution is added 0.4 mL microliters of ethyl 2-butynoate, ($(CH_3)C_2(CO_2Et)$; 3.4 mmol, 20 equiv). This is left stirring for 3 days in the glovebox at room temperature, after which time a colour change to dark brown-yellow was observed. The solvent is then removed *in vacuo*, with further drying overnight to remove all excess alkyne, to yield a yellow-brown oil as the crude product, with the material now treated as air-stable. Purification by column chromatography (eluent = 4:1 hexane:isopropanol, with the product appearing as a yellow spot with R_f = 0.35 in this eluent system) and removal of all volatiles *in vacuo* yielded the product as a yellow solid (24 mg, 0.06 mmol, 35 %). Yellow single crystals of **9** suitable for X-ray diffraction were grown by slow evaporation of a concentrated hexane solution of **9**. ^1H (500.1 MHz, tol-d_8, 298 K): δ 6.76 (2H, s; *m*-Ar*H*), δ 3.96 (2H, q, $^3J_{H\text{-}H}$ = 7.3 Hz; $CO_2CH_2CH_3$), δ 2.20 (3H, s; *p*-CH_3), δ 2.165 (3H, d, $^3J_{H\text{-}P}$ = 10.6Hz; C=C-CH_3), δ 2.159 (6H, s; *o*-CH_3), δ 1.31 (18H, d, $^3J_{H\text{-}P}$ = 14.3 Hz; $P(C(CH_3)_3)_2$), δ 0.88 (3H, t, $^3J_{H\text{-}H}$ = 7.3 Hz; $CO_2CH_2CH_3$). $^{13}C\{^1H\}$ (125.7 MHz, tol-d_8, 298 K): δ 162.3 (d, $^3J_{C\text{-}P}$ = 18.8 Hz; *C*(=O)CC(Me)P), δ 145.7 (d, $^2J_{C\text{-}P}$ = 21.0 Hz; *C*=C-P), δ 139.8 (d, $^3J_{C\text{-}P}$ = 11.7 Hz; *i*-C_{Ar}(Mes)), δ 136.8 (s; *p*-

C_{Ar}(Mes)), δ 136.6 (s; *o*-C_{Ar} (Mes)), δ 128.6 (s; *m*-C_{Ar} (Mes)), δ 69.5 (d, $^{1}J_{C\text{-}P}$ = 68.2 Hz; C=*C*-P), δ 60.5 (s; $CO_2CH_2CH_3$), δ 40.6 (d, $^{1}J_{C\text{-}P}$ = 48.4 Hz; $C(CH_3)_3$), δ 27.5 (s; $C(CH_3)_3$), δ 21.0 (s; *p*-CH_3 (Mes)), δ 18.3 (s; *o*-CH_3 (Mes)), δ 13.5 (s; $CO_2CH_2CH_3$), δ 12.2 (d, $^{2}J_{C\text{-}P}$ = 4.4 Hz; $CO_2CH_2CH_3$). $^{31}P\{^{1}H\}$ (202.4 MHz, tol-d_8, 298 K): δ 74.7 (s). ^{31}P (202.4 MHz, tol-d_8, 298 K): δ 74.7 (m). UV-Vis Spectroscopy: (5 x 10^{-5} M in toluene): 411 nm, 0.1200 absorption. ESI-HRMS m/z for $C_{23}H_{37}O_2N_2P$ $[M+H]^+$: calcd. 405.2671, 406.2703, 407.2733; found 405.2663, 406.2697, 407.2726. IR: ν_{max} (cm^{-1}) 2917 (w), 1703 (m; C=O).

Synthesis of $MesN_2C_2(CO_2Et)_2P^iPr_2C(CH_3)C(CO_2Et)$ (10)

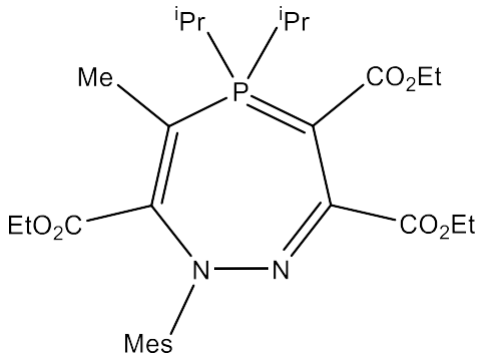

In the glovebox, 40 mg of $MesN_2P^iPr_2$ (0.15 mmol, 1 equiv) is dissolved in 2 mL of toluene in a Schlenk flask. To this solution is added 0.21 mL (1.82 mmol, 12 equiv) of ethyl 2-butynoate, $(CH_3)C_2(CO_2Et)$. This is left stirring in the glovebox overnight, after which time a colour change to deep yellow/orange had been observed, and for which crude $^{31}P\{^{1}H\}$ NMR spectroscopy showed complete reaction of the azophosphine. The solvent is then removed *in vacuo* to yield an orange oil, with further drying *in vacuo* for an hour to remove all excess alkyne. The flask is then transferred back into the glovebox, the orange oil is dissolved in 2 mL of toluene and 0.15 mL of diethyl acetylenedicarboxylate, $C_2(CO_2Et)_2$, is added (0.94 mmol, 6 equiv). This is left stirring in the glovebox overnight, after which time a colour change to pale yellow had been observed. The solvent is then removed in vacuo to yield a yellow oil as the crude product, with the material now treated as air-stable. Purification by column chromatography (eluent = 1:1 hexane:EtOAc, with the product appearing as a yellow spot with R_f = 0.45 in this eluent system) and removal of all volatiles in vacuo yielded the product as a yellow solid (22 mg, 0.040 mmol, 26 %). Yellow single crystals of **10** suitable for X-ray diffraction were grown by slow evaporation of a concentrated hexane solution of **10**. We observed **10** to slowly degrade over the course of weeks at room temperature, in both air and inert atmosphere, thus **10** is best stored in a freezer. ^{1}H (500.1 MHz, $CDCl_3$, 298 K): δ 6.77 (2H, s; m-Ar*H*), δ 4.22 (2H, q, $^{3}J_{H\text{-}H}$ = 7.2 Hz; $CO_2CH_2CH_3$), δ 3.96 (2H, br. q; $CO_2CH_2CH_3$), δ 3.79 (2H, q, $^{3}J_{H\text{-}H}$ = 7.2 Hz;

$CO_2CH_2CH_3$), δ 3.26 (2H, m; $CH(CH_3)_2$), δ 2.30 (6H, s; o-CH_3), δ 2.21 (3H, s; p-CH_3), δ 1.69 (2H, d, $^3J_{H\text{-}P}$ = 11.0 Hz; P-C-CH_3), δ 1.42 (6H; dd, $^3J_{H\text{-}P}$ = 17.5 Hz, $^3J_{H\text{-}H}$ = 7.1 Hz; $CH(CH_3)_2$), δ 1.29 (6H; dd, $^3J_{H\text{-}P}$ = 16.6 Hz, $^3J_{H\text{-}H}$ = 7.2 Hz; $CH(CH_3)_2$), δ 1.28 (3H, t, $^3J_{H\text{-}H}$ = 7.1 Hz; $CO_2CH_2CH_3$), δ 1.12 (3H, t, $^3J_{H\text{-}H}$ = 7.1 Hz; $CO_2CH_2CH_3$), δ 0.93 (3H, t, $^3J_{H\text{-}H}$ = 7.1 Hz; $CO_2CH_2CH_3$). $^{13}C\{^1H\}$ (125.8 MHz, $CDCl_3$, 298 K): δ 168.4 (d, $J_{C\text{-}P}$ = 17.7 Hz; *C*=O), δ 167.4 (d, $^3J_{C\text{-}P}$ = 9.7 Hz; P-C(CH_3)-C(CO_2Et)), δ 164.4 (d, $J_{C\text{-}P}$ = 14.4 Hz; *C*=O), δ 157.0 (br. s; P-C(CO_2Et)-*C*(CO_2Et)), δ 153.9 (br. s; P-C(CH_3)-*C*(CO_2Et)), δ 140.1 (s; *i*-C_{Ar}(Mes)), δ 137.7 (s; *o*-C_{Ar}(Mes)), δ 137.6 (s; *p*-C_{Ar} (Mes)), δ 129.1 (s; *m*-C_{Ar} (Mes)), δ 77.4 (m; P-*C*(CH_3)), δ 61.6 (s; P-C(CH_3)-C($CO_2CH_2CH_3$)), δ 61.2 (s; $CO_2CH_2CH_3$), δ 58.5 (s; $CO_2CH_2CH_3$), δ 40.5 (d, $^1J_{C\text{-}P}$ = 110.5 Hz; P-*C*(CO_2Et)), δ 24.1 (br. d, $^1J_{C\text{-}P}$ = 54.5 Hz; P*C*H(CH_3)$_2$), δ 21.1 (s; *p*-CH_3 (Mes)), δ 19.4 (s; *o*-CH_3 (Mes)), δ 17.3 (d, $^2J_{C\text{-}P}$ = 2.3 Hz; PCH(*C*H_3)$_2$), δ 16.4 (br. s; PCH(*C*H_3)$_2$), δ 15.7 (d, $^2J_{C\text{-}P}$ = 7.3 Hz; P-C-*C*H_3), δ 14.7 (s; P-C(CH_3)-C($CO_2CH_2CH_3$)), δ 14.3 (s; $CO_2CH_2CH_3$), δ 13.6 (s; $CO_2CH_2CH_3$). $^{31}P\{^1H\}$ (202.4 MHz, $CDCl_3$, 298 K): δ 40.0 (s). ^{31}P (202.4 MHz, $CDCl_3$, 298 K): δ 40.0 (m). UV-Vis Spectroscopy: (5 x 10^{-5} M in toluene): 305 nm, 0.5767 absorption; 370 nm, 0.1069 absorption. ESI-HRMS m/z for $C_{29}H_{43}O_6N_2P$ $[M+H]^+$: calcd. 547.2937, 548.2969, 549.2998; found 547.2935, 548.2958, 549.2984. IR: ν_{max} (cm^{-1}) 2979 (w), 1729 (m; C=O), 1639 (m; C=O), 1591 (m; C=O). Elemental Analysis Found (Calculated) for $C_{29}H_{43}O_6N_2P$: C, 62.41(63.72); H, 7.94(7.93); N, 5.11(5.12).

S1.7. Trapping of an intermediate

Synthesis of $MesN_2P(^tBu)_2C_2(CO_2Et)_2(C_2(CO_2Et)_2)(B(C_6F_5)_3)$ (11)

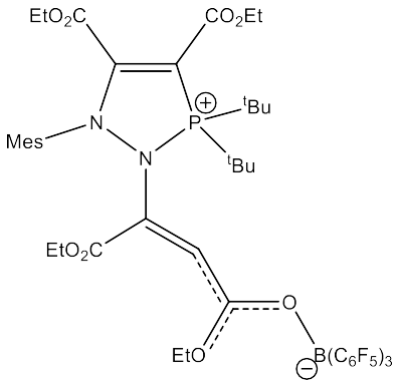

In the glovebox, 11 mg of **6** ($MesN_2P(^tBu)_2C_2(CO_2Et)_2$; 0.024 mmol, 1 equiv) was dissolved in 0.6 mL of d_8-toluene in a glass vial. 3.8 microliters of diethyl acetylenedicarboxylate is then added to this solution by microsyringe ($C_2(CO_2Et)_2$; 0.024 mmol, 1 equiv), followed by 12 mg of tris(pentafluorophenyl)borane ($B(C_6F_5)_3$; 0.024 mmol, 1 equiv); after addition of $B(C_6F_5)_3$, the solution changed colour from off-white/pale yellow to bright yellow. To obtain NMR spectroscopy data, this sample was then immediately analysed in an airtight J-Young NMR

tube. Repeating the same reaction in hexane, followed by slow evaporation of the corresponding hexane solution, allowed for growth of yellowish-orange single crystals of **11** suitable for X-ray diffraction. These crystals were also used for UVVis and IR measurements. ^{1}H (500.1 MHz, tol-d_8, 298 K): δ 6.41 (1H, s; *m*-Ar*H*), δ 6.38 (1H, s; *m*-Ar*H*), δ 3.88 (2H, br. q, $^{3}J_{H\text{-}H}$ = 7.0 Hz; $CO_2CH_2CH_3$), δ 3.72 (2H, m; $CO_2CH_2CH_3$), δ 3.63 (2H, m; $CO_2CH_2CH_3$), δ 3.52 (2H, m; $CO_2CH_2CH_3$), δ 2.22 (3H, s; *o*-CH_3), δ 2.15 (3H, s; *o*-CH_3), δ 1.85 (3H, s; *p*-CH_3), δ 1.44 (9H, d, $^{3}J_{H\text{-}P}$ = 18.5 Hz; P(C(CH_3)$_3$)$_2$), δ 1.40 (9H, d, $^{3}J_{H\text{-}P}$ = 18.5 Hz; P(C(CH_3)$_3$)$_2$), δ 0.87 (3H, t, $^{3}J_{H\text{-}H}$ = 7.0 Hz; $CO_2CH_2CH_3$), δ 0.84 (3H, t, $^{3}J_{H\text{-}H}$ = 7.7 Hz; $CO_2CH_2CH_3$), δ 0.60 (3H, t, $^{3}J_{H\text{-}H}$ = 7.0 Hz; $CO_2CH_2CH_3$), δ 0.59 (3H, t, $^{3}J_{H\text{-}H}$ = 7.7 Hz; $CO_2CH_2CH_3$). ^{13}C{^{1}H} (125.8 MHz, tol-d_8, 298 K): δ 205.9 (s; P(^{t}Bu)$_2$NC=*C*), δ 172.2 (s; *C*(=O-B(C_6F_5)$_3$)), δ 162.6 (d, $^{2}J_{C\text{-}P}$ = 16.3 Hz; P-C-*C*(=O)), δ 162.0 (d, $^{3}J_{C\text{-}P}$ = 6.6 Hz; *C*(=O)), δ 158.7 (d, $^{3}J_{C\text{-}P}$ = 9.7 Hz; *C*(=O)), δ 151.5 (d, $^{2}J_{C\text{-}P}$ = 4.2 Hz; P(^{t}Bu)$_2$N*C*=C), δ 148.7 (d, $^{1}J_{C\text{-}F}$ = 243.7 Hz; C_{BCF}), δ 143.0 (s; *p*-C_{Ar}(Mes)), δ 141.6 (s; *o*-C_{Ar} (Mes)), δ 139.6 (d, $^{1}J_{C\text{-}F}$ = 248.3 Hz; C_{BCF}), δ 139.5 (s; *o*-C_{Ar} (Mes)), δ 137.3 (d, $^{1}J_{C\text{-}F}$ = 246.0 Hz; C_{BCF}), δ 130.5 (d, $^{2}J_{C\text{-}P}$ = 46.4 Hz; *C*=C-P), δ 130.3 (s; *m*-C_{Ar} (Mes)), δ 129.2 (s; *m*-C_{Ar} (Mes)), δ 128.5 (s; *i*-C_{Ar}(Mes)), δ 113.2 (br. s; *i*-C_{BCF}), δ 73.1 (d, $^{1}J_{C\text{-}P}$ = 86.0 Hz; C=*C*-P), δ 65.0 (s; $CO_2CH_2CH_3$), δ 63.2 (s; $CO_2CH_2CH_3$), δ 62.0 (s; $CO_2CH_2CH_3$), δ 61.3 (s; $CO_2CH_2CH_3$), δ 45.3 (d, $^{1}J_{C\text{-}P}$ = 33.1 Hz; *C*(CH_3)$_3$), δ 43.1 (d, $^{1}J_{C\text{-}P}$ = 31.9 Hz; *C*(CH_3)$_3$), δ 27.2 (s; C(*C*H_3)$_3$),δ 26.5 (s; C(*C*H_3)$_3$), δ 20.8 (s; *p*-*C*H_3 (Mes)), δ 20.2 (s; *o*-*C*H_3 (Mes)), δ 19.2 (s; *o*-*C*H_3 (Mes)), δ 13.9 (s; $CO_2CH_2CH_3$), δ 13.8 (s; $CO_2CH_2CH_3$), δ 13.3 (s; $CO_2CH_2CH_3$), δ 13.2 (s; $CO_2CH_2CH_3$). ^{31}P{^{1}H} (162.0 MHz, tol-d_8, 298 K): δ 85.5 (s). ^{31}P (162.0 MHz, tol-d_8, 298 K): δ 85.5 (m). ^{19}F{^{1}H} (376.5 MHz, tol-d_8, 298 K): δ -133.6 (d, $^{3}J_{F\text{-}F}$ = 28.8 Hz), -160.9 (t, $^{3}J_{F\text{-}F}$ = 21.6 Hz), -166.2 (t, $^{3}J_{F\text{-}F}$ = 22.8 Hz). ^{11}B{^{1}H} (160.4 MHz, tol-d_8, 298 K): δ -1.9 (br. s). UV-Vis Spectroscopy*:* (5 x 10^{-5} M in toluene): 312 nm, 0.5948 absorption. IR: ν_{max} (cm^{-1}) 2964 (w), 1735 (m; C=O), 1643 (m; C=O), 1606 (m; C=O).

S2. Characterisation Data

S2.1. NMR Spectra

Images of spectra:

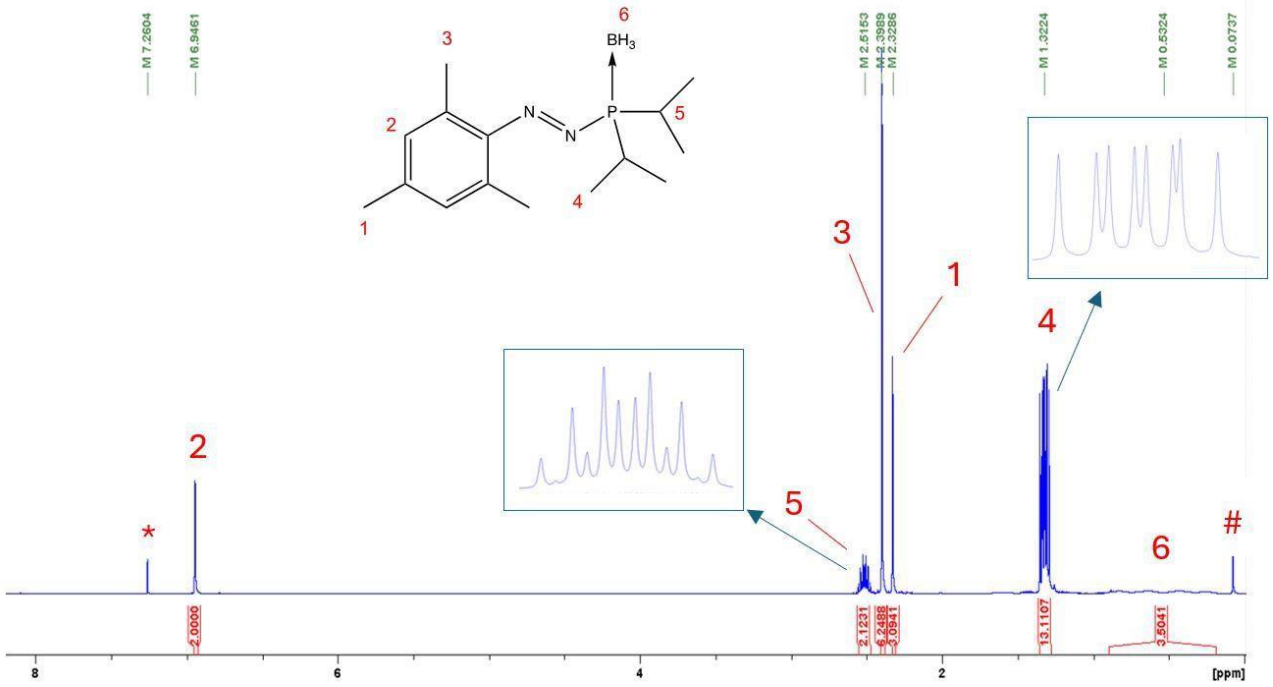

*Figure S1. ^{1}H NMR spectrum of **1.BH3** in $CDCl_3$. * = residual $CHCl_3$, 7.26 ppm, to which the spectrum is calibrated; # = residual silicone grease, 0.07 ppm. Figures inside the blue boxes are zoomed in to show the splittings of the multiplets.*

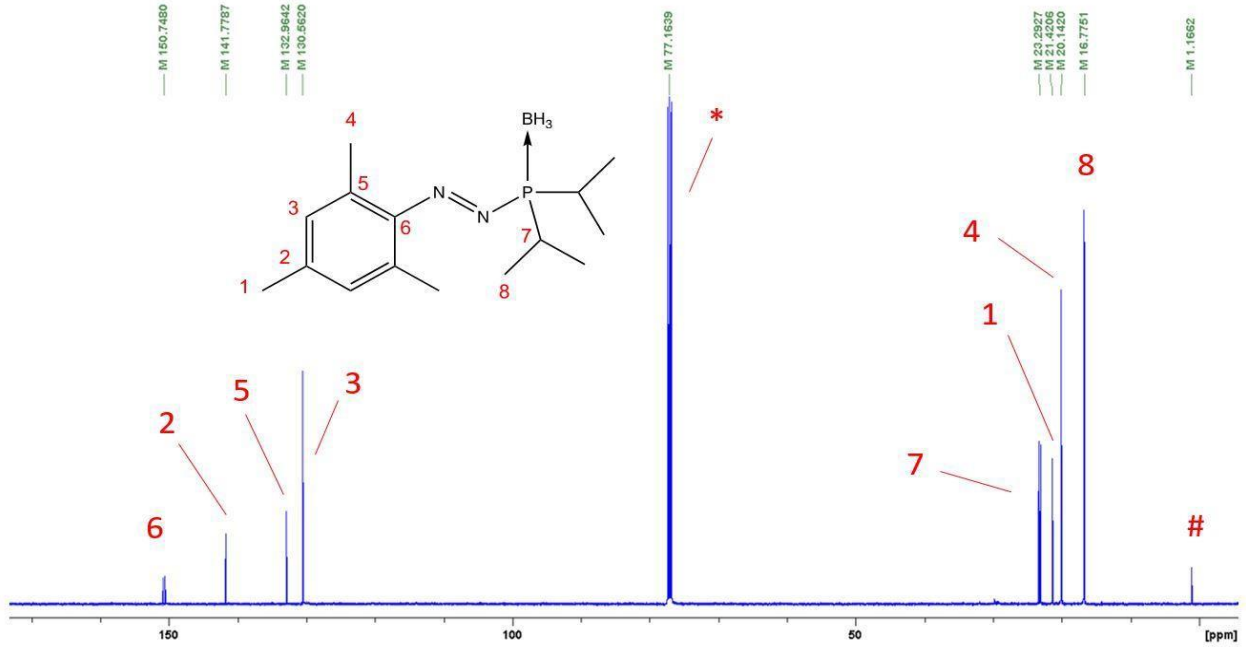

*Figure S2. $^{13}C\{^{1}H\}$ NMR spectrum of **1.BH3** in $CDCl_3$. * = $CDCl_3$ peak, 77.16 ppm, to which the spectrum is calibrated; # = residual silicone grease, 1.17 ppm.*

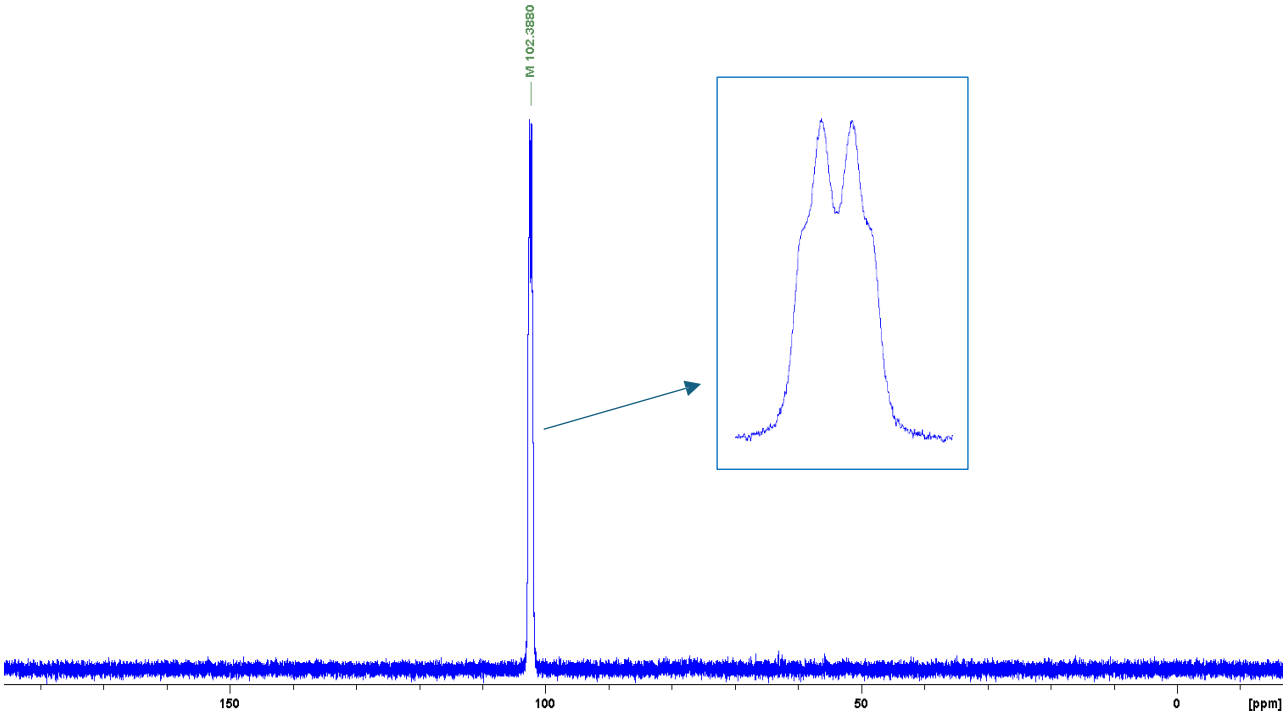

*Figure S3. $^{31}P\{^{1}H\}$ NMR spectrum of **1.BH3** in $CDCl_3$. Figure inside the blue box is zoomed in to show the splittings of the peak.*

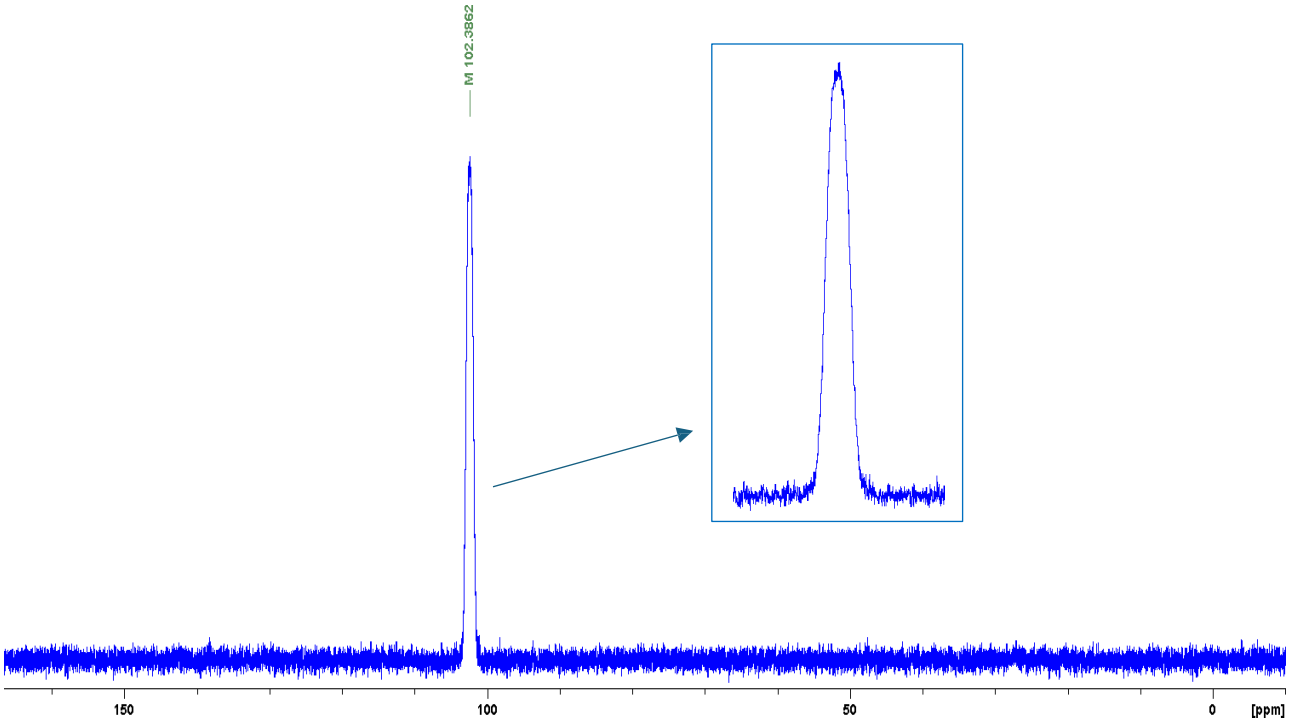

*Figure S4. ^{31}P NMR spectrum of **1.BH3** in $CDCl_3$. Figure inside the blue box is zoomed in to show the splittings of the peak.*

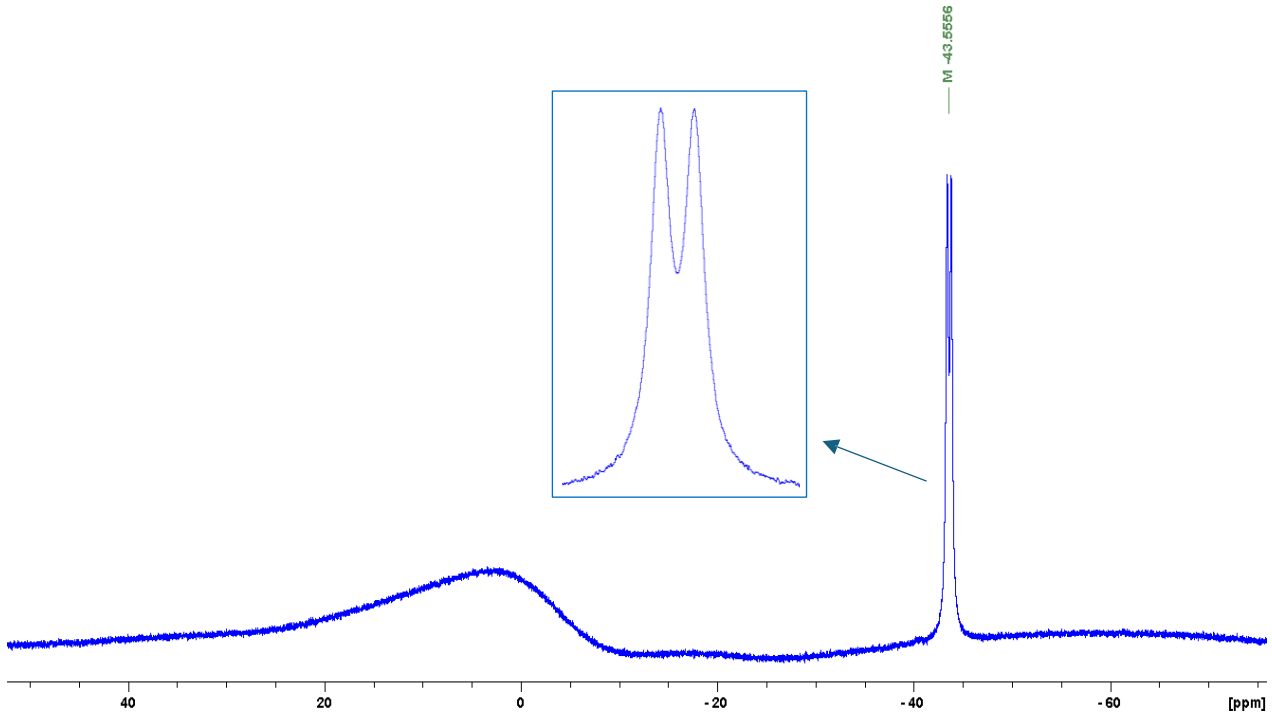

*Figure S5. $^{11}B\{^{1}H\}$ NMR spectrum of **1.BH3** in $CDCl_3$. Figure inside the blue box is zoomed in to show the splittings of the peak.*

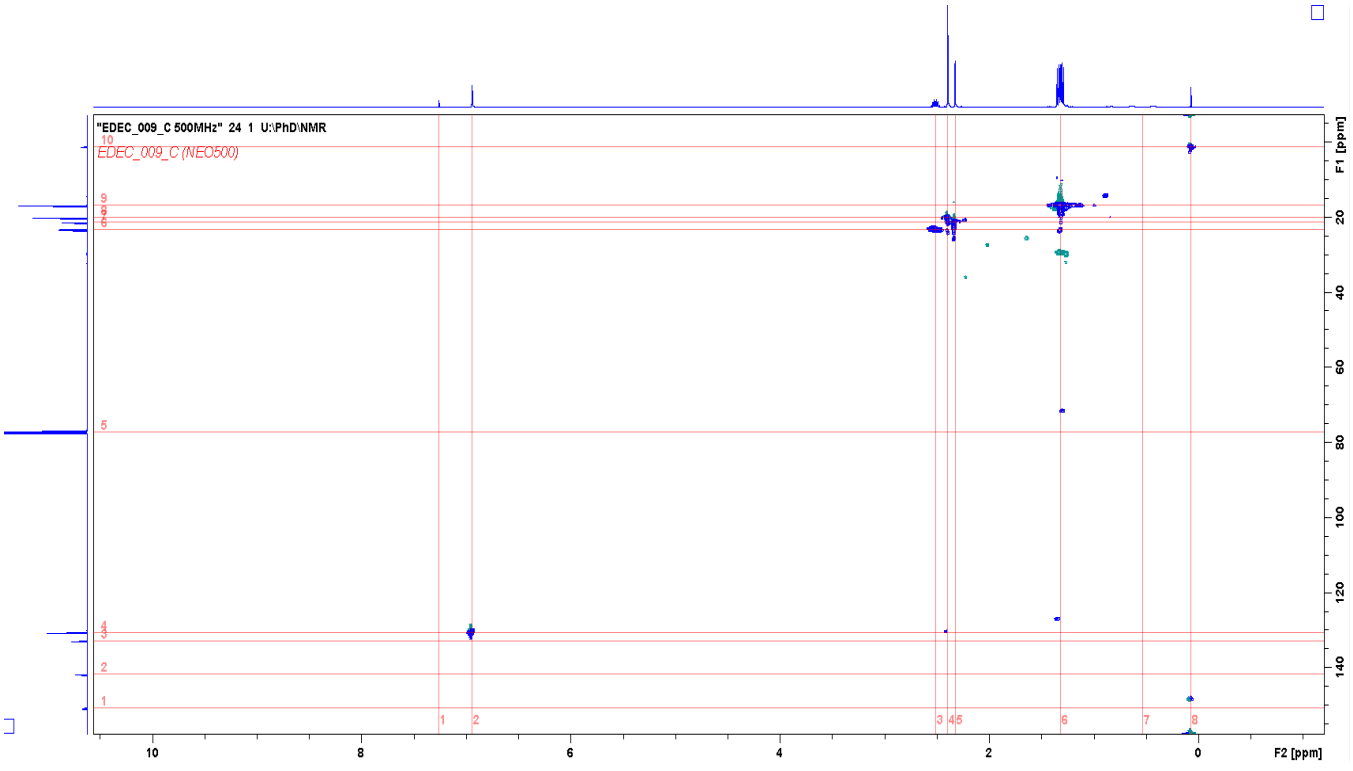

*Figure S6. 2D ^{1}H-^{13}C HSQC NMR spectrum of **1.BH3** in $CDCl_3$*

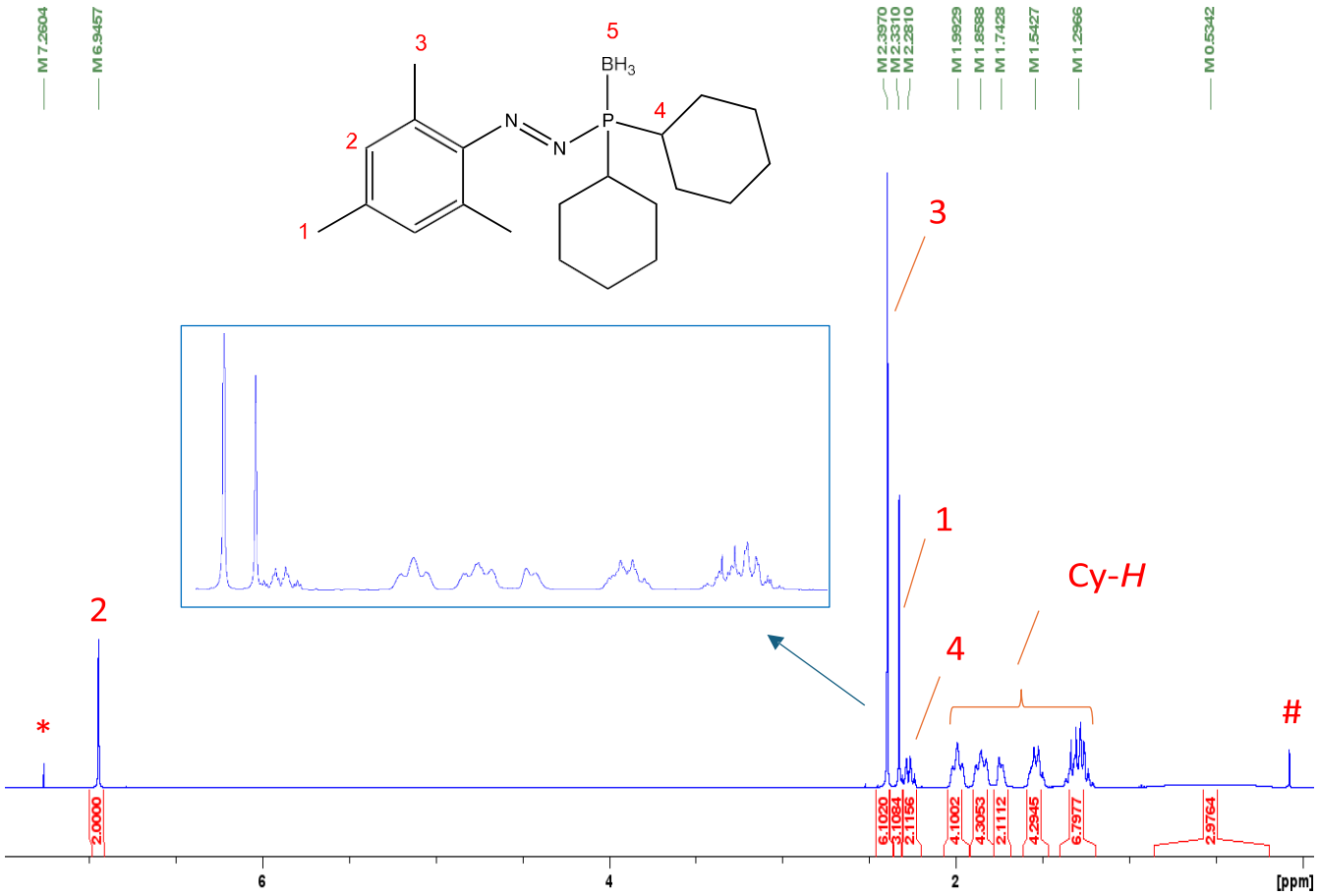

*Figure S7. ^{1}H NMR spectrum of **2.BH3** in $CDCl_3$. * = residual $CHCl_3$, 7.26 ppm, to which the spectrum is calibrated; # = residual silicone grease, 0.07 ppm. Figures inside the blue boxes are zoomed in to show the splittings of the multiplets.*

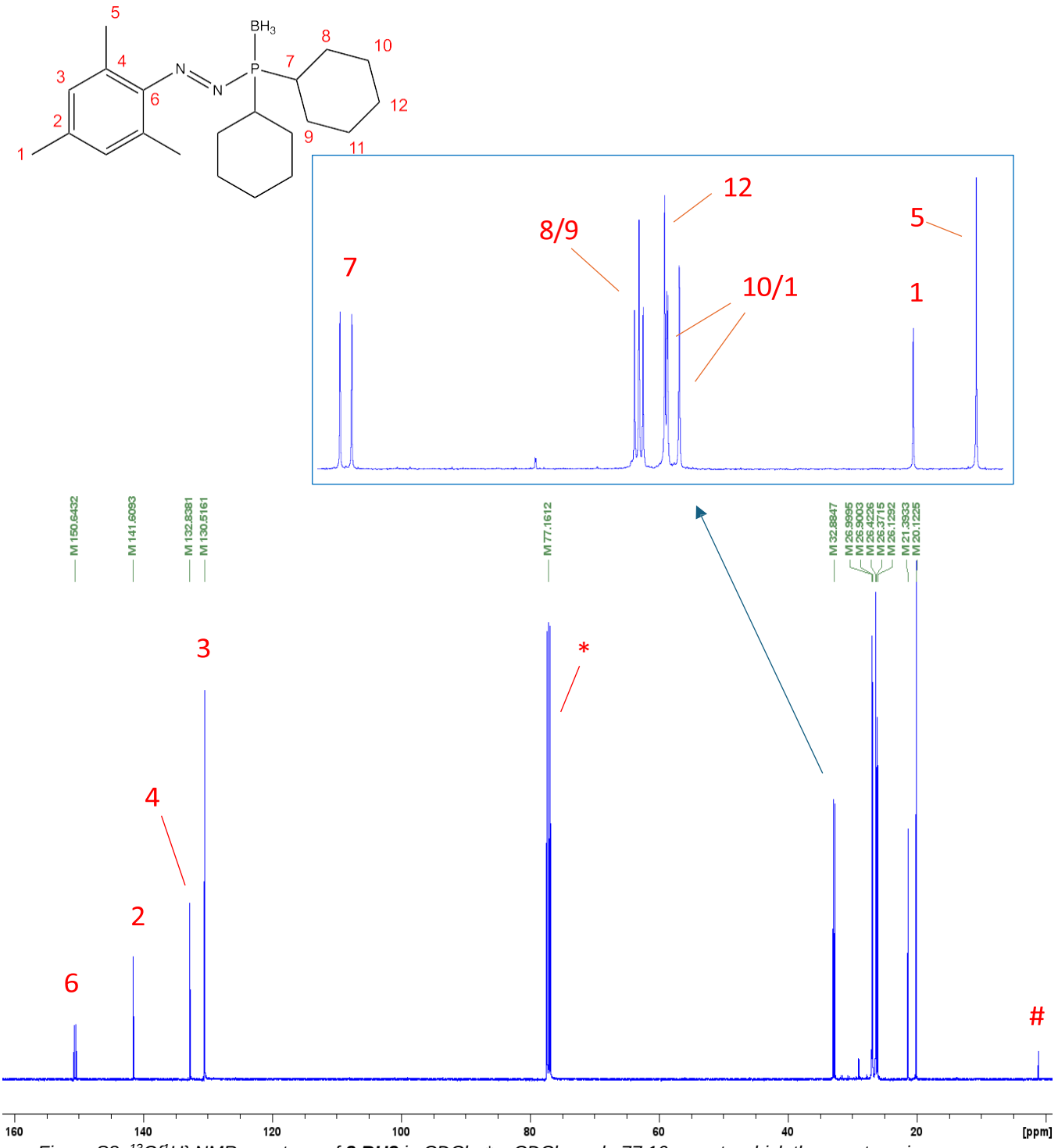

*Figure S8. $^{13}C\{^{1}H\}$ NMR spectrum of **2.BH3** in $CDCl_3$. * = $CDCl_3$ peak, 77.16 ppm, to which the spectrum is calibrated; # = residual silicone grease, 1.17 ppm. Figure inside the blue boxes are zoomed in to show the splittings of the peaks.*

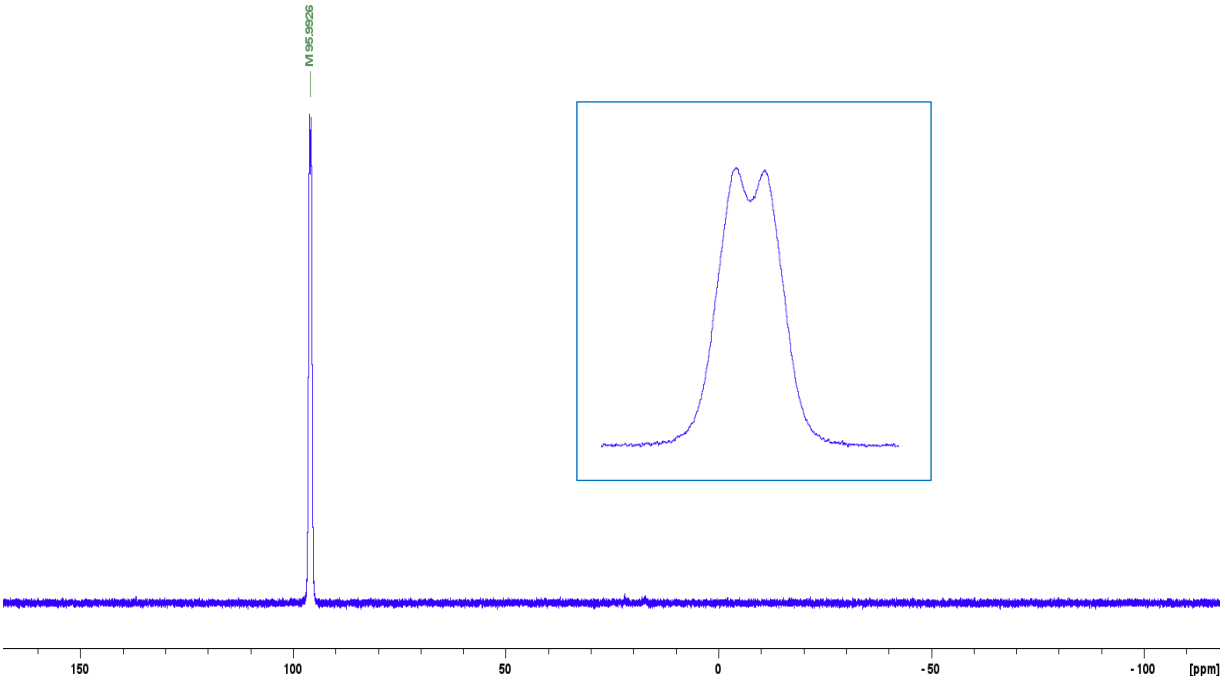

*Figure S9. $^{31}P\{^{1}H\}$ NMR spectrum of **2.BH3** in $CDCl_3$. Figure inside the blue box is zoomed in to show the splittings of the peak.*

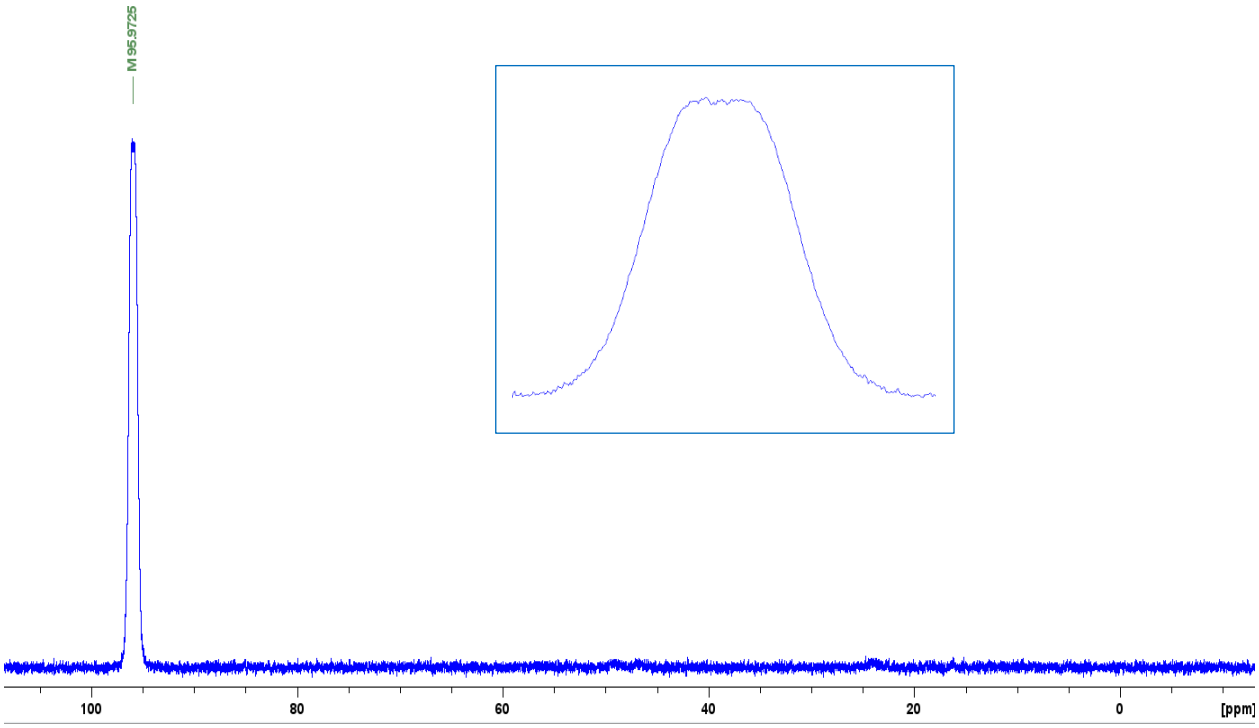

*Figure S10. ^{31}P NMR spectrum of **2.BH3** in $CDCl_3$. Figure inside the blue box is zoomed in to show the splittings of the peak.*

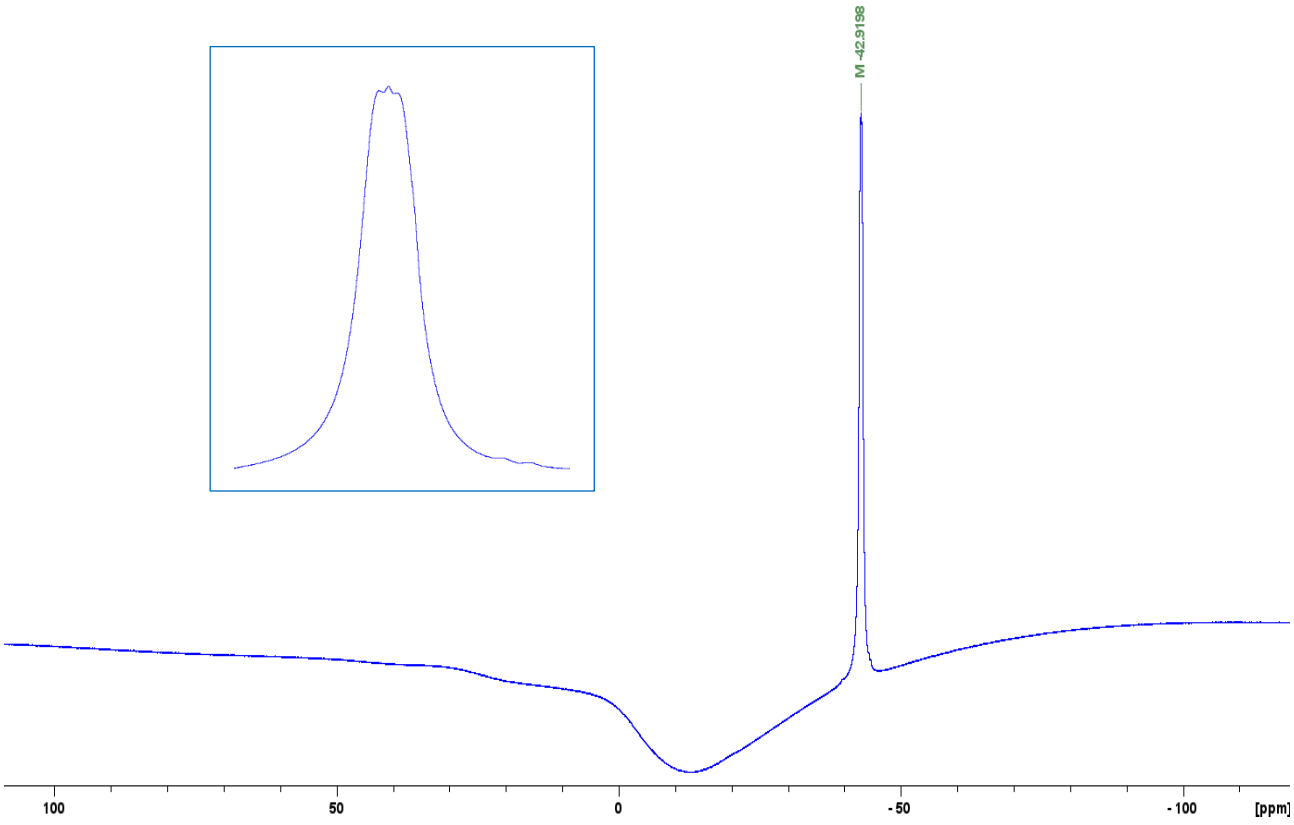

*Figure S11. $^{11}B\{^{1}H\}$ NMR spectrum of **2.BH3** in $CDCl_3$. Figure inside the blue box is zoomed in to show the splittings of the peak.*

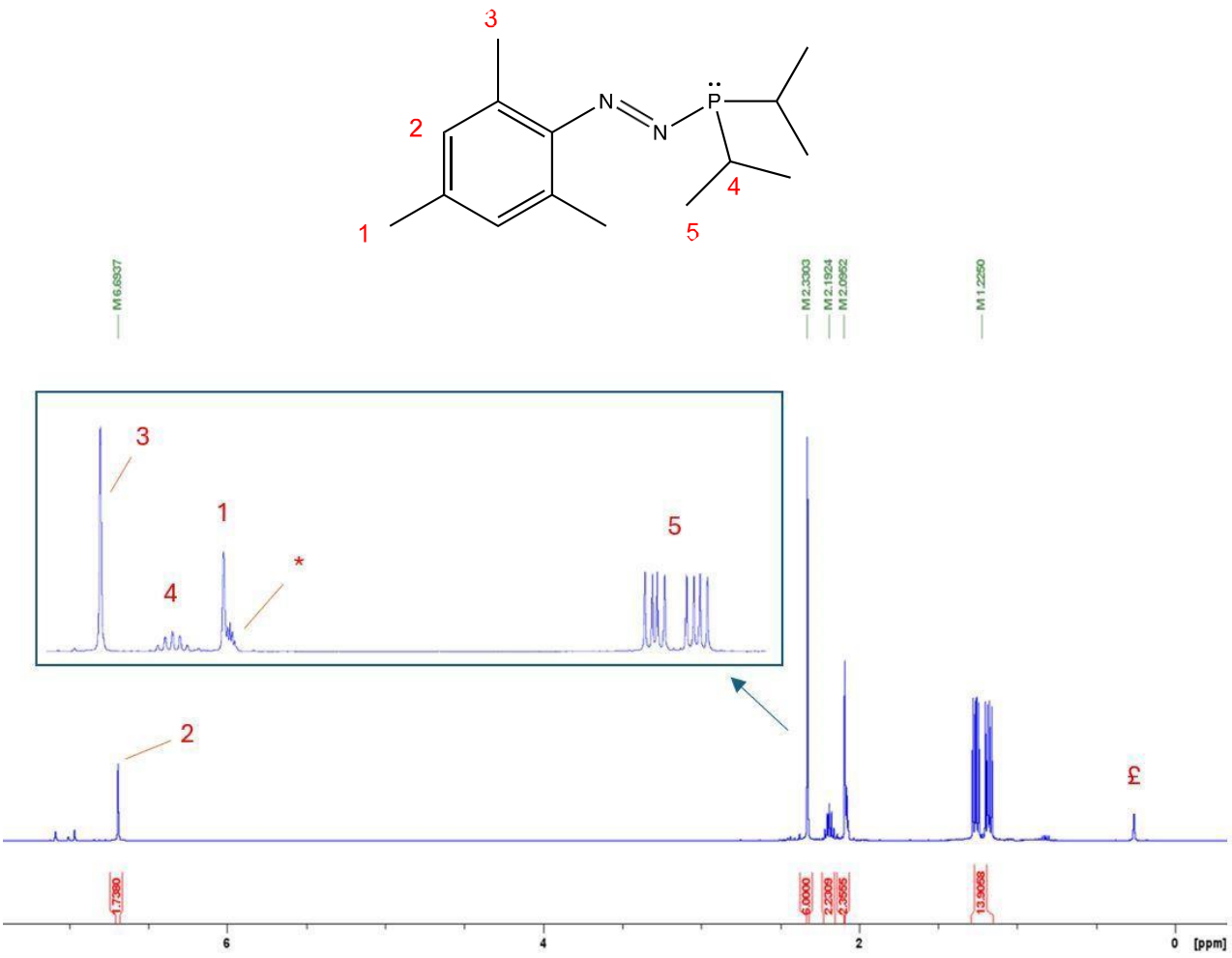

*Figure S12. ^{1}H NMR spectrum of **1** in d_8-toluene. The spectrum is calibrated to the residual Ph-CHD_2 peak at 2.08 ppm, marked with *. £ = residual silicone grease. Figures inside the blue boxes are zoomed in to show the splittings of the multiplets.*

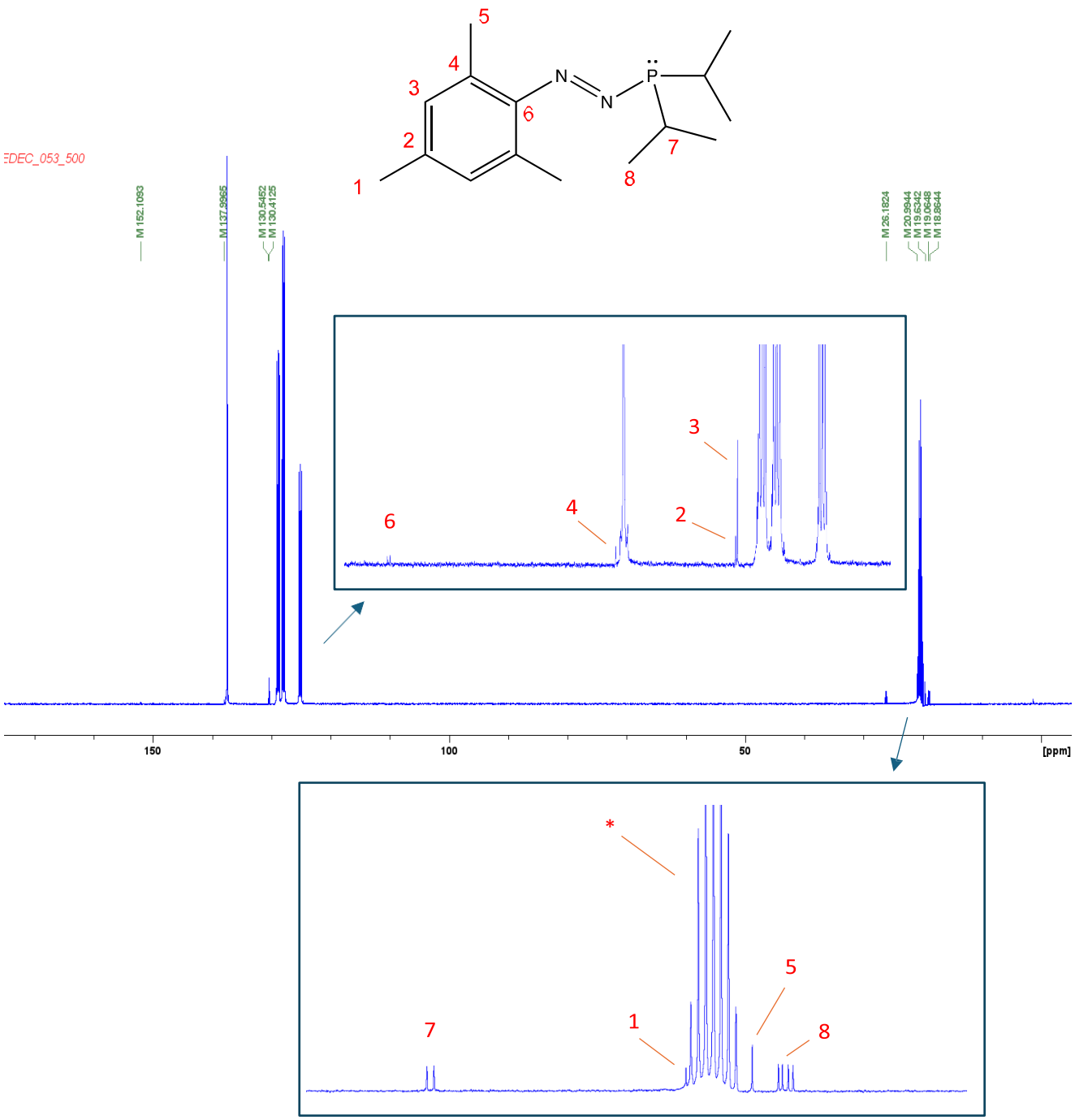

*Figure S13. $^{13}C\{^{1}H\}$ NMR spectrum of **1** in d_8-toluene. * = CD_3 peak of d_8-toluene peak, 20.43 ppm, to which the spectrum is calibrated. Figure inside the blue boxes are zoomed in to show the splittings of the peaks. Assignments were confirmed by HSQC analysis.*

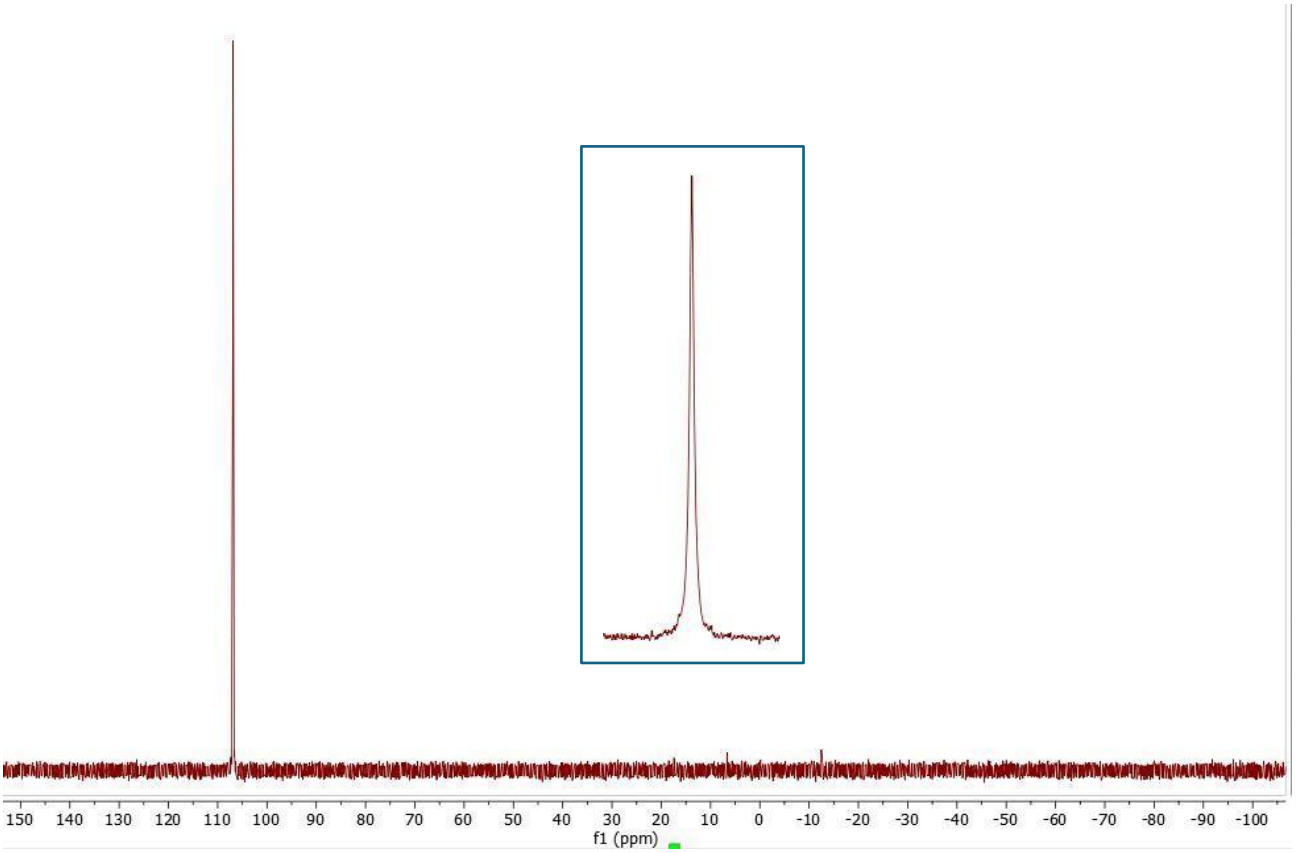

*Figure S14. $^{31}P\{^{1}H\}$ NMR spectrum of **1** in d_8-toluene. Figure inside the blue box is zoomed in to show the splittings of the peak.*

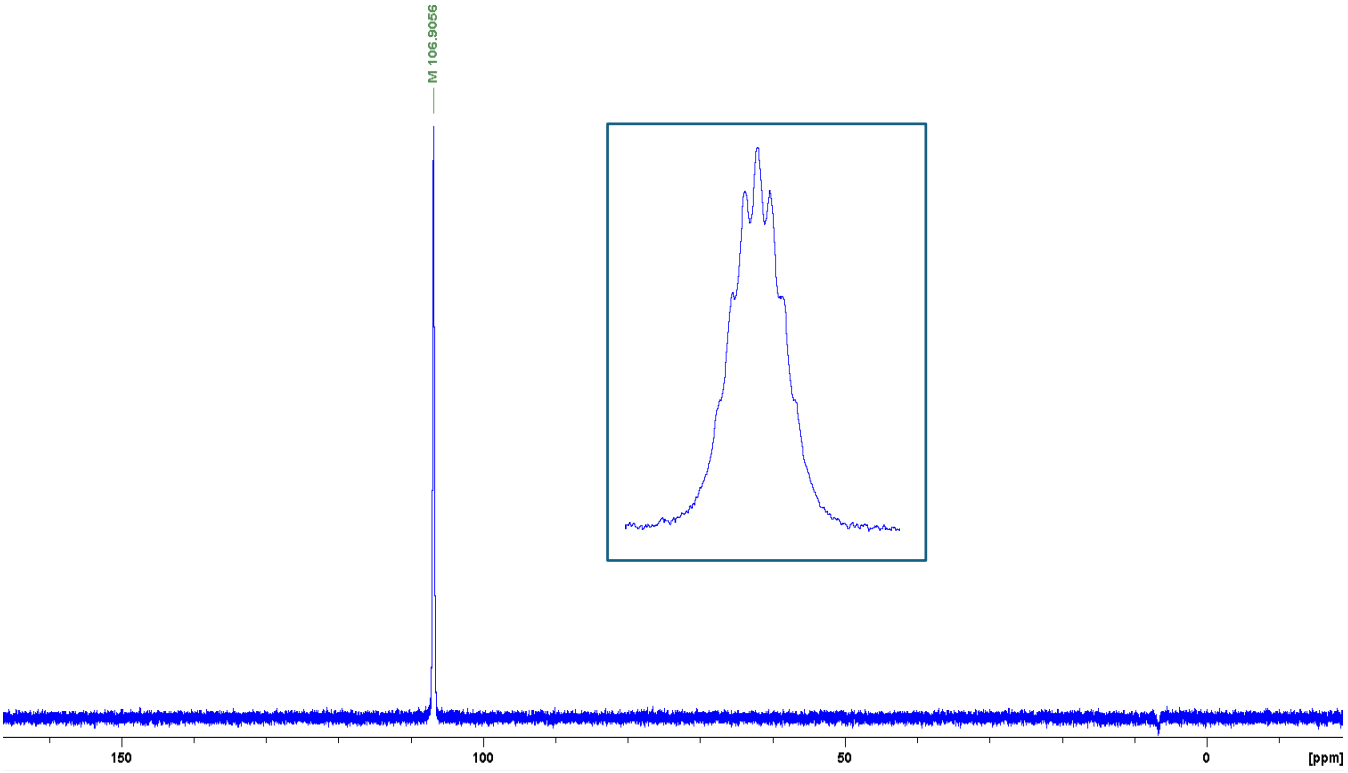

*Figure S15. ^{31}P NMR spectrum of **1** in d_8-toluene. Figure inside the blue box is zoomed in to show the splittings of the peak.*

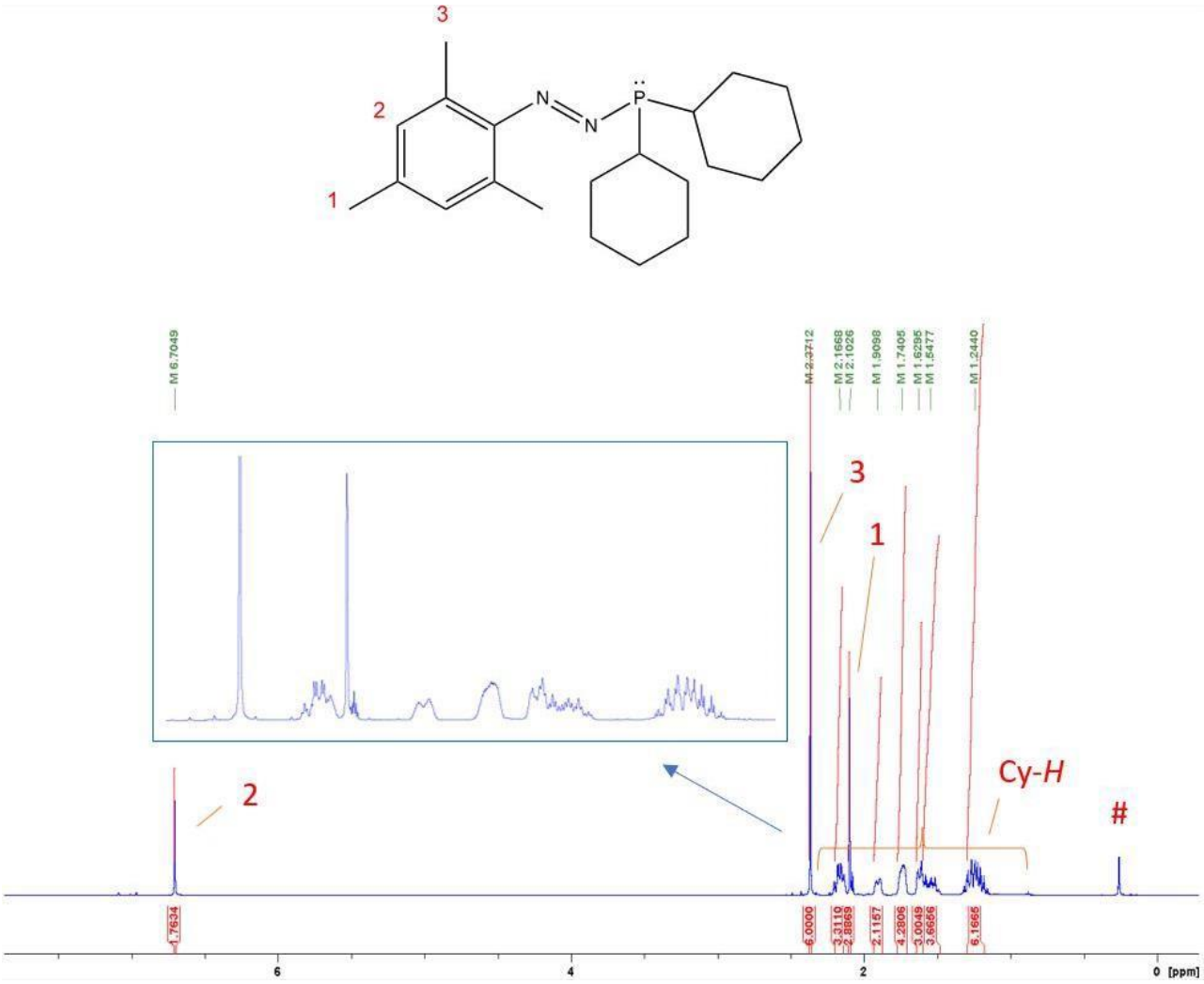

*Figure S16. ^{1}H NMR spectrum of **2** in d_8-toluene. The spectrum is calibrated to the residual Ph-CHD_2 peak at 2.08 ppm; # = residual silicone grease, 0.26 ppm. Figure inside the blue box is zoomed in to show the splittings of the multiplets.*

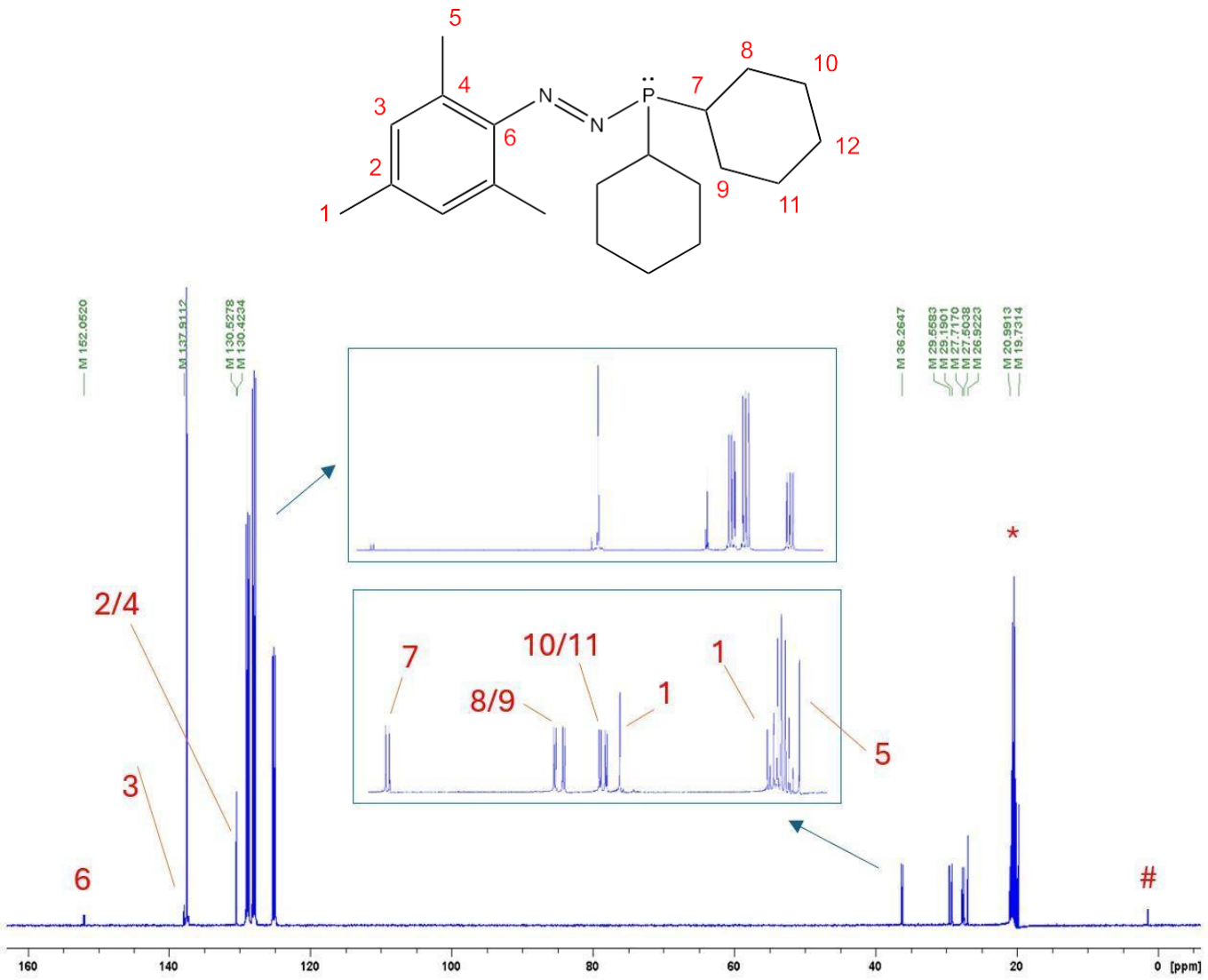

*Figure S17. $^{13}C\{^{1}H\}$ NMR spectrum of **2** in d_8-toluene. * = CD_3 peak of d_8-toluene peak, 20.43 ppm, to which the spectrum is calibrated; # = residual silicone grease, 2.06 ppm. Figure inside the blue boxes are zoomed in to show the splittings of the peaks.*

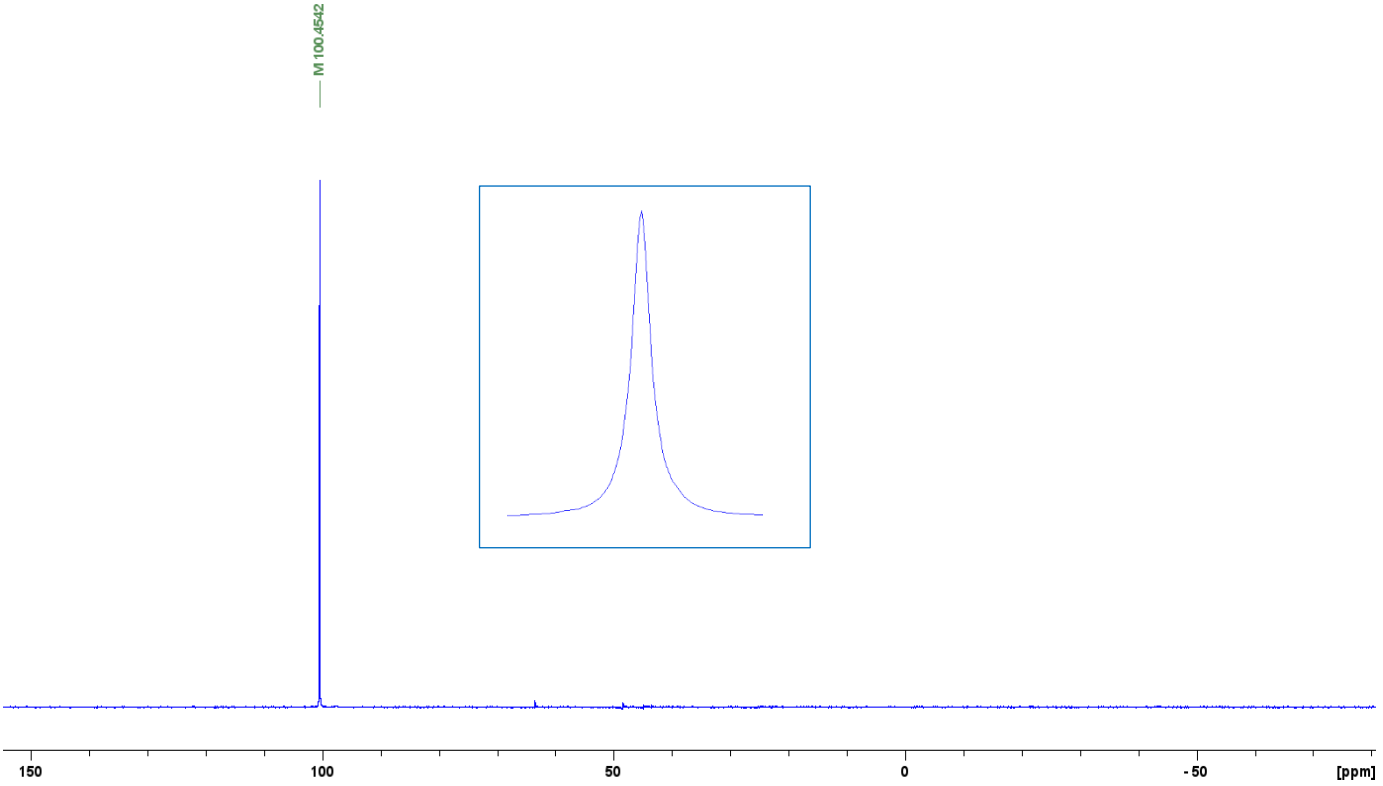

*Figure S18. $^{31}P\{^{1}H\}$ NMR spectrum of **2** in d_8-toluene. Figure inside the blue box is zoomed in to show the splittings of the peak.*

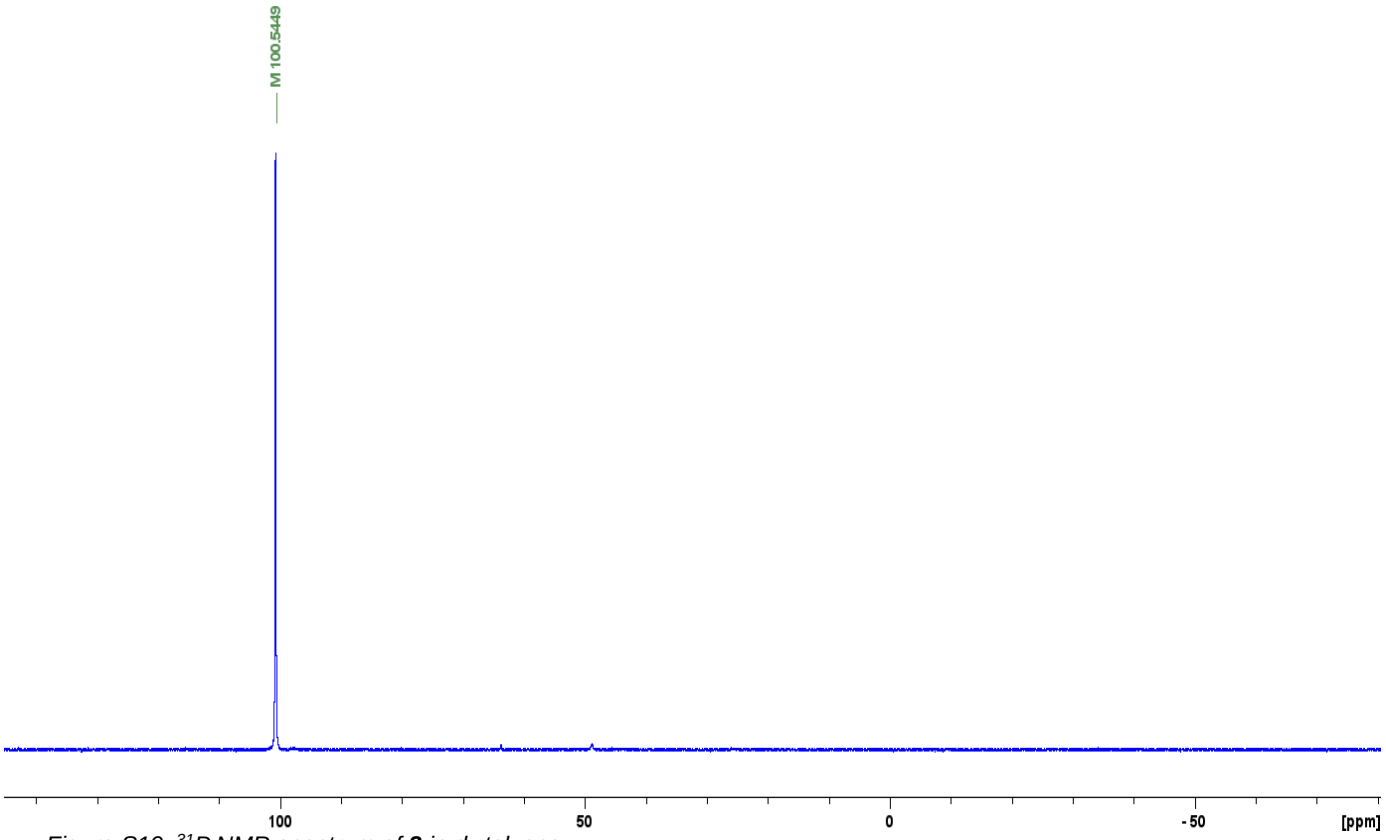

*Figure S19. ^{31}P NMR spectrum of **2** in d_8-toluene.*

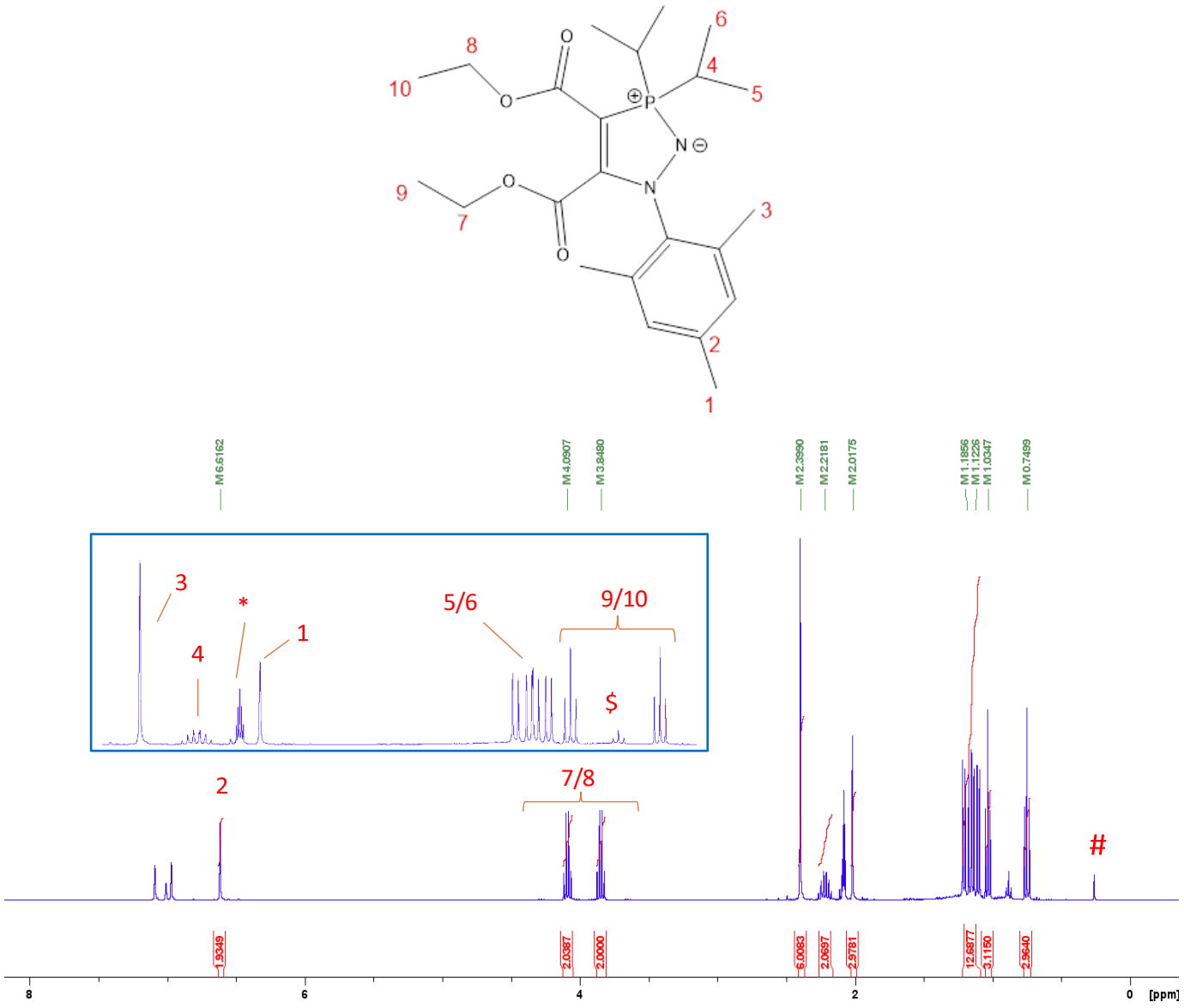

*Figure S20. ^{1}H NMR spectrum of **4** in d_8-toluene. # = residual silicone grease. $ = residual hexane from the NMR solvent. The spectrum is calibrated to the residual Ph-CHD$_2$ peak at 2.08 ppm, marked with *.*

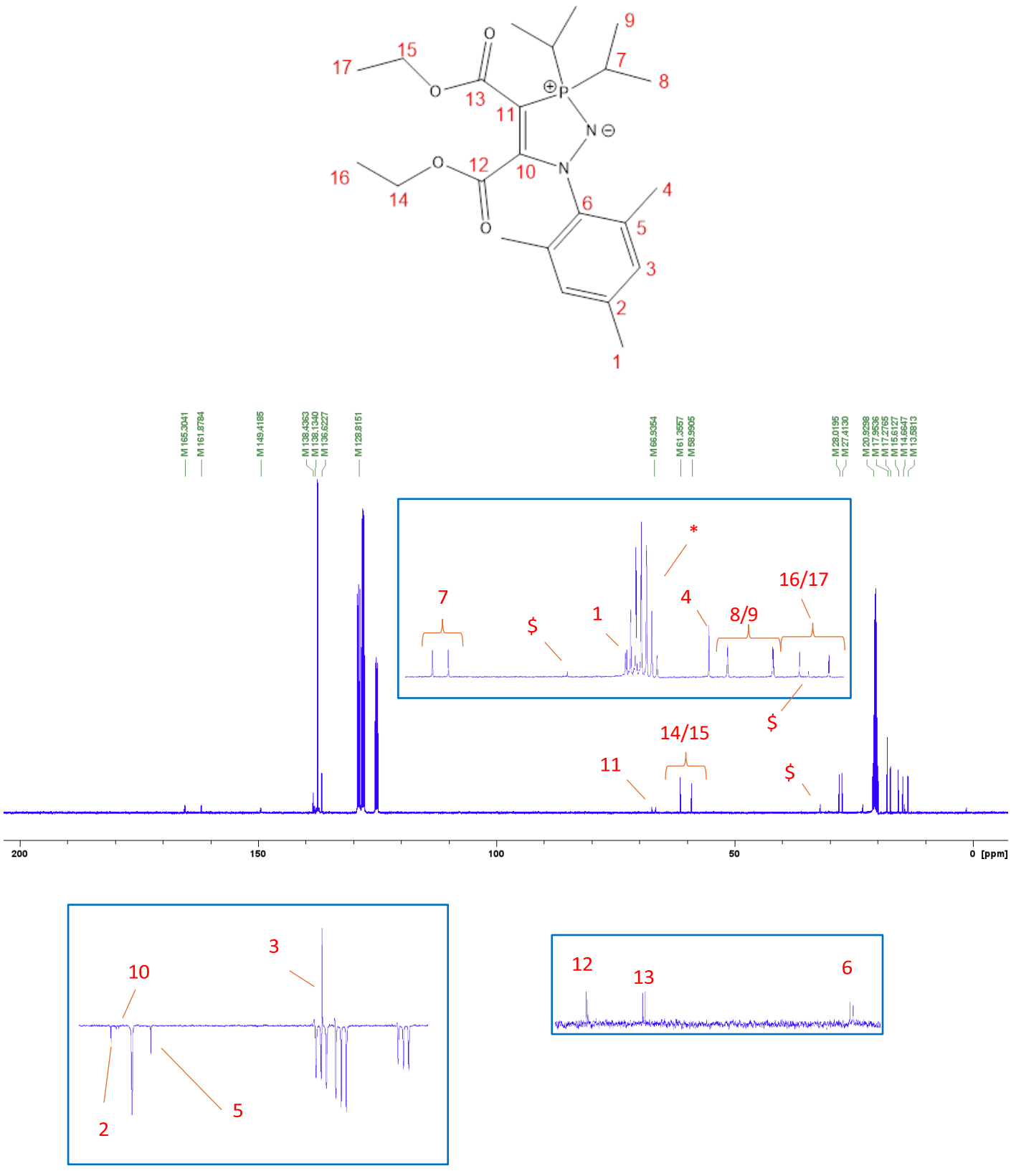

*Figure S21. $^{13}C\{^{1}H\}$ NMR spectrum of **4** in d_8-toluene. * = CD_3 peak of d_8-toluene peak, 20.43 ppm, to which the spectrum is calibrated. The bottom inset shows a JMOD spectrum for the same compound, in which the singlet at 128.8 ppm is much more visible. $ = residual hexane from the NMR solvent.*

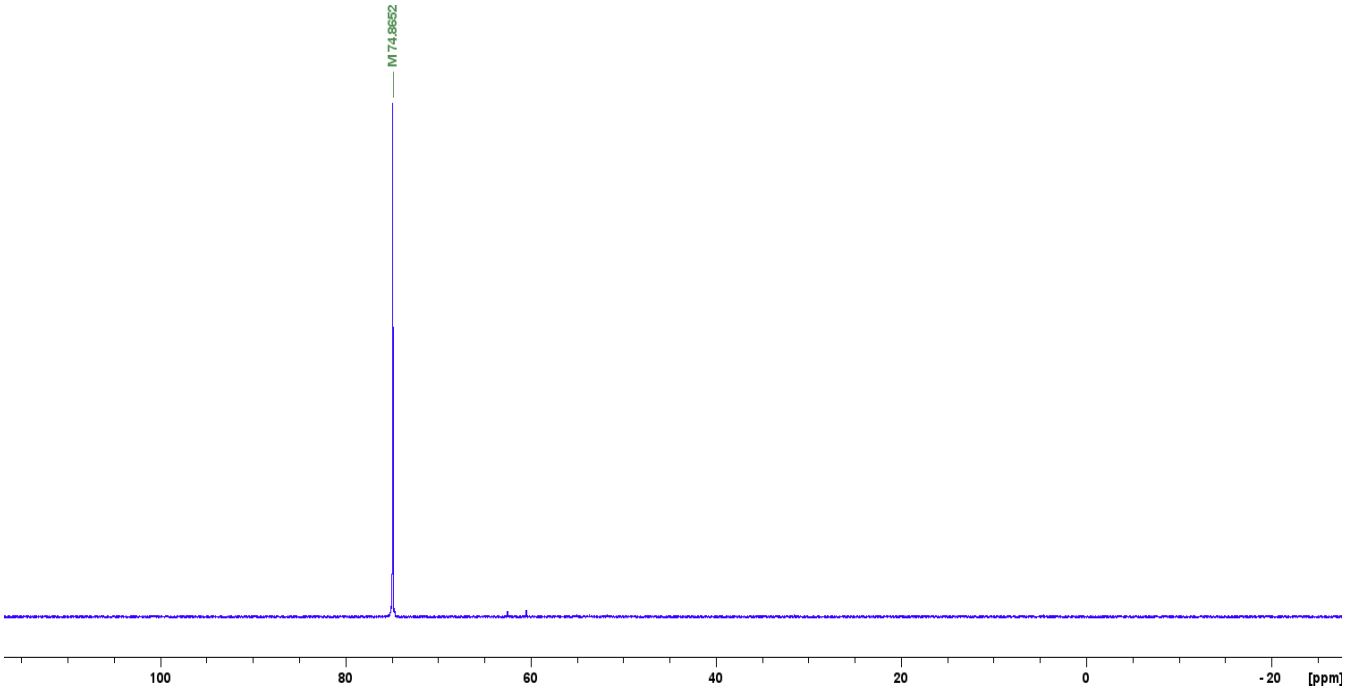

*Figure S22. $^{31}P\{^{1}H\}$ NMR spectrum of **4** in d_8-toluene.*

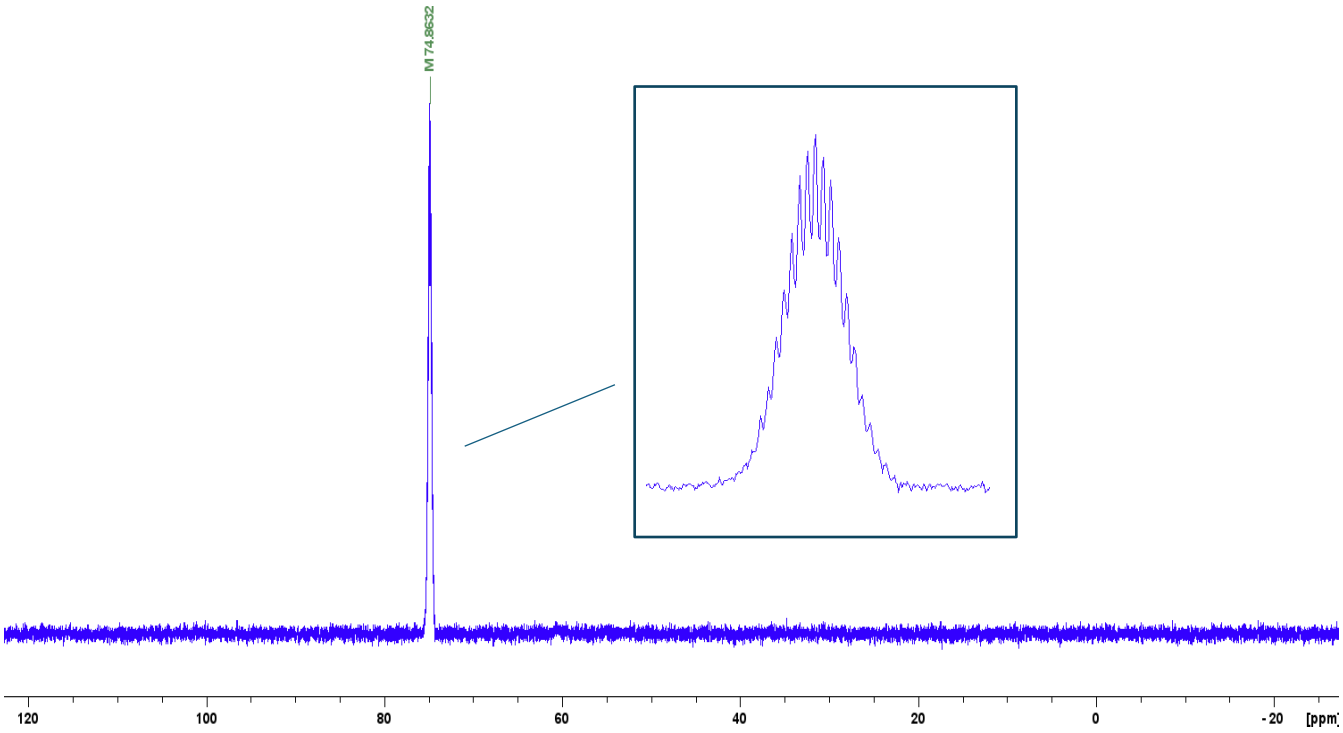

*Figure S23. ^{31}P NMR spectrum of **4** in d_8-toluene. Figure inside the blue box is zoomed in to show the splittings of the peak.*

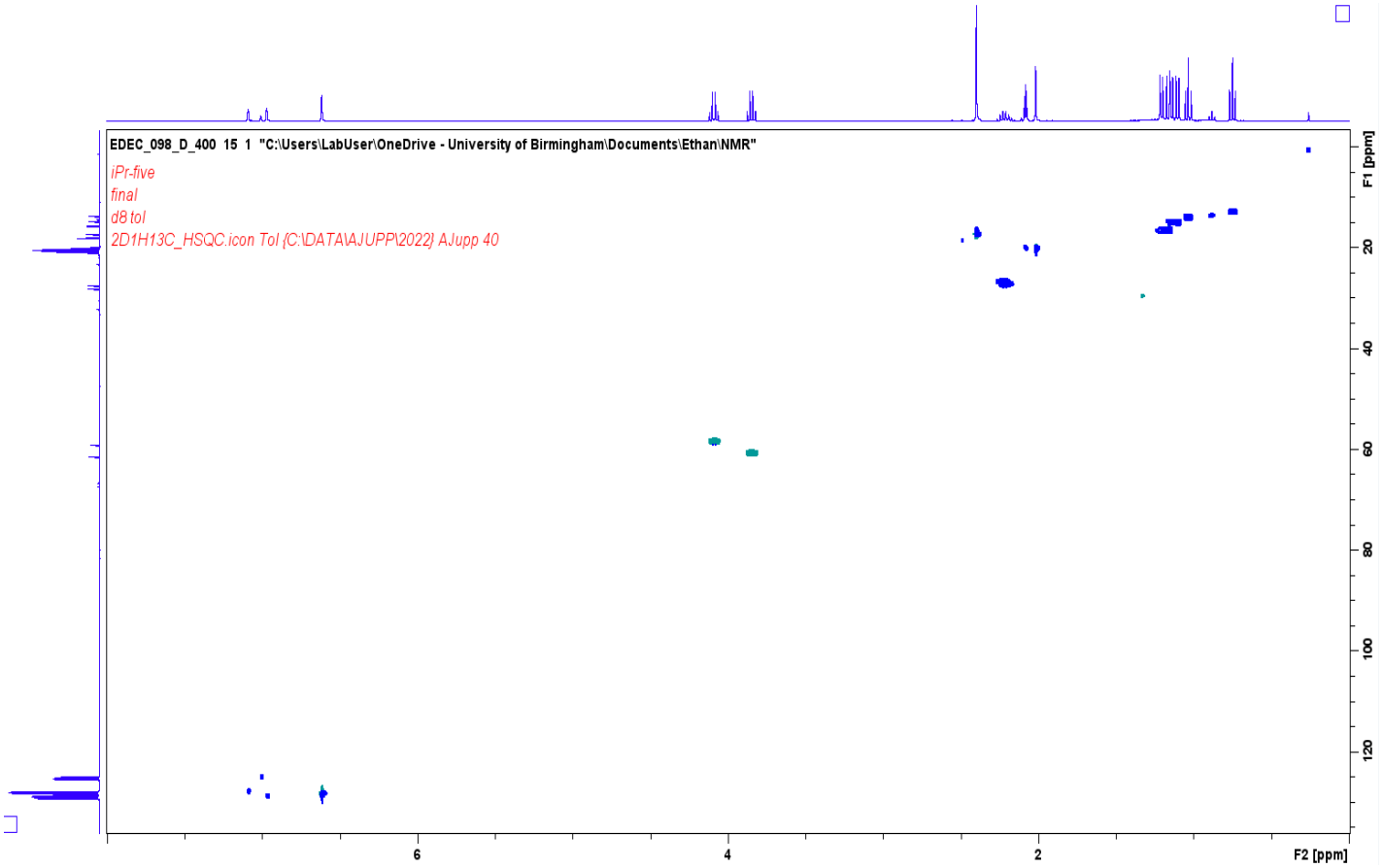

*Figure S24. 2D ^{1}H-^{13}C HSQC NMR spectrum of **4** in d_8-toluene. HSQC was vital for carbon assignments.*

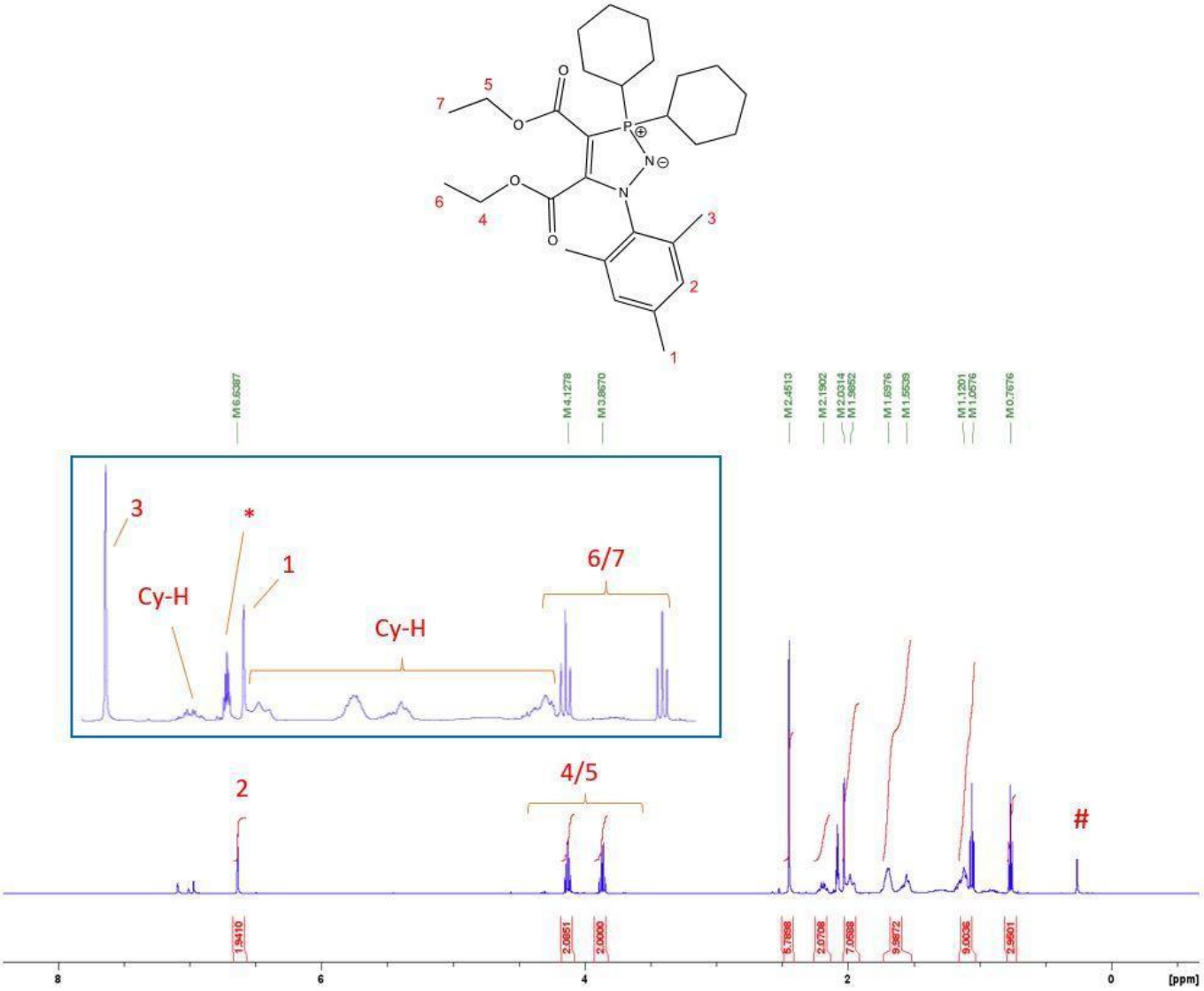

*Figure S25. ^{1}H NMR spectrum of **5** in d_8-toluene. # = residual silicone grease. The spectrum is calibrated to the residual Ph-CHD_2 peak at 2.08 ppm, marked with *.*

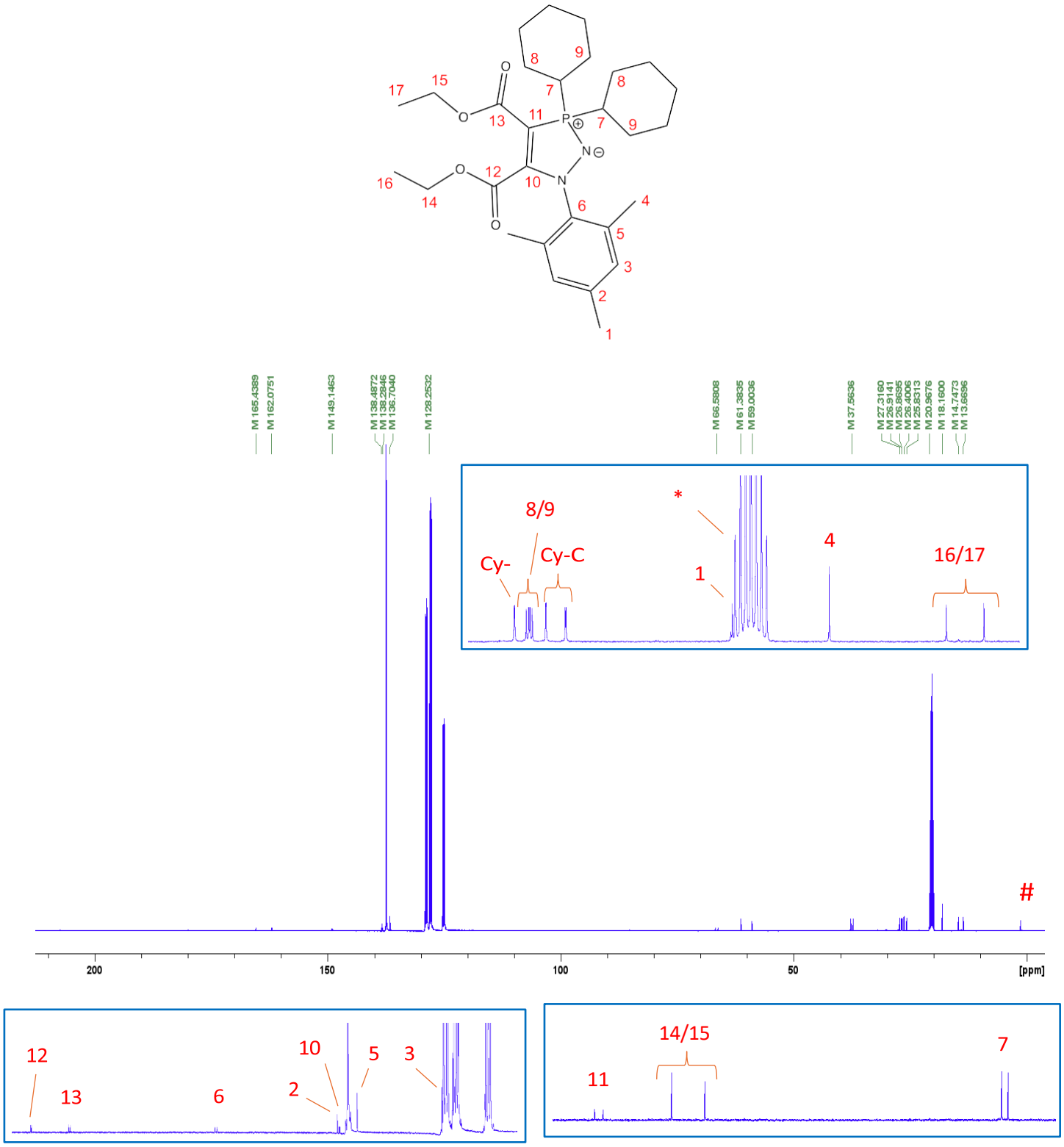

*Figure S26. $^{13}C\{^{1}H\}$ NMR spectrum of **5** in d_8-toluene. * = CD_3 peak of d_8-toluene peak, 20.43 ppm, to which the spectrum is calibrated. Figures inside the blue boxes show insets of the same spectrum for clarity.. # = residual silicone grease, 1.37 ppm.*

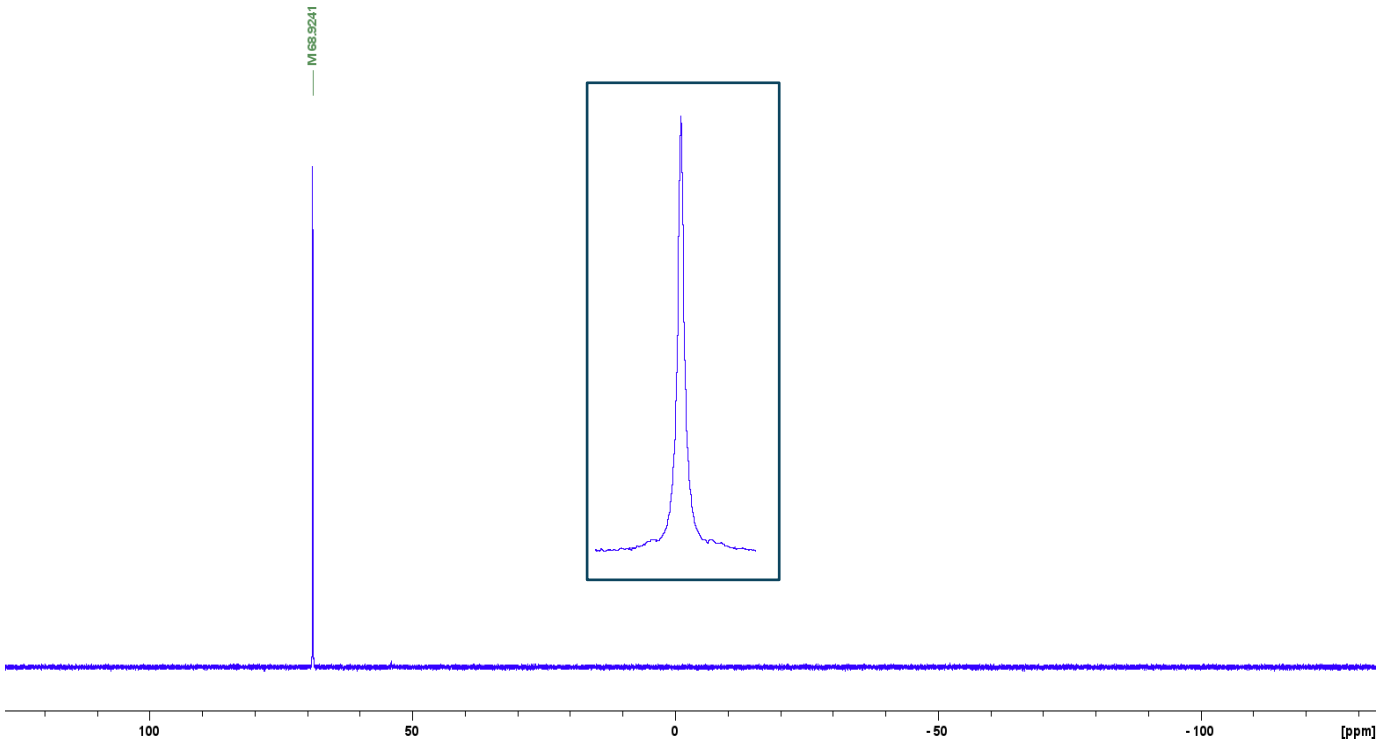

*Figure S27. $^{31}P\{^{1}H\}$ NMR spectrum of **5** in d_8-toluene. Figure in blue box is an inset of the same spectrum.*

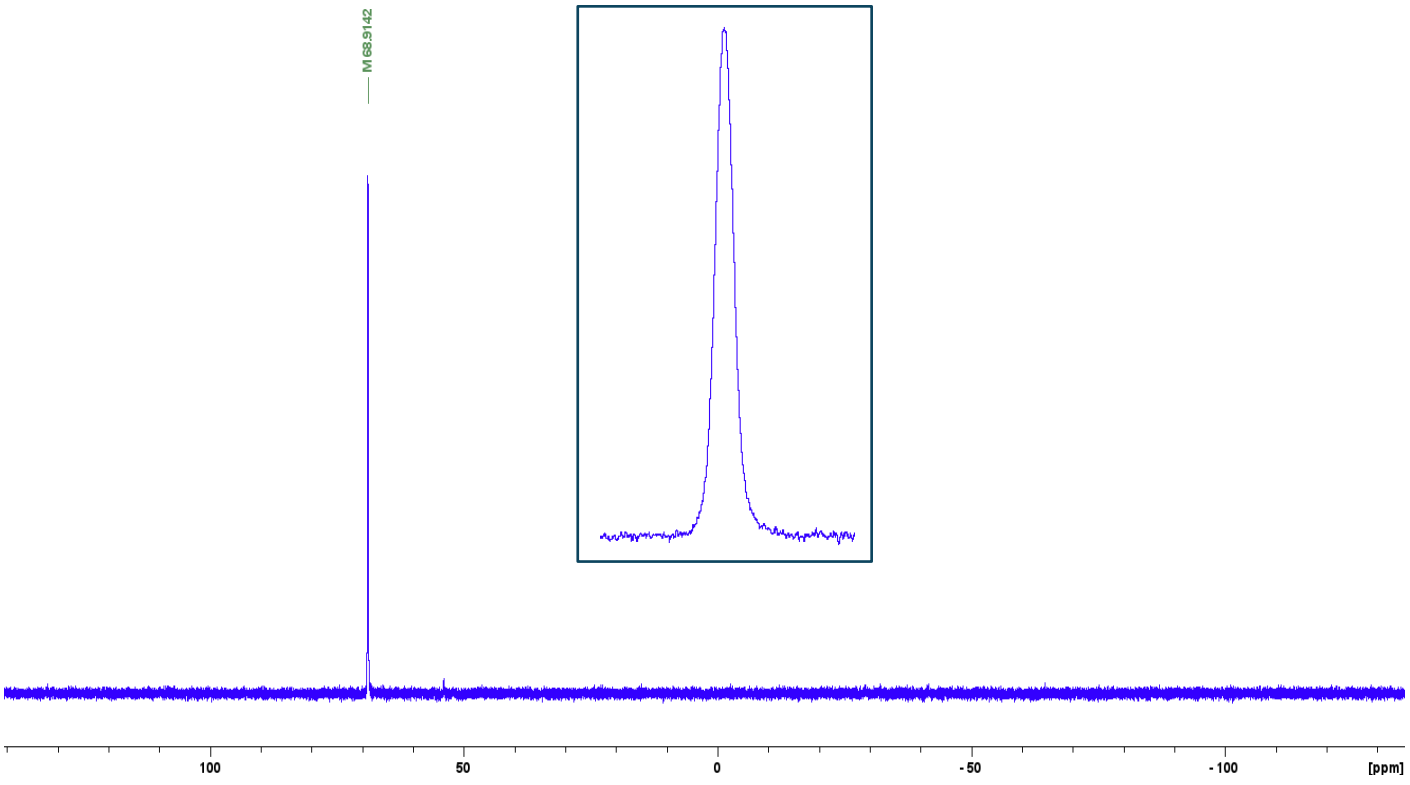

*Figure S28. ^{31}P NMR spectrum of **5** in d_8-toluene. Figure in blue box is an inset of the same spectrum.*

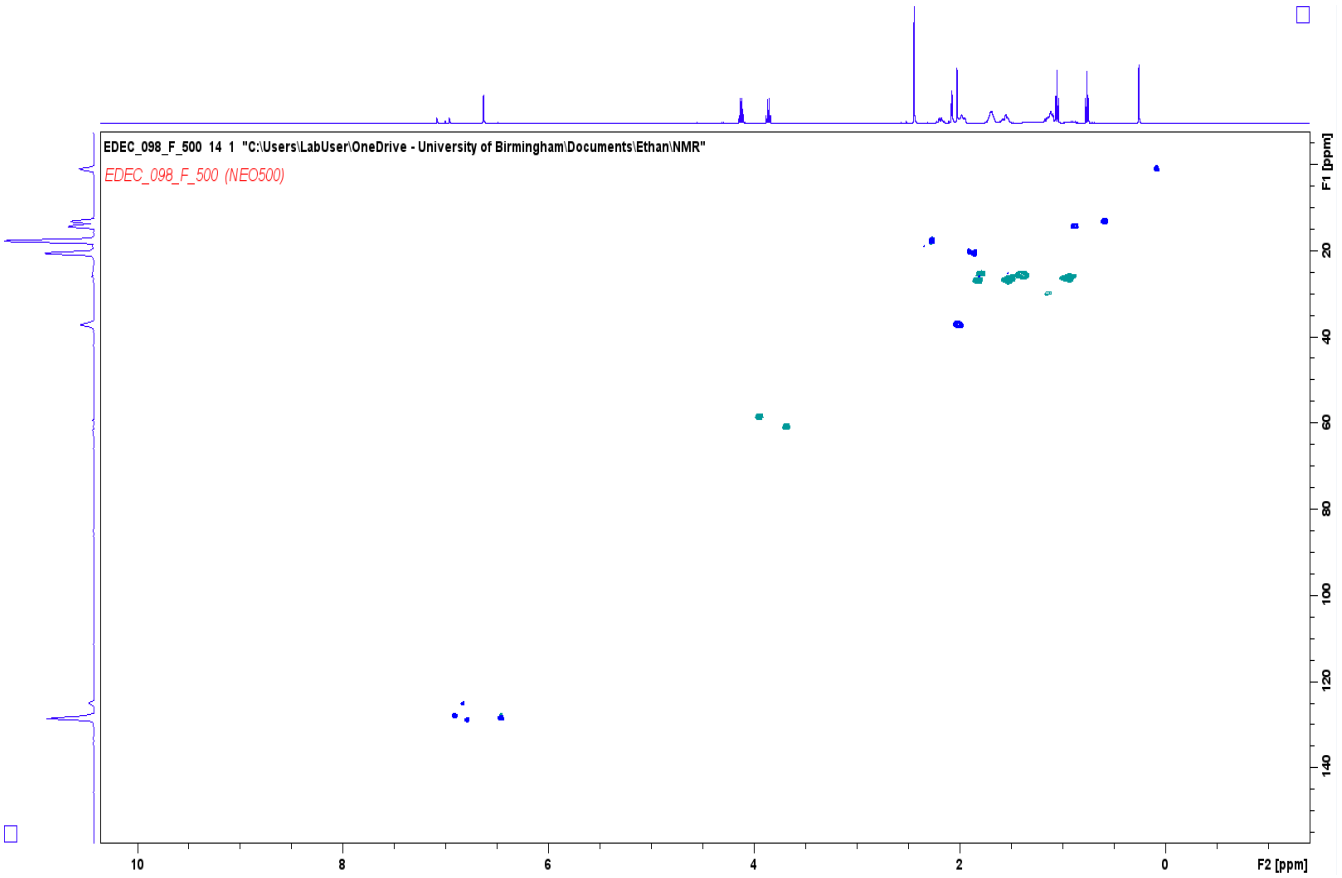

*Figure S29. 2D ^{1}H-^{13}C HSQC NMR spectrum of **5** in d_8-toluene. HSQC was vital for carbon assignments.*

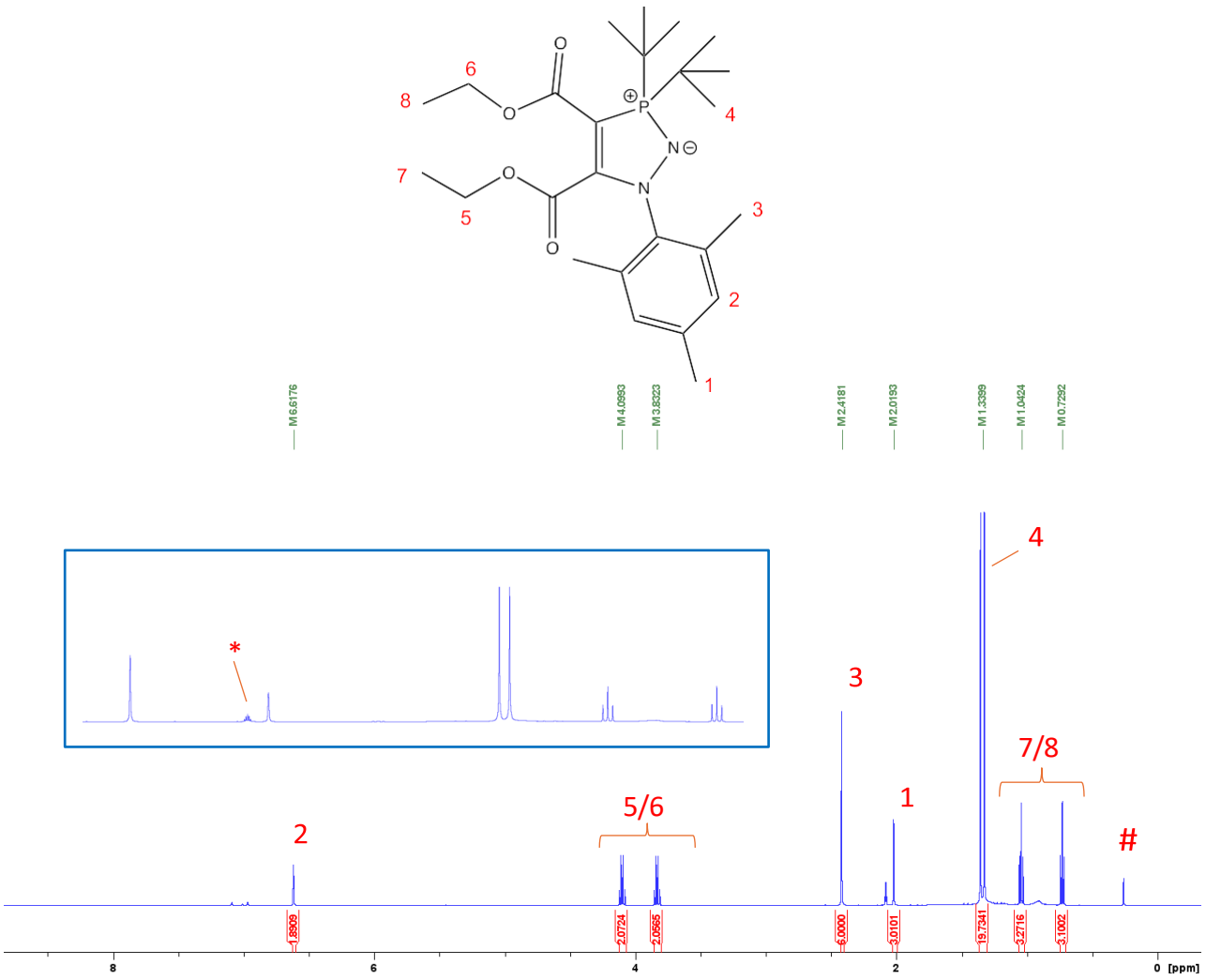

*Figure S30. ^{1}H NMR spectrum of **6** in d_8-toluene. # = residual silicone grease. The spectrum is calibrated to the residual Ph-CHD_2 peak at 2.08 ppm, marked with *.*

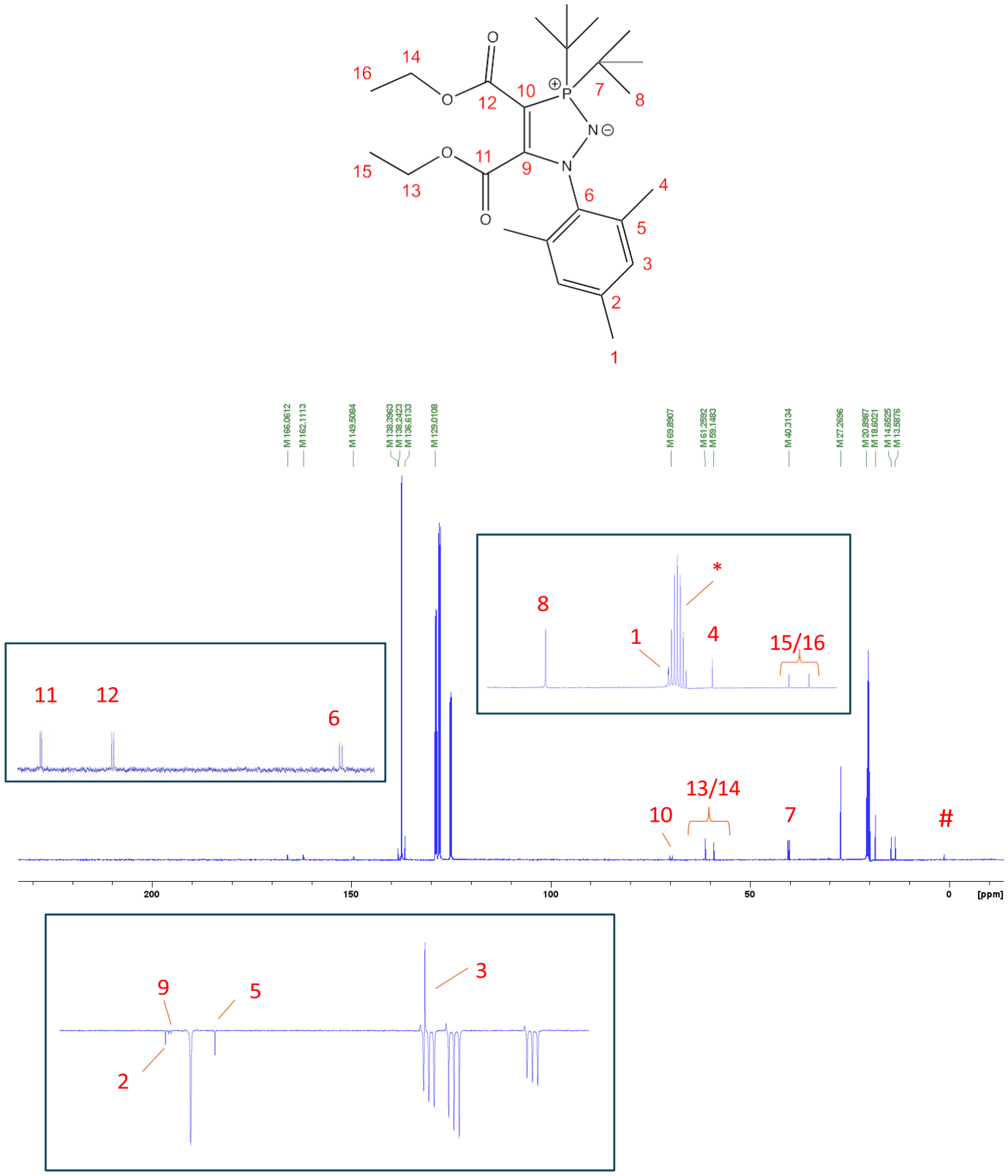

*Figure S31. $^{13}C\{^{1}H\}$ NMR spectrum of **6** in d_8-toluene. * = CD_3 peak of d_8-toluene peak, 20.43 ppm, to which the spectrum is calibrated. The bottom inset shows a JMOD spectrum for the same compound, in which the singlet at 129.0 ppm is much more visible. # = residual silicone grease, 1.37 ppm.*

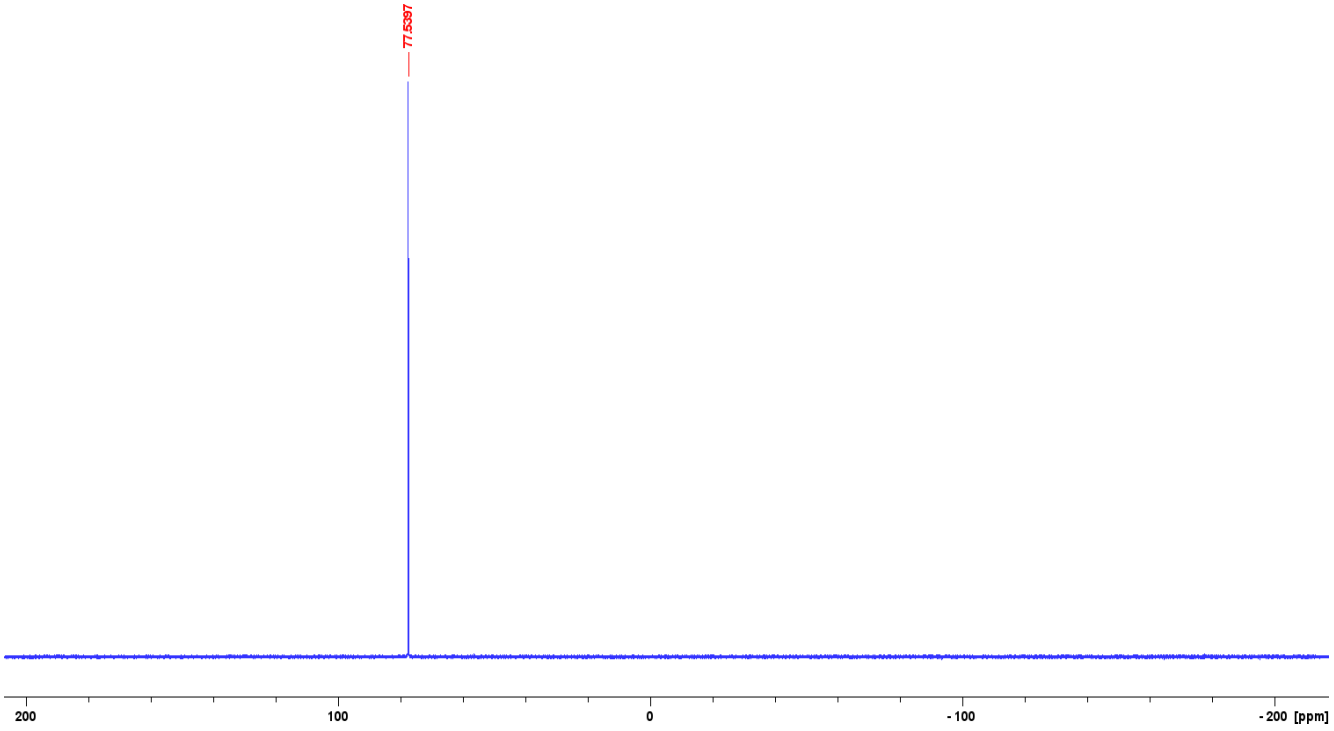

*Figure S32. $^{31}P\{^{1}H\}$ NMR spectrum of **6** in d_8-toluene.*

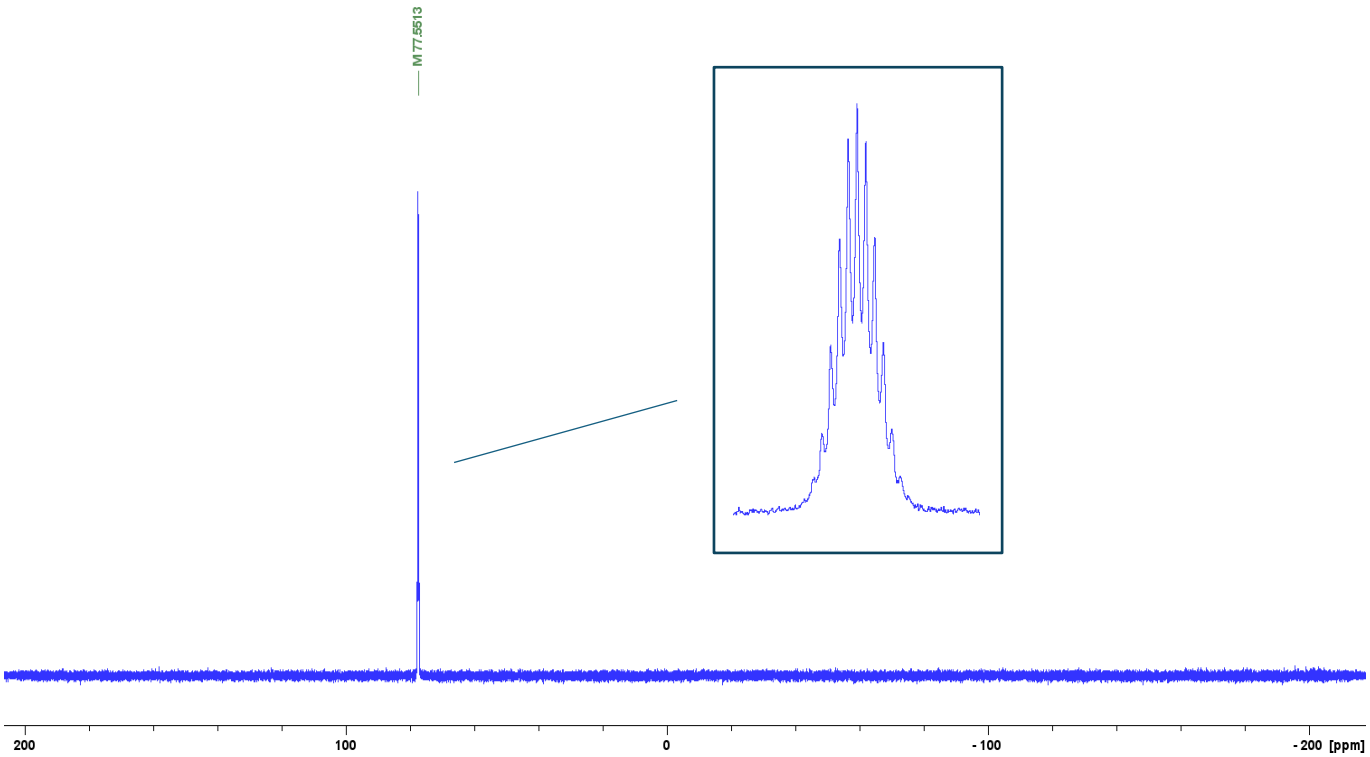

*Figure S33. ^{31}P NMR spectrum of **6** in d_8-toluene. Figure inside the blue box is zoomed in to show the splittings of the peak.*

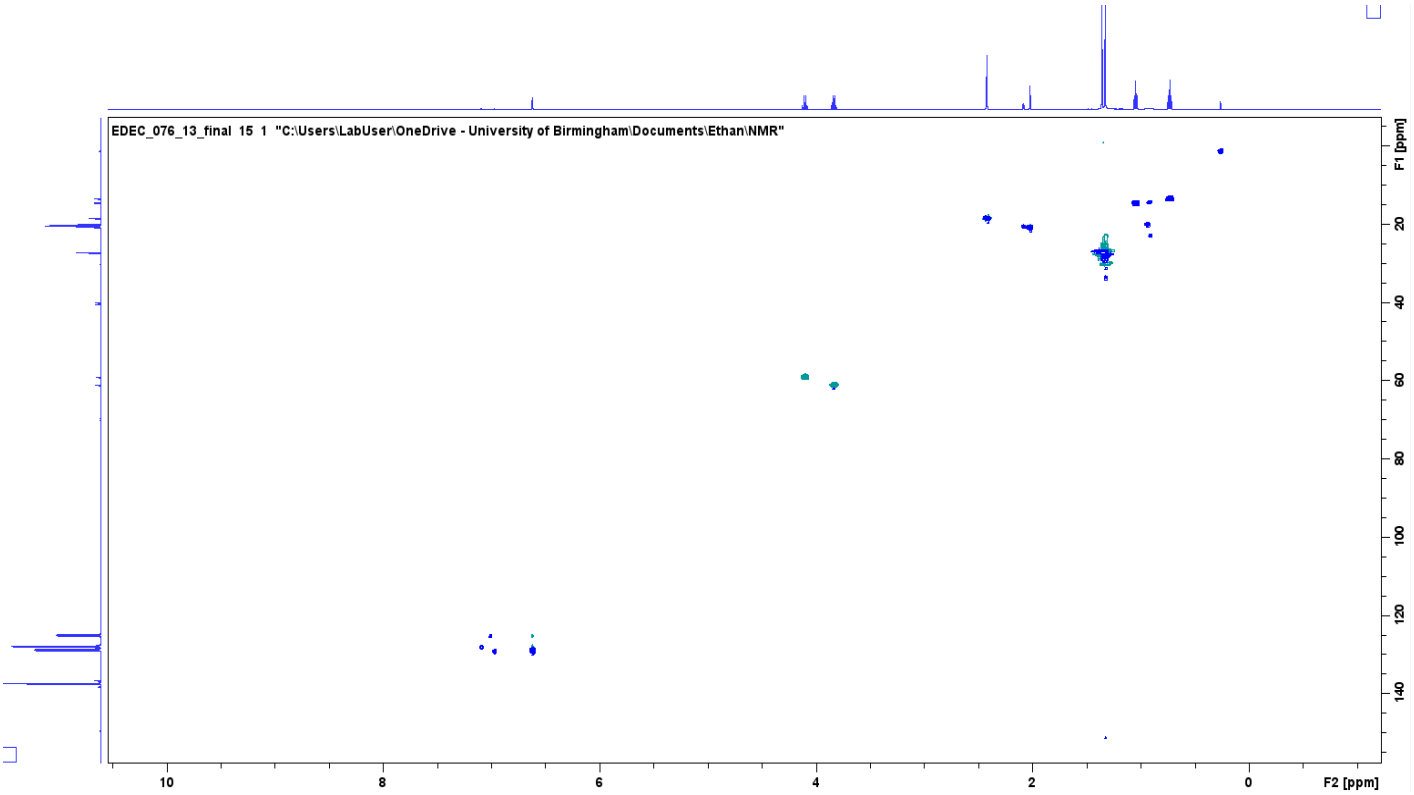

*Figure S34. 2D ^{1}H-^{13}C HSQC NMR spectrum of **6** in d_8-toluene. HSQC was vital for carbon assignments.*

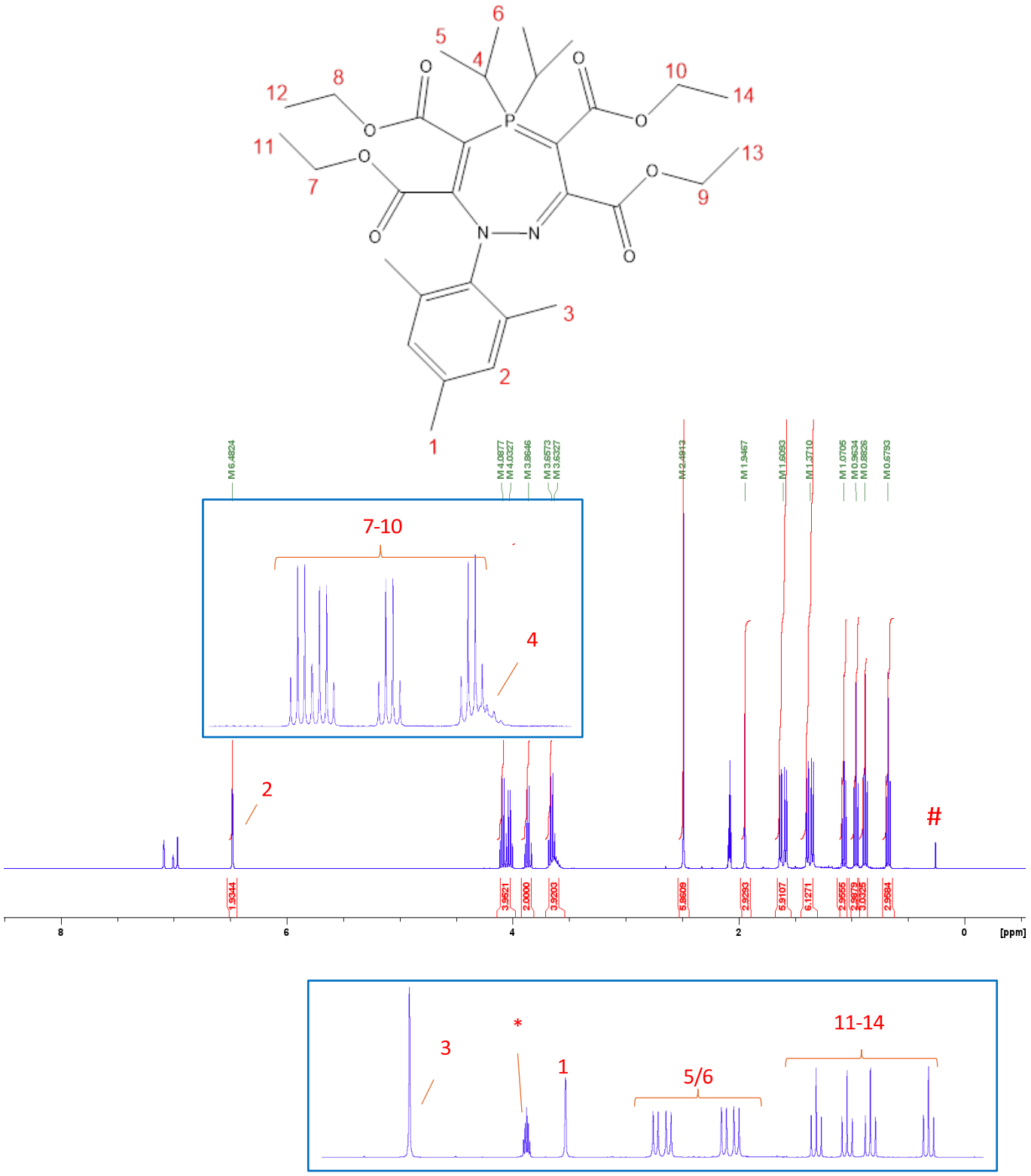

*Figure S35. ^{1}H NMR spectrum of **7** in d_8-toluene. # = residual silicone grease. Figures inside blue boxes show insets of the same spectrum. The spectrum is calibrated to the residual Ph-CHD_2 peak at 2.08 ppm, marked with *.*

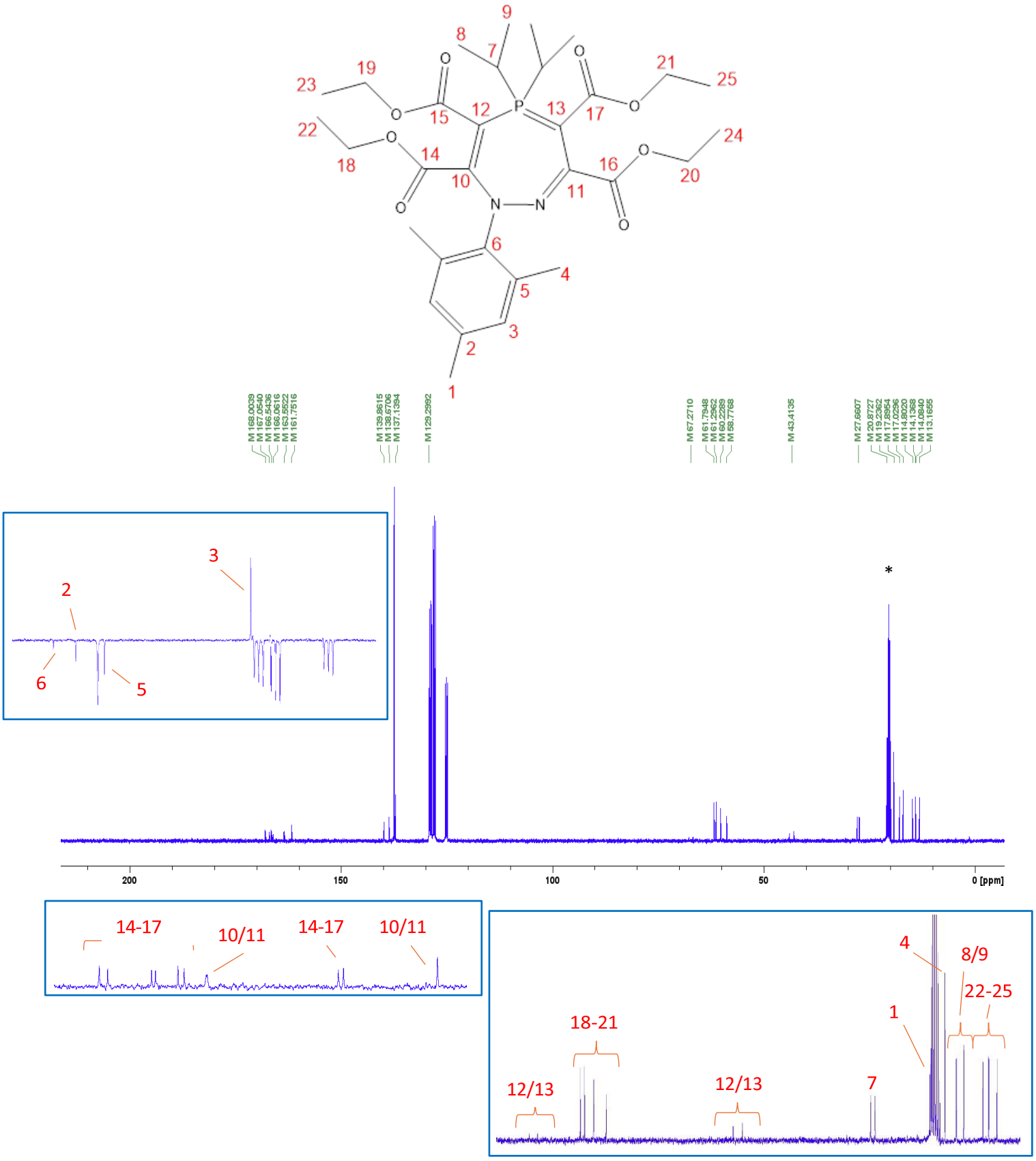

*Figure S36. $^{13}C\{^{1}H\}$ NMR spectrum of **7** in d_8-toluene. * = CD_3 peak of d_8-toluene peak, 20.43 ppm, to which the spectrum is calibrated. The top inset shows a JMOD spectrum for the same compound, in which the singlet at 129.3 ppm is much more visible.*

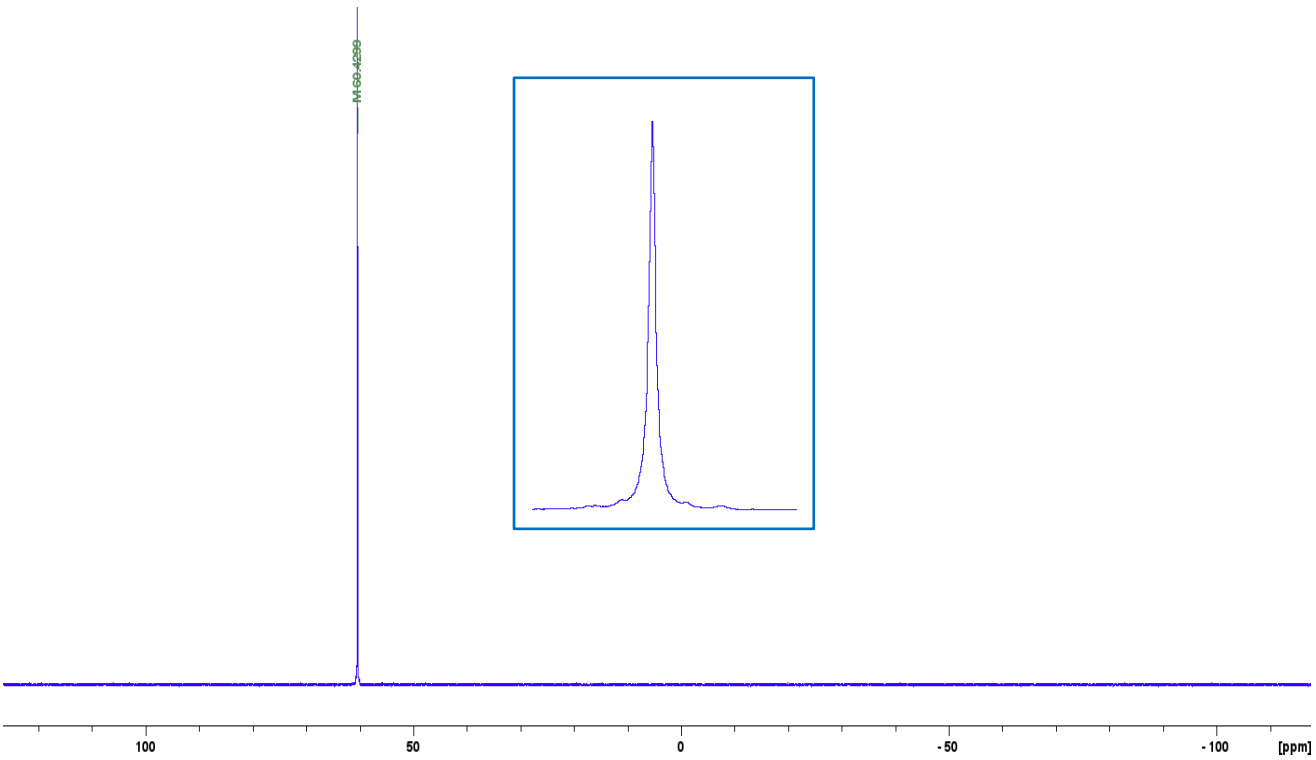

*Figure S37. $^{31}P\{^{1}H\}$ NMR spectrum of **7** in d_8-toluene. Figure inside blue box shows inset of the same spectrum.*

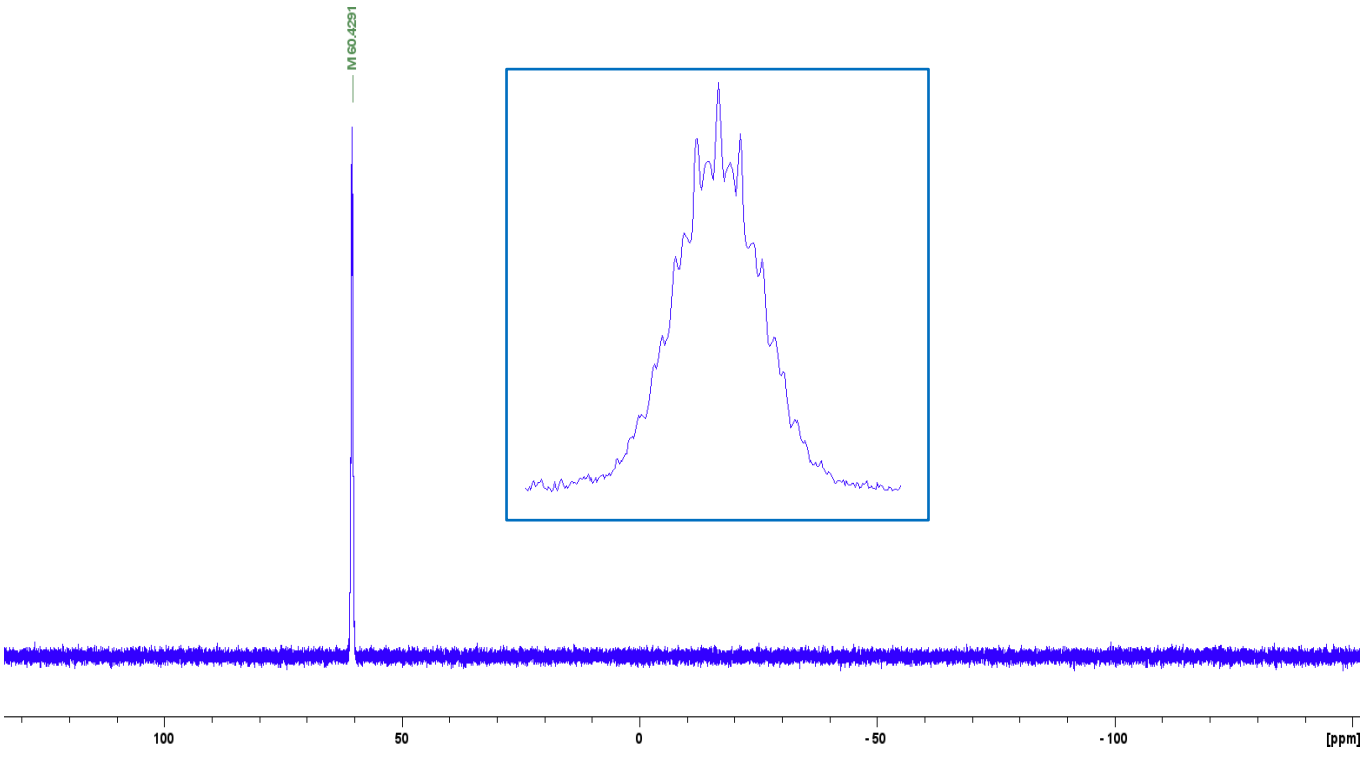

*Figure S38. ^{31}P NMR spectrum of **7** in d_8-toluene. Figure inside blue box shows inset of the same spectrum.*

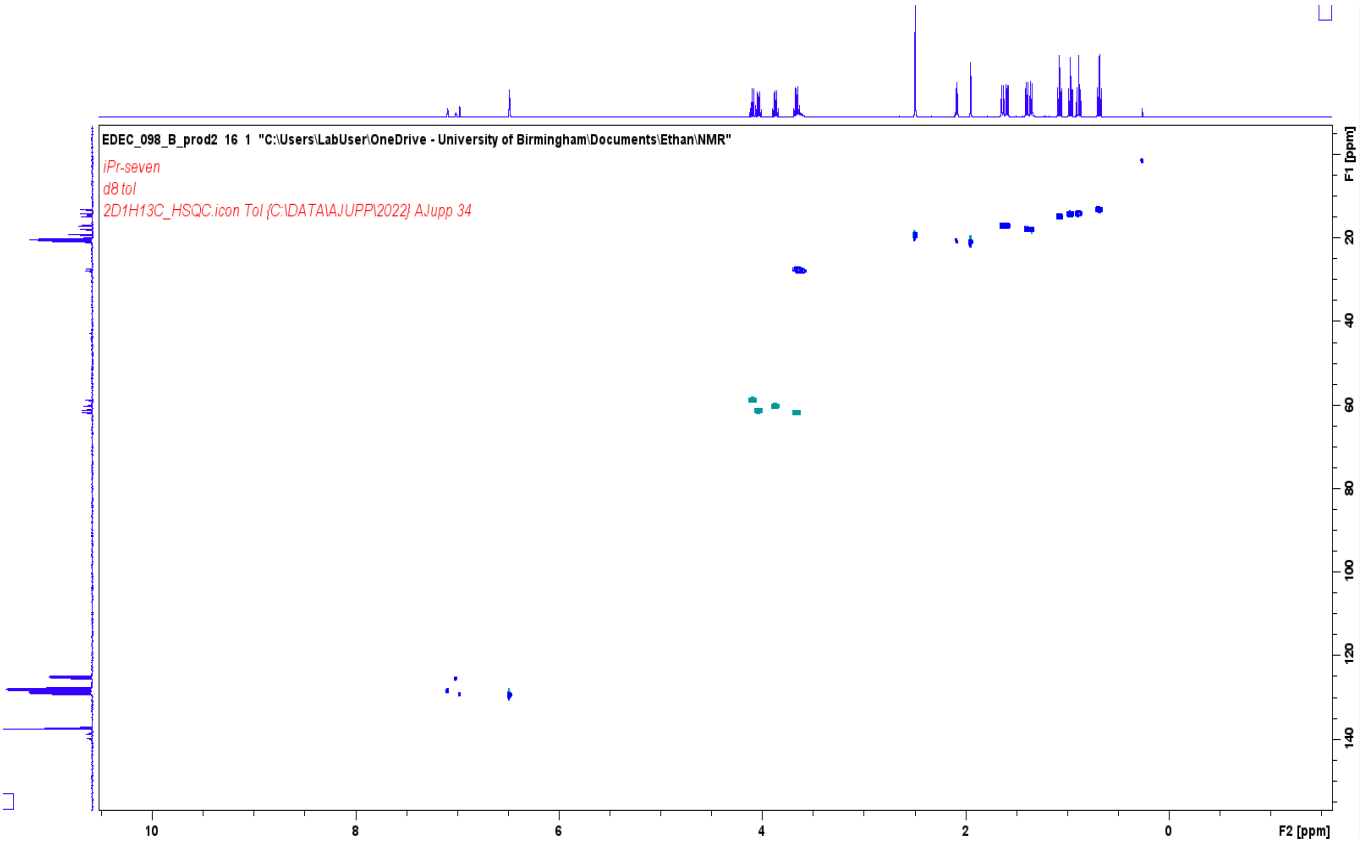

*Figure S39. 2D ^{1}H-^{13}C HSQC NMR spectrum of **7** in d_8-toluene. HSQC was vital for carbon assignments.*

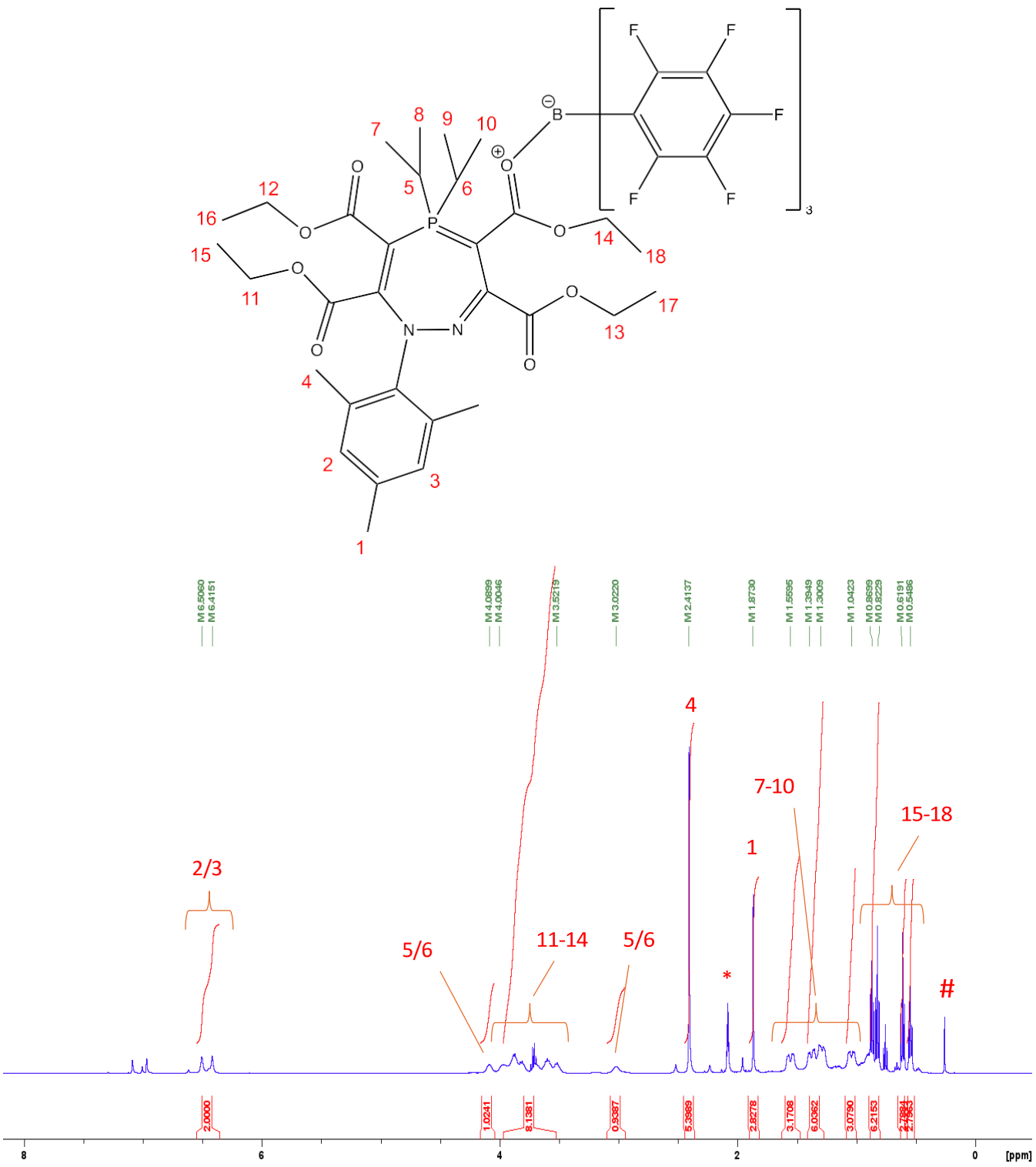

*Figure S40. ^{1}H NMR spectrum of **7·BCF** in d_8-toluene. # = residual silicone grease. The spectrum is calibrated to the residual Ph-CHD_2 peak at 2.08 ppm, marked with *.*

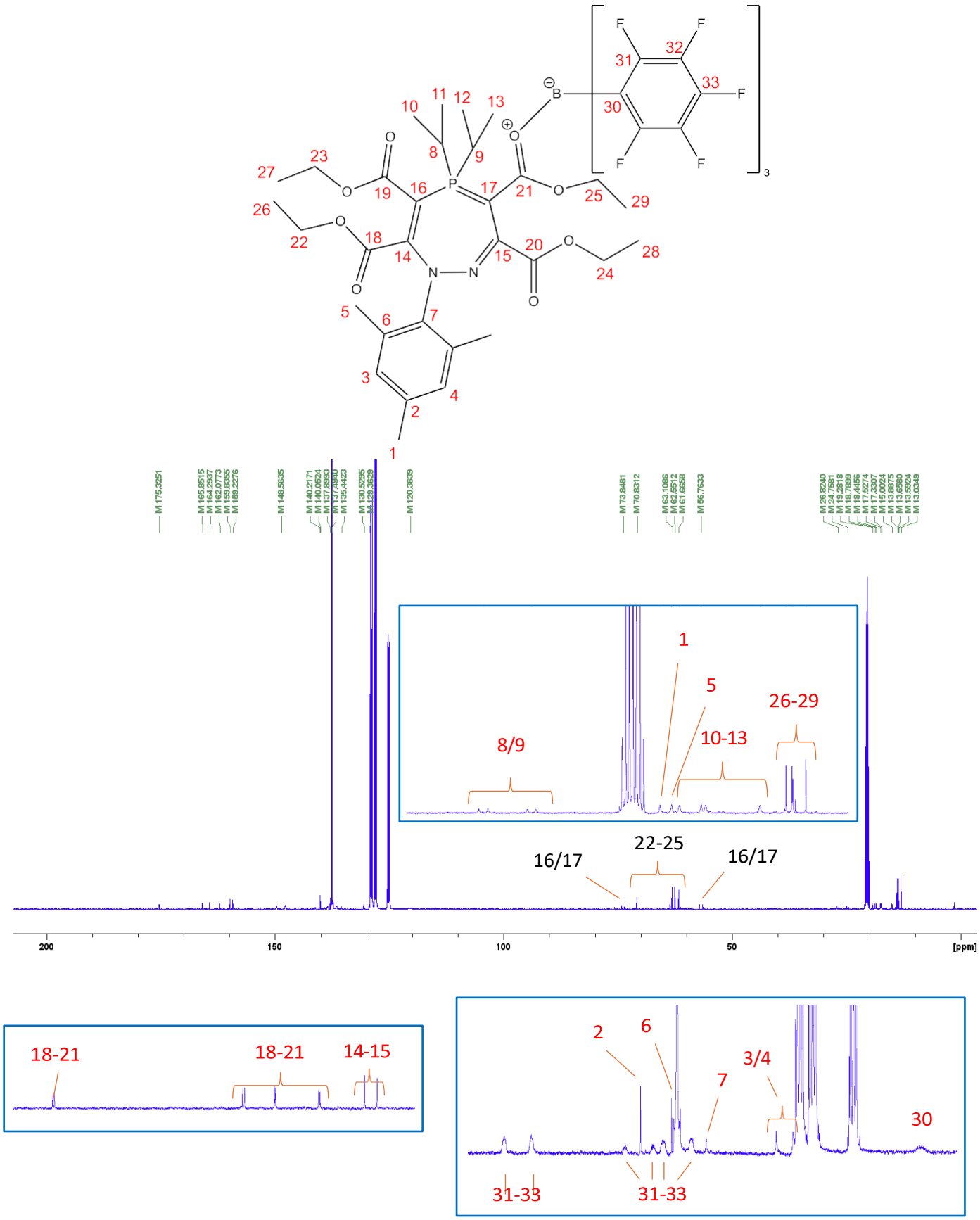

*Figure S41. $^{13}C\{^{1}H\}$ NMR spectrum of **7·BCF** in d_8-toluene. * = CD_3 peak of d_8-toluene peak, 20.43 ppm, to which the spectrum is calibrated. Figures inside blue boxes are insets of the same spectrum, in which certain peaks are much more visible.*

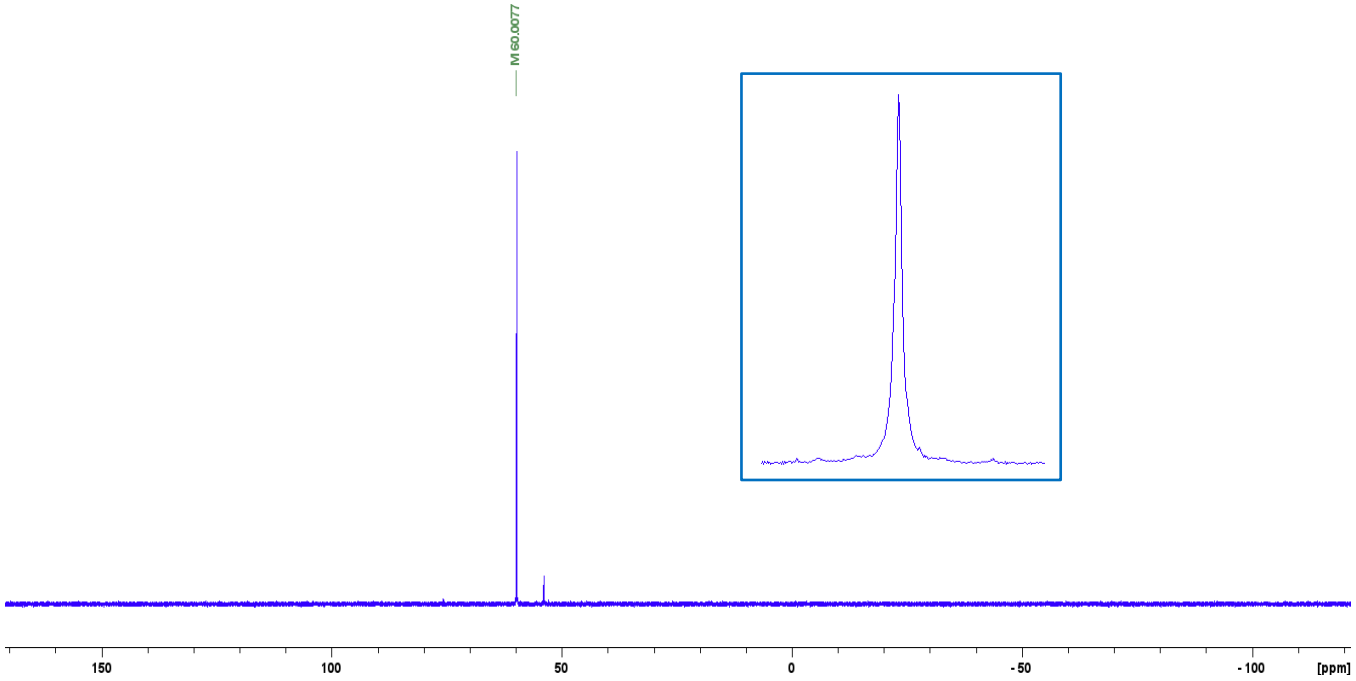

*Figure S42. $^{31}P\{^{1}H\}$ NMR spectrum of **7·BCF** in d_8-toluene. Figure inside the blue box is zoomed in to show the splittings of the peak. * = impurity at 54.1 ppm. The identity of this impurity is unknown; it does not match any other compounds reported in this manuscript, and could not been removed after several recrystallisations. We tentatively ascribe it to coordination of $B(C_6F_5)_3$ to another $-CO_2Et$ group on the seven-membered ring; this may exist in equilibrium with the major product in solution, rationalizing why it could not be removed after several attempts.*

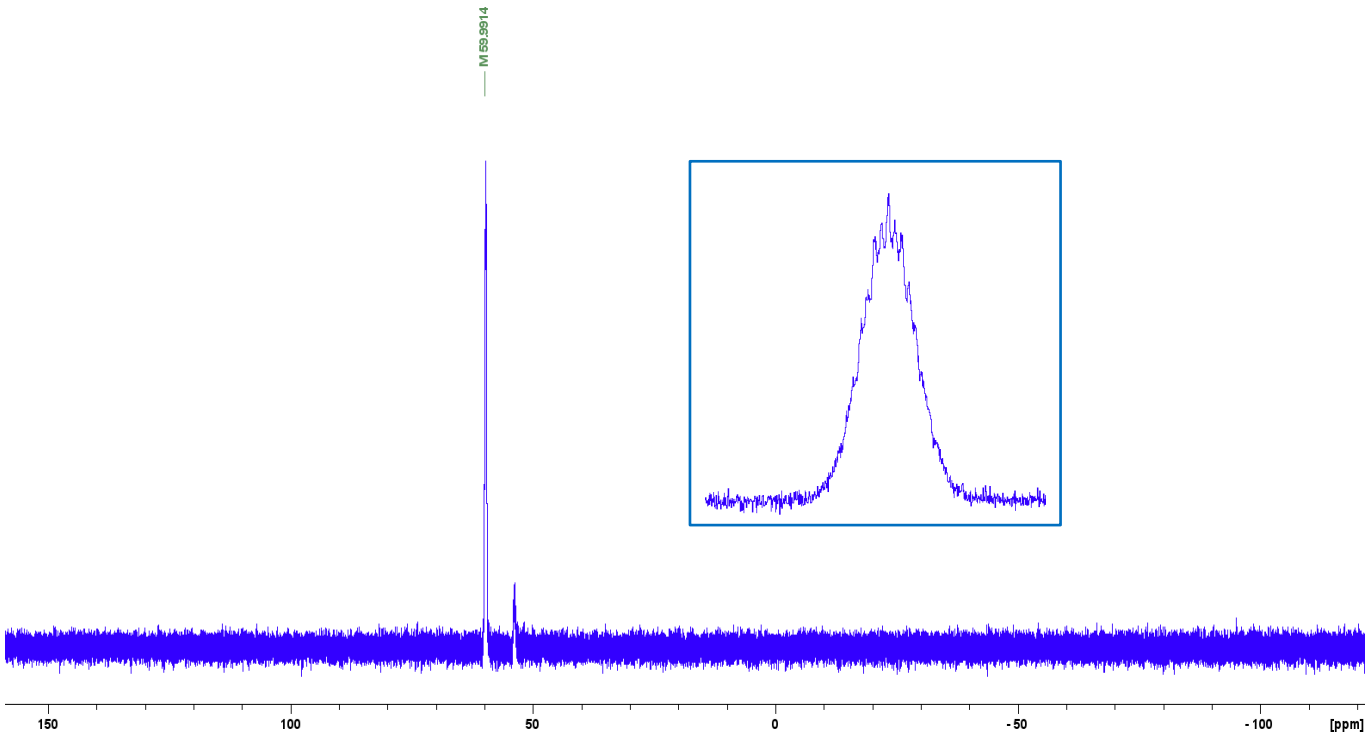

*Figure S43. ^{31}P NMR spectrum of **7·BCF** in d_8-toluene. Figure inside the blue box is zoomed in to show the splittings of the peak. * = impurity at 54.1 ppm. See caption for S42 for further details relating to this impurity.*

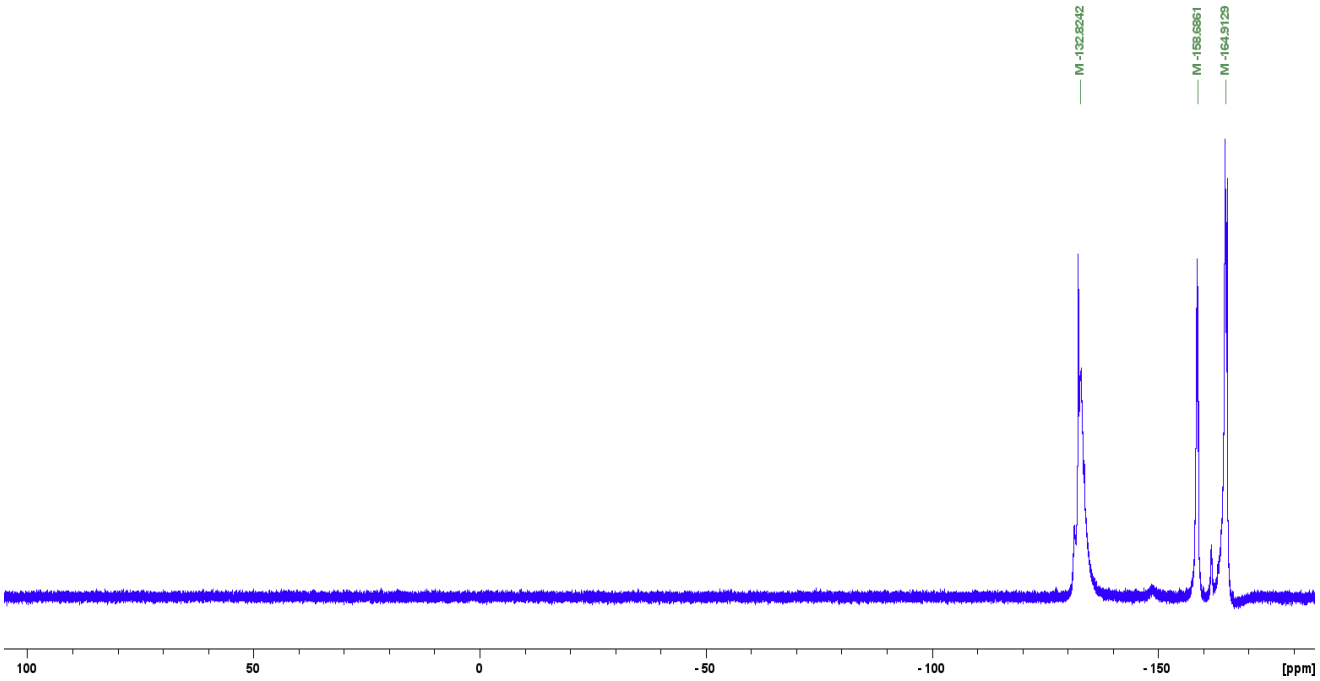

*Figure S44. $^{19}F\{^{1}H\}$ NMR spectrum of **7·BCF** in d_8-toluene.*

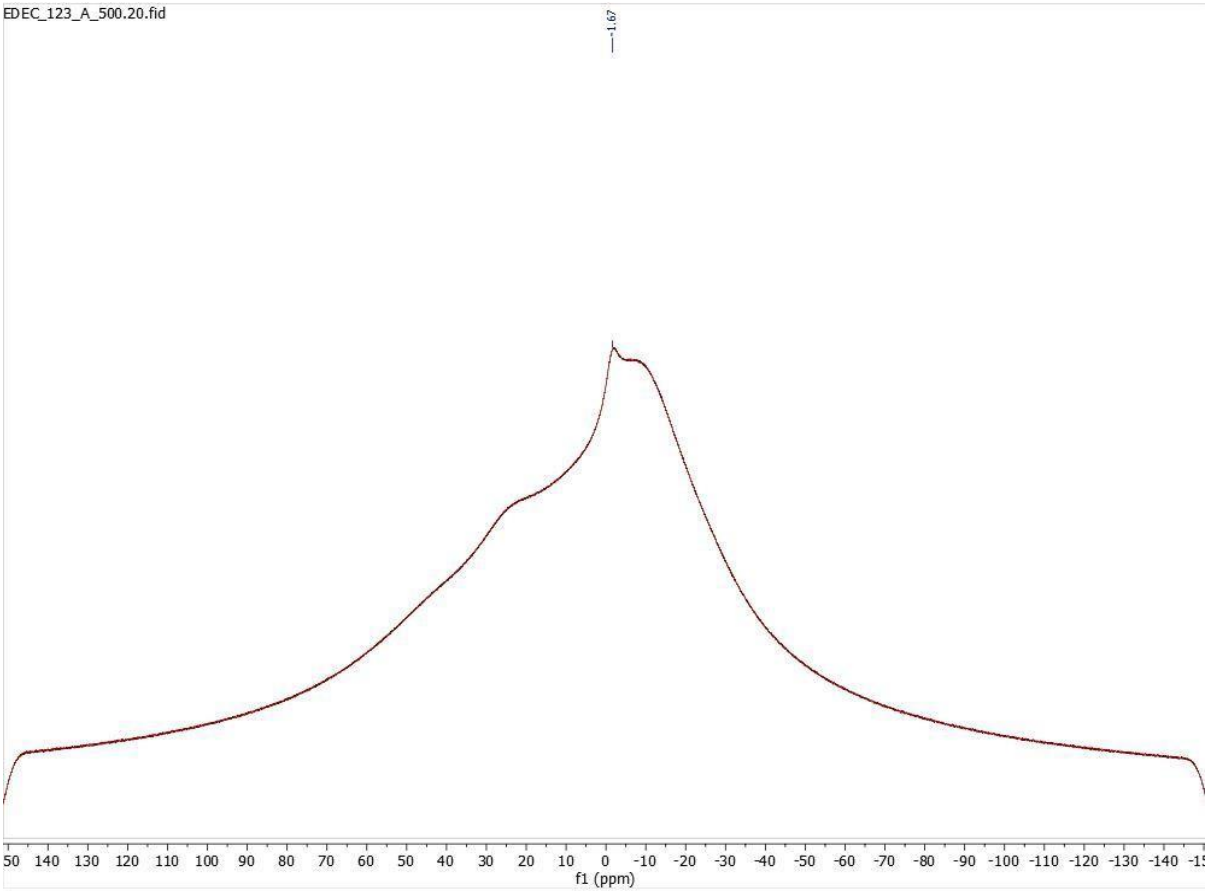

*Figure S45. $^{11}B\{^{1}H\}$ NMR spectrum of **7·BCF** in d_8-toluene.*

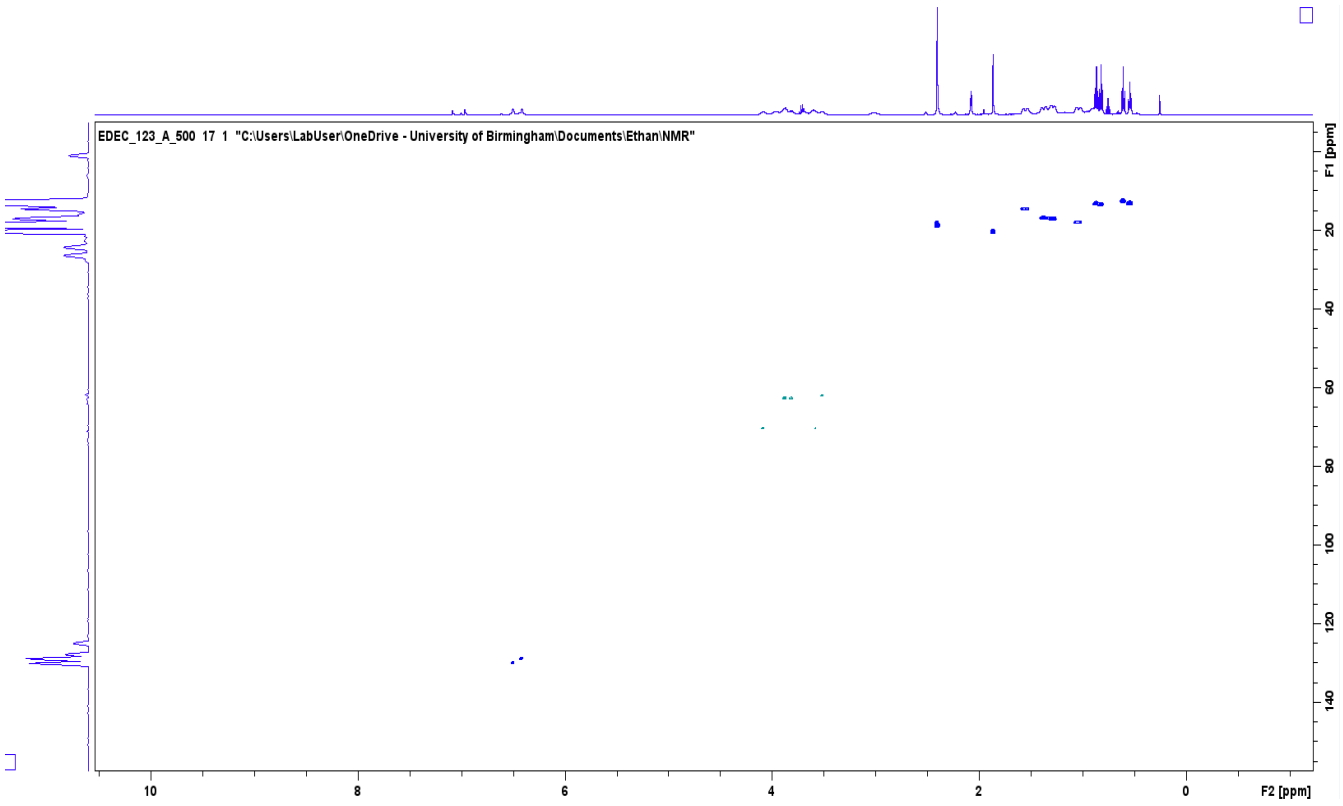

*Figure S46. 2D ^{1}H-^{13}C HSQC NMR spectrum of **7·BCF** in d_8-toluene. HSQC was vital for carbon assignments.*

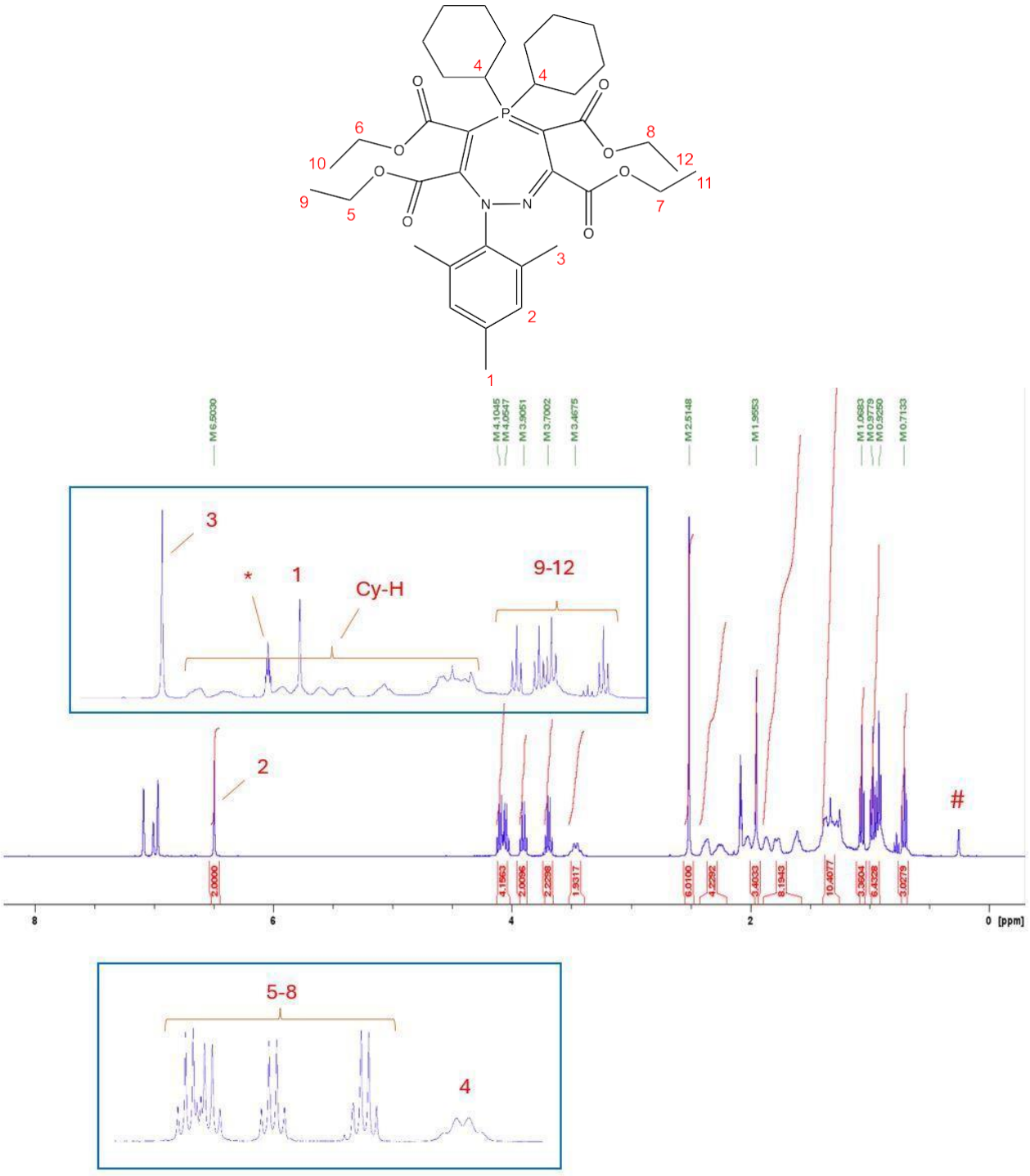

*Figure S47. ^{1}H NMR spectrum of **8** in d_8-toluene. # = residual silicone grease. The spectrum is calibrated to the residual Ph-CHD_2 peak at 2.08 ppm, marked with *.*

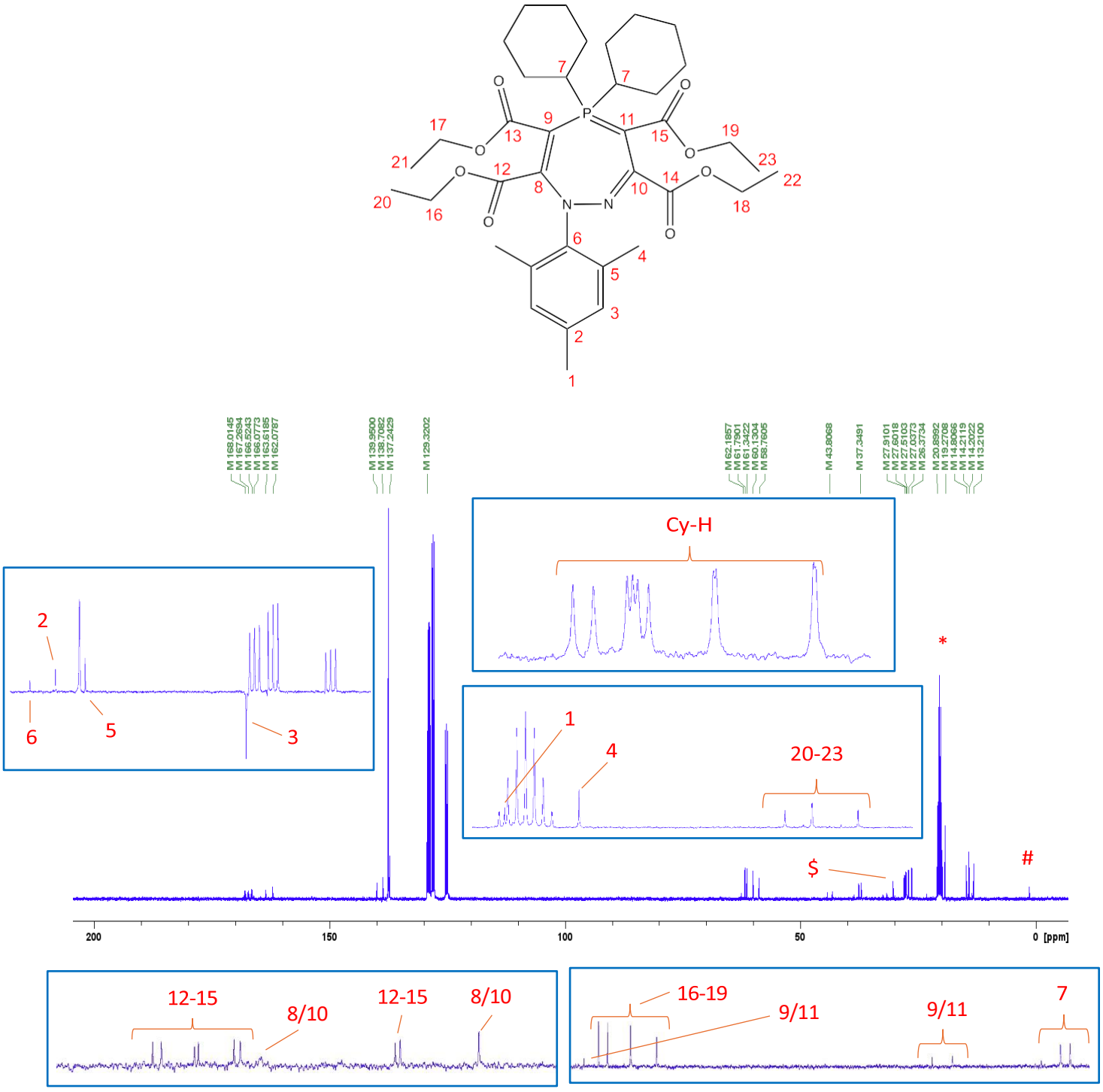

*Figure S48. $^{13}C\{^{1}H\}$ NMR spectrum of **8** in d_8-toluene. * = CD_3 peak of d_8-toluene peak, 20.43 ppm, to which the spectrum is calibrated. Figures inside blue boxes show insets of the same spectrum. The top-left inset shows a JMOD spectrum for the same compound, in which the singlet at 129.3 ppm is much more visible. Note that for the doublet at 62.2 ppm, one of the peaks is 'hidden' by the singlet at 61.8 ppm. # = residual silicone grease, 1.37 ppm. $ = residual H-grease, 30.33 ppm.*

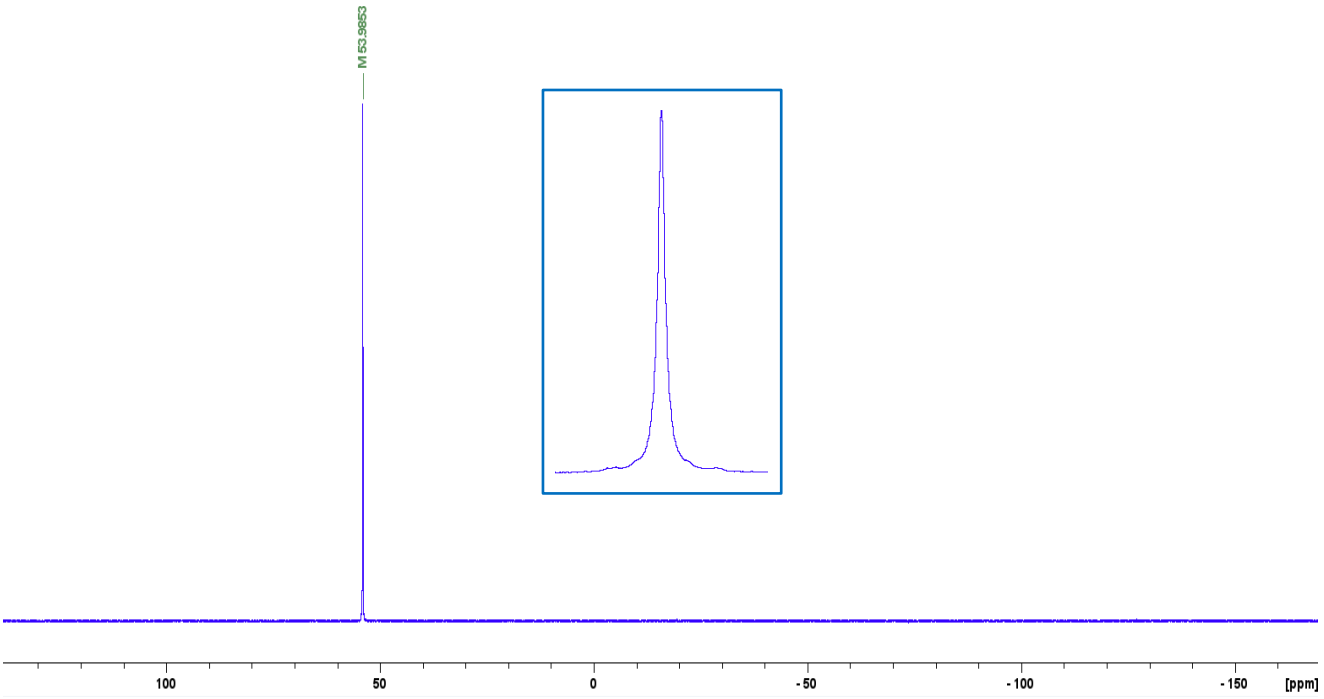

*Figure S49. $^{31}P\{^{1}H\}$ NMR spectrum of **8** in d_8-toluene. Figure inside blue box shows inset of the same spectrum.*

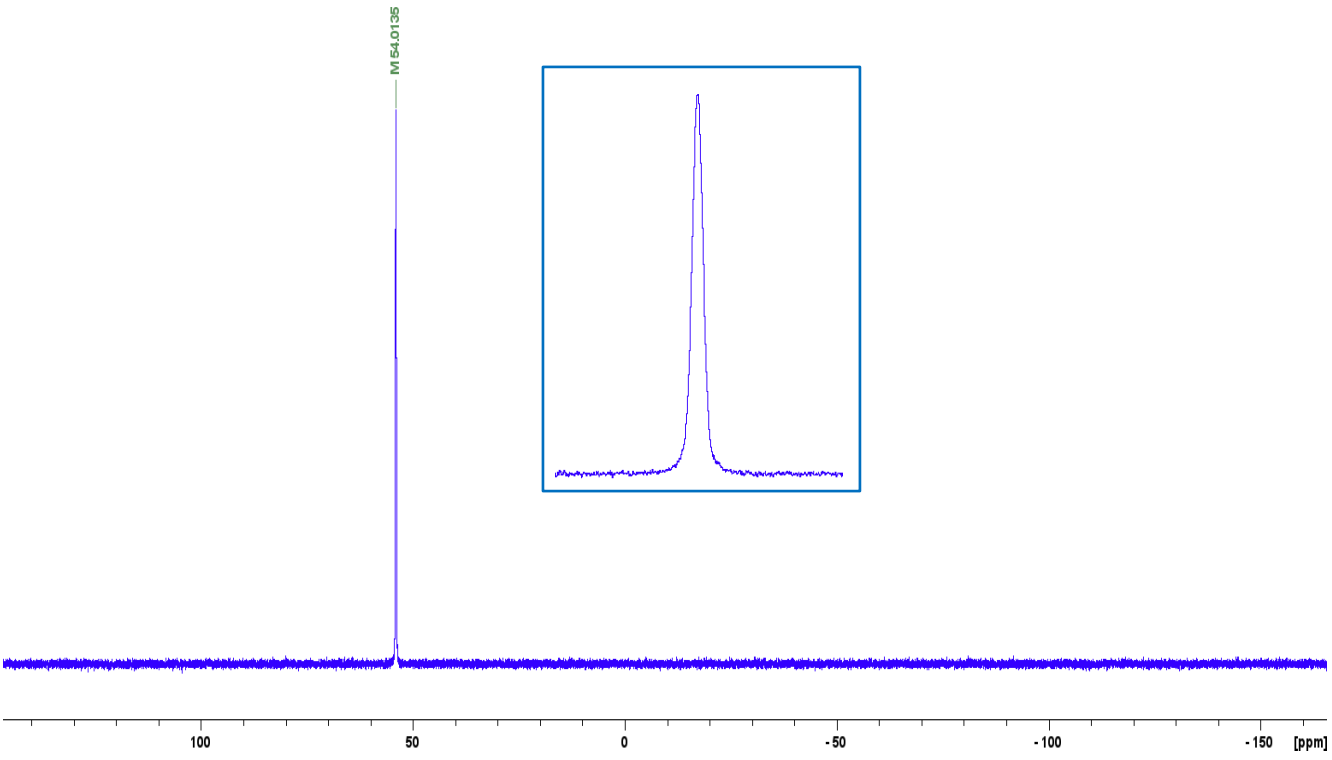

*Figure S50. ^{31}P NMR spectrum of **8** in d_8-toluene. Figure inside blue box shows inset of the same spectrum.*

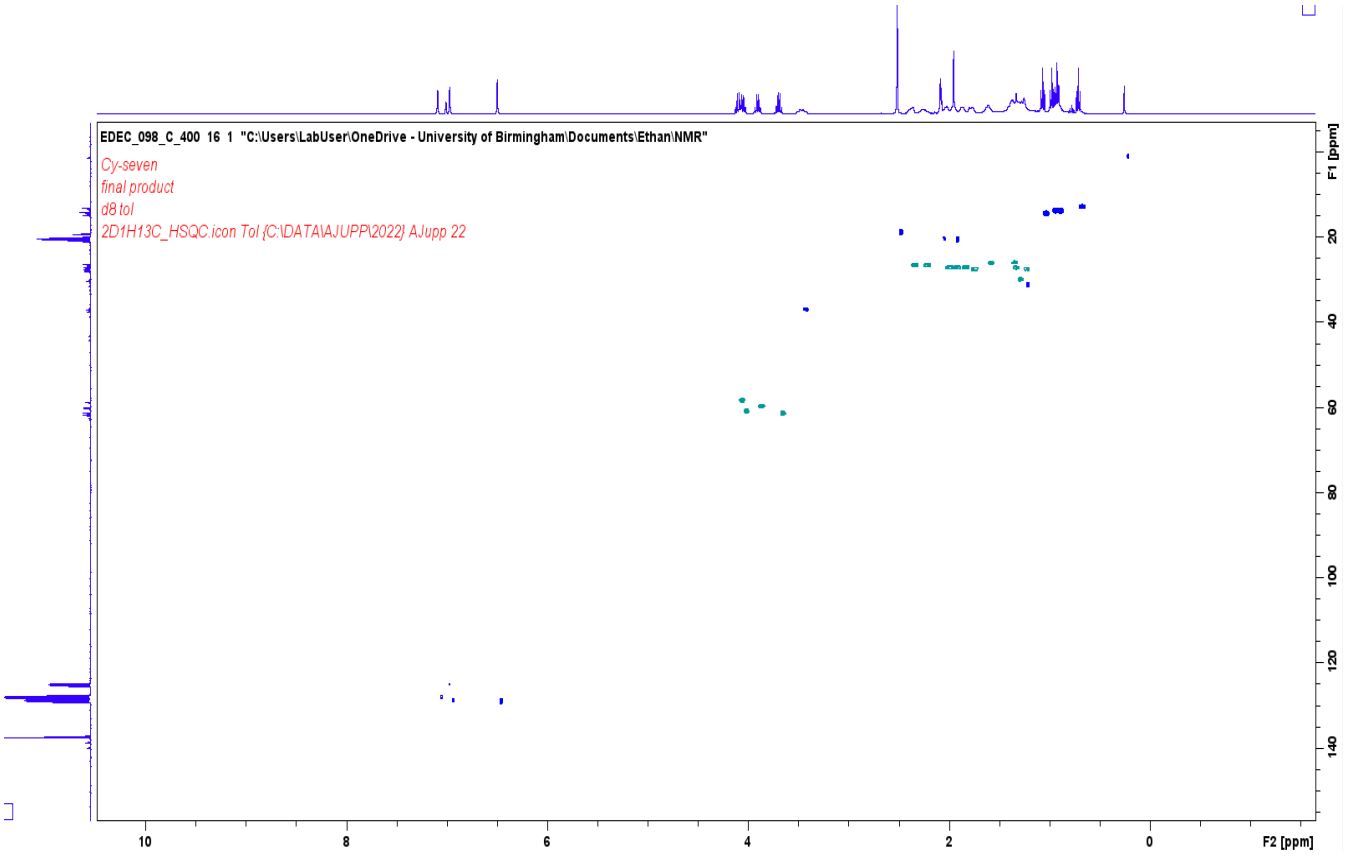

*Figure S51. 2D ^{1}H-^{13}C HSQC NMR spectrum of **8** in d_8-toluene. HSQC was vital for carbon assignments.*

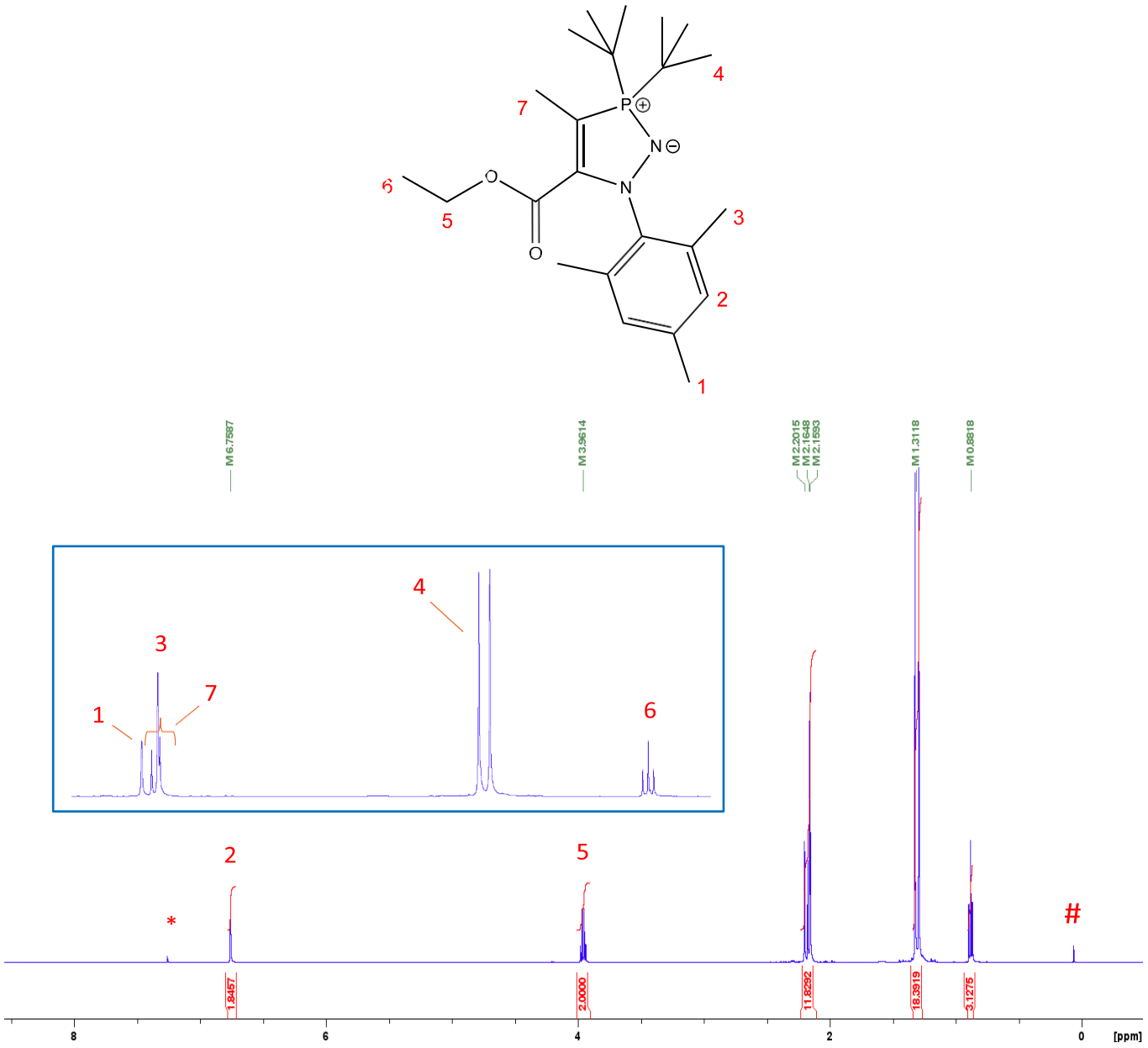

*Figure S52. ^{1}H NMR spectrum of **9** in $CDCl_3$. # = residual silicone grease. Figures inside blue box shows inset of the same spectrum. The spectrum is calibrated to the residual $CDCl_3$ peak at 7.26 ppm, marked with *.*

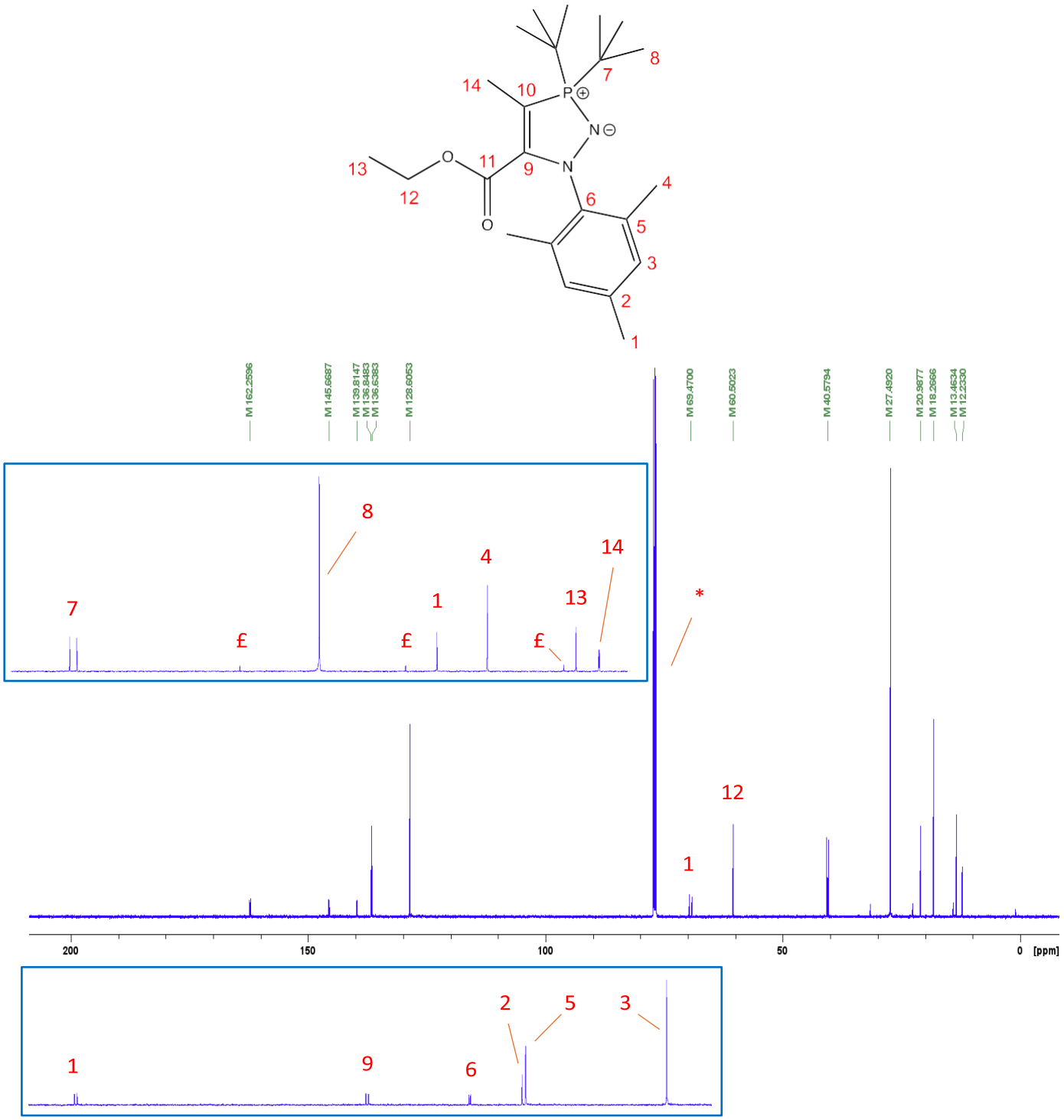

*Figure S53. $^{13}C\{^{1}H\}$ NMR spectrum of **9** in $CDCl_3$. * = CDCl3 peak, 77.16 ppm, to which the spectrum is calibrated. Figures inside blue boxes show insets of the same spectrum, in which the splittings of the peaks are clearer. £ = residual hexane (14.14 ppm, 22.70 ppm, 31.64 ppm).*

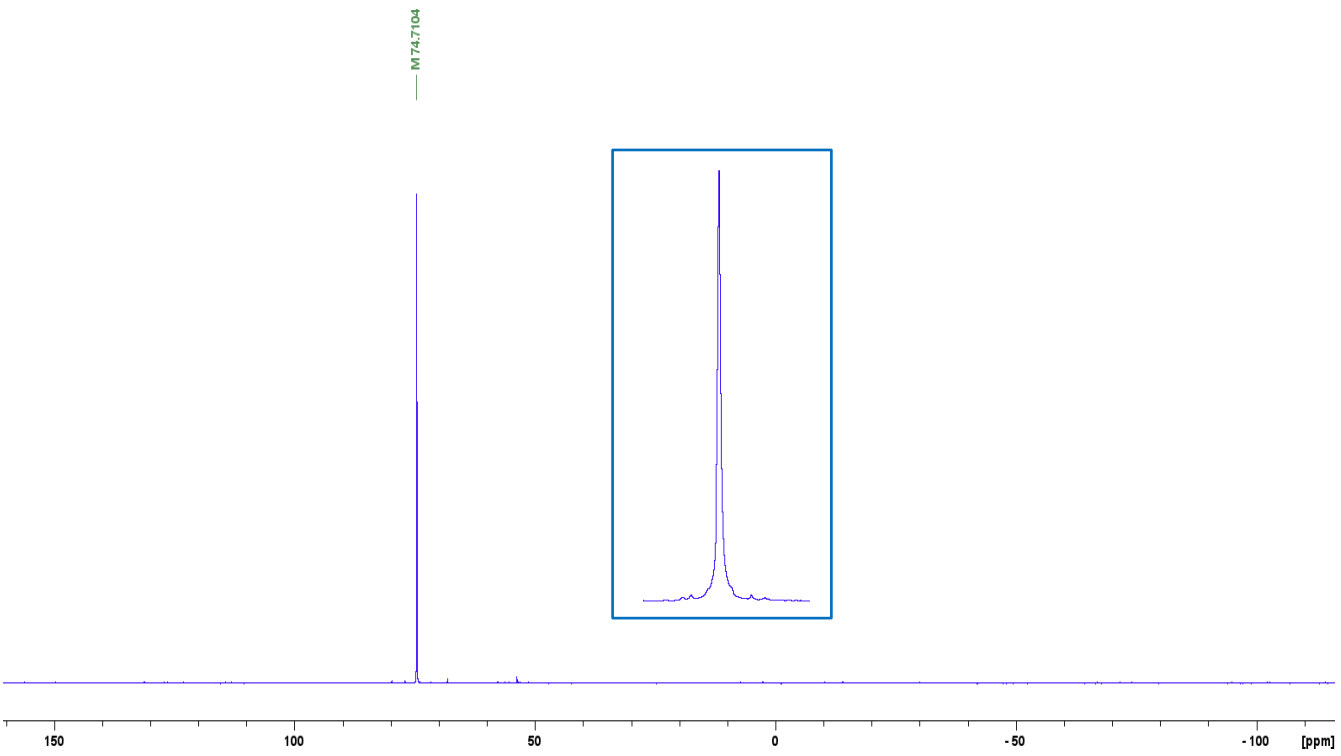

*Figure S54. $^{31}P\{^{1}H\}$ NMR spectrum of **9** in $CDCl_3$. Figure inside blue box shows inset of the same spectrum.*

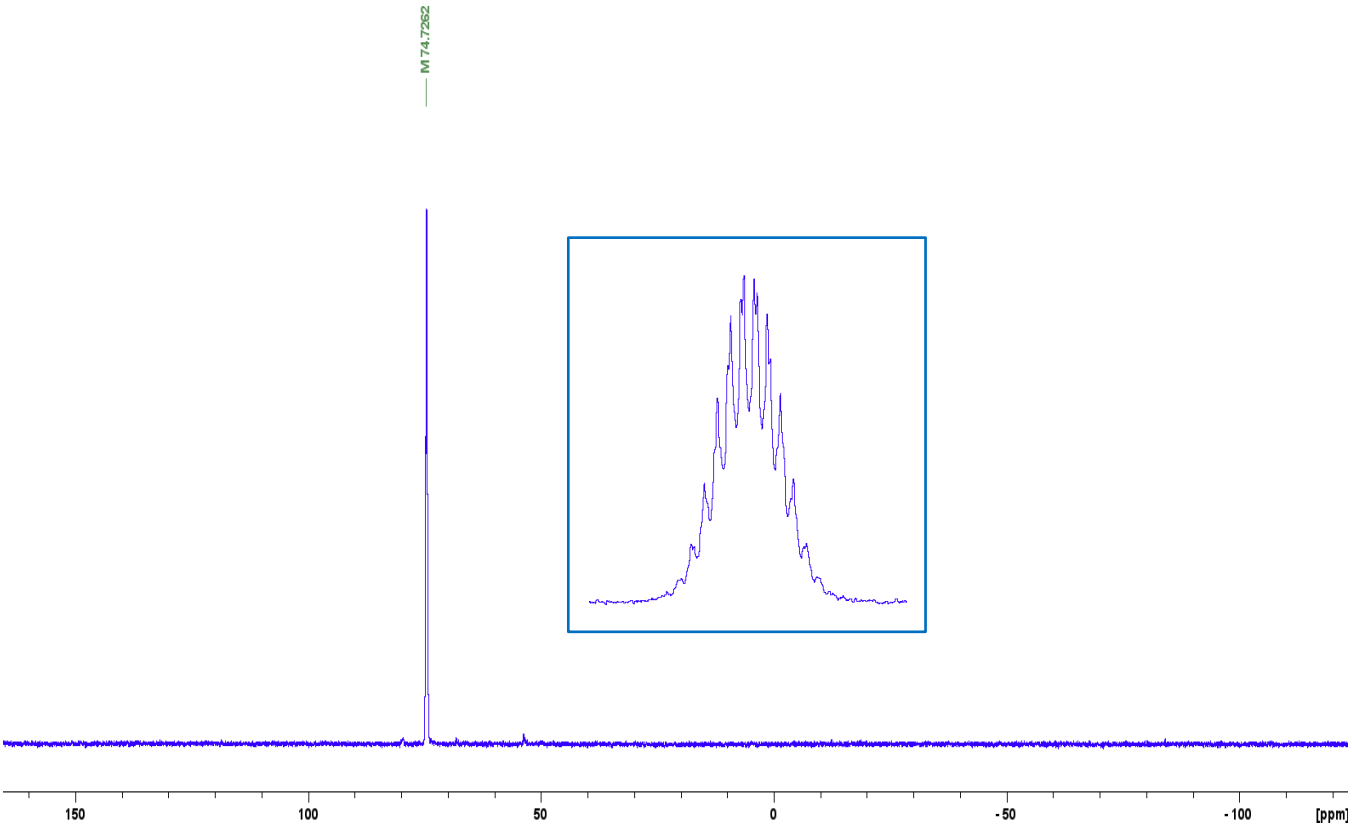

*Figure S55. ^{31}P NMR spectrum of **9** in $CDCl_3$. Figure inside blue box shows inset of the same spectrum.*

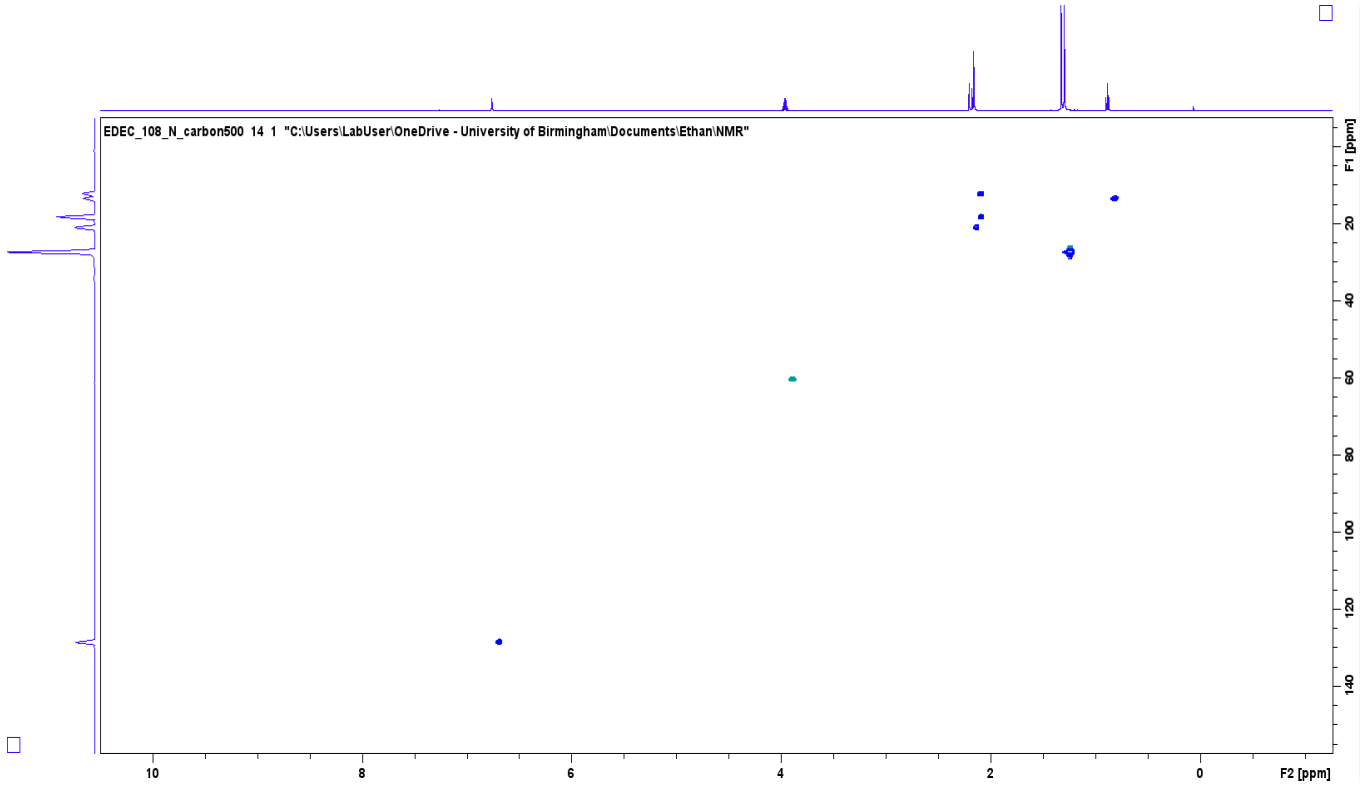

*Figure S56. 2D ^{1}H-^{13}C HSQC NMR spectrum of **9** in $CDCl_3$. HSQC was vital for carbon assignments.*

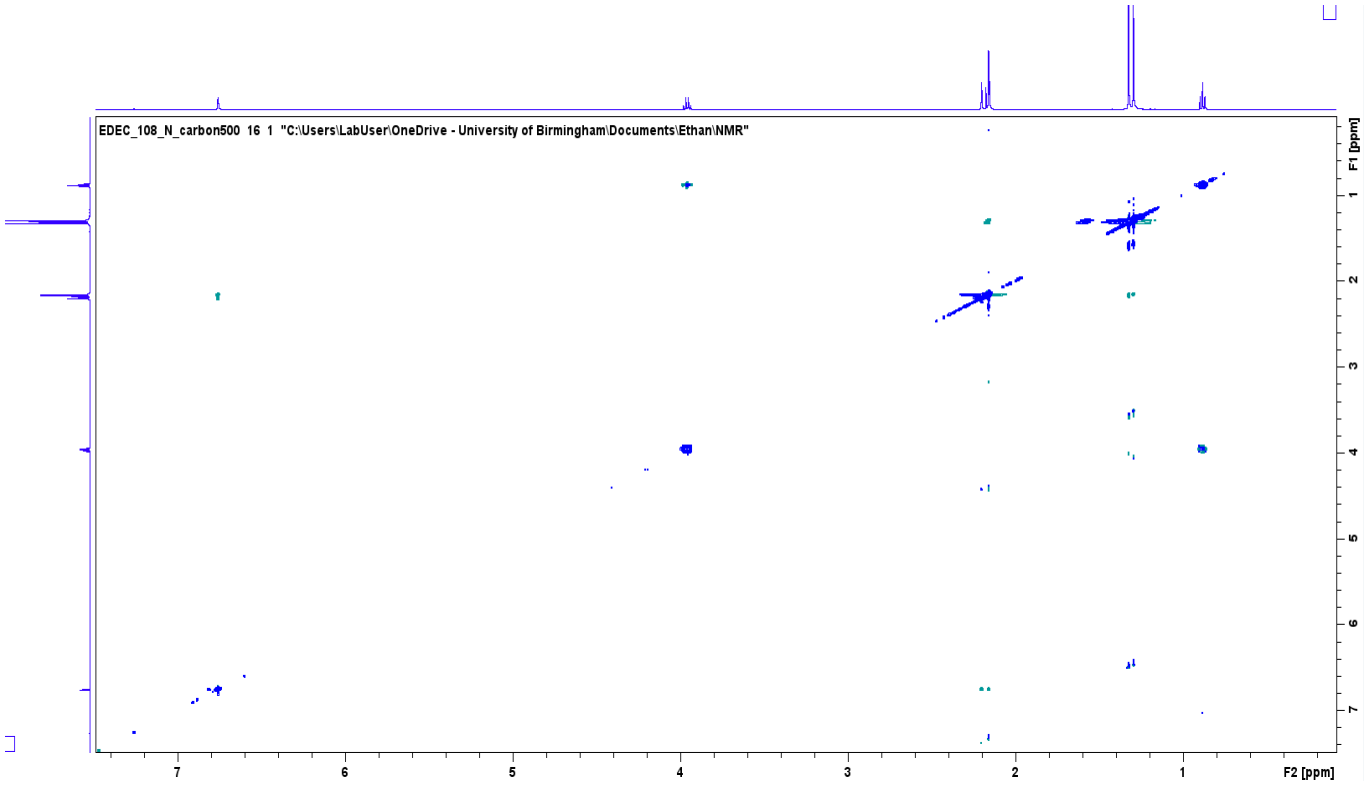

*Figure S57. 2D ^{1}H-^{1}H NOESY NMR spectrum of **9** in $CDCl_3$. NOESY was useful for the determination of regiochemistry.*

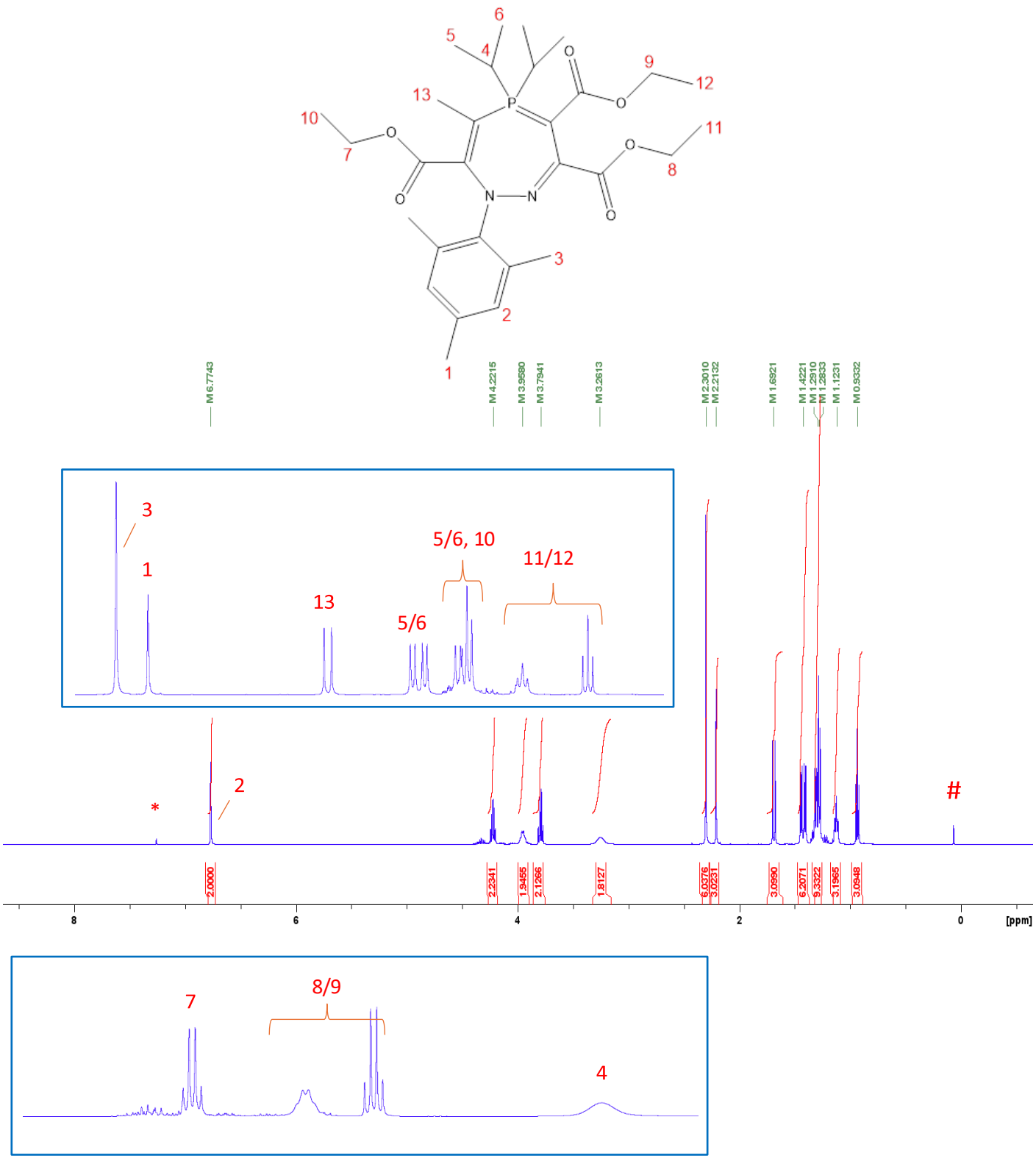

*Figure S58. ^{1}H NMR spectrum of **10** in $CDCl_3$. # = residual silicone grease. Figures inside blue boxes show insets of the same spectrum. The spectrum is calibrated to the residual $CHCl_3$ peak at 7.26 ppm, marked with *.*

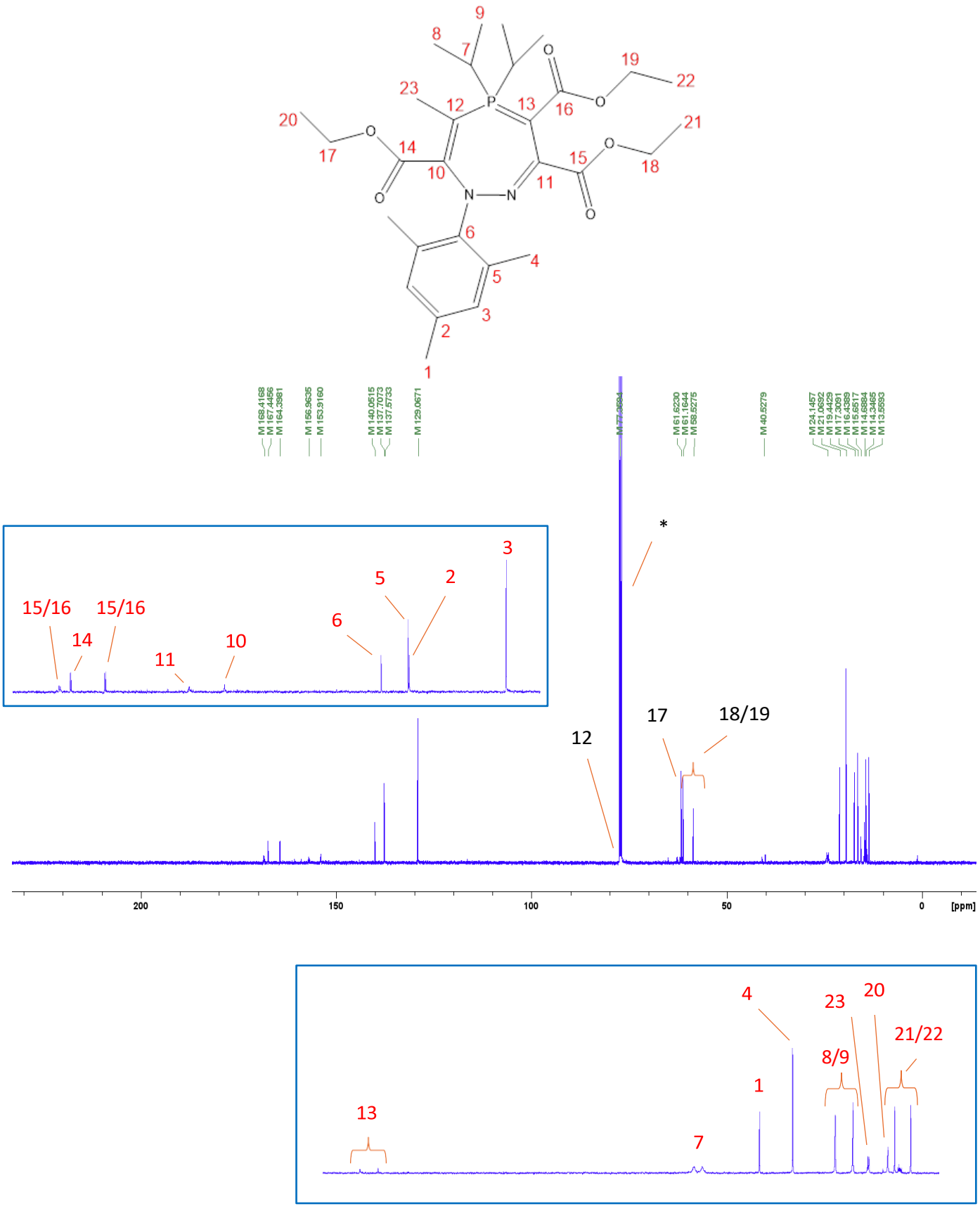

*Figure S59. $^{13}C\{^{1}H\}$ NMR spectrum of **10** in $CDCl_3$. * = $CDCl_3$ peak, 77.16 ppm, to which the spectrum is calibrated. Figures inside blue boxes show insets of the same spectrum. The peak at 77.4 ppm is obscured under the $CDCl_3$ peak; this peak showed a strong HMBC coupling to proton 13, supporting its assignment as carbon 12.*

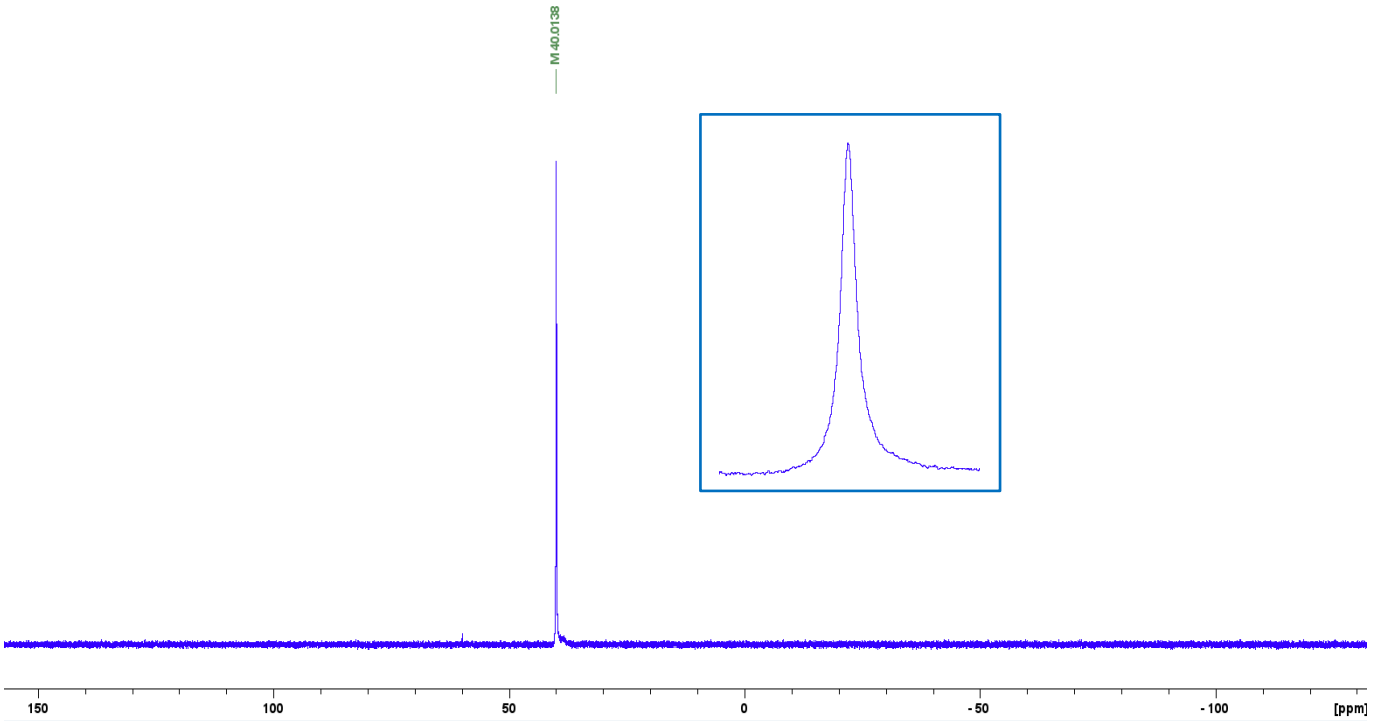

*Figure S60. $^{31}P\{^{1}H\}$ NMR spectrum of **10** in $CDCl_3$. Figure inside blue box shows inset of the same spectrum.*

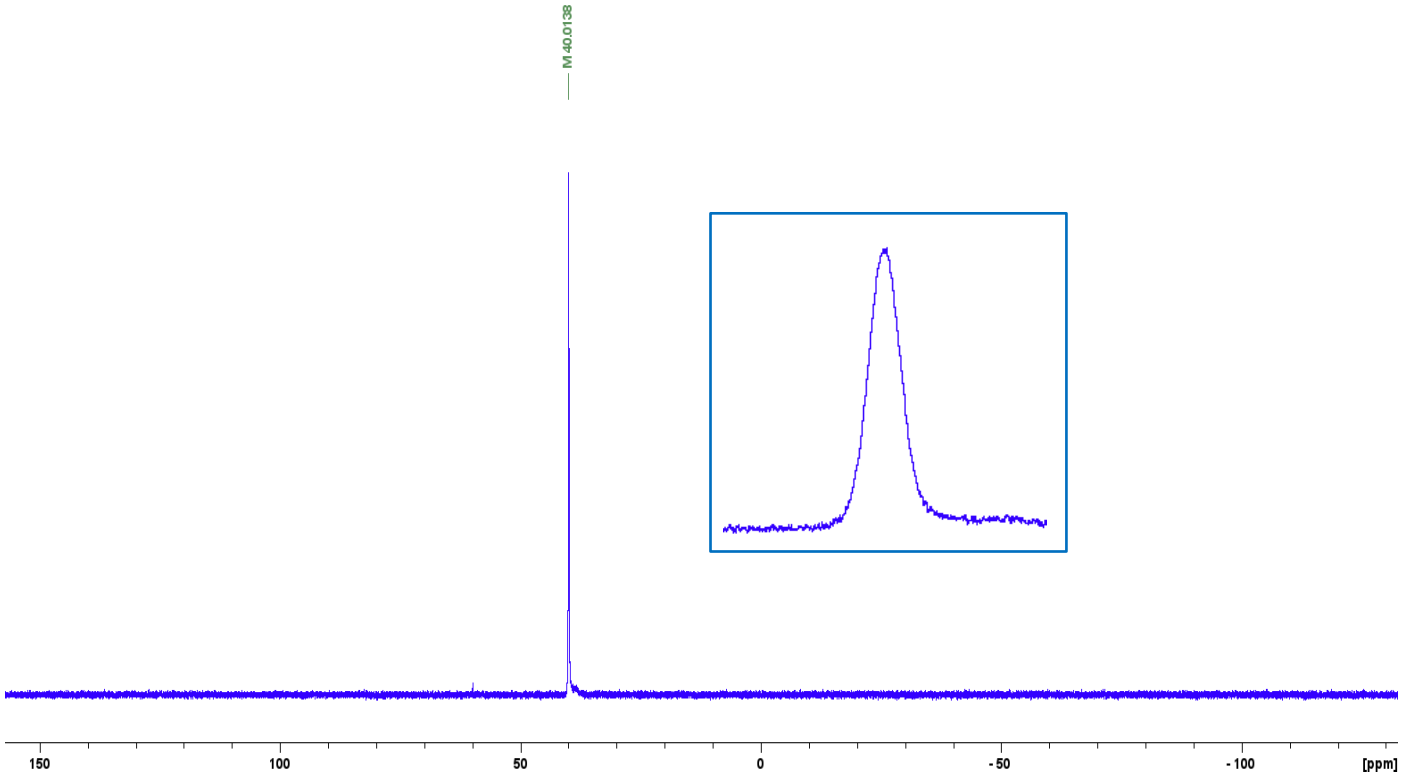

*Figure S61. ^{31}P NMR spectrum of **10** in $CDCl_3$. Figure inside blue box shows inset of the same spectrum.*

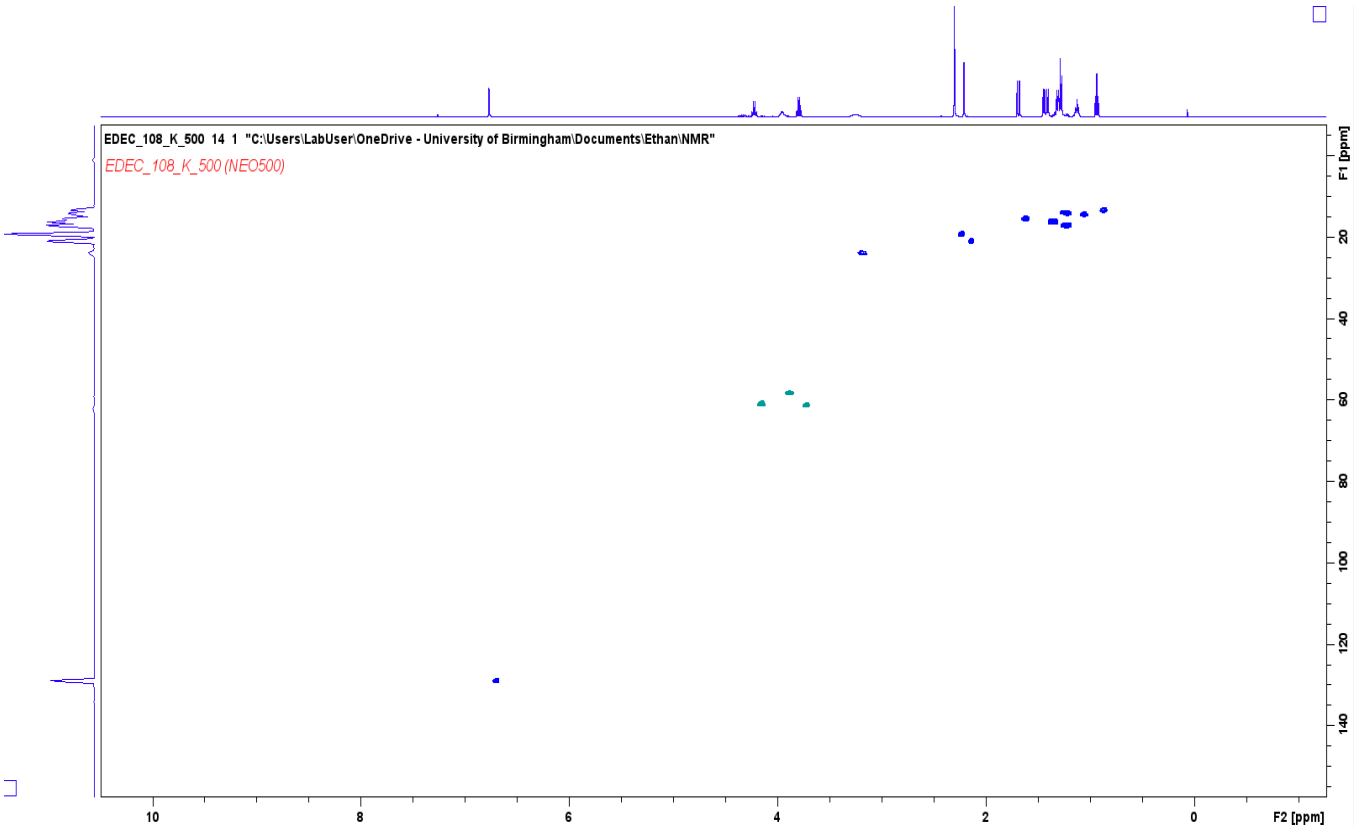

*Figure S62. 2D ^{1}H-^{13}C HSQC NMR spectrum of **10** in $CDCl_3$. HSQC was vital for carbon assignments.*

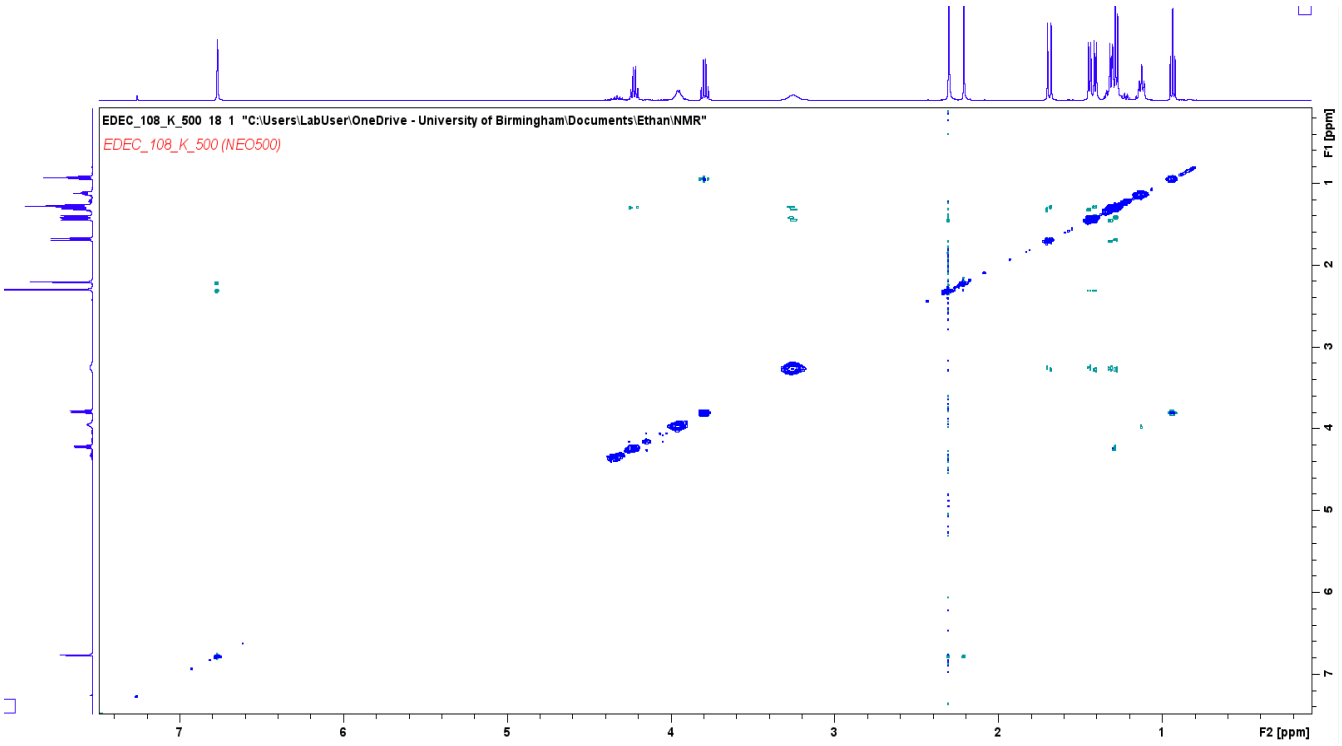

*Figure S63. 2D NOESY NMR spectrum of **10** in $CDCl_3$. NOESY assisted in working out the carbon/proton assignments, and thus regioselectivity.*

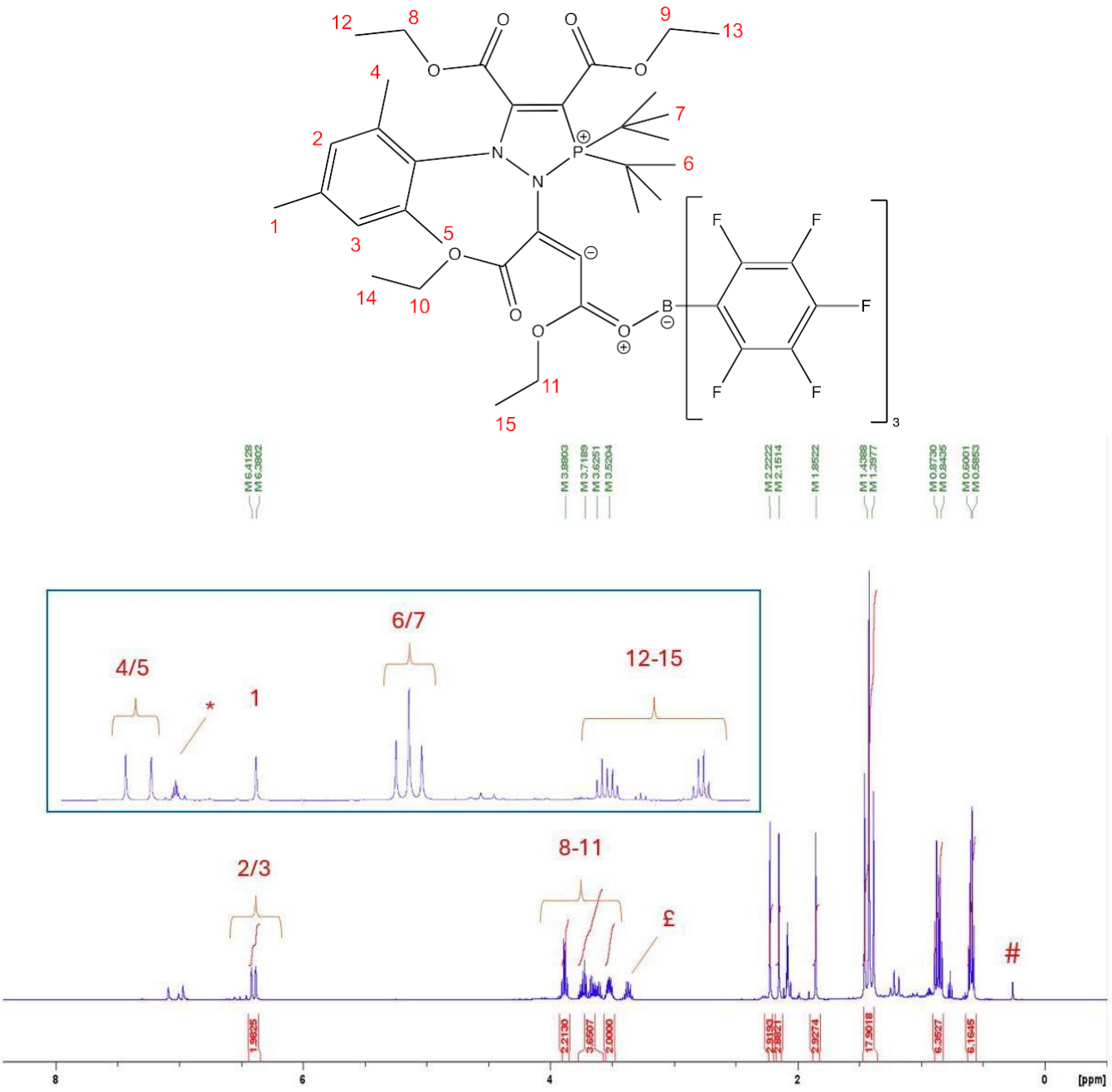

*Figure S64. ^{1}H NMR spectrum of **11** in d_8-toluene. # = residual silicone grease. £ = residual diethylacetylene dicarboxylate. The spectrum is calibrated to the residual Ph-CHD_2 peak at 2.08 ppm, marked with *.*

The peaks corresponding to 6/7 appear as a triplet, but are actually two overlapping doublets; similarly, the peaks corresponding to 12-15 are overlapping triplets. Both these assignments were confirmed by running the same spectrum again at different frequencies (400 vs 500 MHz); in both cases, this gave deconvolution of the peaks into their constituent doublets/triplets.

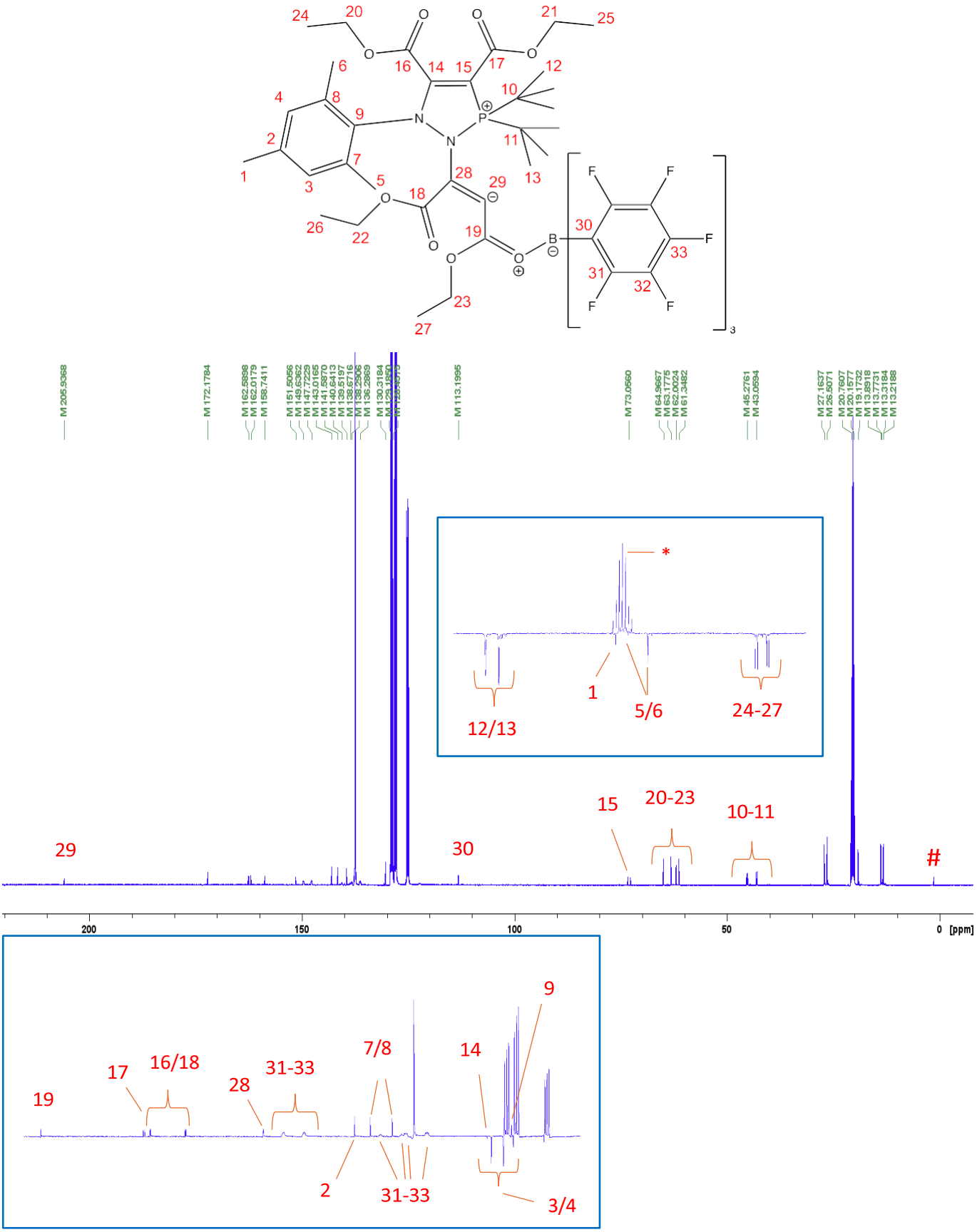

*Figure S65. $^{13}C\{^{1}H\}$ NMR spectrum of **11** in d_8-toluene. * = CD_3 peak of d_8-toluene peak, 20.43 ppm, to which the spectrum is calibrated. The insets show a JMOD spectrum for the same compound, in which certain peaks are much more visible. # = residual silicone grease, 1.37 ppm.*

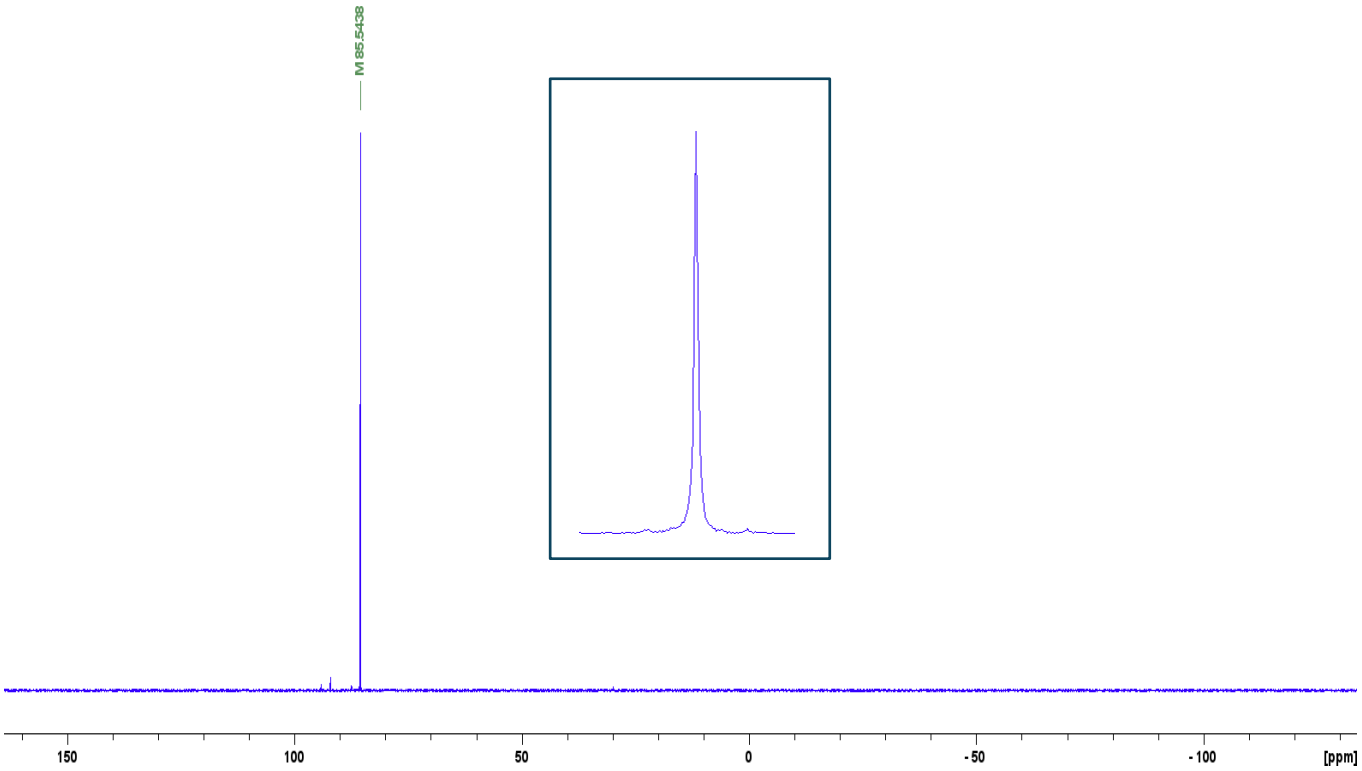

*Figure S66. $^{31}P\{^{1}H\}$ NMR spectrum of **11** in d_8-toluene. Figure inside the blue box is zoomed in to show the splittings of the peak.*

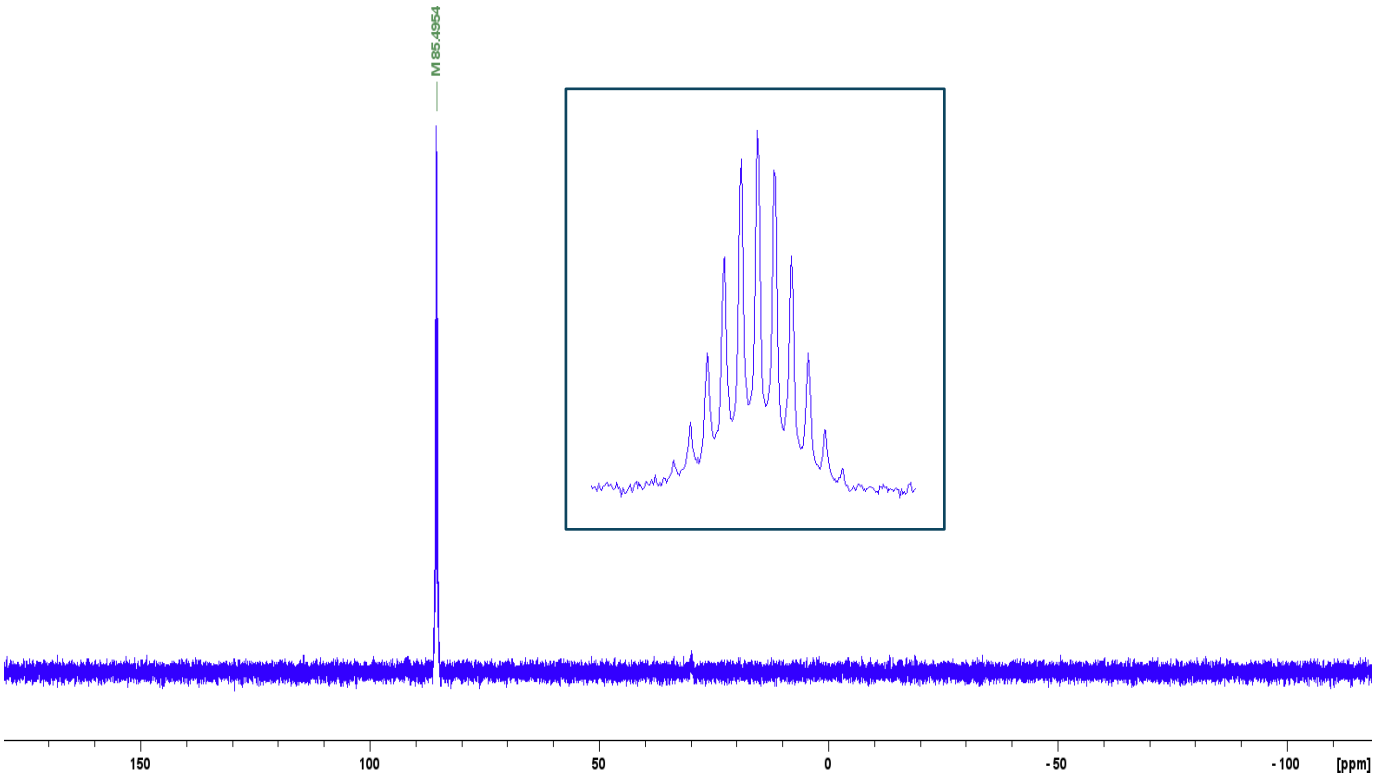

*Figure S67. ^{31}P NMR spectrum of **11** in d_8-toluene. Figure inside the blue box is zoomed in to show the splittings of the peak*

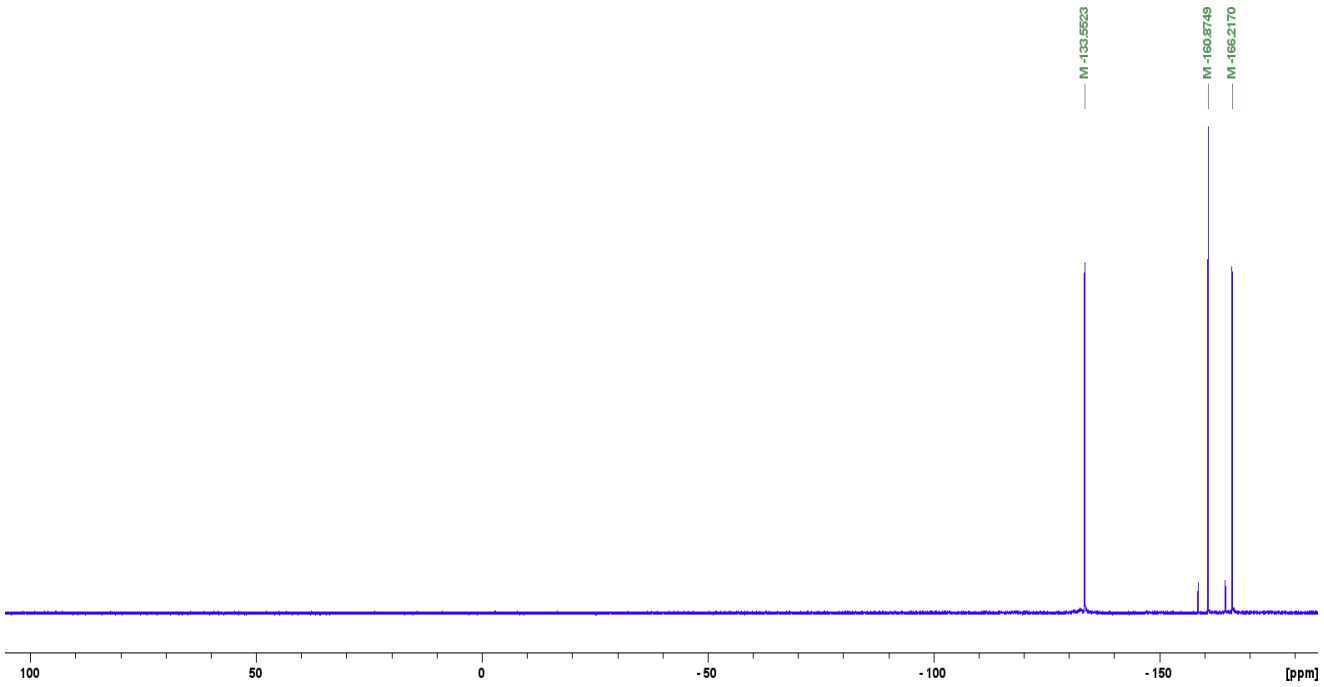

*Figure S68. $^{19}F\{^{1}H\}$ NMR spectrum of **11** in d_8-toluene.*

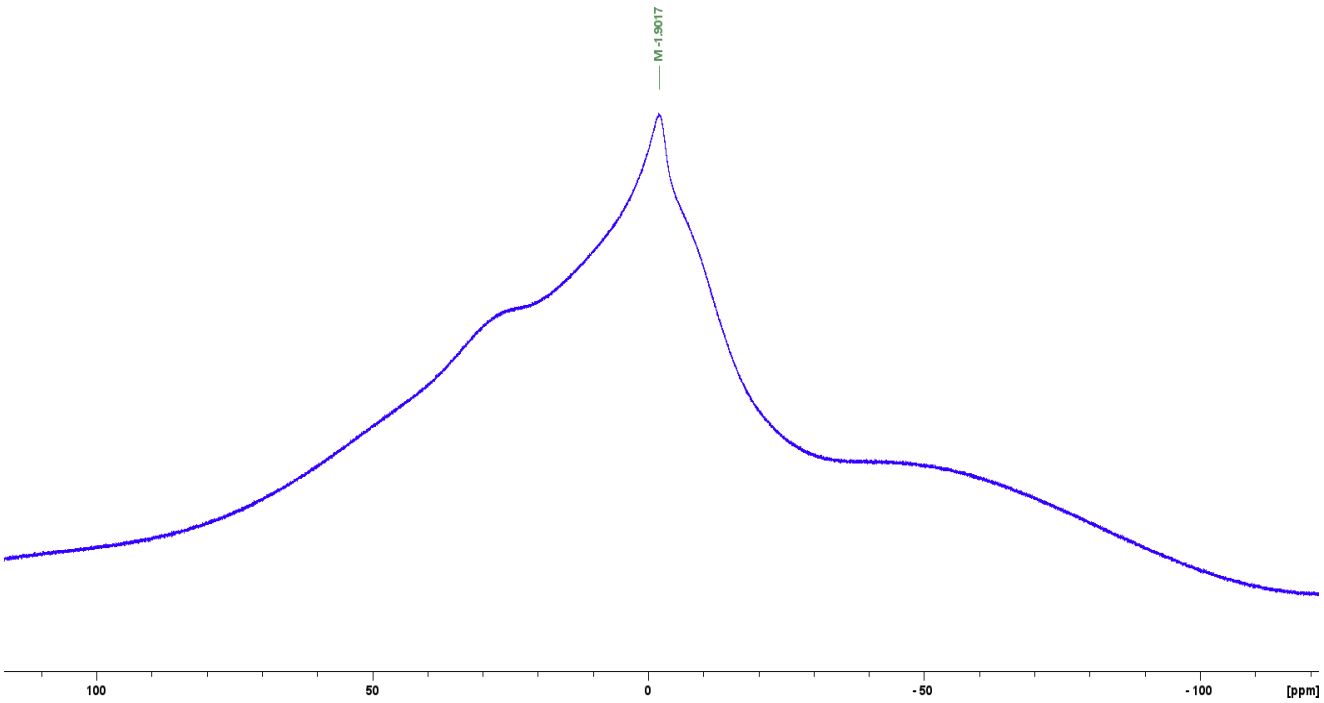

*Figure S69. $^{11}B\{^{1}H\}$ NMR spectrum of **11** in d_8-toluene.*

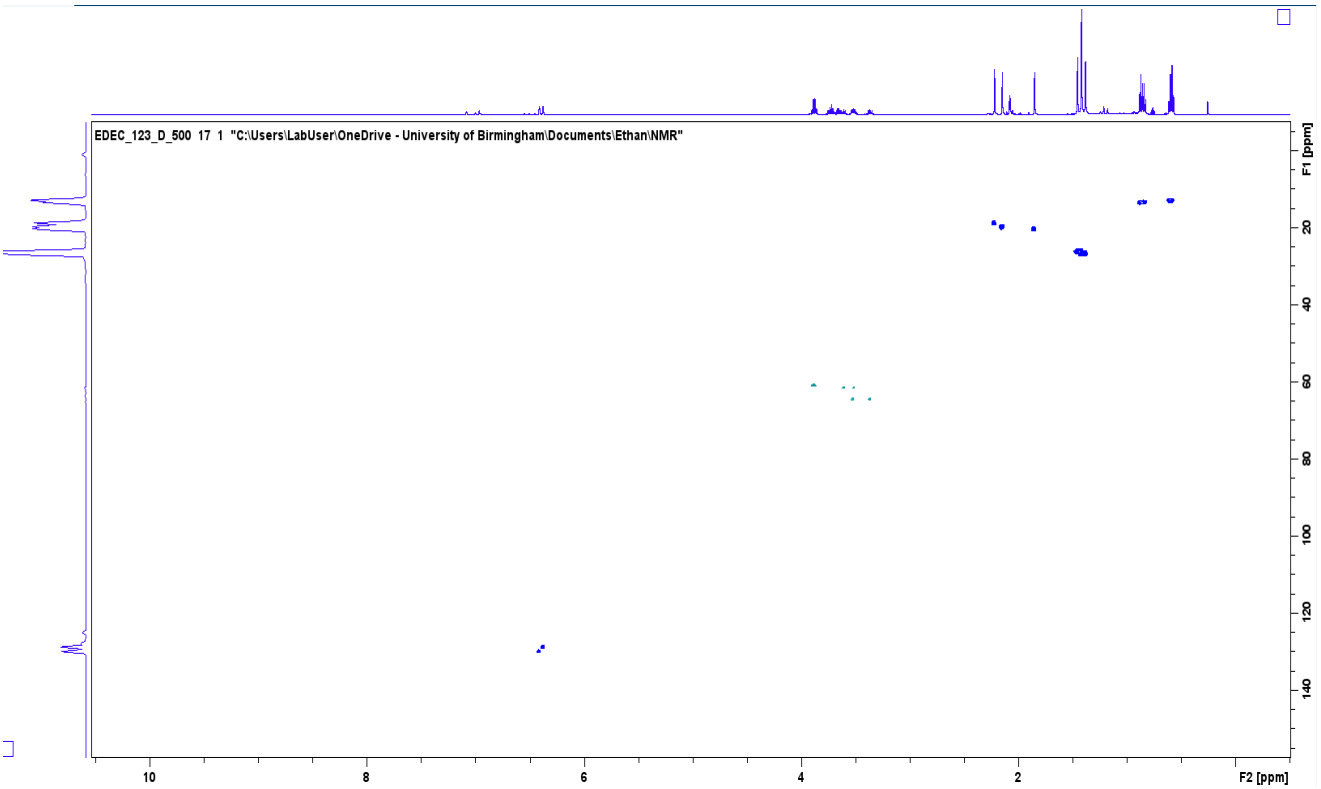

*Figure S70. 2D ^{1}H-^{13}C HSQC NMR spectrum of **11** in d_8-toluene. HSQC was vital for carbon assignments.*

S2.2. UVVis Spectra

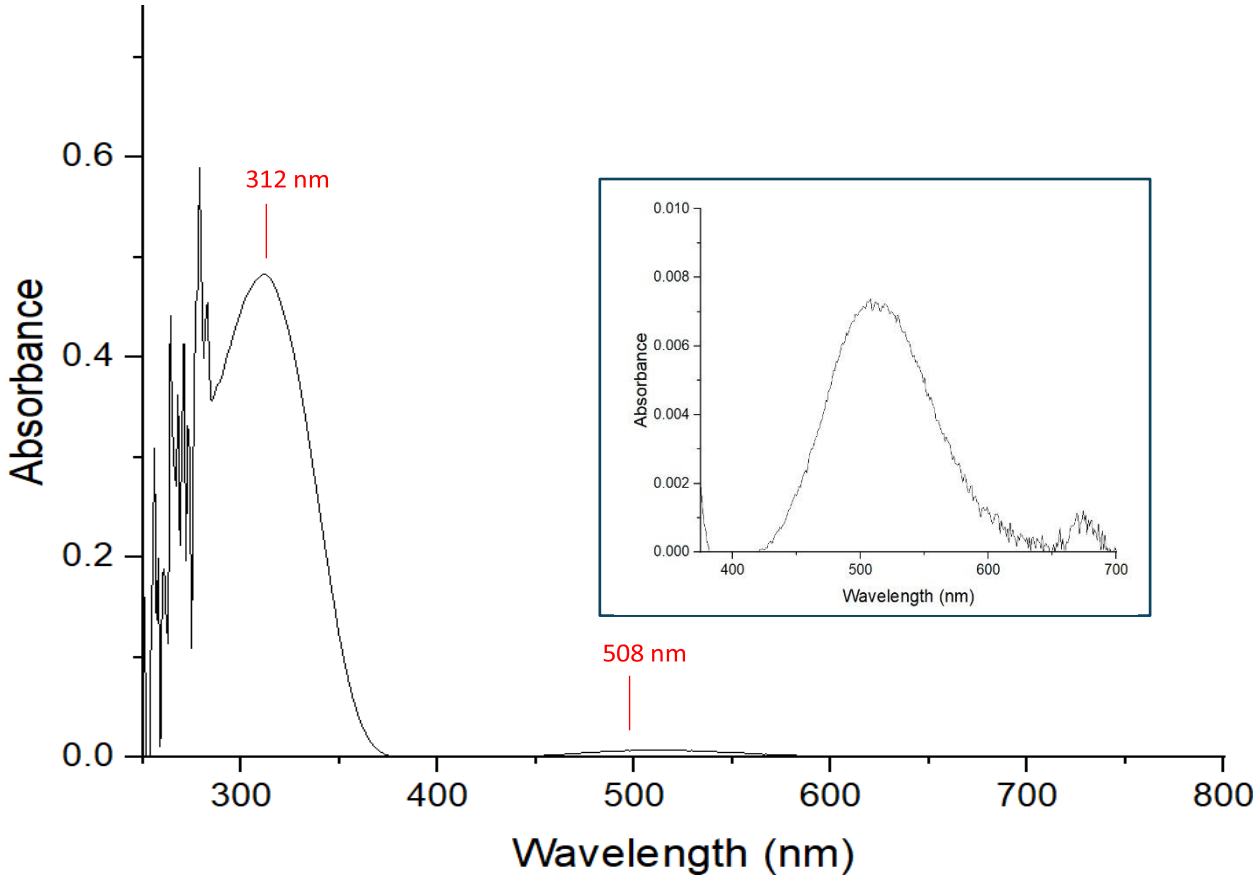

*Figure S71. UV/Vis Spectrum of **1.BH3** (5 x 10^{-5} M in toluene). Figure inside the blue box is zoomed in to show the absorbance peak at 508 nm.*

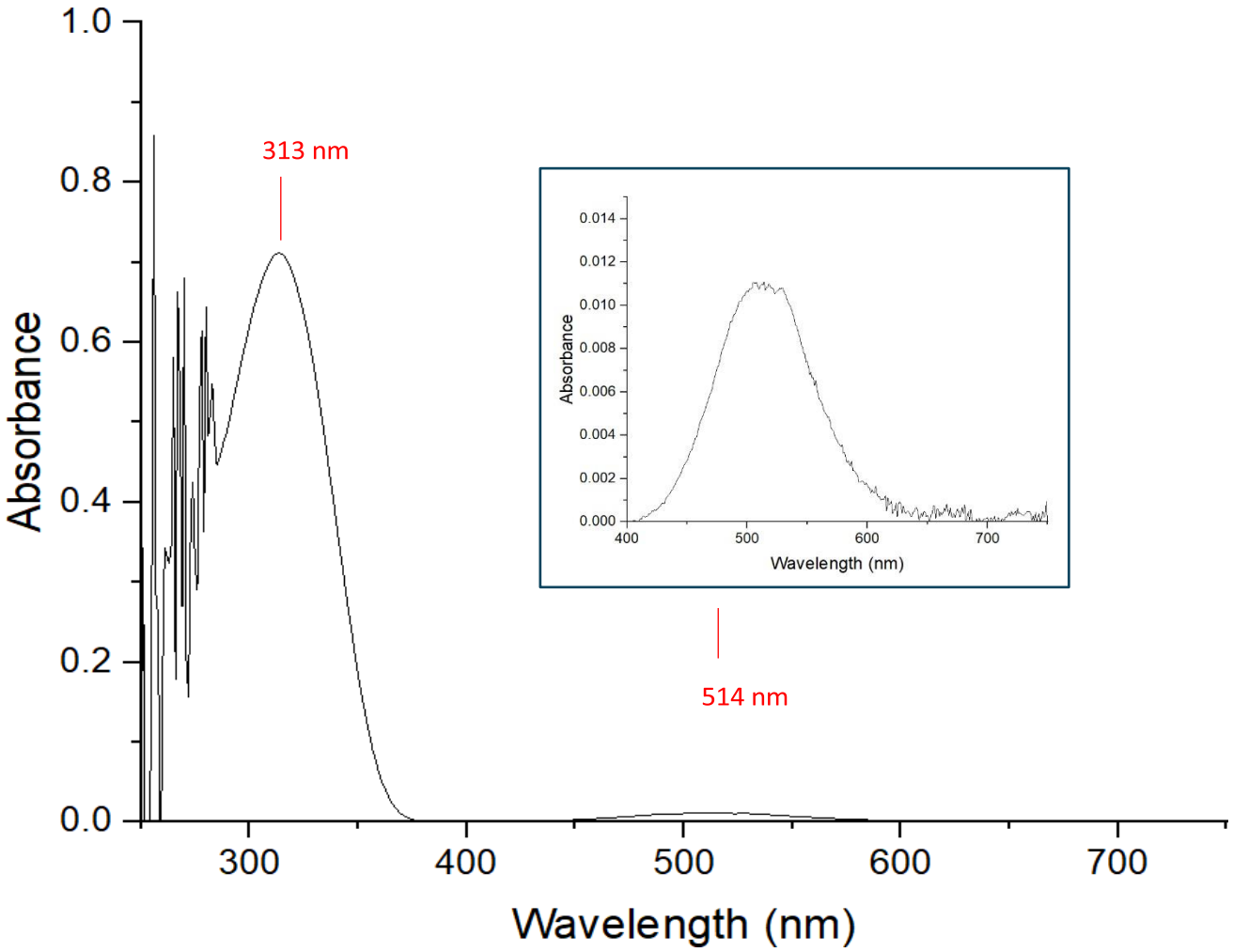

*Figure S72. UV/Vis Spectrum of **2.BH3** (5 x 10^{-5} M in toluene). Figure in the blue box is zoomed in to show the small absorbance peak at 513.99 nm.*

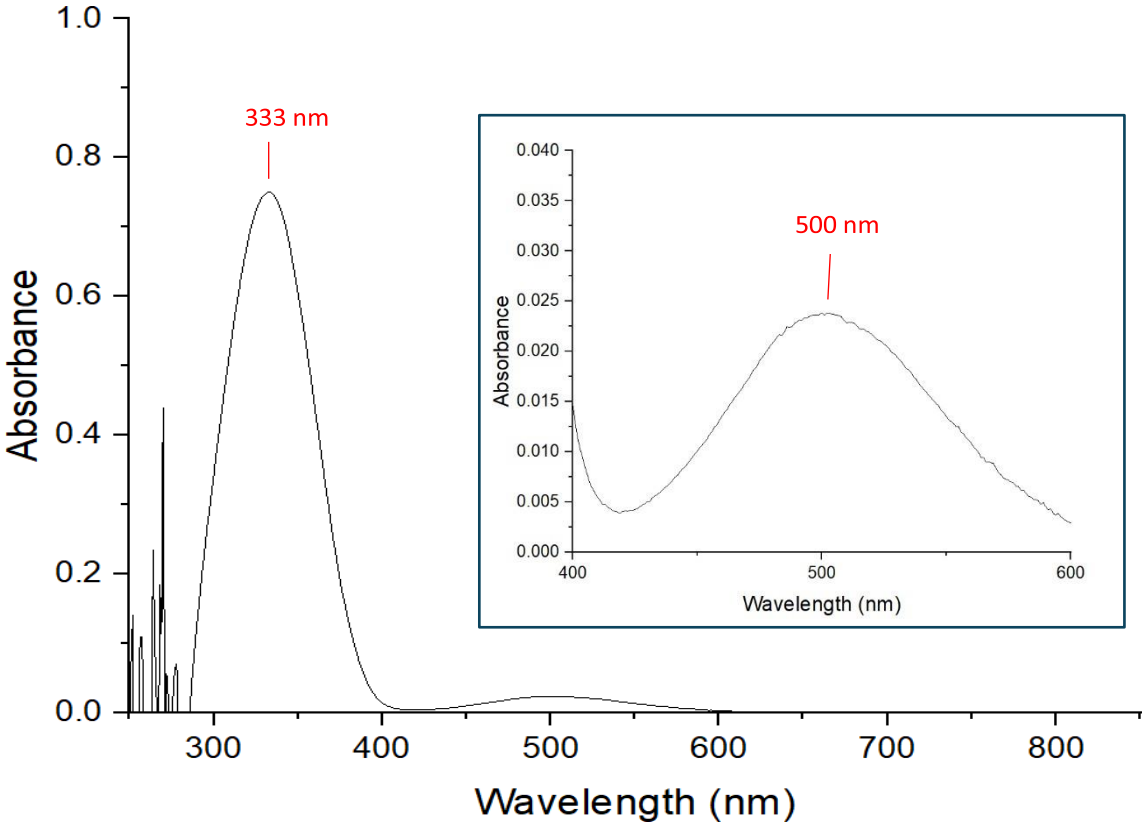

*Figure S73. UV/Vis Spectrum of **1** (5 x 10^{-5} M in toluene). Figure inside the blue box is zoomed in to show the absorbance peak*

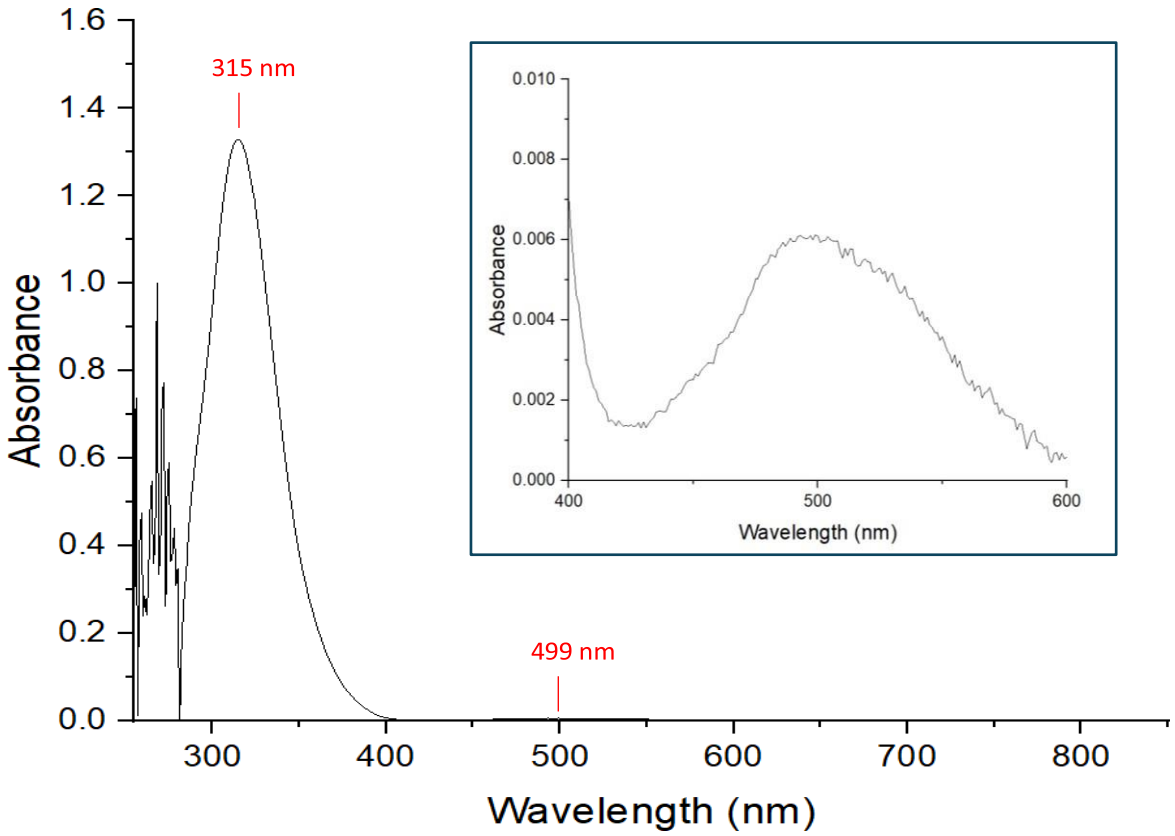

*Figure S74. UV/Vis Spectrum of **2** (5 x 10^{-5} M in toluene). Figure inside the blue box is zoomed in to show the absorbance peak at 499 nm.*

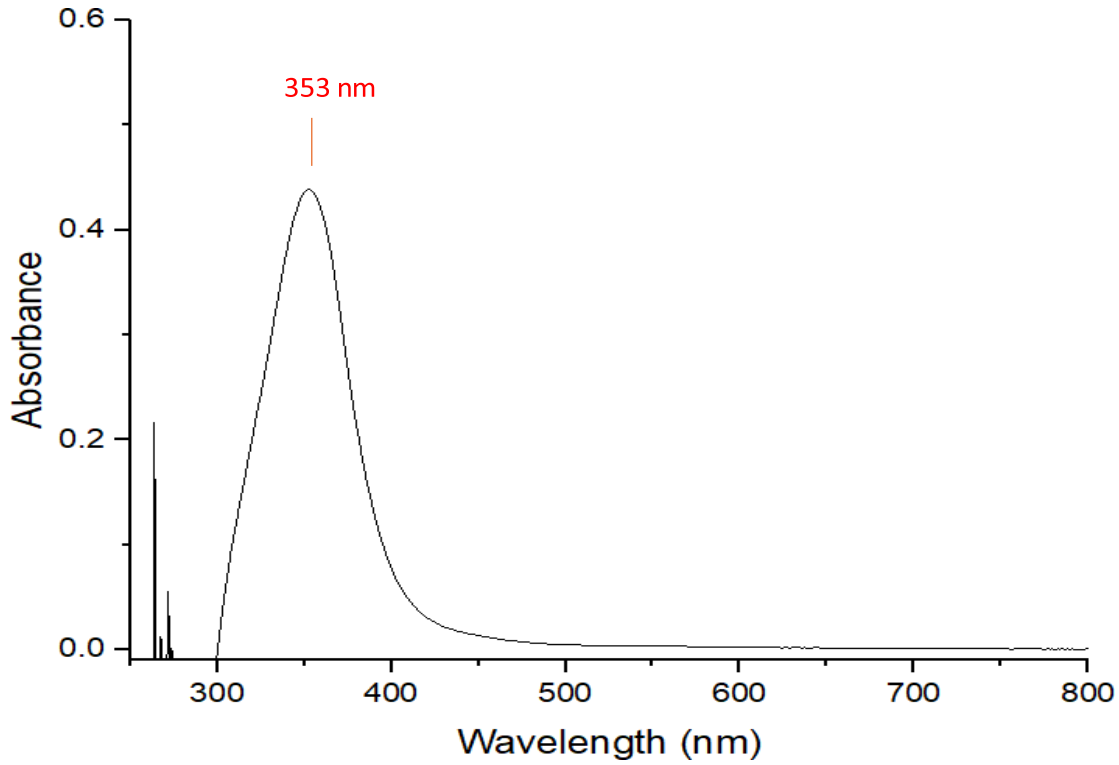

*Figure S75. UV/Vis Spectrum of **4** (5 x 10^{-5} M in toluene).*

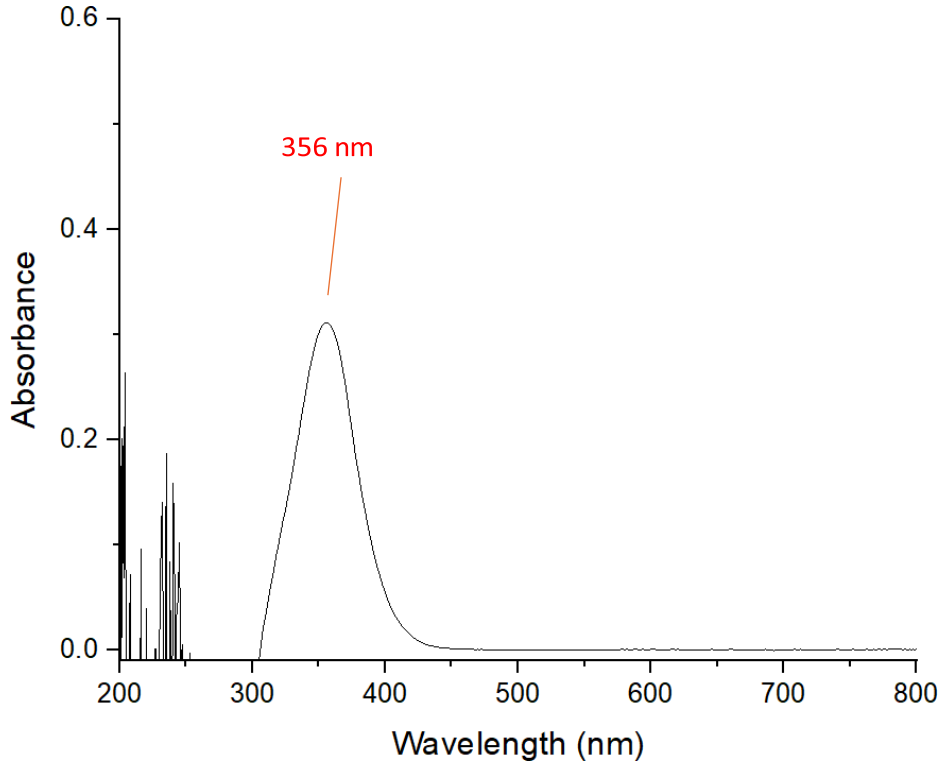

*Figure S76. UV/Vis Spectrum of **5** (5 x 10^{-5} M in toluene).*

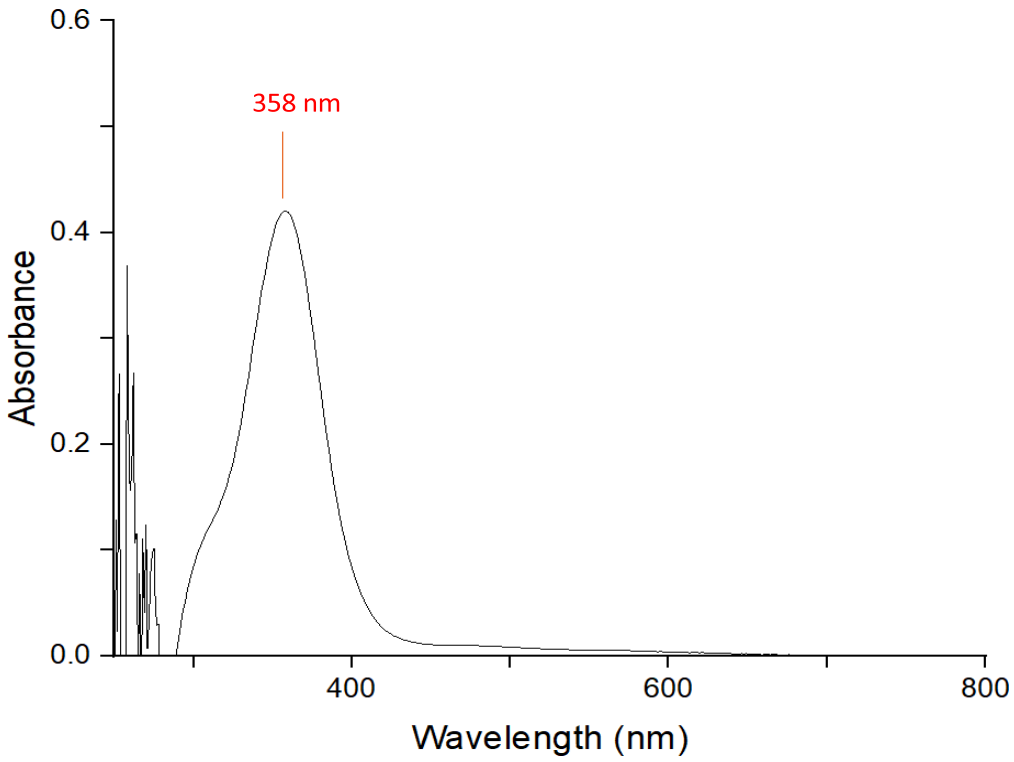

*Figure S77. UV/Vis Spectrum of **6** (5 x 10^{-5} M in toluene).*

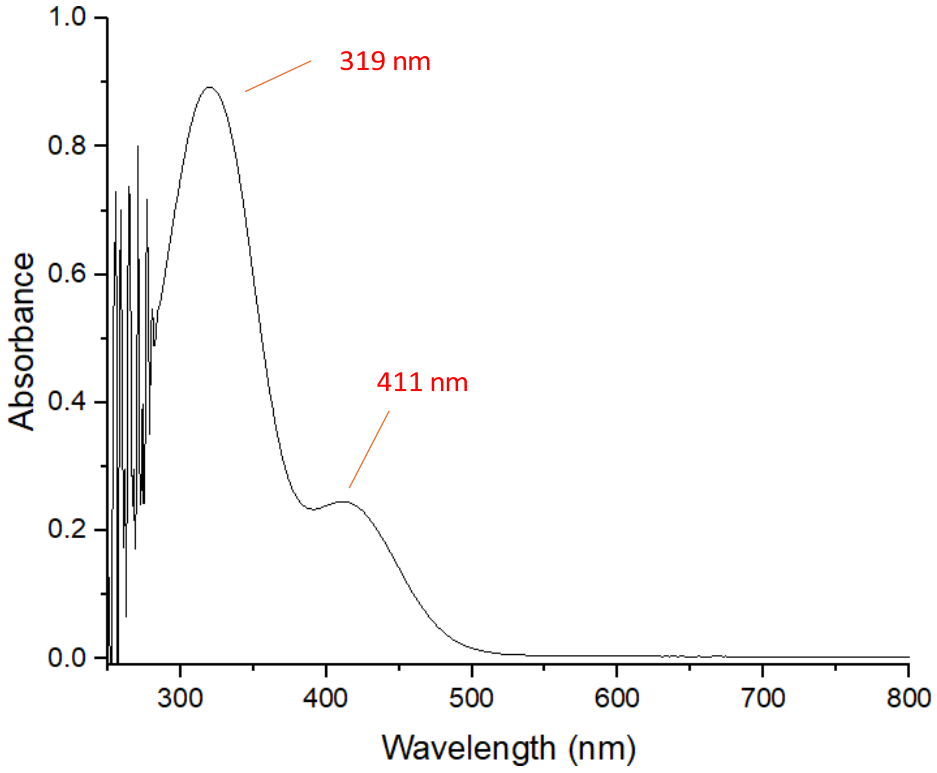

*Figure S78. UV/Vis Spectrum of **7** (5 x 10^{-5} M in toluene).*

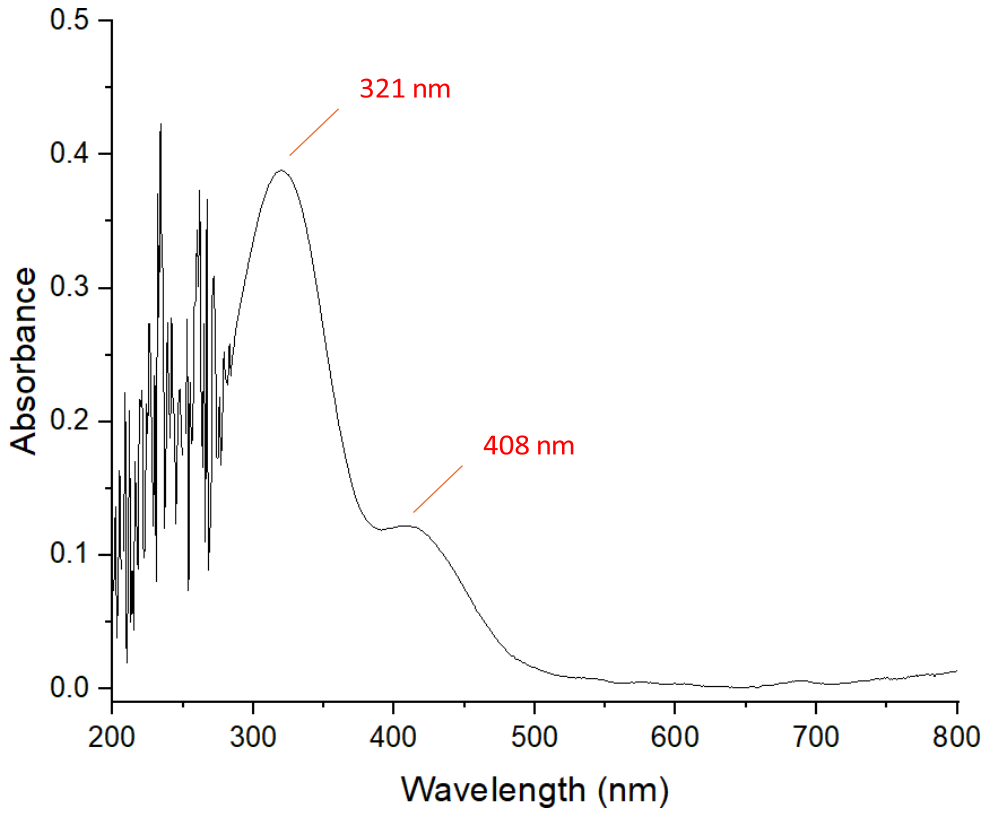

*Figure S79. UV/Vis Spectrum of **7·BCF** (5 x 10^{-5} M in toluene).*

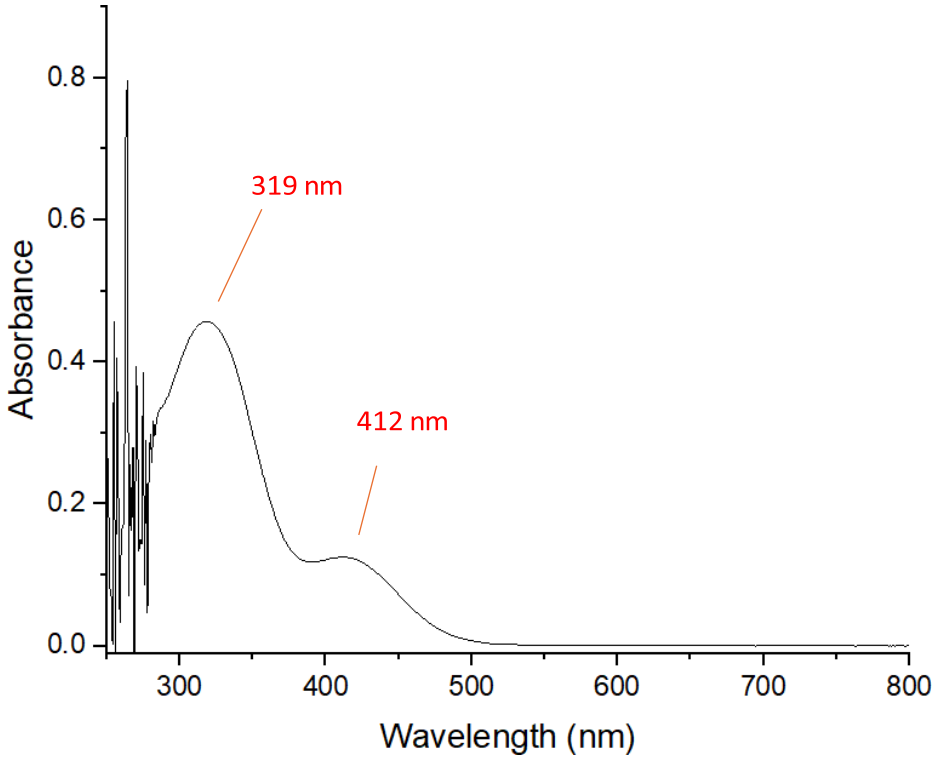

*Figure S80. UV/Vis Spectrum of **8** (5 x 10^{-5} M in toluene).*

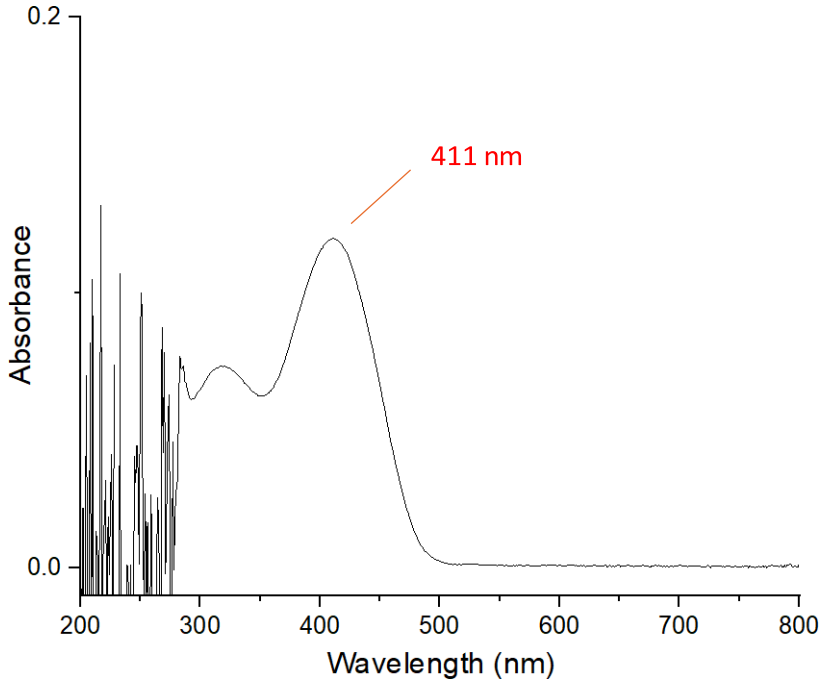

*Figure S81. UV/Vis Spectrum of **9** (5 x 10^{-5} M in toluene).*

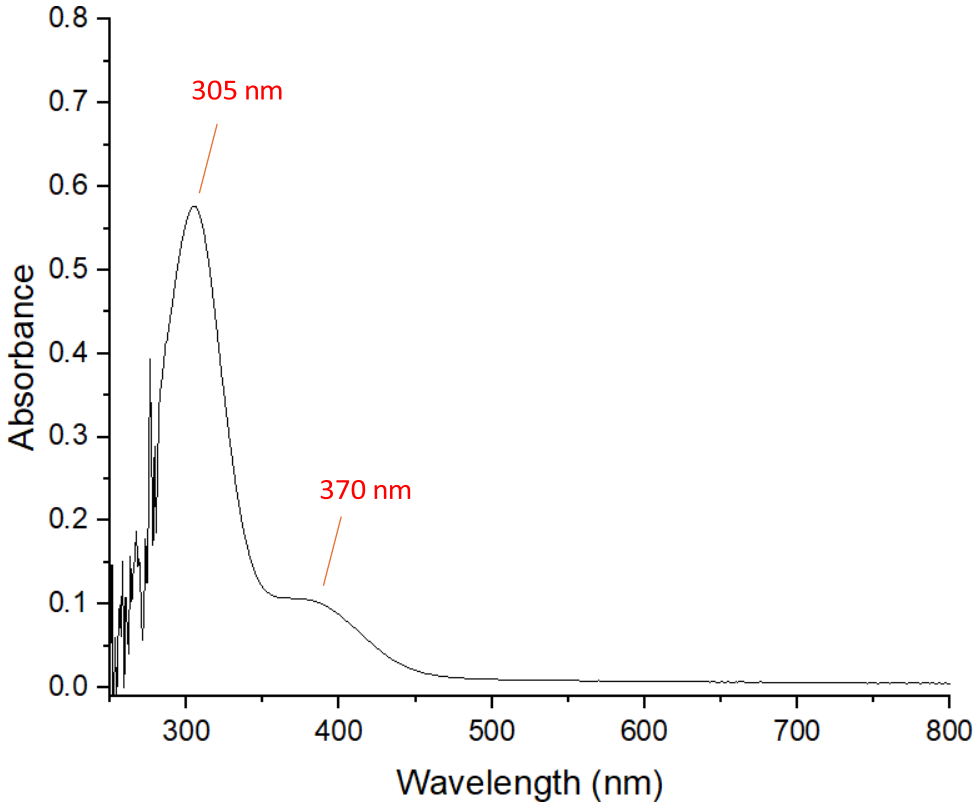

*Figure S82. UV/Vis Spectrum of **10** (5 x 10^{-5} M in toluene).*

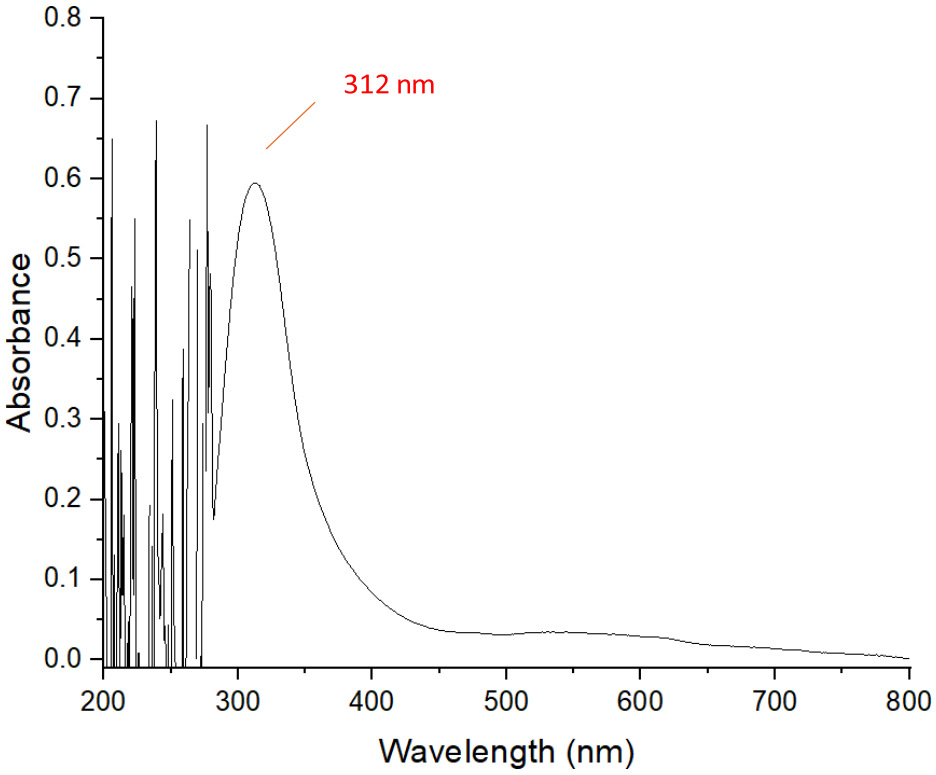

*Figure S83. UV/Vis Spectrum of **11** (5 x 10^{-5} M in toluene).*

S2.3. Mass Spectra

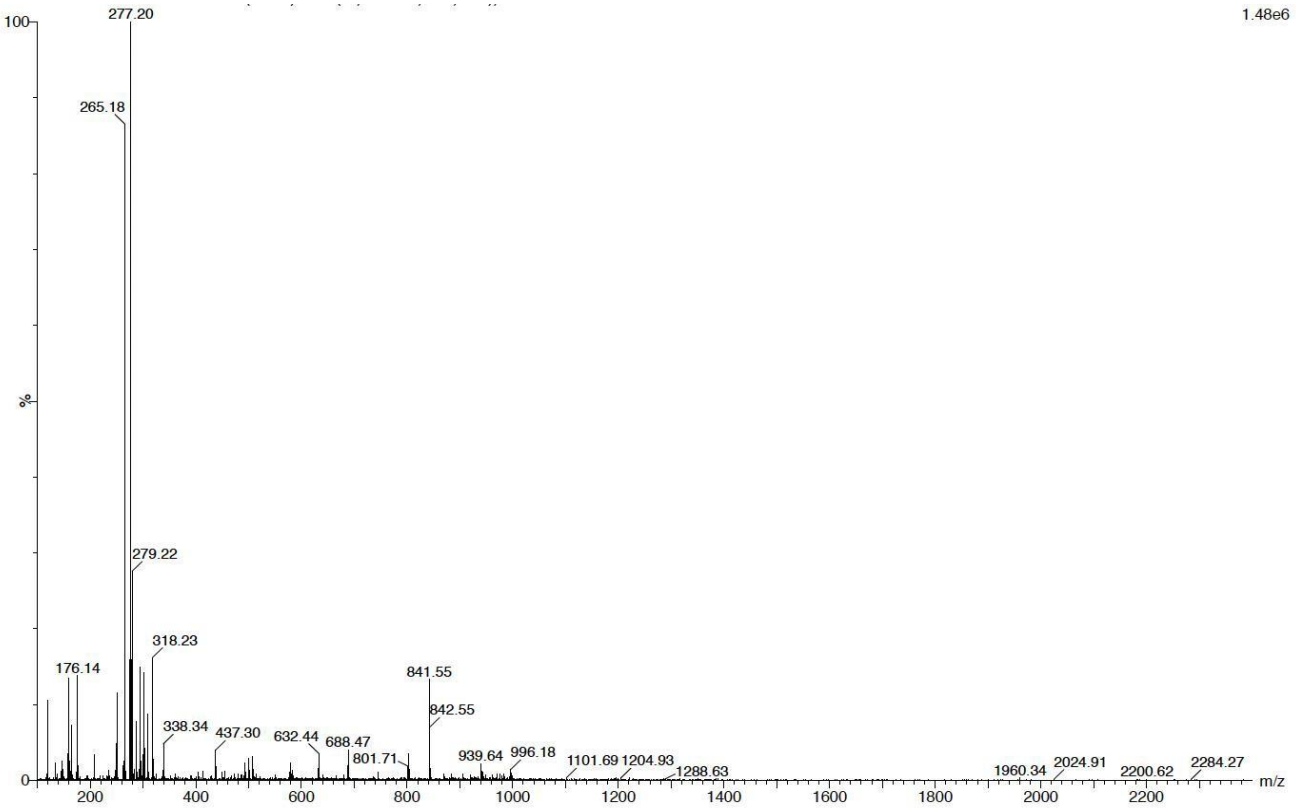

*Figure S84. Mass spectrum of **1.BH3** in acetonitrile.*

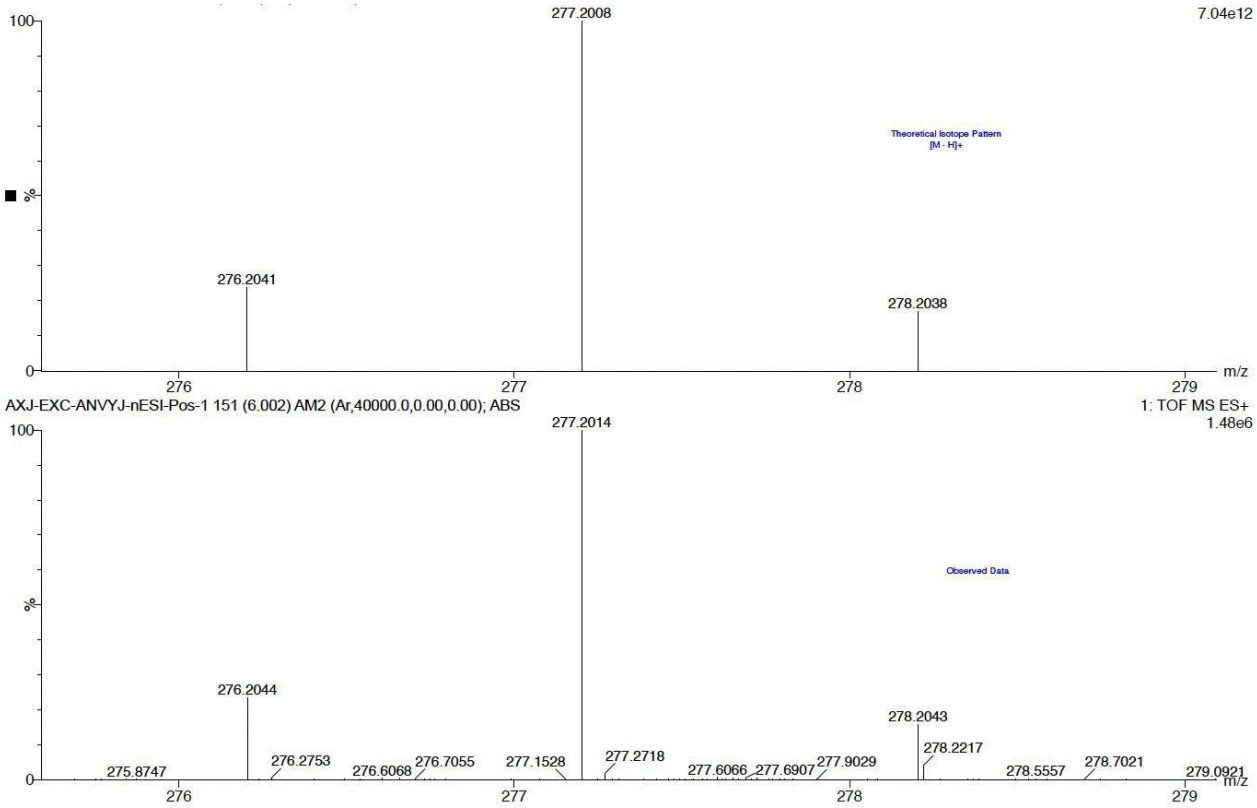

*Figure S85. High-res mass spectrum of **1.BH3** in acetonitrile. Top shows the theoretical isotope pattern based on {M - H}$^+$; bottom shows the observed data.*

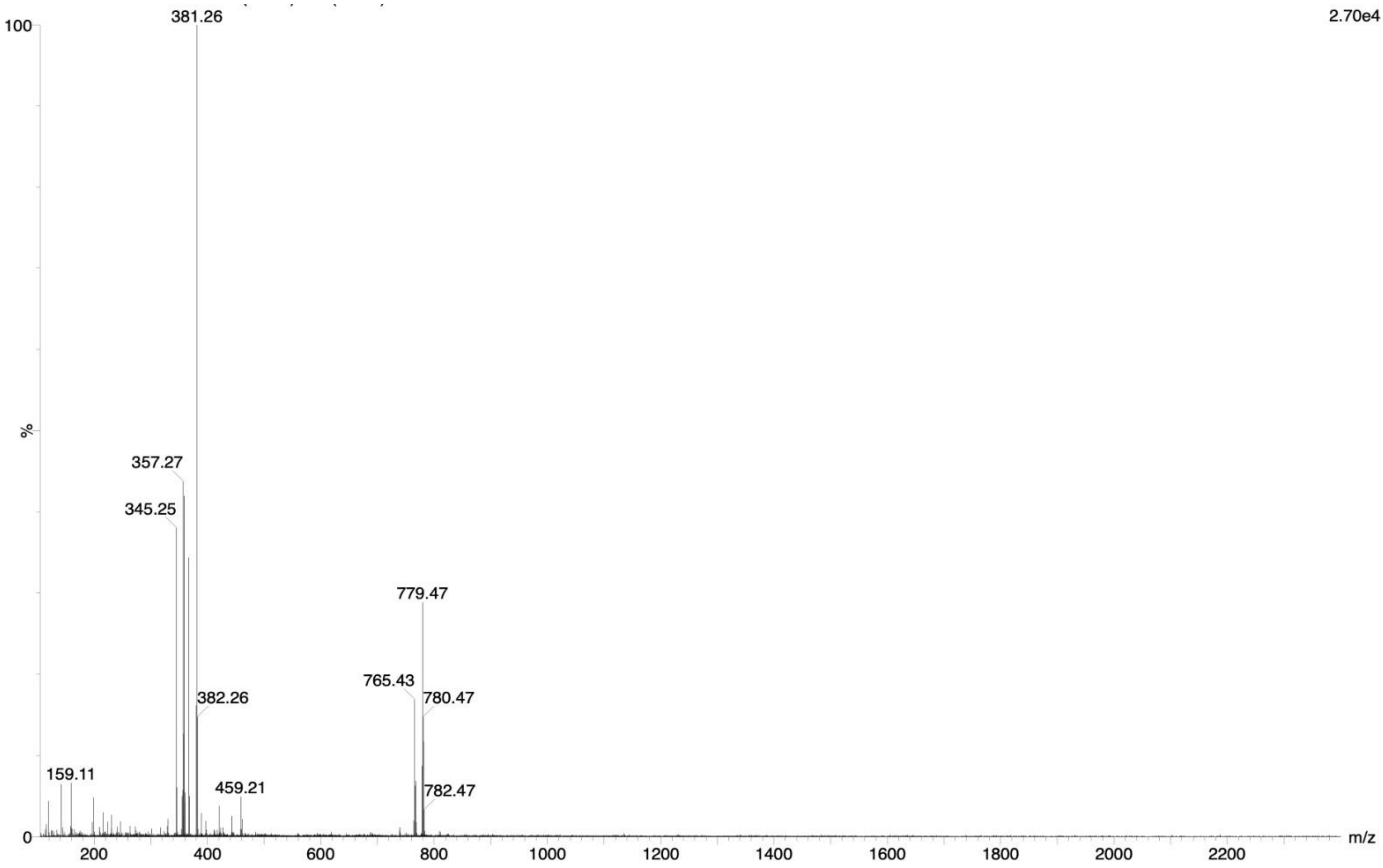

*Figure S86. Mass spectrum of **2.BH3** in acetonitrile.*

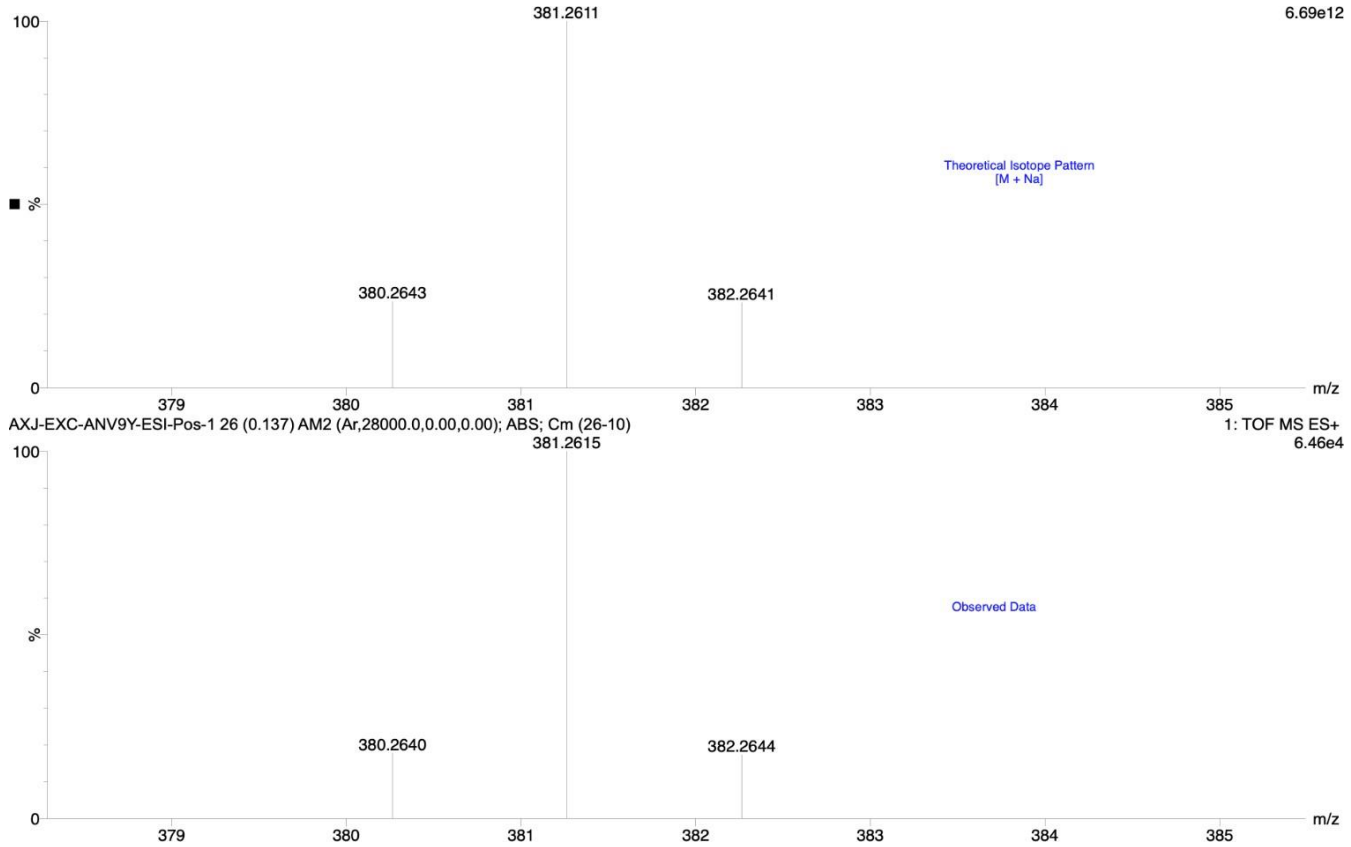

*Figure S87. High-res mass spectrum of **2.BH3** in acetonitrile. Top shows the theoretical isotope pattern based on $[M + Na]^+$; bottom shows the observed data.*

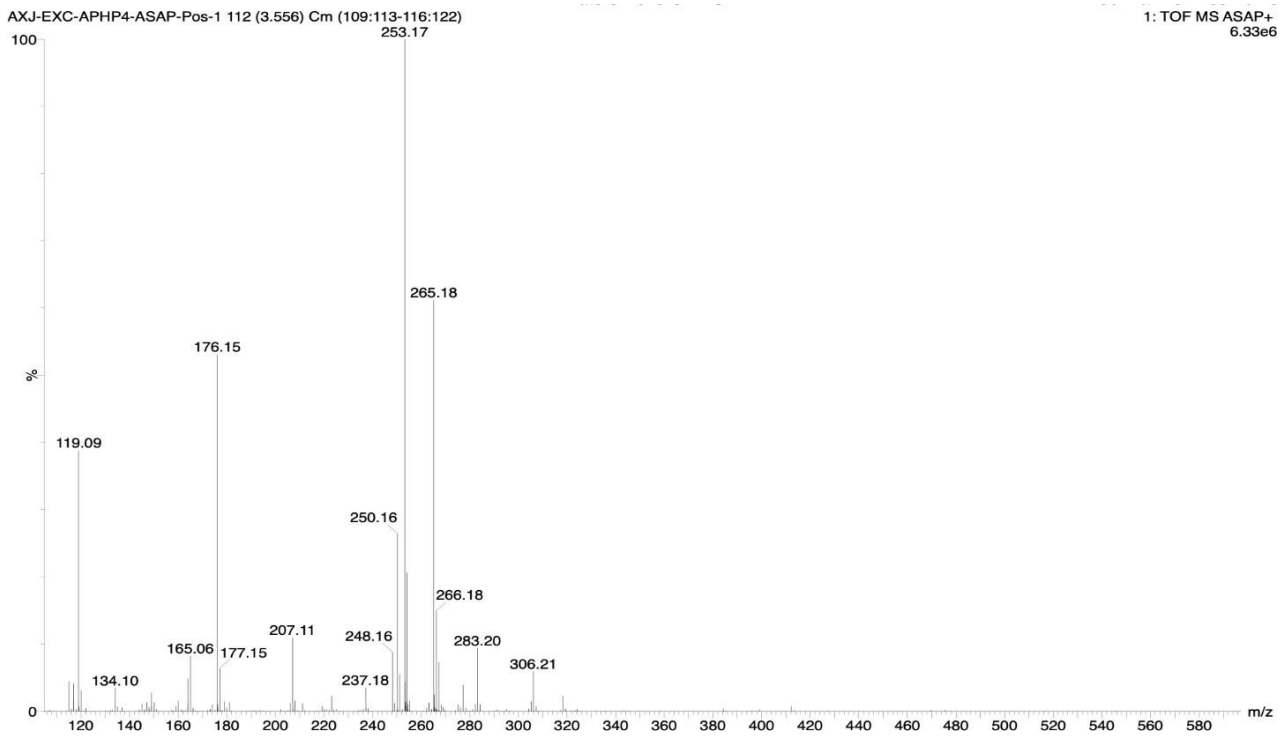

*Figure S88. Mass spectrum of **1** in acetonitrile.*

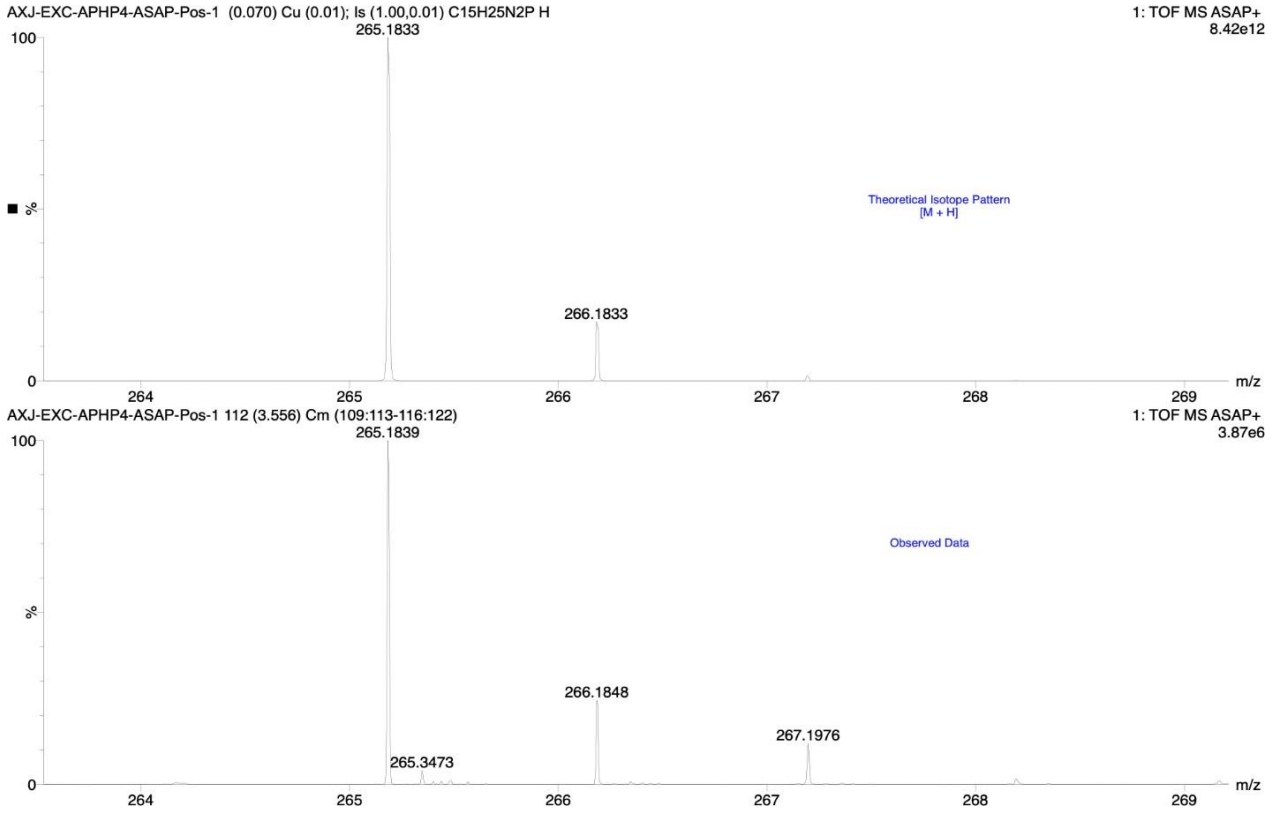

*Figure S89. High-res mass spectrum of **1** in acetonitrile. Top shows the theoretical isotope pattern based on {M + H}$^+$; bottom shows the observed data.*

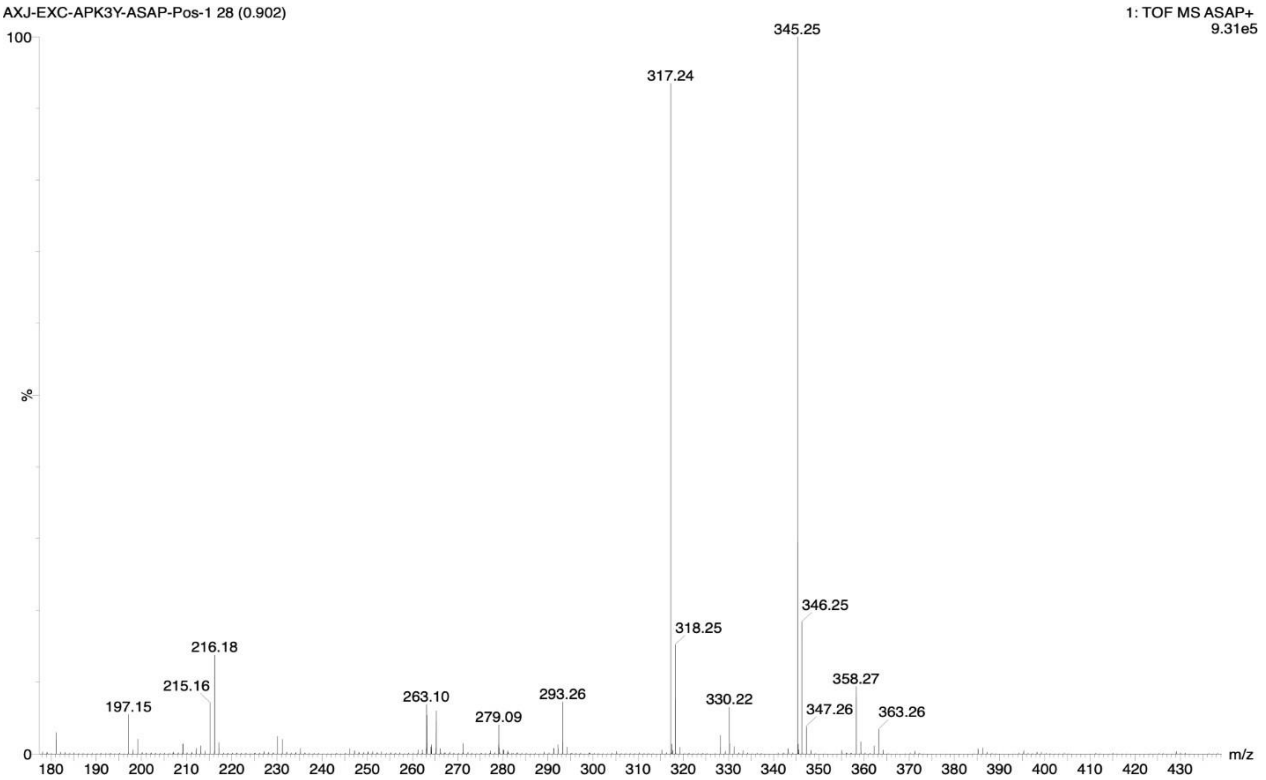

*Figure S90. Mass spectrum of **2** in acetonitrile.*

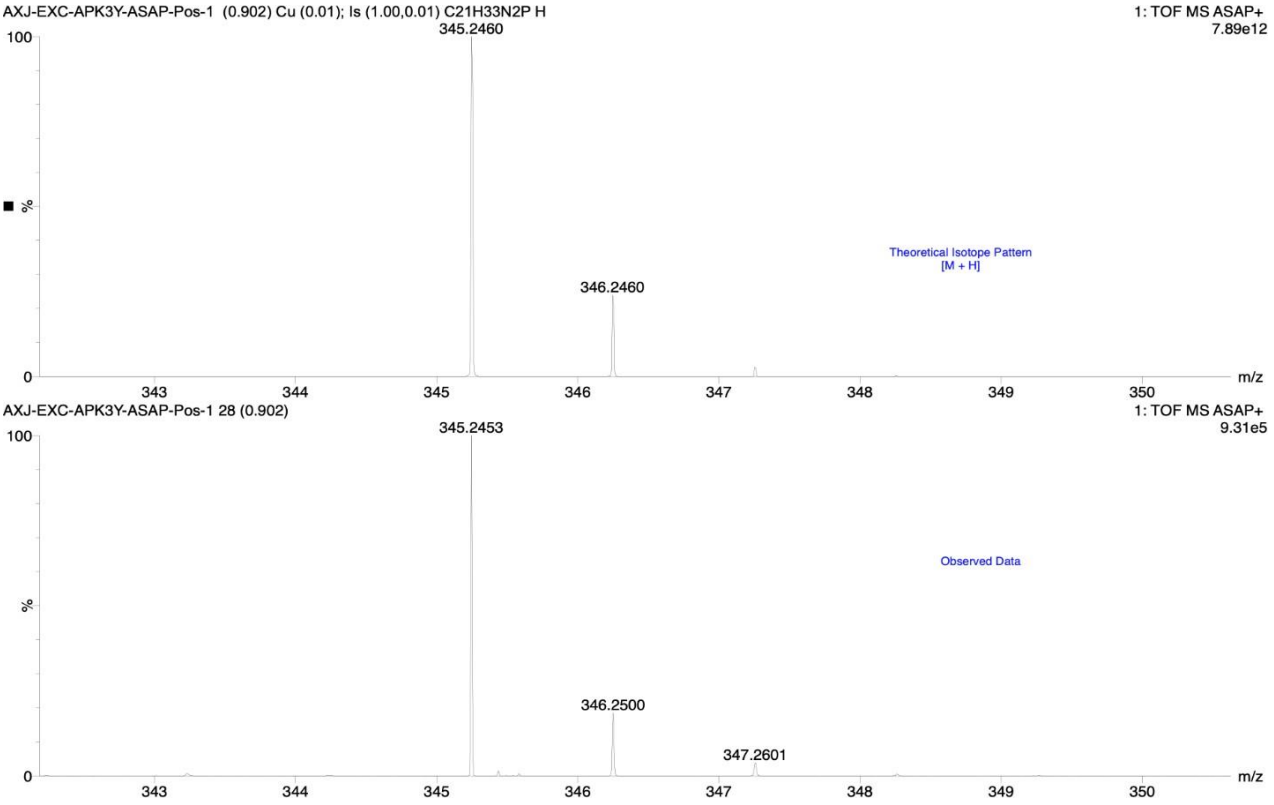

*Figure S91. High-res mass spectrum of **2** in acetonitrile. Top shows the theoretical isotope pattern based on {M + H}$^+$; bottom shows the observed data.*

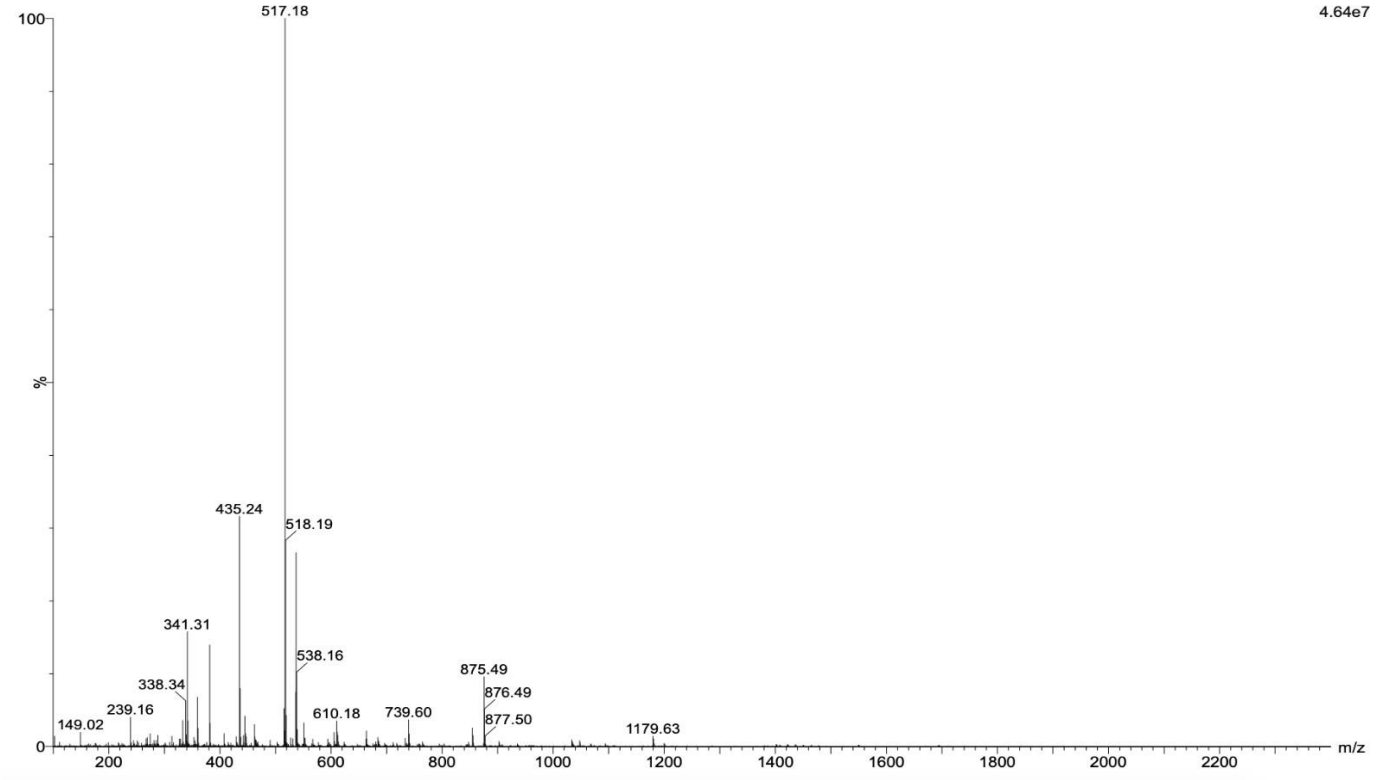

*Figure S92. Mass spectrum of **4** in dichloromethane.*

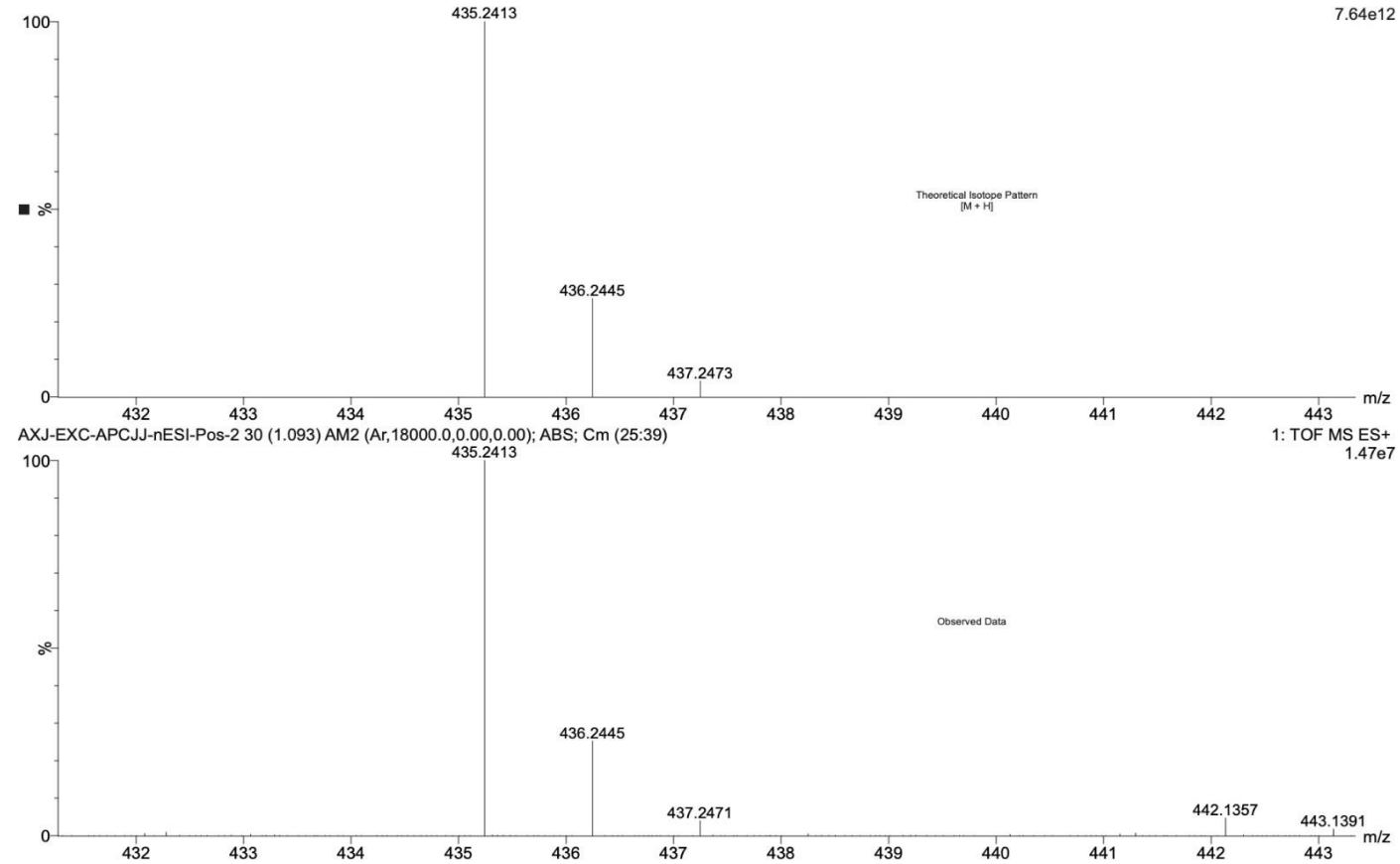

*Figure S93. High-res mass spectrum of **4** in dichloromethane. Top shows the theoretical isotope pattern based on $\{M + H\}^+$; bottom shows the observed data.*

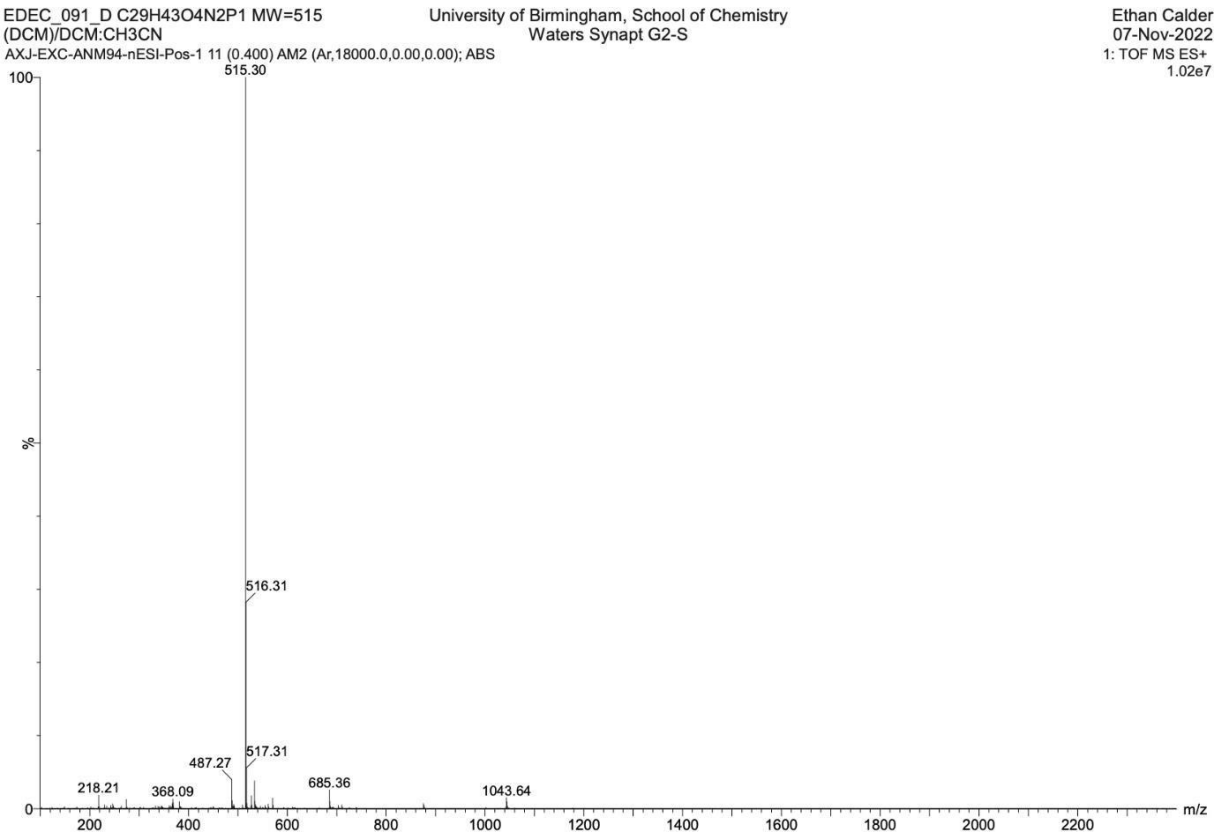

*Figure S94. Mass spectrum of **5** in dichloromethane.*

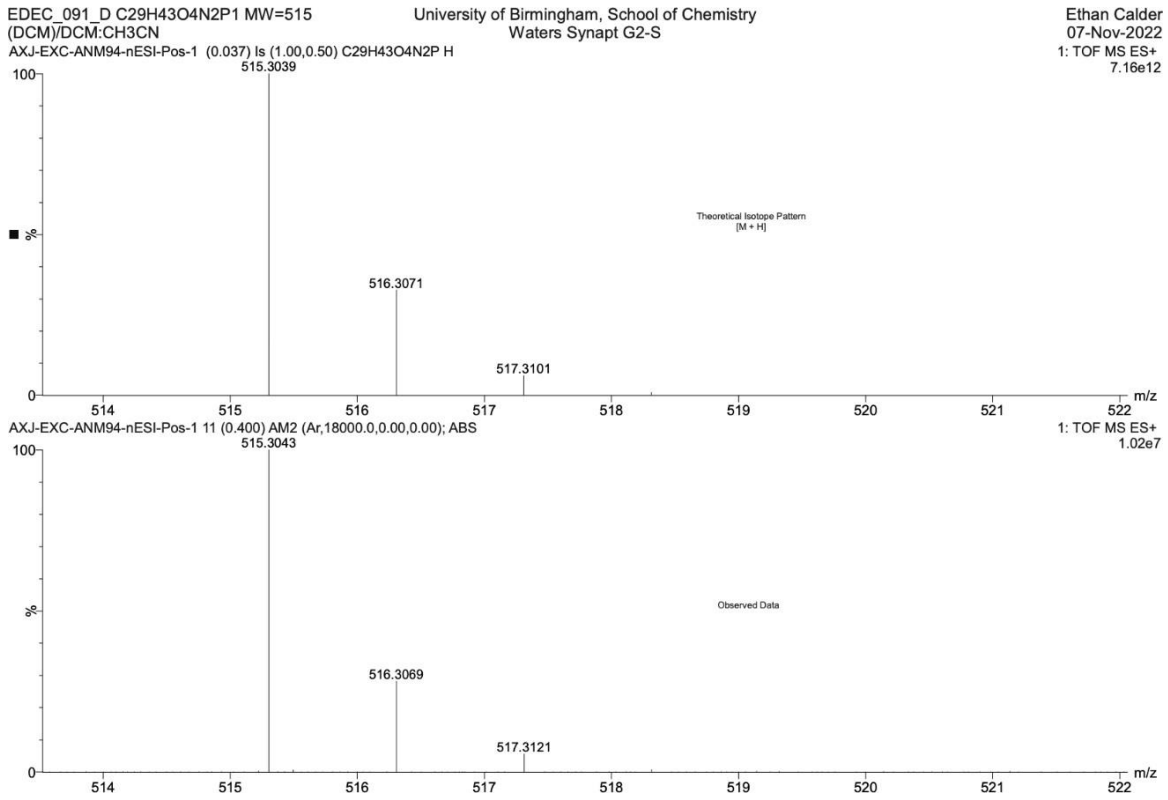

*Figure S95. High-res mass spectrum of **5** in dichloromethane. Top shows the theoretical isotope pattern based on {M + H}$^+$; bottom shows the observed data.*

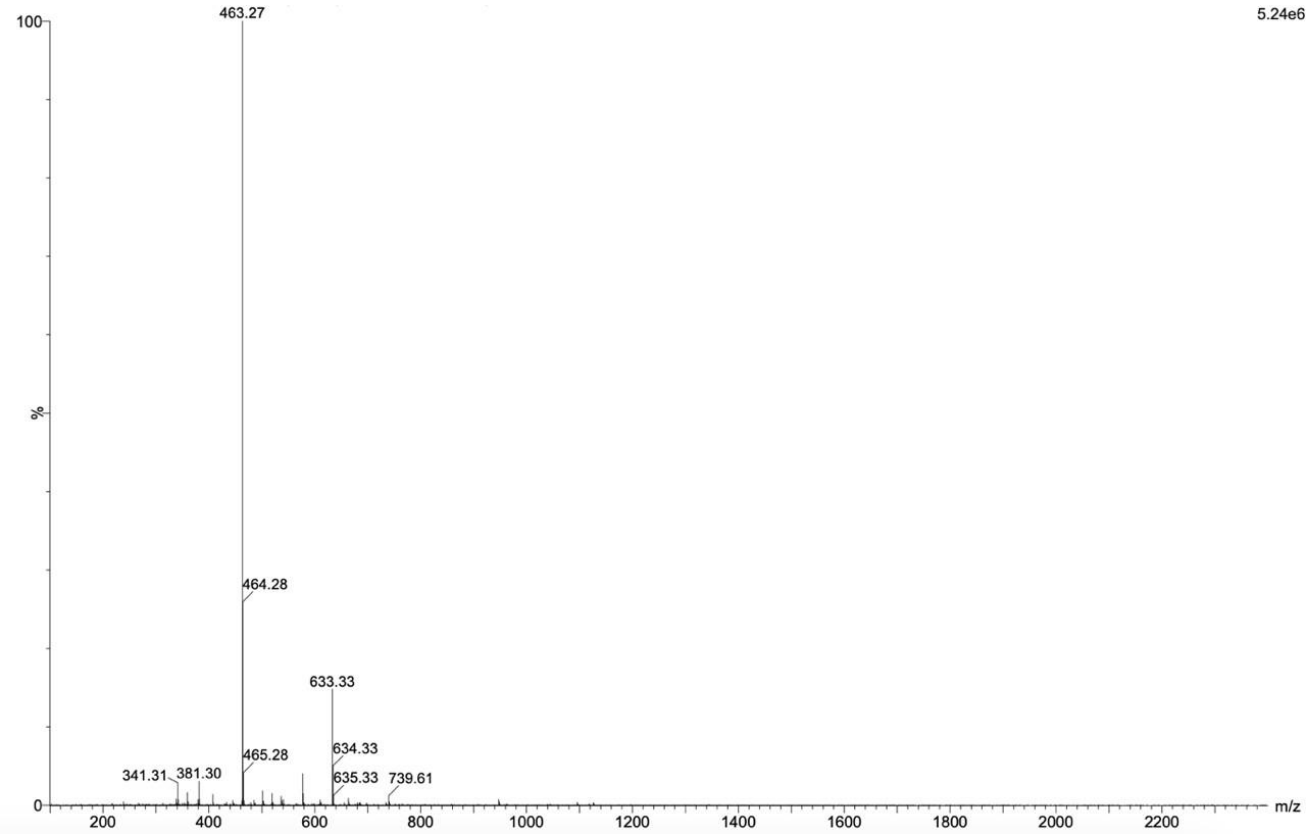

*Figure S96. Mass spectrum of **6** in dichloromethane.*

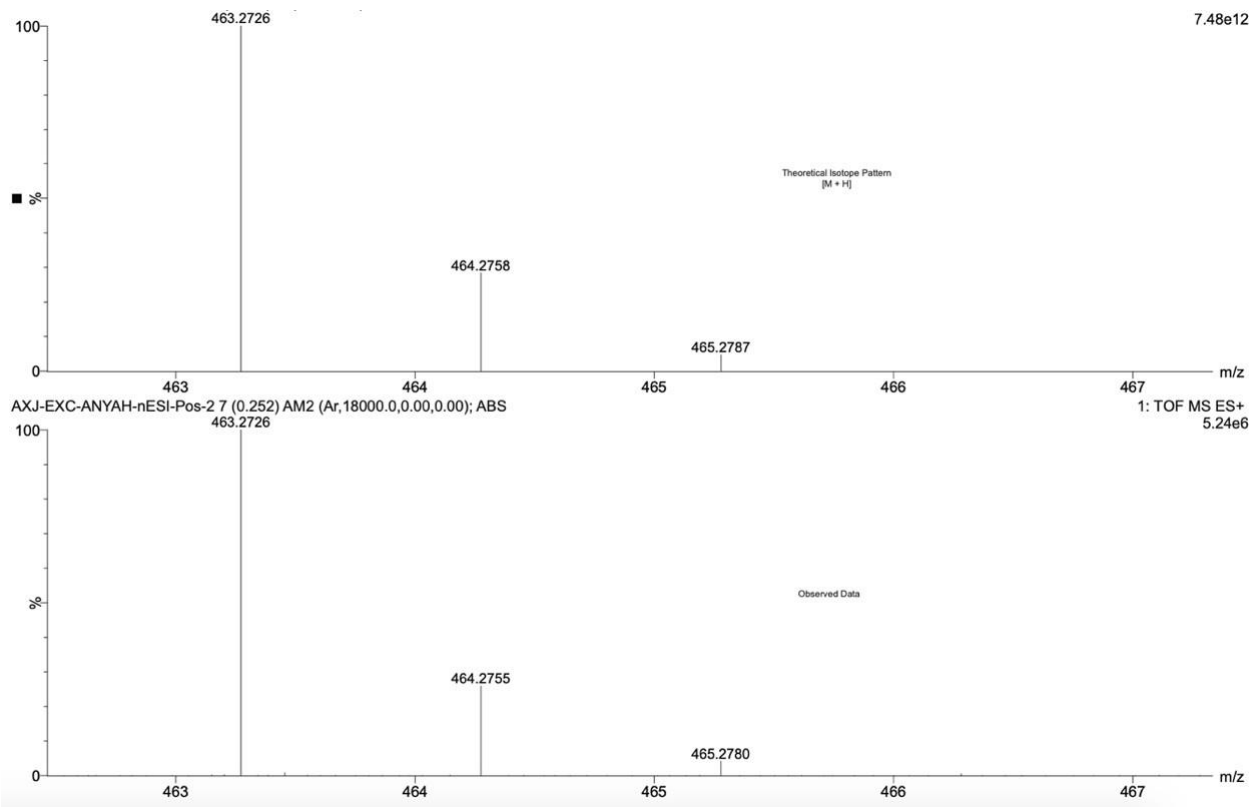

*Figure S97. High-res mass spectrum of **6** in dichloromethane. Top shows the theoretical isotope pattern based on {M - H}$^+$; bottom shows the observed data.*

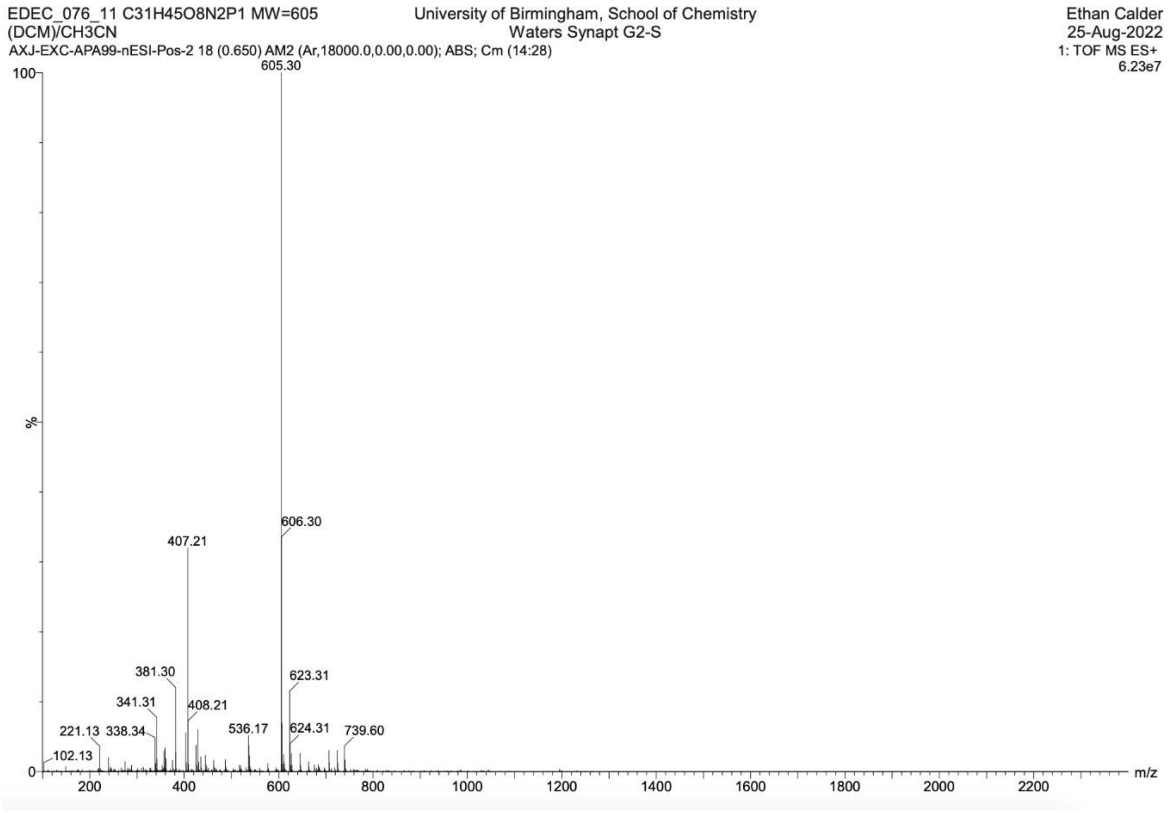

*Figure S98. Mass spectrum of **7** in dichloromethane*

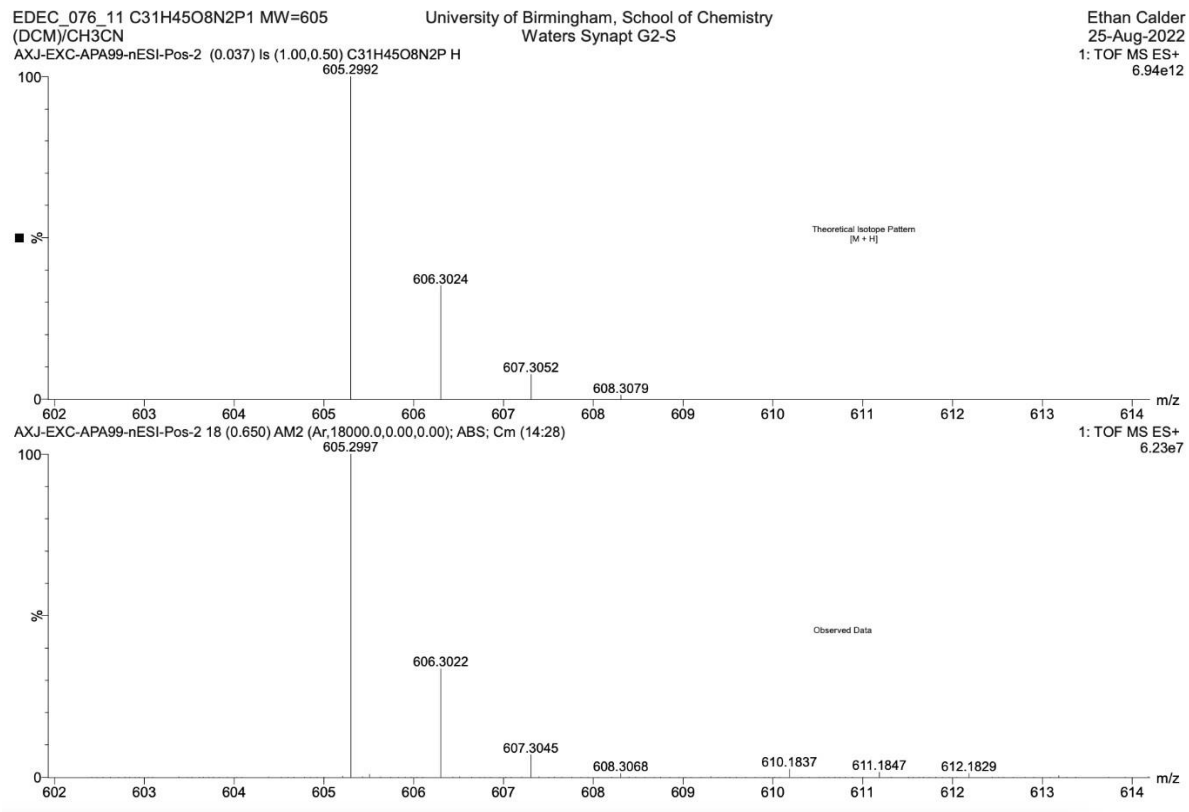

*Figure S99. High-res mass spectrum of **7** in dichloromethane. Top shows the theoretical isotope pattern based on {M + H}$^+$; bottom shows the observed data.*

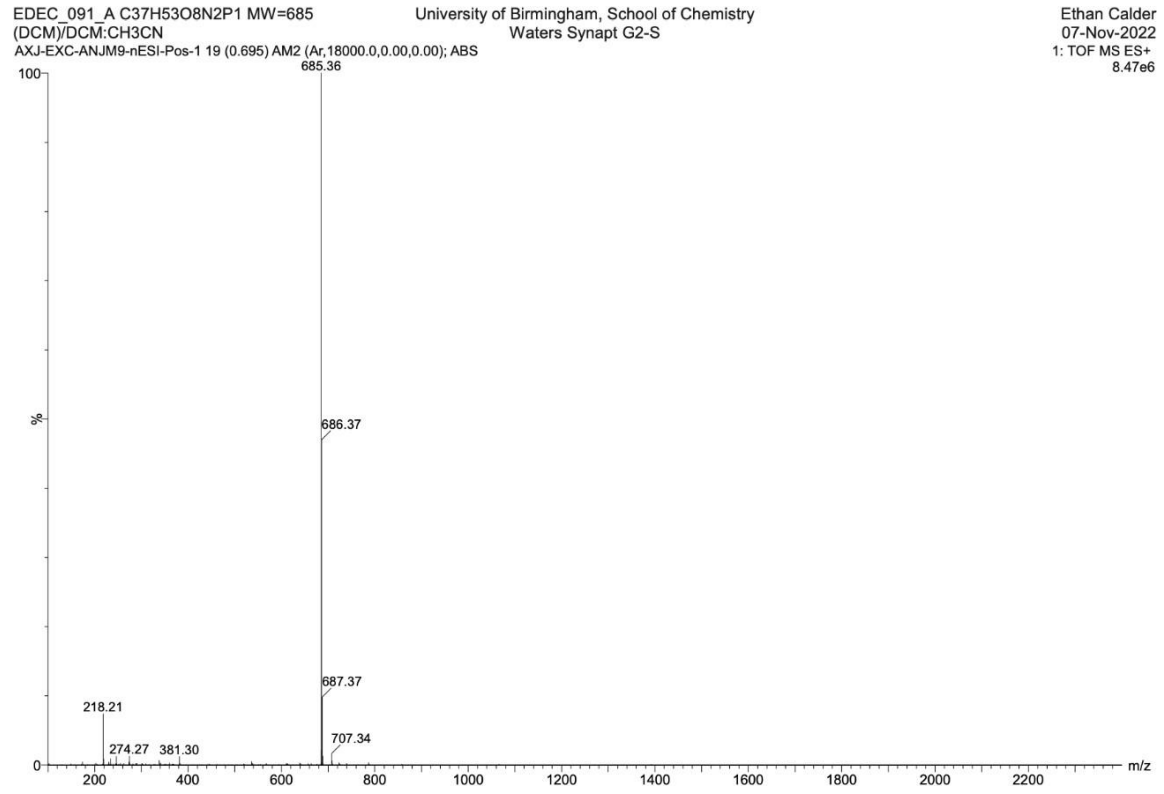

*Figure S100. Mass spectrum of **8** in dichloromethane*

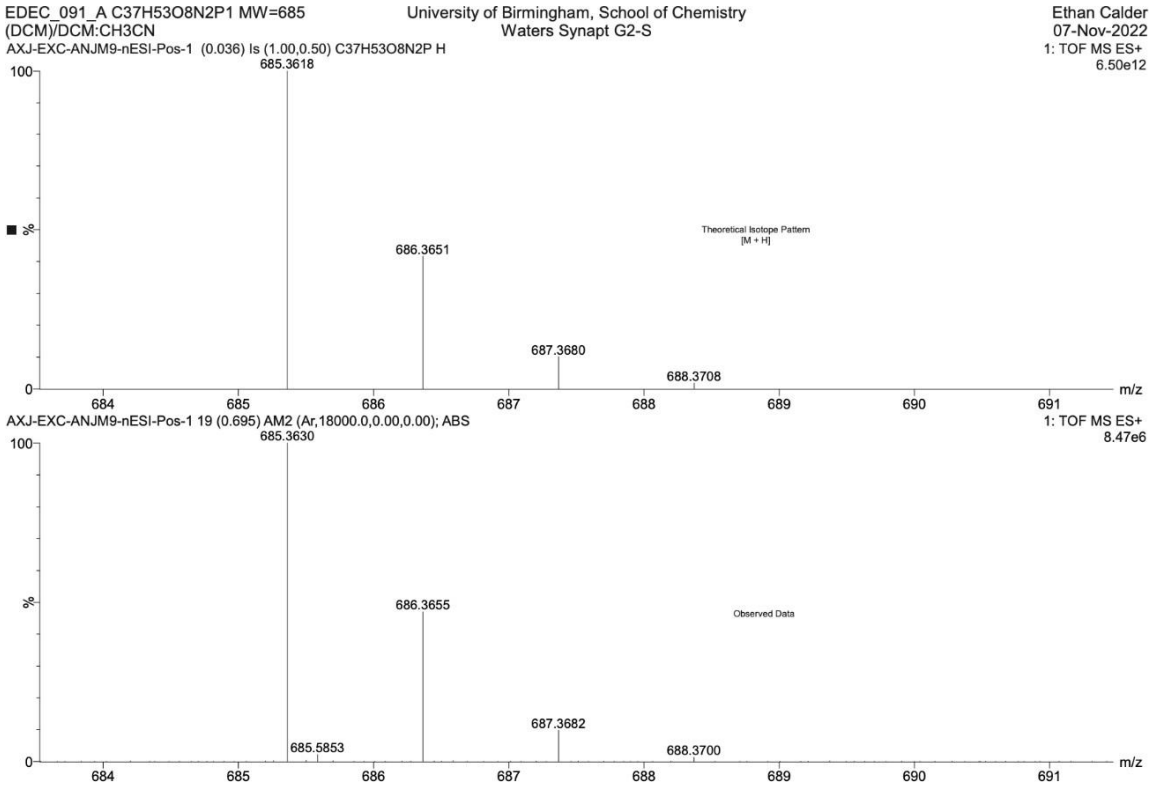

*Figure S101. High-res mass spectrum of **8** in dichloromethane. Top shows the theoretical isotope pattern based on {M + H}$^+$; bottom shows the observed data.*

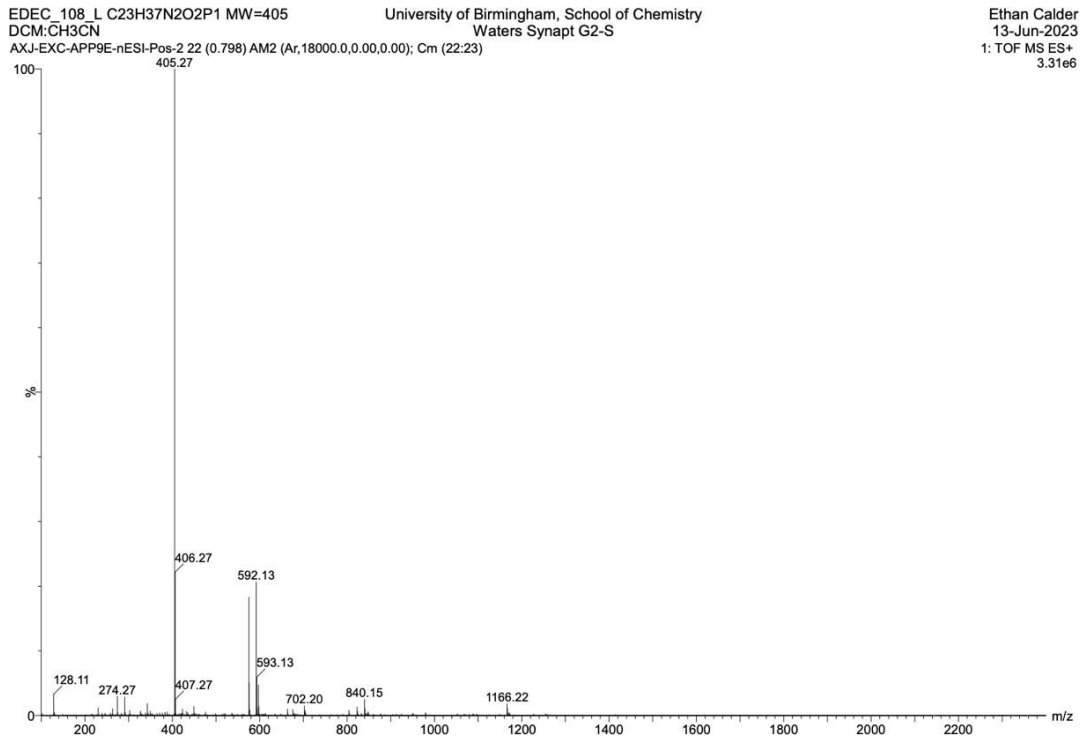

*Figure S102. Mass spectrum of **9** in dichloromethane*

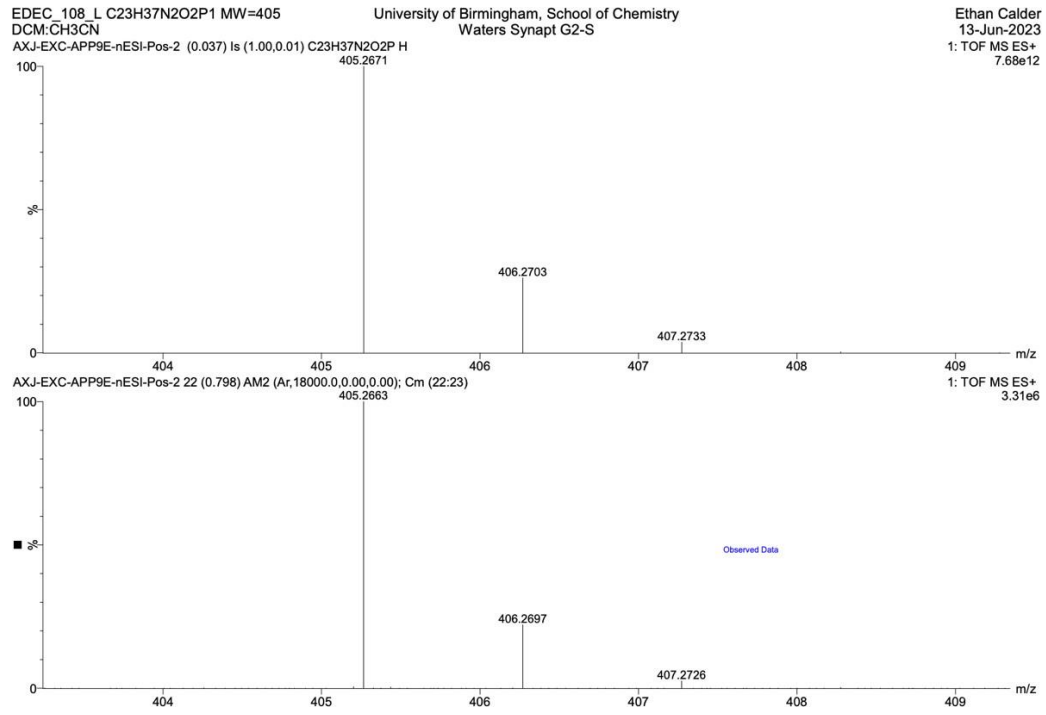

*Figure S103. High-res mass spectrum of **9** in dichloromethane. Top shows the theoretical isotope pattern based on {M + H}⁺; bottom shows the observed data.*

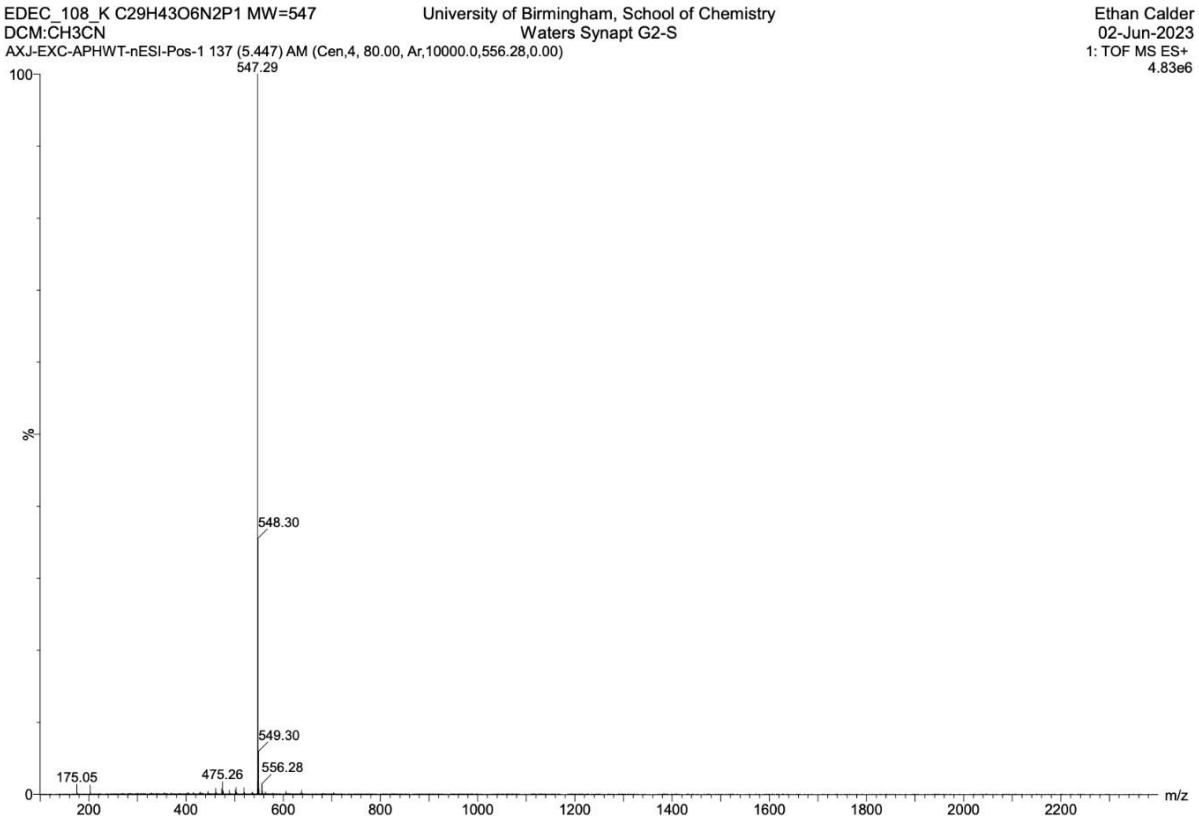

*Figure S104. Mass spectrum of **10** in dichloromethane*

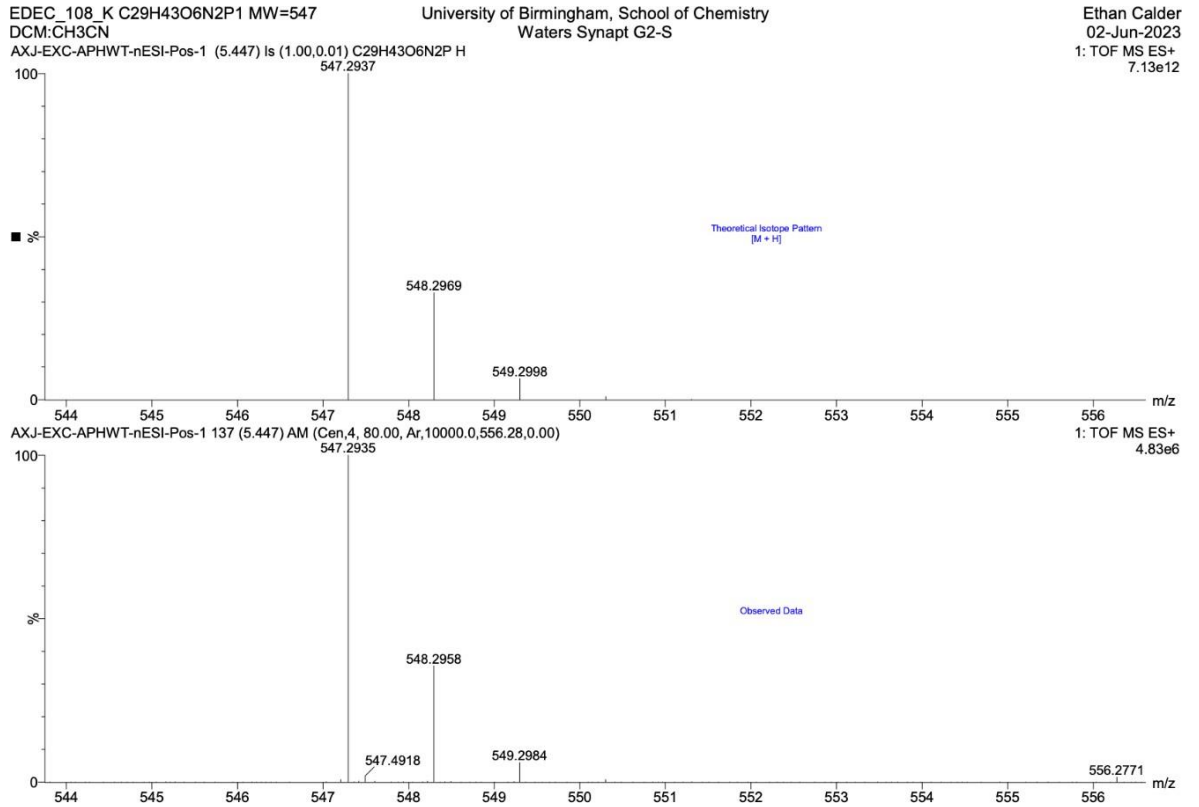

*Figure S105. High-res mass spectrum of **10** in dichloromethane. Top shows the theoretical isotope pattern based on {M + H}⁺; bottom shows the observed data.*

S2.4. IR Spectra

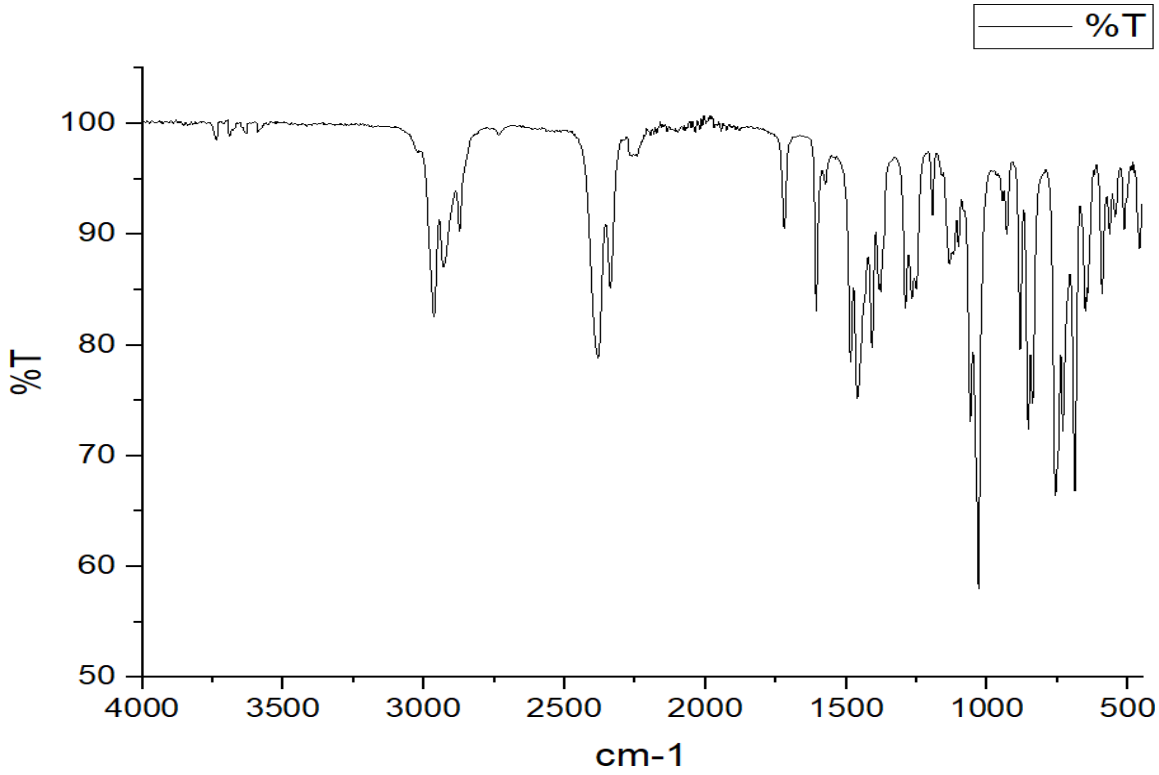

*Figure S106. IR Spectrum of **1.BH3***

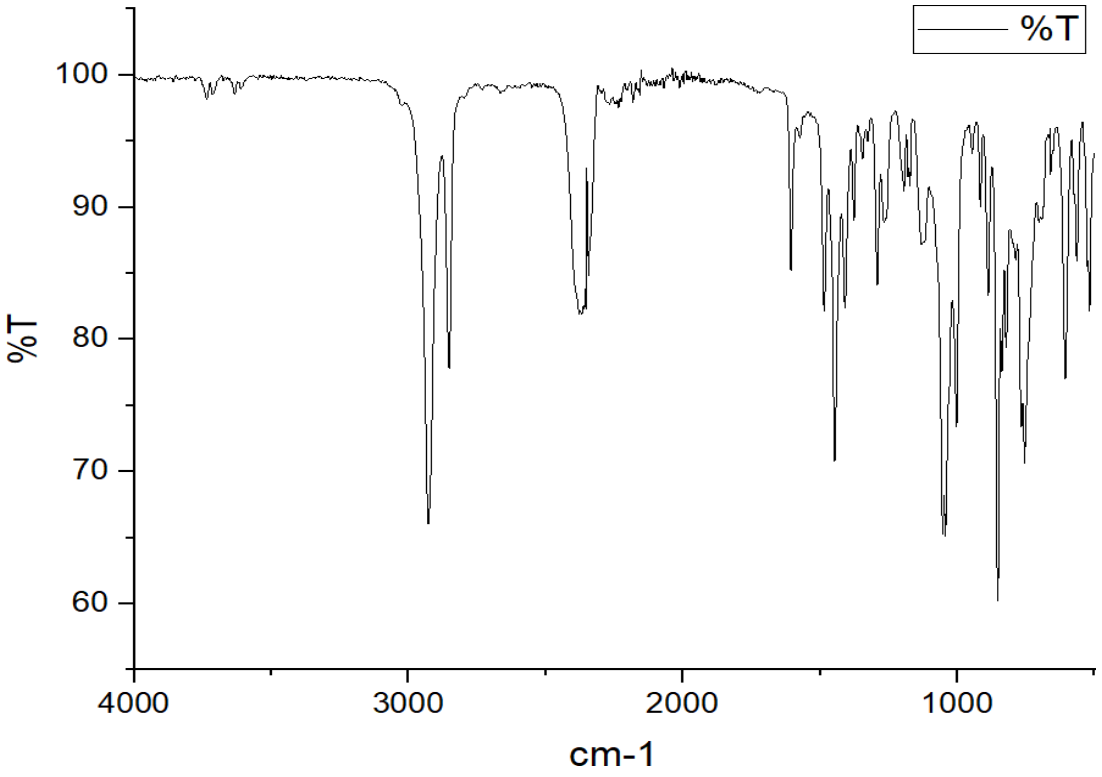

*Figure S107. IR Spectrum of **2.BH3***

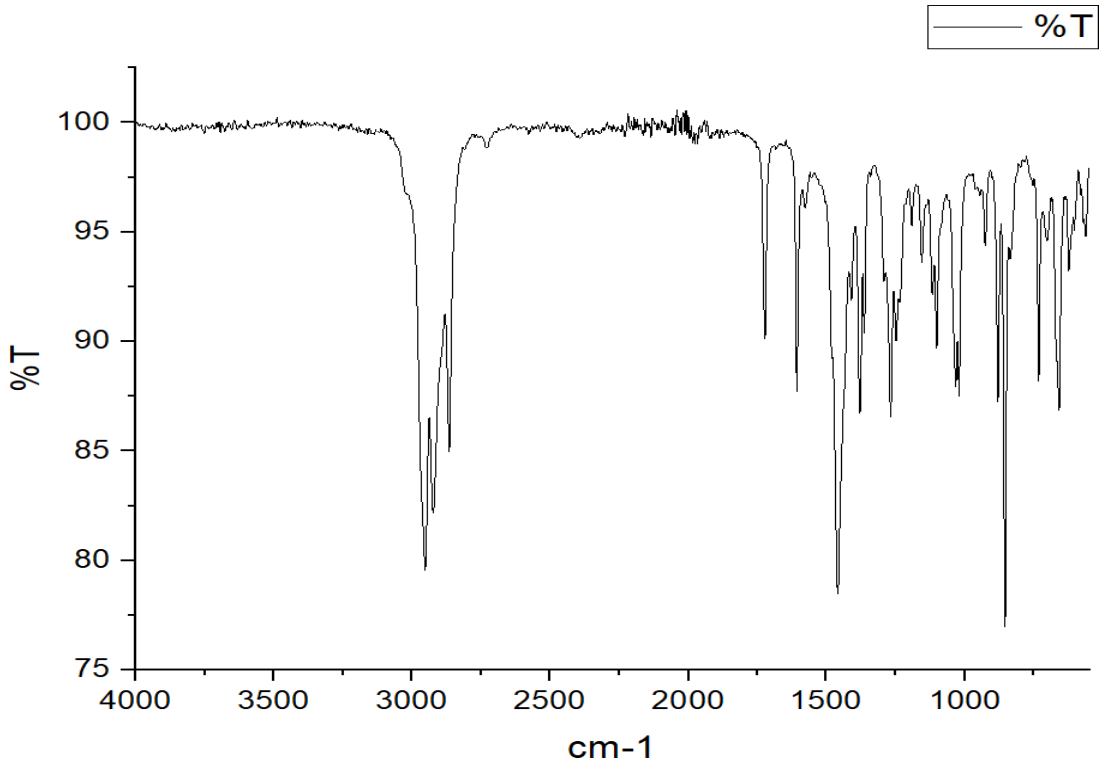

*Figure S108. IR Spectrum of **1***

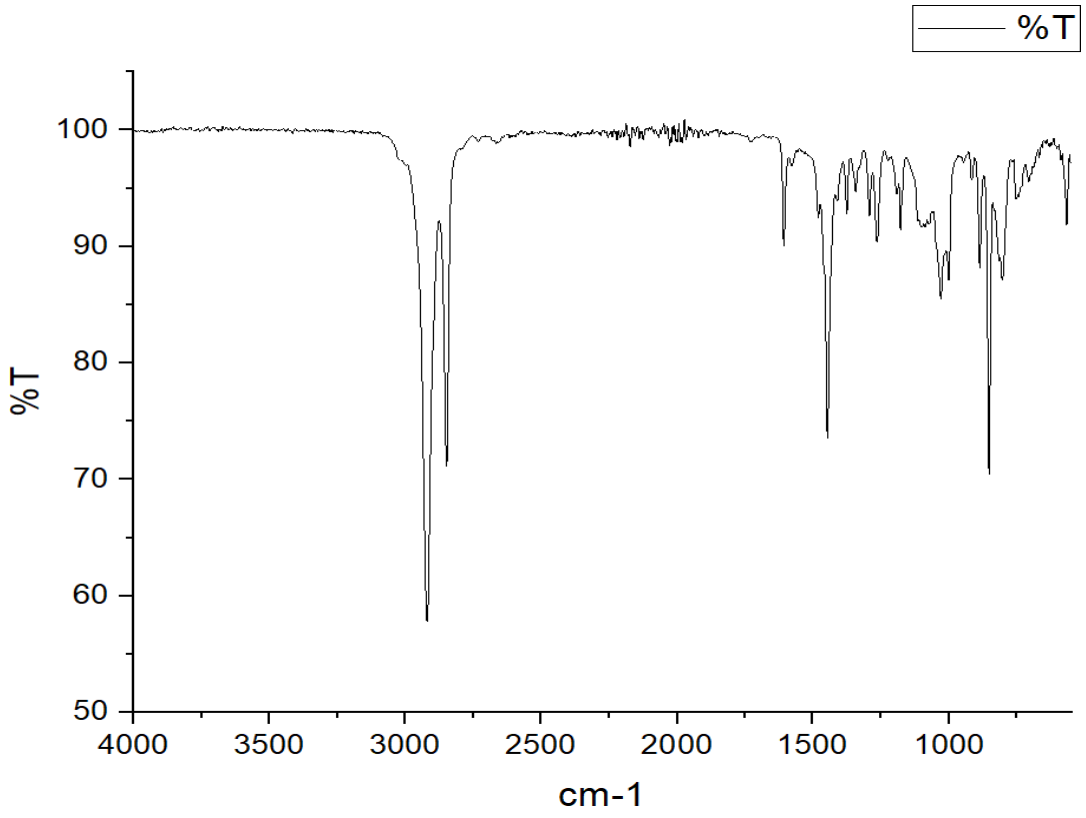

*Figure S109. IR Spectrum of **2***

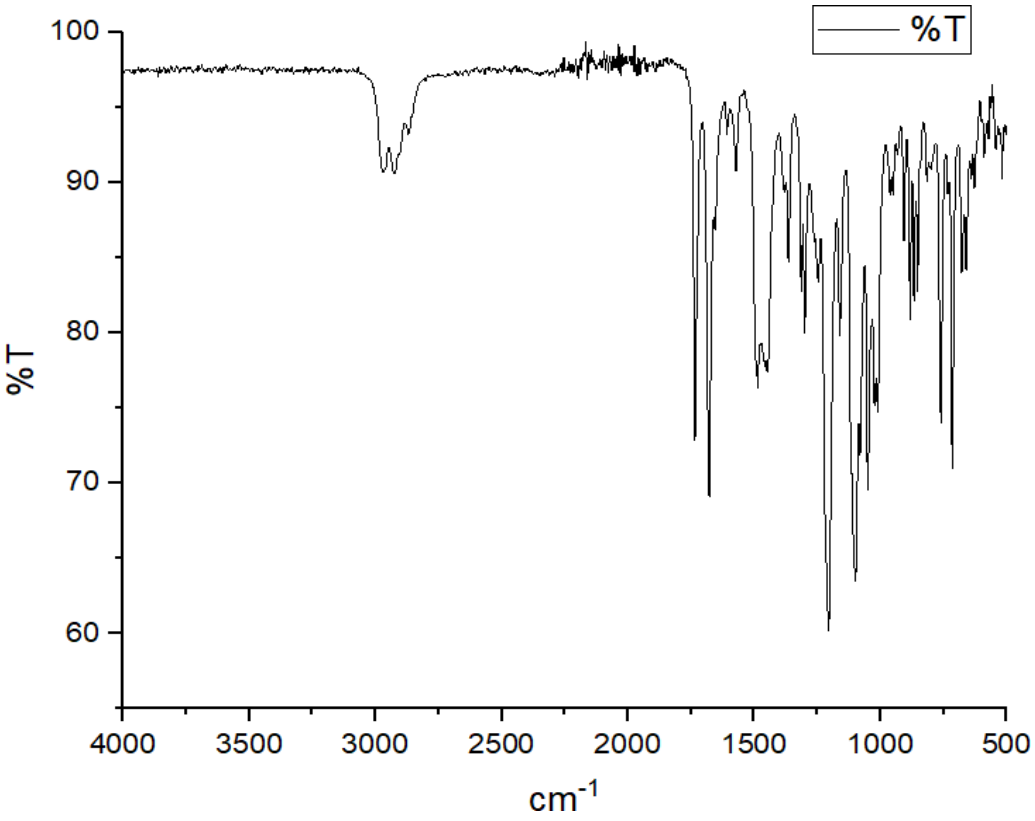

*Figure S110. IR Spectrum of **4***

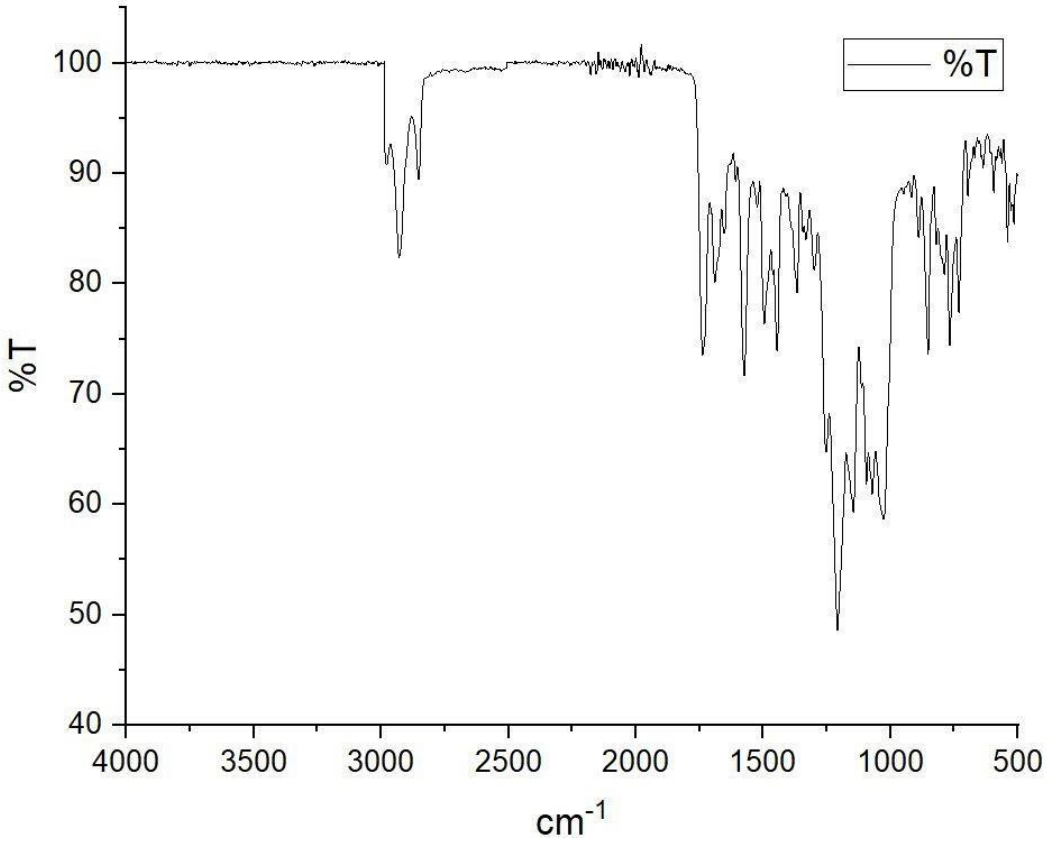

*Figure S111. IR Spectrum of **5***

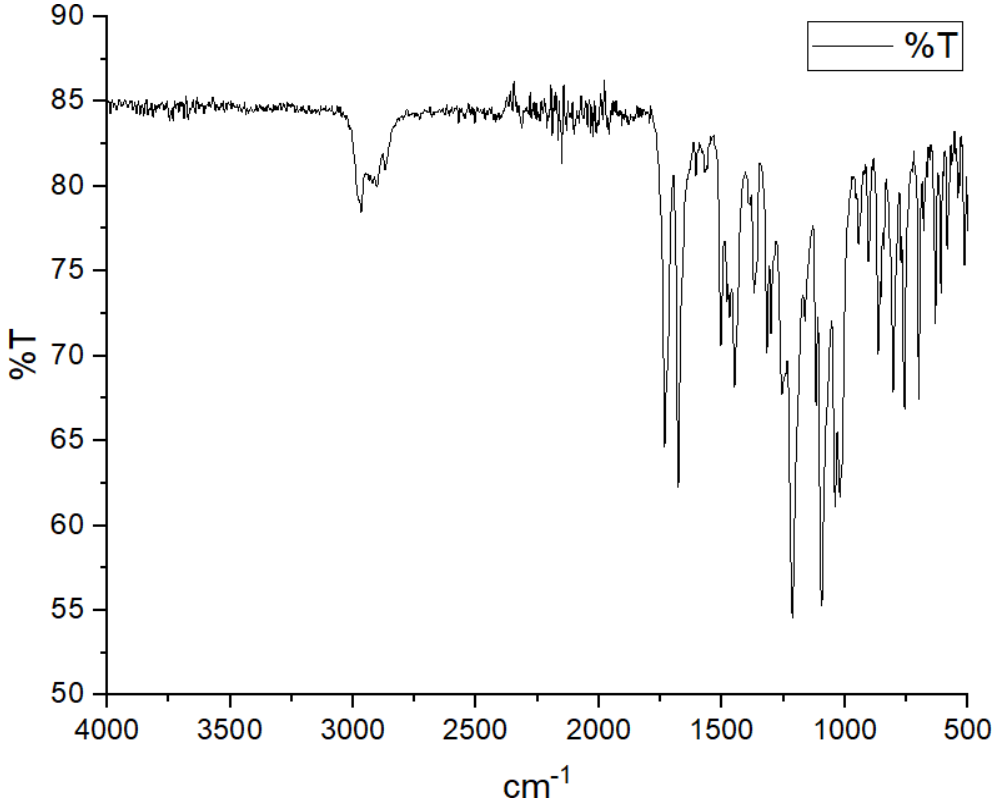

*Figure S112. IR Spectrum of **6***

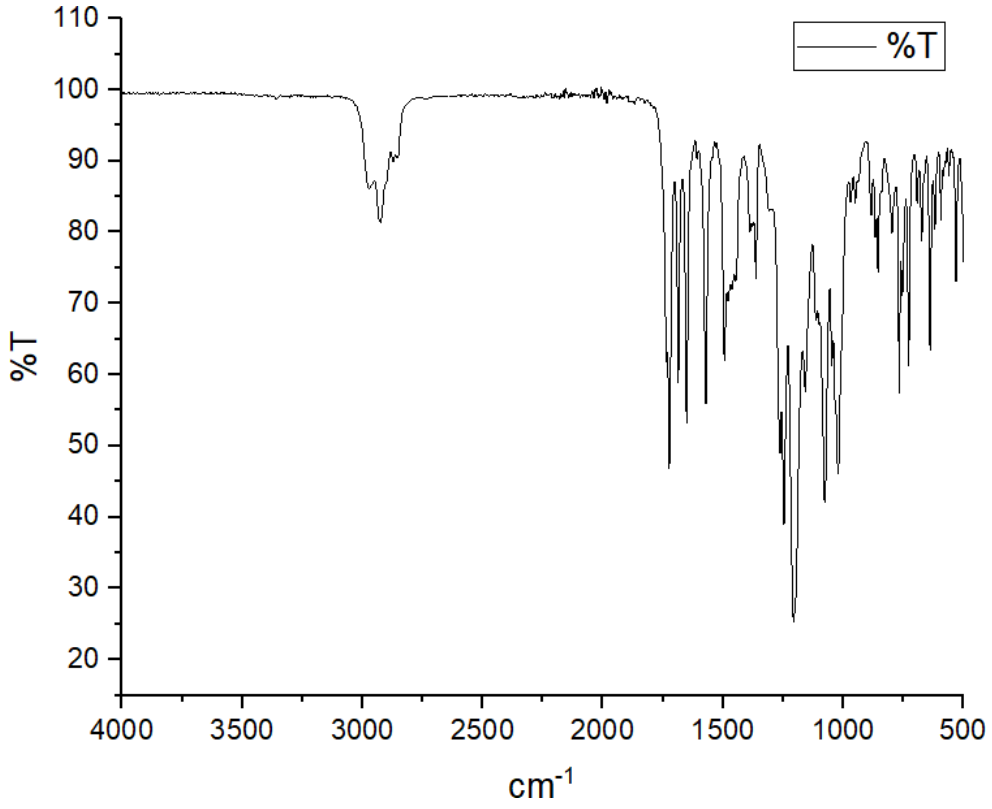

*Figure S113. IR Spectrum of **7***

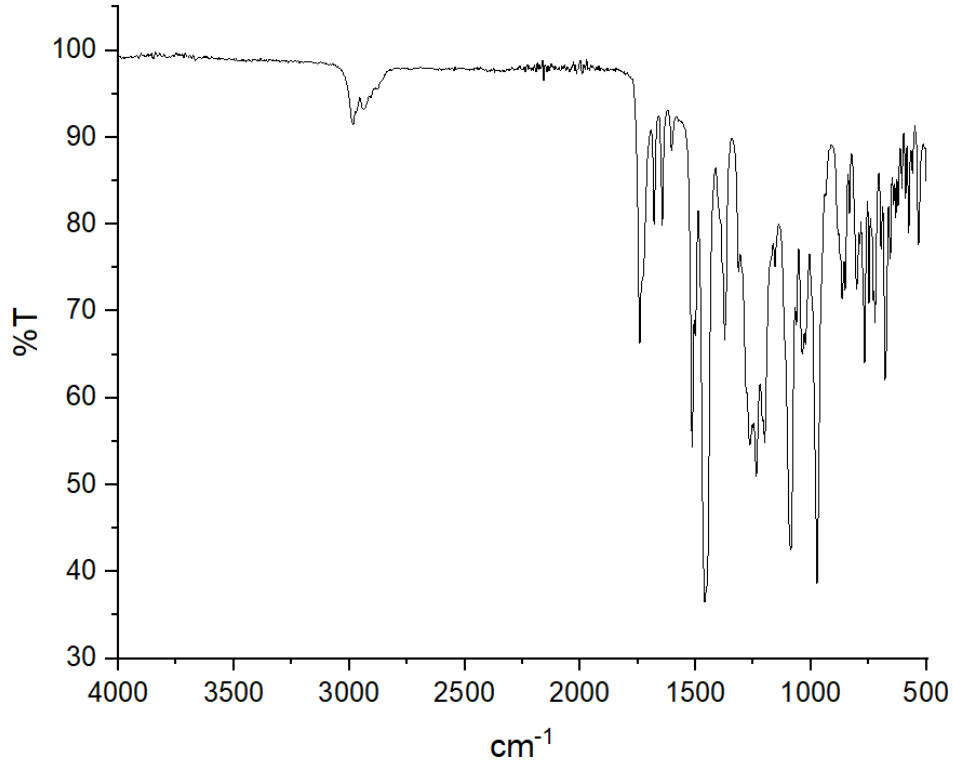

*Figure S114. IR Spectrum of **7·BCF***

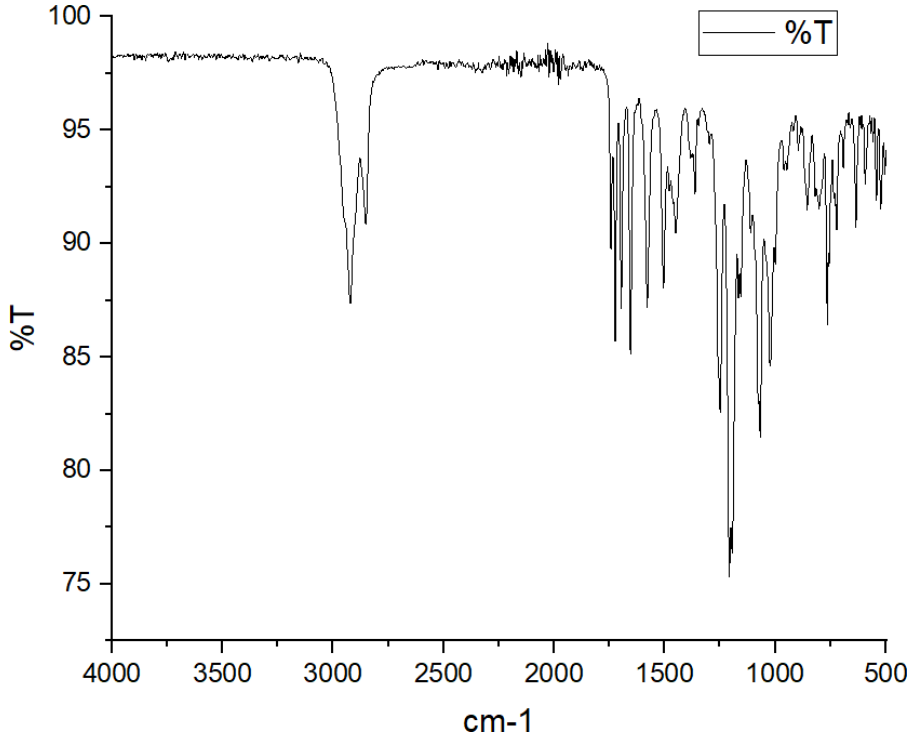

*Figure S115. IR Spectrum of **8**.*

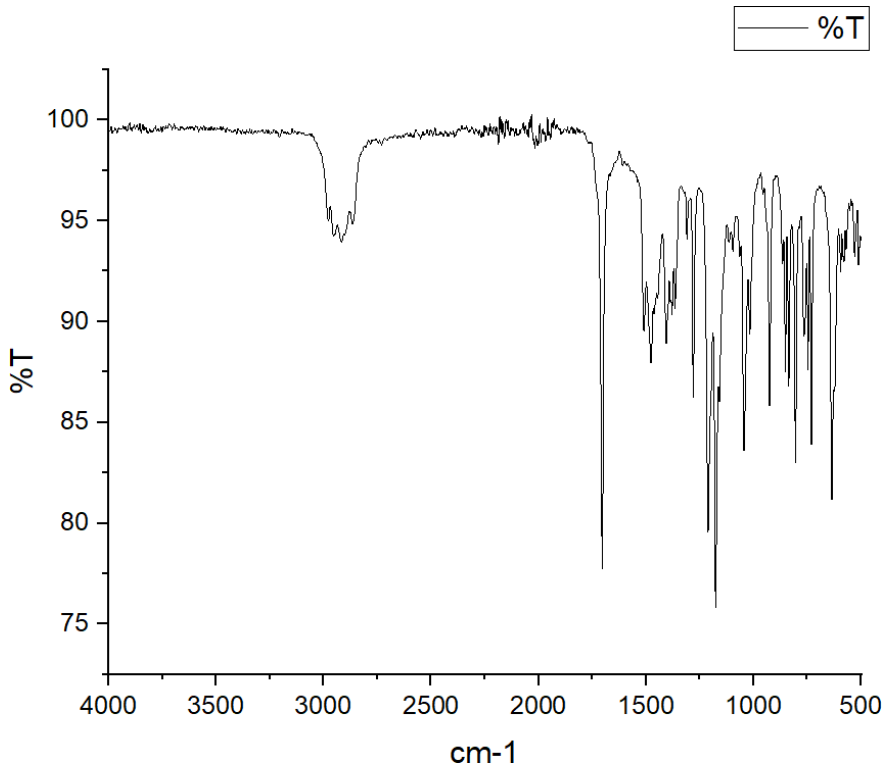

*Figure S116. IR Spectrum of **9***

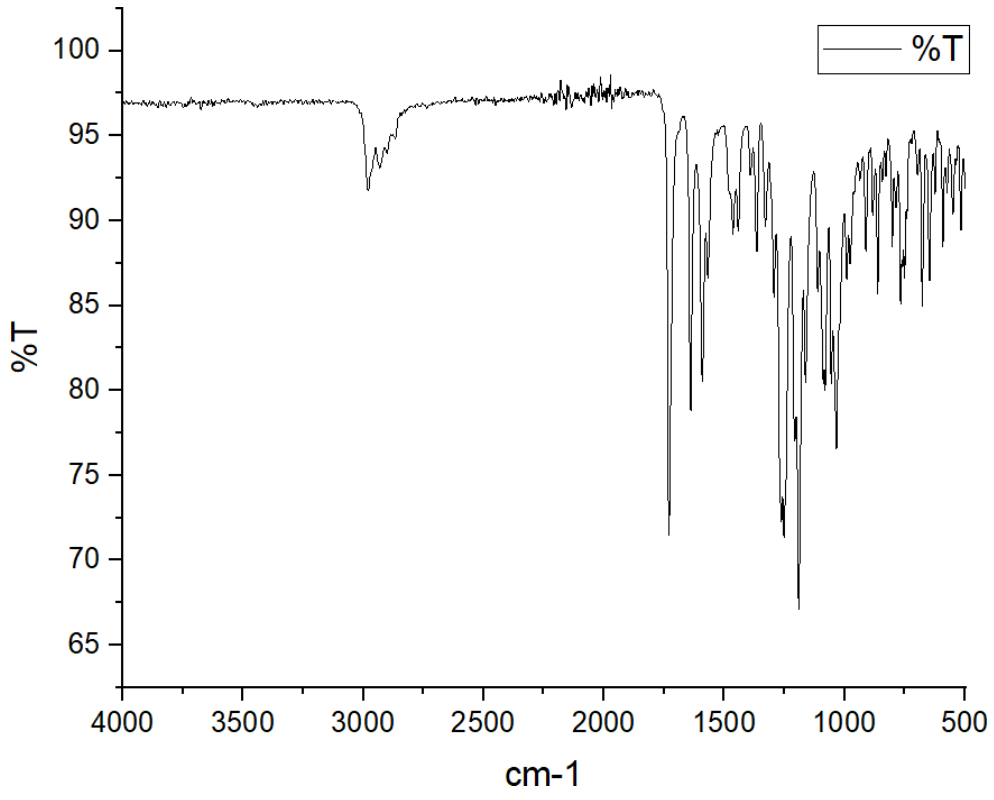

*Figure S117. IR Spectrum of **10***

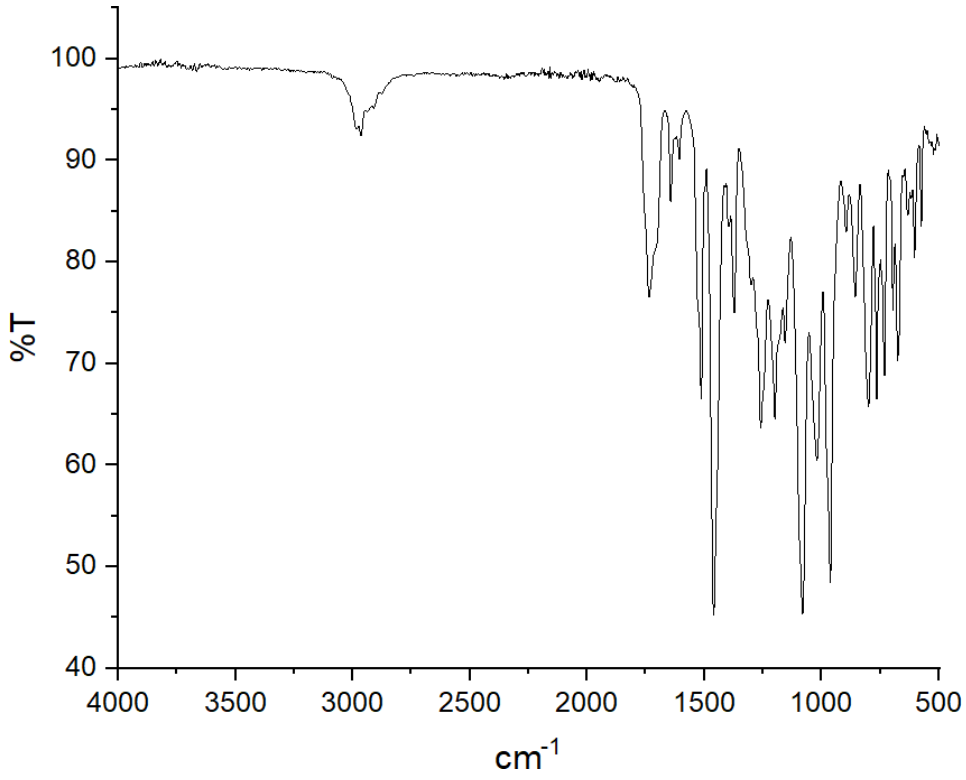

Figure S118. IR Spectrum of ***11***

S3. Crystallographic Details

S3.1. General Crystallographic Information

Single crystals suitable for X-ray diffraction were transferred from recrystallisation vials onto a microscope slide under oil. A suitable single crystal was then selected and mounted on the loop. The datasets for species **4**, **6**, **7, 8,** and **10** were measured at 100 K using Cu-Kα radiation (λ = 1.54184) on a Rigaku SuperNova diffractometer using an Atlas detector. The dataset for **7·BCF** was measured at 120 K using Cu-Kα radiation (λ = 1.54184) on a Rigaku SuperNova diffractometer using an Atlas detector. The dataset for **9** was measured at 100 K using Cu-Kα radiation (λ = 1.54184) on a Rigaku XtaLAB Synergy diffractometer using a HyPix detector. The data collections for these species were driven and processed and absorption corrections were applied using CrysAlisPro.[2] Using OLEX2,[3] the structures were solved using ShelXT,[4] and were refined by a full-matrix least-squares procedure on F^2 in ShelXL.[5] The dataset for **11** was measured at 100 K at the Diamond Light Source, Beamline I19-1, using a Dectris PILATUS 2M detector.[8] These data were processed and an absorption correction was applied using XIA2.[9,10] Using OLEX2,[3] the structure was solved using ShelXT,[4] and was refined by a full-matrix least-squares procedure on F^2 in ShelXL.[5] In all structures, all non-hydrogen atoms were refined with anisotropic displacement parameters. All hydrogen atoms were fixed as riding models and the isotropic thermal parameters (U_{iso}) were based on the U_{eq} of the parent atom. Deposition numbers 2356186 (for **4**), 2356185 (for **6**), 2356190 (for **7**), 2356192 (for **7·BCF**), 2356188 (for **8**), 2356189 (for **9**), 2356187 (for **10**) and 2356191 (for **11**) contains the supplementary crystallographic data for this paper . These can be obtained free of charge by the joint Cambridge Crystallographic Data Centre and Fachinformationszentrum Karlsruhe *via* http://www.ccdc.cam.ac.uk/structures, or *via* https://www.ccdc.cam.ac.uk/services/structures?id=doi:10.1002/chem.202401358.

Single crystals of **4**, in the form of colourless plates, were grown from slow evaporation of a concentrated *n*-hexane solution of **4** in a nitrogen atmosphere. The structure was solved in the monoclinic space group $P2_1/c$ with two molecules of **4**, no solvent molecules, and no disorder. Single crystals of **6**, in the form of colourless blocks, were grown from slow evaporation of a mixed THF/*n*-hexane solution (approximately 1:10 THF:hexane, v/v) of **6**. The structure was solved in the triclinic space group P-1 with one molecule of **6**, no solvent molecules, and no disorder. Single crystals of **7**, in the form of yellow blocks, were grown from slow diffusion of *n*-hexane into a concentrated THF solution of **7** at -35°C in a nitrogen

atmosphere (although the product itself was observed to be air-stable). The structure was solved in the monoclinic space group $P2_1/c$ with one molecule of **7**, no solvent molecules, and no disorder. Single crystals of **8**, in the form of yellow blocks, were grown by slow evaporation of a concentrated *n*-hexane solution of **8**. The structure was solved in the triclinic space group P-1, with one molecule of **8**, no solvent molecules, and no disorder. Single crystals of **9**, in the form of yellow plates, were grown by slow evaporation of a concentrated *n*-hexane solution of **9**. The structure was solved in the orthorhombic space group Pbca, with two molecules of **9**, no solvent molecules, and no disorder. Single crystals of **10**, in the form of yellow blocks, were grown by slow evaporation of a concentrated *n*-hexane solution of **10**. The structure was solved in the monoclinic space group $P2_1/n$, with one molecule of **10**, no solvent molecules, and no disorder. Single crystals of **7·BCF**, in the form of yellow needles, were grown by slow evaporation of a concentrated *n*-hexane solution of **7·BCF**. The structure was solved in the triclinic space group P-1, with one molecule of **7·BCF**, no solvent molecules, and no disorder. Single crystals of **11**, in the form of orange blocks, were grown by slow evaporation of a concentrated *n*-hexane solution of **11** in a nitrogen atmosphere. The structure was solved in the monoclinic space group $P2_1/c$, with two molecules of **11**, and one hexane molecule; the terminal CH_3 groups on the hexane, C206/C26A and C201/C21A, are disordered over two positions at a percentage occupancy ratio of 40:60 respectively.

S3.2. Tables of Crystallographic Data

*Table S1. Crystallographic Data for **4**.*

Identification code	EDEC_098_F_gaussian
CCDC Deposition Number	2356186
Empirical formula	$C_{23}H_{35}N_2O_4P$
Formula weight	434.50
Temperature/K	99.96(14)
Crystal system	monoclinic
Space group	$P2_1/c$
a/Å	17.0832(4)
b/Å	9.8167(2)
c/Å	28.9289(6)
α/°	90
β/°	96.910(2)
γ/°	90
Volume/Å^3	4816.16(18)
Z	8
ρ_{calc}g/cm^3	1.198
μ/mm^{-1}	1.251
F(000)	1872.0
Crystal size/mm^3	0.231 × 0.164 × 0.049
Radiation	Cu Kα (λ = 1.54184)
2Θ range for data collection/°	7.574 to 146.018
Index ranges	$-17 \leq h \leq 21$, $-12 \leq k \leq 9$, $-35 \leq l \leq 34$
Reflections collected	36542
Independent reflections	9464 [R_{int} = 0.0435, R_{sigma} = 0.0375]
Data/restraints/parameters	9464/0/559
Goodness-of-fit on F^2	1.029
Final R indexes [I>=2σ (I)]	R_1 = 0.0393, wR_2 = 0.0990
Final R indexes [all data]	R_1 = 0.0579, wR_2 = 0.1100
Largest diff. peak/hole / e Å^{-3}	0.30/-0.32

*Table S2. Crystallographic Data for **6**.*

Identification code	EDEC_076_7B_gaussian
CCDC Deposition Number	2356185
Empirical formula	$C_{25}H_{39}N_2O_4P$
Formula weight	462.55
Temperature/K	100.01(10)
Crystal system	triclinic
Space group	P-1
a/Å	8.0234(3)
b/Å	8.2718(3)
c/Å	19.6948(7)
α/°	94.526(3)
β/°	97.708(3)
γ/°	103.731(3)
Volume/Å^3	1249.92(8)
Z	2
ρ_{calc}g/cm^3	1.229
μ/mm^{-1}	1.234
F(000)	500.0
Crystal size/mm^3	0.2 × 0.09 × 0.05
Radiation	Cu Kα (λ = 1.54184)
2Θ range for data collection/°	9.122 to 145.676
Index ranges	$-9 \leq h \leq 6$, $-9 \leq k \leq 10$, $-24 \leq l \leq 24$
Reflections collected	13829
Independent reflections	4852 [R_{int} = 0.0455, R_{sigma} = 0.0461]
Data/restraints/parameters	4852/0/300
Goodness-of-fit on F^2	1.037
Final R indexes [I>=2σ (I)]	R_1 = 0.0416, wR_2 = 0.0984
Final R indexes [all data]	R_1 = 0.0525, wR_2 = 0.1051
Largest diff. peak/hole / e Å^{-3}	0.32/-0.43

*Table S3. Crystallographic Data for **7**.*

Identification code	EDEC_076_1_final_gaussian
CCDC Deposition Number	2356190
Empirical formula	$C_{31}H_{45}N_2O_8P$
Formula weight	604.66
Temperature/K	99.96(13)
Crystal system	monoclinic
Space group	$P2_1/c$
a/Å	16.6739(3)
b/Å	12.9998(2)
c/Å	14.7844(3)
α/°	90
β/°	95.755(2)
γ/°	90
Volume/Å^3	3188.48(10)
Z	4
ρ_{calc}g/cm^3	1.260
μ/mm^{-1}	1.189
F(000)	1296.0
Crystal size/mm^3	0.258 × 0.157 × 0.127
Radiation	Cu Kα (λ = 1.54184)
2Θ range for data collection/°	8.642 to 145.922
Index ranges	$-20 \leq h \leq 20$, $-16 \leq k \leq 15$, $-17 \leq l \leq 18$
Reflections collected	30825
Independent reflections	6275 [R_{int} = 0.0400, R_{sigma} = 0.0271]
Data/restraints/parameters	6275/0/390
Goodness-of-fit on F^2	1.045
Final R indexes [I>=2σ (I)]	R_1 = 0.0358, wR_2 = 0.0859
Final R indexes [all data]	R_1 = 0.0443, wR_2 = 0.0921
Largest diff. peak/hole / e Å^{-3}	0.29/-0.33

*Table S4. Crystallographic Data for **7·BCF**.*

Identification code	EDEC_107_C_120_gaussian
CCDC Deposition Number	2356192
Empirical formula	$C_{49}H_{45}BF_{15}N_2O_8P$
Formula weight	1116.65
Temperature/K	119.99(10)
Crystal system	triclinic
Space group	P-1
a/Å	12.6836(4)
b/Å	14.3392(5)
c/Å	15.9046(5)
α/°	112.034(3)
β/°	97.787(3)
γ/°	107.389(3)
Volume/Å^3	2456.51(15)
Z	2
ρ_{calc}g/cm^3	1.510
μ/mm^{-1}	1.515
F(000)	1144.0
Crystal size/mm^3	0.253 × 0.153 × 0.147
Radiation	Cu Kα (λ = 1.54184)
2Θ range for data collection/°	7.158 to 145.646
Index ranges	$-15 \leq h \leq 15$, $-17 \leq k \leq 17$, $-18 \leq l \leq 19$
Reflections collected	32120
Independent reflections	9592 [R_{int} = 0.0418, R_{sigma} = 0.0353]
Data/restraints/parameters	9592/0/696
Goodness-of-fit on F^2	1.018
Final R indexes [I>=2σ (I)]	R_1 = 0.0356, wR_2 = 0.0886
Final R indexes [all data]	R_1 = 0.0457, wR_2 = 0.0958
Largest diff. peak/hole / e Å^{-3}	0.27/-0.33

*Table S5. Crystallographic Data for **8**.*

Identification code	EDEC_098_C_gaussian
CCDC Deposition Number	2356188
Empirical formula	$C_{37}H_{53}N_2O_8P$
Formula weight	684.78
Temperature/K	99.98(13)
Crystal system	triclinic
Space group	P-1
a/Å	11.0797(3)
b/Å	12.5123(4)
c/Å	13.9655(5)
α/°	110.174(3)
β/°	93.849(3)
γ/°	98.359(3)
Volume/Å^3	1783.60(10)
Z	2
ρ_{calc}g/cm^3	1.275
μ/mm^{-1}	1.123
F(000)	736.0
Crystal size/mm^3	0.171 × 0.103 × 0.075
Radiation	Cu Kα (λ = 1.54184)
2Θ range for data collection/°	7.652 to 145.49
Index ranges	$-13 \leq h \leq 13$, $-15 \leq k \leq 15$, $-17 \leq l \leq 17$
Reflections collected	33249
Independent reflections	7013 [R_{int} = 0.0464, R_{sigma} = 0.0330]
Data/restraints/parameters	7013/0/440
Goodness-of-fit on F^2	1.027
Final R indexes [I>=2σ (I)]	R_1 = 0.0384, wR_2 = 0.0915
Final R indexes [all data]	R_1 = 0.0480, wR_2 = 0.0981
Largest diff. peak/hole / e Å^{-3}	0.29/-0.39

*Table S6. Crystallographic Data for **9**.*

Identification code	EDEC_108_L_new_gaussian
CCDC Deposition Number	2356189
Empirical formula	$C_{46}H_{74}N_4O_4P_2$
Formula weight	809.03
Temperature/K	100.00(10)
Crystal system	orthorhombic
Space group	Pbca
a/Å	12.63150(10)
b/Å	23.1136(2)
c/Å	31.6638(3)
α/°	90
β/°	90
γ/°	90
Volume/Å^3	9244.55(14)
Z	8
ρ_{calc}g/cm^3	1.163
μ/mm^{-1}	1.199
F(000)	3520.0
Crystal size/mm^3	0.26 × 0.12 × 0.11
Radiation	Cu Kα (λ = 1.54184)
2Θ range for data collection/°	7.65 to 157.164
Index ranges	$-14 \le h \le 16$, $-29 \le k \le 25$, $-38 \le l \le 38$
Reflections collected	45381
Independent reflections	8841 [R_{int} = 0.0393, R_{sigma} = 0.0322]
Data/restraints/parameters	8841/0/527
Goodness-of-fit on F^2	1.043
Final R indexes [I>=2σ (I)]	R_1 = 0.0433, wR_2 = 0.1159
Final R indexes [all data]	R_1 = 0.0511, wR_2 = 0.1213
Largest diff. peak/hole / e Å^{-3}	0.32/-0.34

*Table S7. Crystallographic Data for **10**.*

Identification code	EDEC_108_K_2_gaussian
CCDC Deposition Number	2356187
Empirical formula	$C_{29}H_{43}N_2O_6P$
Formula weight	546.62
Temperature/K	120.01(10)
Crystal system	monoclinic
Space group	$P2_1/n$
a/Å	8.7981(3)
b/Å	38.1963(13)
c/Å	9.2377(4)
α/°	90
β/°	106.619(4)
γ/°	90
Volume/Å^3	2974.7(2)
Z	4
ρ_{calc}g/cm^3	1.221
μ/mm^{-1}	1.168
F(000)	1176.0
Crystal size/mm^3	0.219 × 0.188 × 0.115
Radiation	Cu Kα (λ = 1.54184)
2Θ range for data collection/°	9.262 to 154.76
Index ranges	$-11 \leq h \leq 10$, $-48 \leq k \leq 36$, $-11 \leq l \leq 11$
Reflections collected	30309
Independent reflections	6237 [R_{int} = 0.0450, R_{sigma} = 0.0356]
Data/restraints/parameters	6237/0/354
Goodness-of-fit on F^2	1.034
Final R indexes [I>=2σ (I)]	R_1 = 0.0418, wR_2 = 0.1012
Final R indexes [all data]	R_1 = 0.0558, wR_2 = 0.1104
Largest diff. peak/hole / e Å^{-3}	0.25/-0.28

*Table S8. Crystallographic Data for **11**.*

Identification code	EDEC_141_A
CCDC Deposition Number	2356191
Empirical formula	$C_{54}H_{56}BF_{15}N_2O_8P$
Formula weight	1187.78
Temperature/K	100.15
Crystal system	monoclinic
Space group	$P2_1/c$
a/Å	45.26149(17)
b/Å	14.39164(5)
c/Å	18.01887(8)
α/°	90
β/°	101.4583(4)
γ/°	90
Volume/Å^3	11503.33(8)
Z	8
ρ_{calc}g/cm^3	1.372
μ/mm^{-1}	0.139
F(000)	4904.0
Crystal size/mm^3	0.251 × 0.075 × 0.02
Radiation	Synchrotron (λ = 0.6889)
2Θ range for data collection/°	2.236 to 57.162
Index ranges	$-62 \leq h \leq 62$, $-19 \leq k \leq 19$, $-25 \leq l \leq 24$
Reflections collected	348690
Independent reflections	32216 [R_{int} = 0.0732, R_{sigma} = 0.0463]
Data/restraints/parameters	32216/81/1506
Goodness-of-fit on F^2	0.908
Final R indexes [I>=2σ (I)]	R_1 = 0.0553, wR_2 = 0.1449
Final R indexes [all data]	R_1 = 0.0729, wR_2 = 0.1494
Largest diff. peak/hole / e Å^{-3}	1.04/-0.35

S4. Catalysis Studies

S4.1. Procedure

In the glovebox, 12 mg (0.0276 mmol; 1 equiv) of five-membered heterocycle **4** was dissolved in 0.6 mL $CDCl_3$ in a glass vial, yielding a pale-yellow solution. This vial was charged with 4.4 microliters (0.0276 mmol; 1 equiv) *via* micropipette of $(C(CO_2Et))_2$; no immediate colour change was seen. This solution was then transferred to a separate vial containing 2.8 mg of $B(C_6F_5)_3$ (prepared by dilution; 0.00552 mmol; 0.2 equiv), and stirred until full dissolution of the $B(C_6F_5)_3$ was seen. This solution was then transferred to a sealed J-Young NMR tube.

Separately in the glovebox, another portion of 12 mg (0.0276 mmol; 1 equiv) of five-membered heterocycle **4** was dissolved in 0.6 mL $CDCl_3$ in a glass vial, yielding a pale-yellow solution. This vial was then charged with 4.4 microliters *via* micropipette (0.0276 mmol; 1 equiv) of $(C(CO_2Et))_2$; no immediate colour change was seen. This solution was then transferred to a sealed J-Young NMR tube.

S4.2. Results and Analysis

Both samples were then monitored at set time points by $^{31}P\{^1H\}$ NMR spectroscopy. ^1H NMR spectroscopy was not used as the presence of overlapping peaks made it difficult to accurately integrate **4** and **7** separately, whereas the peaks are clearly distinct in the $^{31}P\{^1H\}$ NMR spectrum (**4** = 74.9 ppm; **7** = 60.4 ppm).

When $B(C_6F_5)_3$ is included, both **7** and **7·BCF** form in-situ; these can be differentiated by their subtly different $^{31}P\{^1H\}$ NMR shifts (**7** = 60.4 ppm; **7·BCF** = 60.0 ppm). In Figure S120, the integrals for **7** and **7·BCF** are combined into one value. In Figure S121, the integrals for **7** and **7·BCF** are plotted separately. The proportion of **7·BCF** is observed to remain roughly constant across time, while the proportion of **7** increases over time.

S4.3. Deprotection of **7·BCF** to **7**

To convert **7·BCF** to **7**, in the glovebox, **7·BCF** (30.8 mg, 0.0276 mmol; 1 equiv) was dissolved in 1 mL of toluene in a glass vial, and 16.9 mg of 4-(dimethylamino)pyridine (DMAP; 0.138 mmol; 5 equiv.) were added to the reaction mixture. This gave a colour change within 10 minutes from bright yellow to dark green/brown, although crude $^{31}P\{^1H\}$ NMR spectroscopy showed only one peak present, which corresponded to **7**. Removal of the solvent *in vacuo* and filtration through a short silica plug, using an eluent system of 4:1 hexane:ethyl acetate, allowed for elution of **7** as a yellow band (R_f = 0.35). Removal of the solvent in vacuo yielded

spectroscopically pure **7**, with the removal of the DMAP-BCF adduct confirmed by both $^{11}B\{^1H\}$ and $^{19}F\{^1H\}$ NMR spectroscopy, which showed no peaks. The mass of product obtained was calculated by adding in a known quantity of mesitylene and comparing the ^1H NMR integrals of **7** and mesitylene (0.021 mmol, 76% yield, 12.7 mg; this compares to an 88% yield for the formation of **7** with no catalyst).

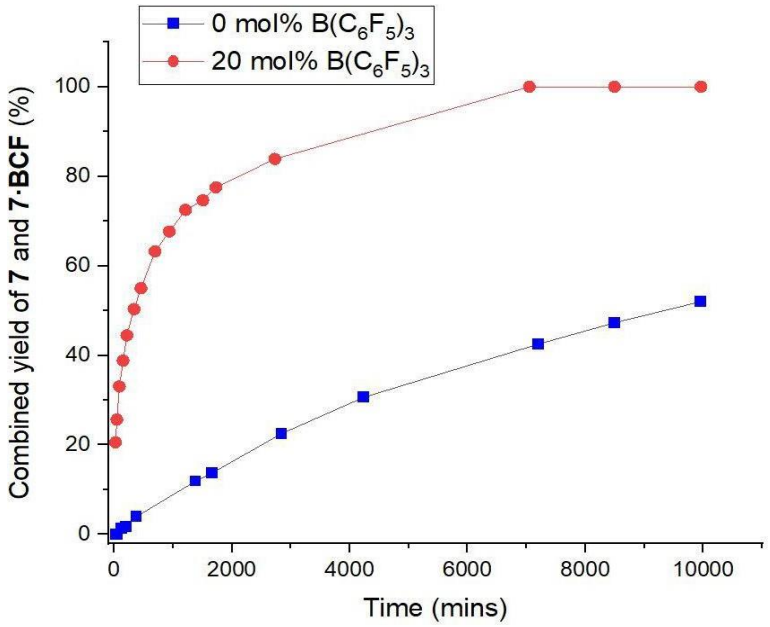

*Figure S119. Conversion from **4** to **7/7·BCF** against time, based on $^{31}P\{^1H\}$ NMR integrals, depending on the inclusion or exclusion of $B(C_6F_5)_3$. The integrals for **7** and **7·BCF** are combined into one value for the purposes of this figure.*

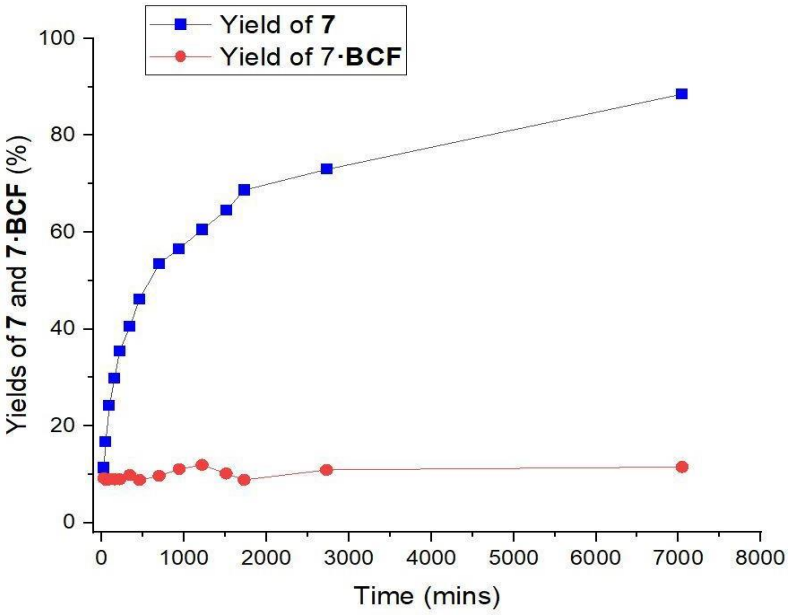

*Figure S120. Proportion of **7** and **7·BCF** in the reaction mixture, based on $^{31}P\{^1H\}$ NMR integrals, for the reaction in which 20 mol% $B(C_6F_5)_3$ is included.*

S5. Computational Details

S5.1. General Computational Information

Unless otherwise stated, calculations for all complexes under study were performed using DFT in Gaussian 09.[11] Geometry optimisations and frequency calculations were carried out using the ωB97XD functional and the def2-TZVP basis set,[12,13] with symmetry disabled (keyword = nosymm). Optimisations were carried out in the gas phase. For computational efficacy, the *para*-Me group on all structures was replaced with a *p*-H group, with the assumption that this would have negligible impact on the optimised structures. Frequency calculations were then carried out on all optimised structures. For non-transition state structures, the absence of any imaginary frequencies confirmed that each optimised structure was located at a minimum. For transition state structures, the presence of exactly one imaginary frequency clearly corresponding to the transformation in question confirmed the structure as a valid transition state. Where necessary, IRC (intrinsic reaction coordinate) calculations were also performed to confirm the validity of transition states. Single point energy corrections were then carried out on these optimised structures using the ωB97XD functional and def2-QZVP basis set.[12,13] Solvent interactions were modelled using the polarisable continuum model (using toluene as the solvent, as toluene was also the solvent used experimentally).[14] Where desired, NBO calculations (including Wiberg bond indices and NPA values) were carried out on optimised geometries using the NBO package in Gaussian 09, using the keywords Pop=(FULL,NBOREAD,SAVENBO).[15] Full cartesian coordinates for all optimised structures can be found in section S5.4.

The optimised structure for **11** was calculated using the ωB97XD functional and the def2-SVP basis set,[12,13] with symmetry disabled (keyword = nosymm). Optimisations were carried out in the gas phase. A subsequent frequency calculation confirmed the optimised structure was located at a minimum by the absence of any imaginary frequencies. NBO calculations (including Wiberg bond indices and NPA values) were then carried out on this optimised geometry using the NBO package in Gaussian 09, using the keywords Pop=(FULL,NBOREAD,SAVENBO).[15] Cartesian coordinates for the optimised structure of **11** can be found in section S5.4.

S5.2. Pertinent Energies and Data on Structures

Five-membered ring formation, R = ^{i}Pr

Structure	*Single-point electronic energy[a] (Hartree)*	*Thermal correction to Gibbs free energy[b] (Hartree)*	*Total Gibbs energy[c] (kcal.mol^{-1})*	*Relative Gibbs energy[d] (kcal.mol^{-1})*
Azophosphine **1**	-998.2661833	0.299756	-626233.5136	N/A
$(C(CO_2Et))_2$	-611.797567	0.13028	-383827.0946	N/A
1 + $(C(CO_2Et))_2$	-1610.06375	0.430036	-1010060.608	0
TS1 (R = ^{i}Pr)	-1610.064016	0.459495	-1010042.289	+ 18.3193358
I1 (R = ^{i}Pr)	-1610.076	0.461491	-1010048.557	+ 12.0514122
TS2 (R = ^{i}Pr)	-1610.074559	0.46082	-1010048.073	+ 12.5348519
Five-membered heterocycle **4**	-1610.167905	0.464664	-1010104.237	- 43.6284245

Five-membered ring formation, R = ^{t}Bu

Structure	*Single-point electronic energy[a] (Hartree)*	*Thermal correction to Gibbs free energy[b] (Hartree)*	*Total Gibbs energy[c] (kcal.mol^{-1})*	*Relative Gibbs energy[d] (kcal.mol^{-1})*
Azophosphine **3**	-1076.899747	0.354024	-675542.7763	N/A
$(C(CO_2Et))_2$	-611.797567	0.13028	-383827.0946	N/A
3 + $(C(CO_2Et))_2$	-1688.697314	0.484304	-1059369.871	0
TS1 (R = ^{t}Bu)	-1688.696136	0.515664	-1059349.453	+ 20.418046
I1 (R = ^{t}Bu)	-1688.711472	0.515803	-1059358.989	+ 10.8819835
TS2 (R = ^{t}Bu)	-1688.708915	0.518578	-1059355.643	+ 14.2275321
Five-membered heterocycle **6**	-1688.812224	0.519235	-1059420.058	- 50.0872132

Seven-membered ring formation, R = ^{i}Pr

Structure	*Single-point electronic energy[a] (Hartree)*	*Thermal correction to Gibbs free energy[b] (Hartree)*	*Total Gibbs energy[c] (kcal.mol^{-1})*	*Relative Gibbs energy[d] (kcal.mol^{-1})*
Five-membered heterocycle **4**	-1610.167905	0.464664	-1010104.237	N/A
$(C(CO_2Et))_2$	-611.797567	0.13028	-383827.0946	N/A
4 + $(C(CO_2Et))_2$	-2221.965472	0.594944	-1393931.331	0
TS3 (R = ^{i}Pr)	-2221.964377	0.622706	-1393913.223	+ 18.1078569
I2 (R = ^{i}Pr)	-2221.993748	0.627179	-1393928.847	+ 2.48397228
I3 (R = ^{i}Pr)	-2221.998666	0.62417	-1393933.821	- 2.48999512
Seven-membered heterocycle **7**	-2222.015738	0.627242	-1393942.607	- 11.2752927

Seven-membered ring formation, R = ^{t}Bu

Structure	*Single-point electronic energy[a] (Hartree)*	*Thermal correction to Gibbs free energy[b] (Hartree)*	*Total Gibbs energy[c] (kcal.mol^{-1})*	*Relative Gibbs energy[d] (kcal.mol^{-1})*
Five-membered heterocycle **6**	-1688.812224	0.519235	-1059420.058	N/A
$(C(CO_2Et))_2$	-611.797567	0.13028	-383827.0946	N/A
6 + $(C(CO_2Et))_2$	-2300.609791	0.649515	-1443247.153	0
TS3 (R = ^{t}Bu)	-2300.598825	0.677913	-1443222.452	+ 24.701232
I2 (R = ^{t}Bu)	-2300.621754	0.680443	-1443235.252	+ 11.9007578
Hypothetical seven-membered heterocycle, R = ^{t}Bu	-2300.65467	0.683308	-1443254.109	- 6.95650805

a = Single point electronic energies calculated at ωB97XD(toluene)/def2QZVP level of theory.
b = Thermal correction to Gibbs free energy calculated at ωB97XD/def2TZVP level of theory.
c = Total Gibbs energy is calculated by summing the electronic energy and thermal correction to Gibbs free energy for a given system, and converting units from Hartree to kcal.mol^{-1}.
d = The reference compound, set to zero relative energy, is highlighted by a value of '0' in this column. All other values in this column are relative to the zero relative energy.

Pertinent NBO Data

*NBO Data for five-membered heterocycles **4** and **6**:*

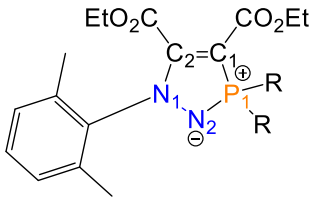

Bond in question	**4** (R = ^{i}Pr)		**6** (R = ^{t}Bu)	
	Optimised bond length (Å)	**Wiberg bond index (WBI)**	**Optimised bond length (Å)**	**Wiberg bond index (WBI)**
N_2-P_1	1.62781	1.0656	1.63123	1.0511
N_1-N_2	1.39080	1.0516	1.38988	1.0515
N_1-C_2	1.32077	1.3547	1.31792	1.3586
P_1-C_1	1.75512	0.9682	1.76162	0.9626
C_1-C_2	1.39930	1.3394	1.39694	1.3376
N_1-Ar	1.43228	0.9378	1.43101	0.9393
P_1-C(R)	1.83269 1.83536	0.8259 0.8220	1.86609 1.86626	0.8010 0.7878

	4 (R = ^{i}Pr)	**6** (R = ^{t}Bu)
NPA value for **N_2**-P_1 atom	-0.85930	-0.87379
NPA value for N_2-**P_1** atom	1.80922	1.84126

*NBO Data for seven-membered heterocycle **7**:*

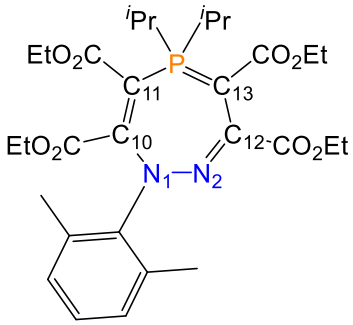

Bond in question	Optimised bond length (Å)	Wiberg bond index (WBI)
N_2=C_{12}	1.28112	1.7010
C_{12}-C_{13}	1.43258	1.1254
C_{13}=P	1.72934	0.9972
C_{11}=P	1.79655	0.8645
C_{10}=C_{11}	1.37070	1.5540
N_1=C_{10}	1.36965	1.2048
N_1=N_2	1.39515	1.0455
C_{13}-C(=O)	1.42766	1.1610

C_{12}-C(=O)	1.51781	0.9060
C_{11}-C(=O)	1.46525	1.0442
C_{10}-C(=O)	1.53103	0.9087
N_1-Ar	1.44894	0.9373
P_1-C(^{i}Pr)	1.84128, 1.84059	0.9147, 0.8883

NPA value for (Ar)-**N_1**-N_2 atom	-0.25217
NPA value for (Ar)-N_1-**N_2** atom	-0.28559

*NBO Data for **11**:*

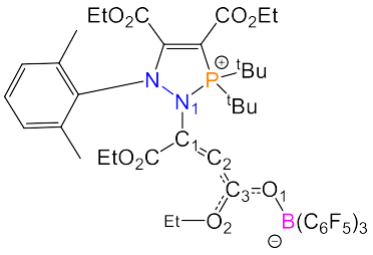

Bond in question	Optimised bond length (Å)	Wiberg bond index (WBI)
N_1-C_1	1.43078	0.9591
C_1=C_2	1.33022	1.8194
C_2-C_3	1.39480	1.3583
C_3-O_1	1.27163	1.2249
C_3-O_2	1.32482	1.0879

S5.3. Potential energy surface scans for seven-membered rings

In order to search for any transition states between **I2**, **I3**, and the product seven-membered rings, various relaxed potential energy surface (PES) scans were performed, using the following keywords:

#N wB97XD def2SVP opt=(modredundant) freq nosymm

Following these scans, and finer scans on the obtained maxima, the maxima were submitted as separate transition state calculations, using the following keywords:

#P wB97XD def2SVP opt=(ts,noeigen,calcfc/calcall) freq nosymm*

* Both opt=calcfc and opt=calcall were used separately in various calculations.

The results of these PES scans, and the subsequent transition state calculations, are summarised below. While maxima could be found on the potential energy surface, subsequent transition state and IRC calculations on these maxima did not yield any structure that could be unambiguously be assigned as an accurate transition state, thus we do not claim any of them to be valid transition states. The PES scans also highlighted that these maxima are clearly not rate-limiting steps, as the predicted energy barrier is never higher than 7 kcal.mol^{-1} (results shown below).

*First scan; extension of P-N bond starting from **I1**, R = ^{i}Pr*

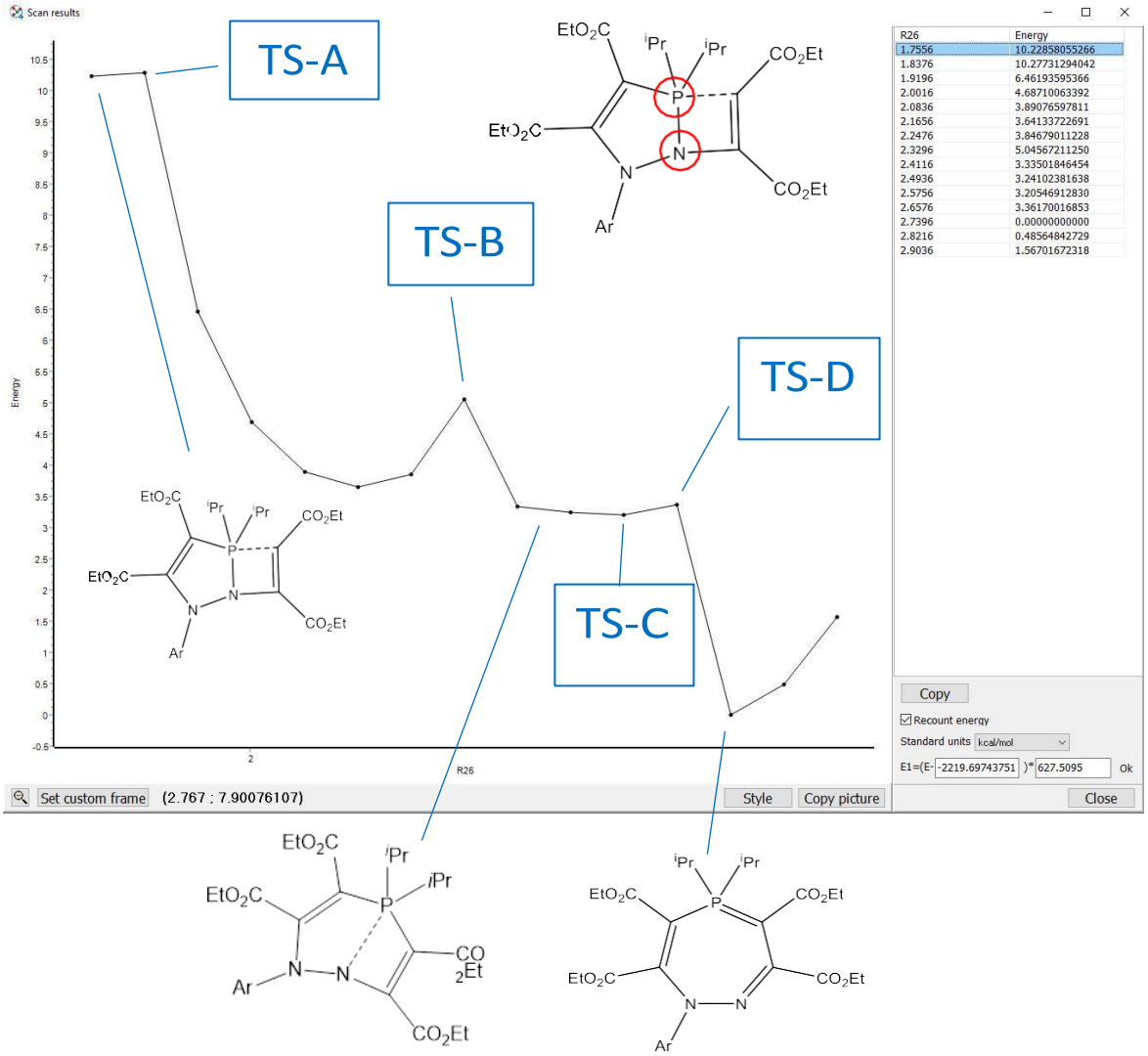

Subsequent transition state calculations

The negative frequency obtained in **TS-A** corresponded to twisting of an *ortho*-CH_3 group on the aryl ring, with the overall structure resembling **I1**.

The negative frequency obtained in **TS-B** corresponded to twisting of a CH_3 group on an ^{i}Pr substituent, with the overall structure resembling **I2**.

The negative frequency obtained in **TS-C** corresponded to twisting of an *ortho*-CH_3 group on the aryl ring, with the overall structure resembling the product.

The negative frequency obtained in **TS-D** corresponded to twisting of a CH_3 group on an ^{i}Pr substituent, with the overall structure resembling the product.

*Second scan; contraction of P-C bond starting from **I1**, R = ^{i}Pr*

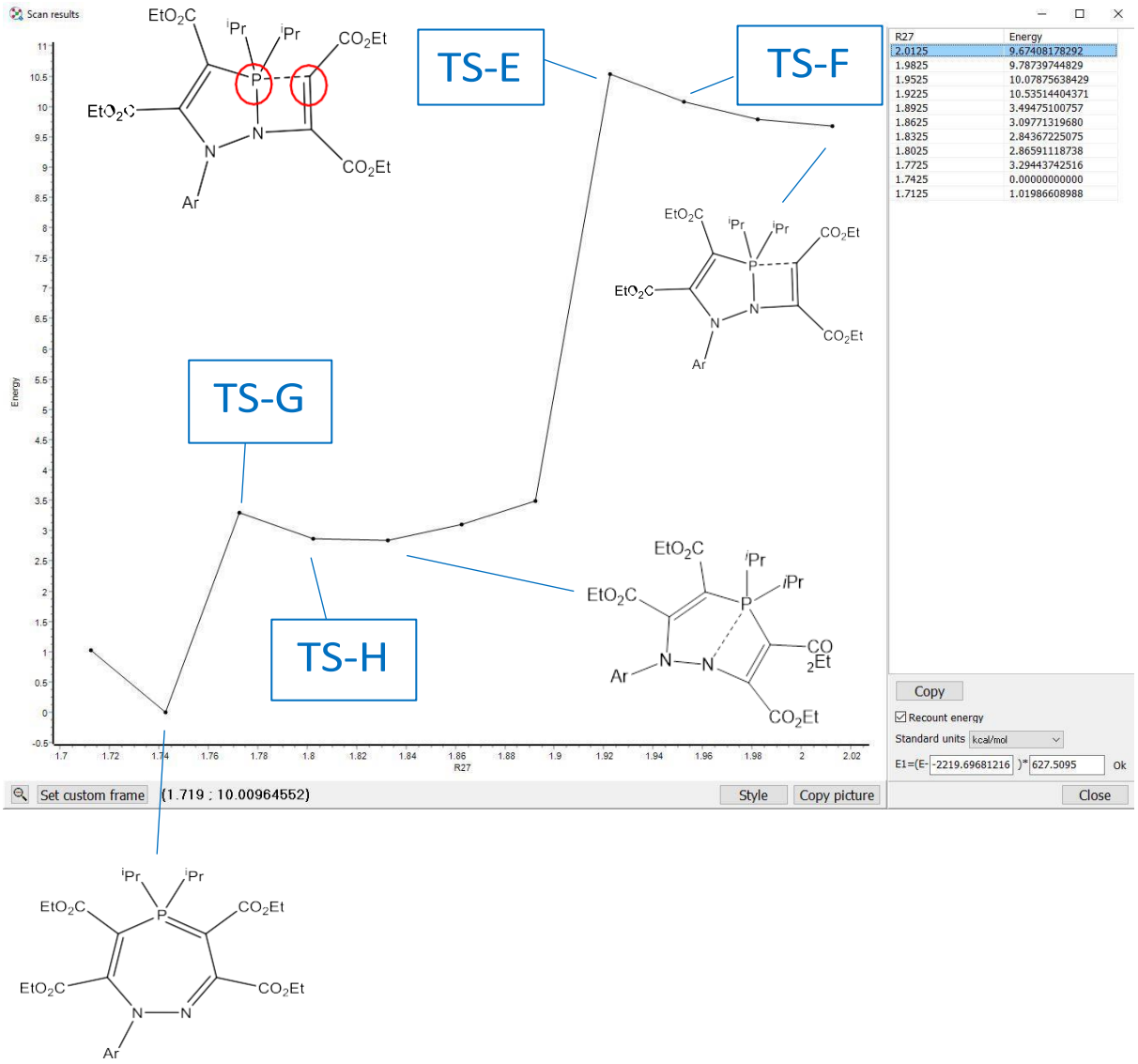

Subsequent transition state calculations

The negative frequency obtained in **TS-E** corresponded to rotation of an ^{i}Pr substituent, with the overall structure resembling **I1**.

The negative frequency obtained in **TS-F** corresponded to twisting of an *ortho*-CH_3 group on the aryl ring, with the overall structure resembling **I1**.

The negative frequency obtained in **TS-G** corresponded to twisting of an *ortho*-CH_3 group on the aryl ring, with the overall structure resembling the product.

The negative frequency obtained in **TS-H** corresponded to twisting of an *ortho*-CH_3 group on the aryl ring, with the overall structure resembling the product.

*Third scan; extension of P-N bond starting from **I1**, R = ^{t}Bu*

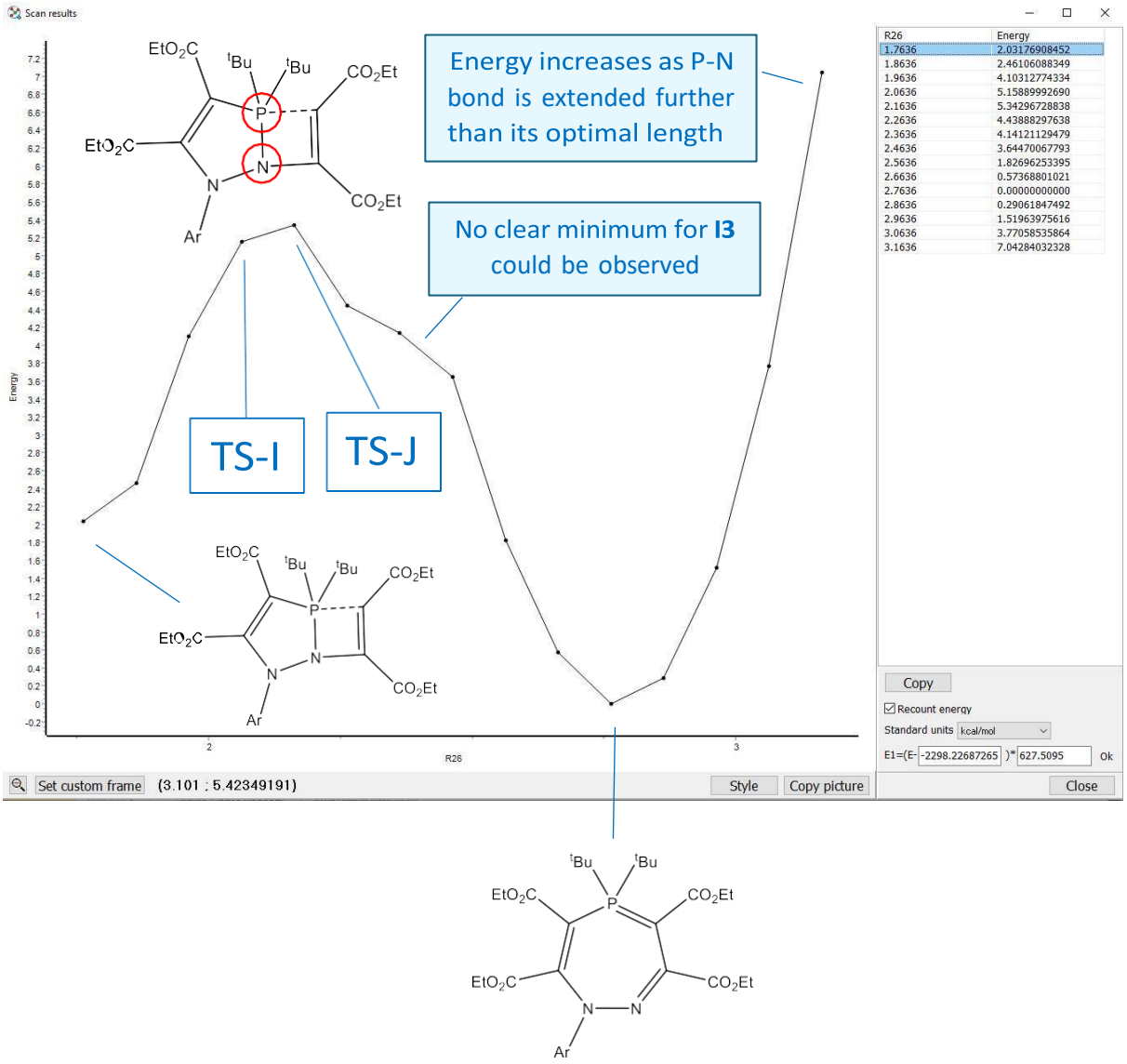

Subsequent transition state calculations

The negative frequency obtained in **TS-I** appeared visually though it may correspond to a valid transition state between **I1** and the product. However, when this structure was re-optimised at a higher level of theory (def2TZVP), the structure 'fell' down the energy well and resembled the product. In addition, IRC calculations did not support this structure being a valid transition state for this step. Subsequently, this structure was not assigned as a valid transition state, though even if it was it would be a low barrier (approximately 5 kcal.mol^{-1}).

Like **TS-I**, the negative frequency obtained in **TS-J** appeared visually though it may correspond to a valid transition state between **I1** and the product. However, when this structure was re-optimised at a higher level of theory (def2TZVP), the structure 'fell' down the energy well and resembled the product. In addition, IRC calculations did not support this structure being a valid transition state for this step. Subsequently, this structure was not assigned as a valid transition state.

*Fourth scan; contraction of P-C bond starting from **I1**, R = ^{t}Bu*

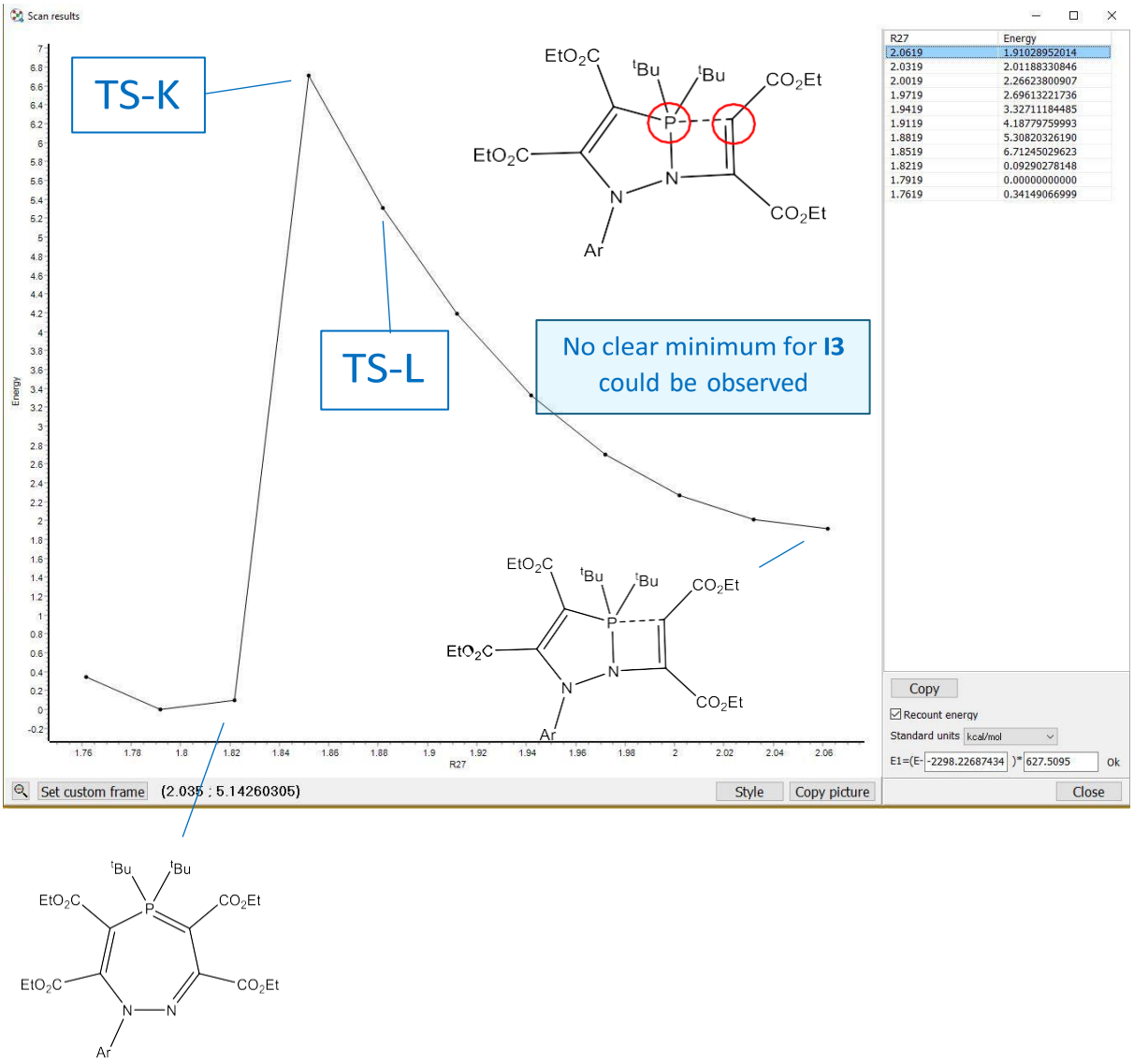

Subsequent transition state calculations

The negative frequency obtained in **TS-K** corresponded to twisting of an *ortho*-CH_3 group on the aryl ring, with the overall structure resembling **I1**.

The negative frequency obtained in **TS-L** corresponded to twisting of an *ortho*-CH_3 group on the aryl ring, with the overall structure resembling **I1**.

*Fifth scan; extension of P-N bond starting from **I1** (exact structure below)*

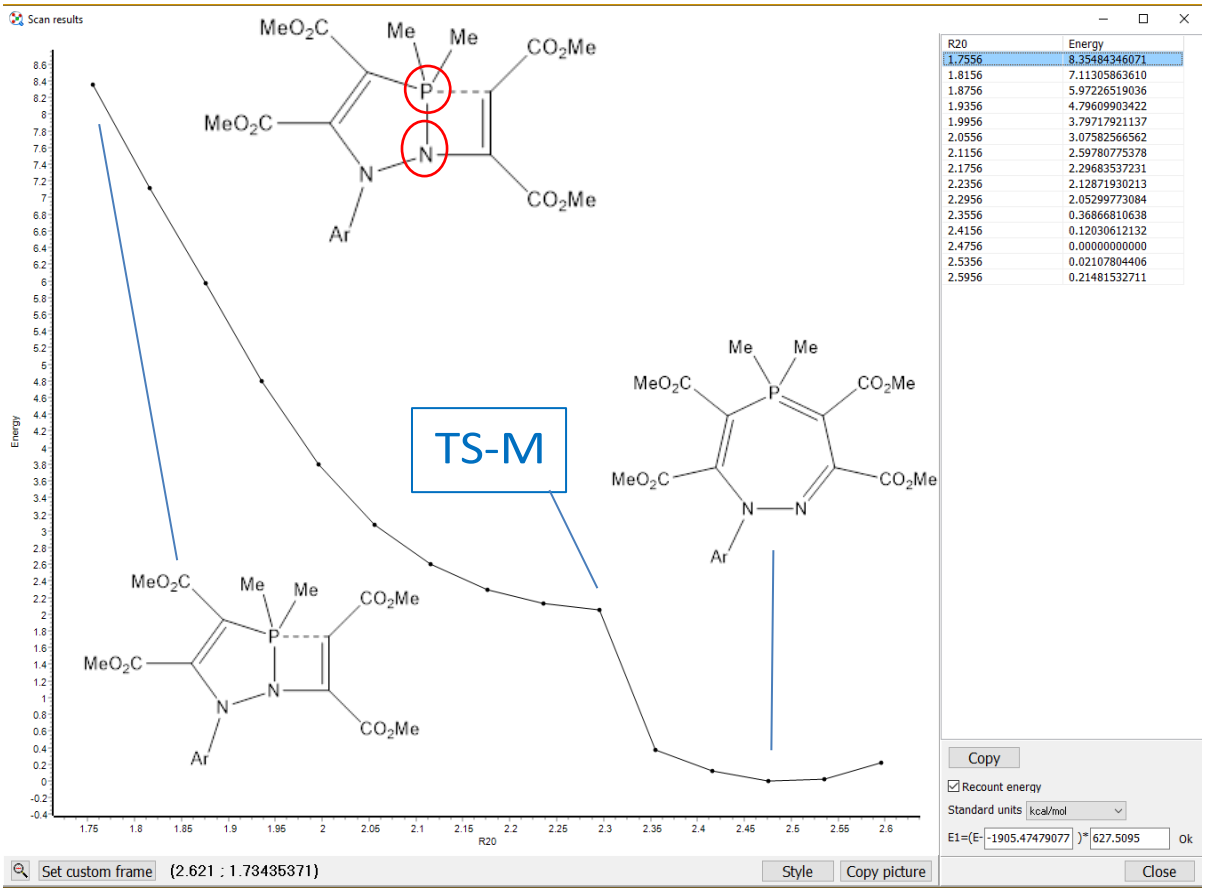

Subsequent transition state calculations

The negative frequency obtained in **TS-M** corresponded to twisting of a CH_3 group on one of the ester groups, with the overall structure resembling the product.

*Sixth scan; contraction of P-C bond starting from **I1** (exact structure below)*

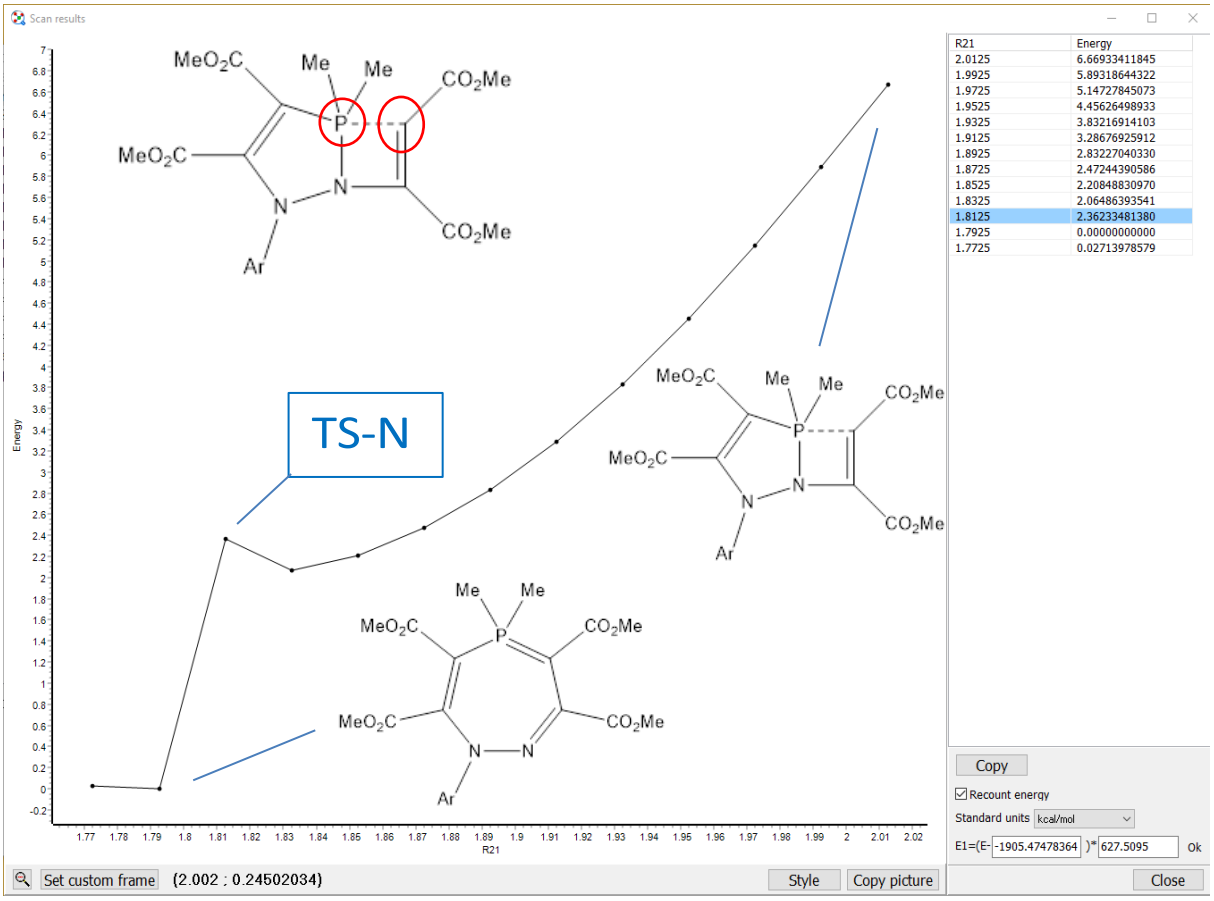

Subsequent transition state calculations

The negative frequency obtained in **TS-N** corresponded to twisting of a CH_3 group on one of the ester groups, with the overall structure resembling the product.

*Seventh scan; extension of P-N bond starting from **I1** (exact structure below)*

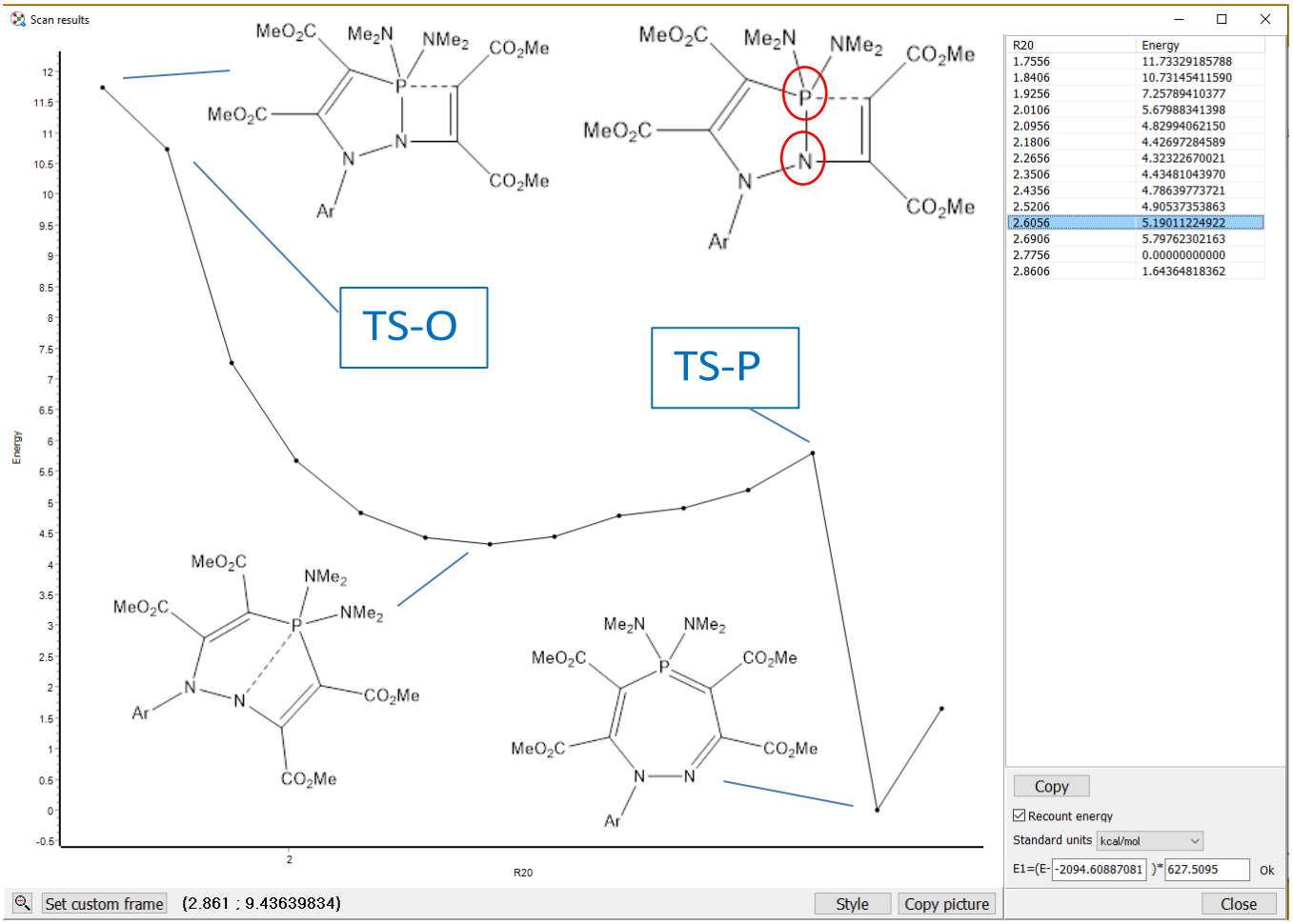

R20	Energy
1.7556	11.73329185788
1.8406	10.73145411590
1.9256	7.25789410377
2.0106	5.67988341398
2.0956	4.82994062150
2.1806	4.42697284589
2.2656	4.32322670021
2.3506	4.43481043970
2.4356	4.78639773721
2.5206	4.90537353863
2.6056	5.19011224922
2.6906	5.79762302163
2.7756	0.00000000000
2.8606	1.64364818362

Subsequent transition state calculations

The negative frequency obtained in **TS-O** corresponded to twisting of an *ortho*-CH_3 group on the aryl ring, with the overall structure resembling the product.

The negative frequency obtained in **TS-P** corresponded to dynamic rocking of the whole molecule (clearly not corresponding to a relevant transition state), with the overall structure resembling the product.

*Eighth scan; contraction of P-C bond starting from **I1** (exact structure below)*

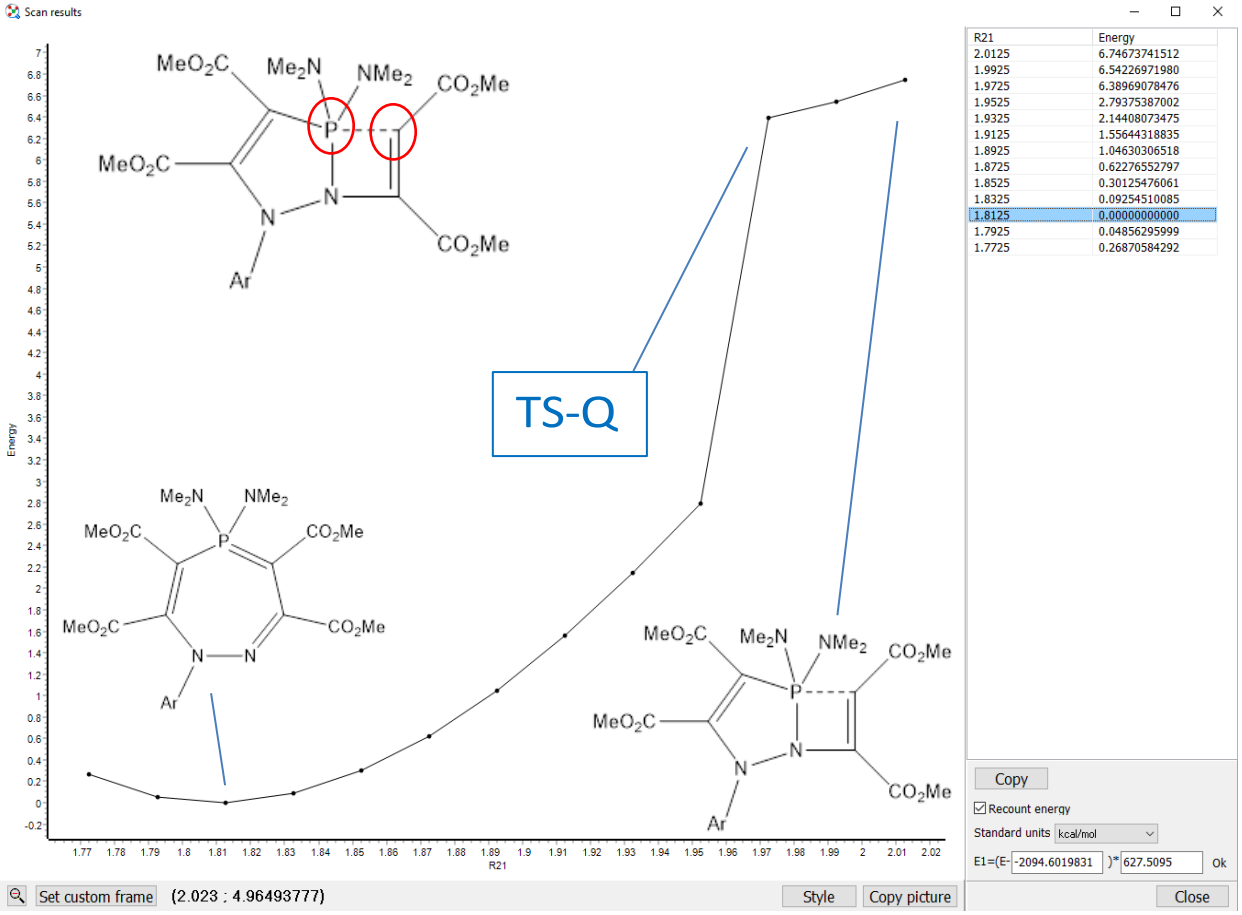

R21	Energy
2.0125	6.74673741512
1.9925	6.54226971980
1.9725	6.38969078476
1.9525	2.79375387002
1.9325	2.14408073475
1.9125	1.55644318835
1.8925	1.04630306518
1.8725	0.62276552797
1.8525	0.30125476061
1.8325	0.09254510085
1.8125	0.00000000000
1.7925	0.04856295999
1.7725	0.26870584292

Subsequent transition state calculations

The negative frequency obtained in **TS-Q** corresponded to twisting of a -CH_3 group on one of the -NMe_2 groups, with the overall structure resembling **I1**.

*Ninth scan; extension of P-N bond starting from **I1** (exact structure below)*

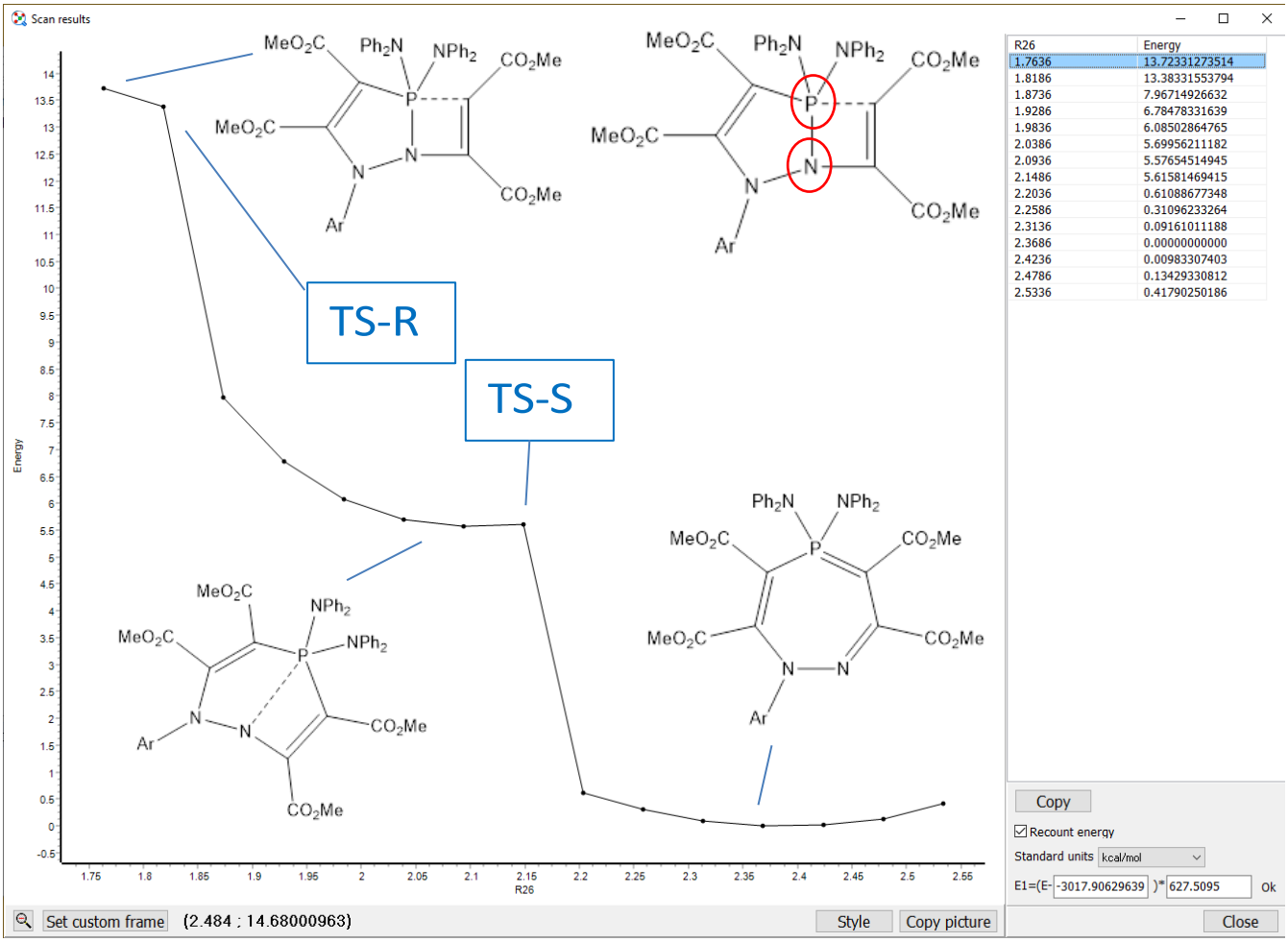

R26	Energy
1.7636	13.72331273514
1.8186	13.38331553794
1.8736	7.96714926632
1.9286	6.78478331639
1.9836	6.08502864765
2.0386	5.69956211182
2.0936	5.57654514945
2.1486	5.61581469415
2.2036	0.61088677348
2.2586	0.31096233264
2.3136	0.09161011188
2.3686	0.00000000000
2.4236	0.00983307403
2.4786	0.13429330812
2.5336	0.41790250186

Subsequent transition state calculations

The negative frequency obtained in **TS-R** corresponded to twisting of an *ortho*-CH_3 group on the aryl ring, with the overall structure resembling the product.

The negative frequency obtained in **TS-S** corresponded to twisting of an *ortho*-CH_3 group on the aryl ring, with the overall structure resembling the product.

*Tenth scan; contraction of P-C bond starting from **I1** (exact structure below)*

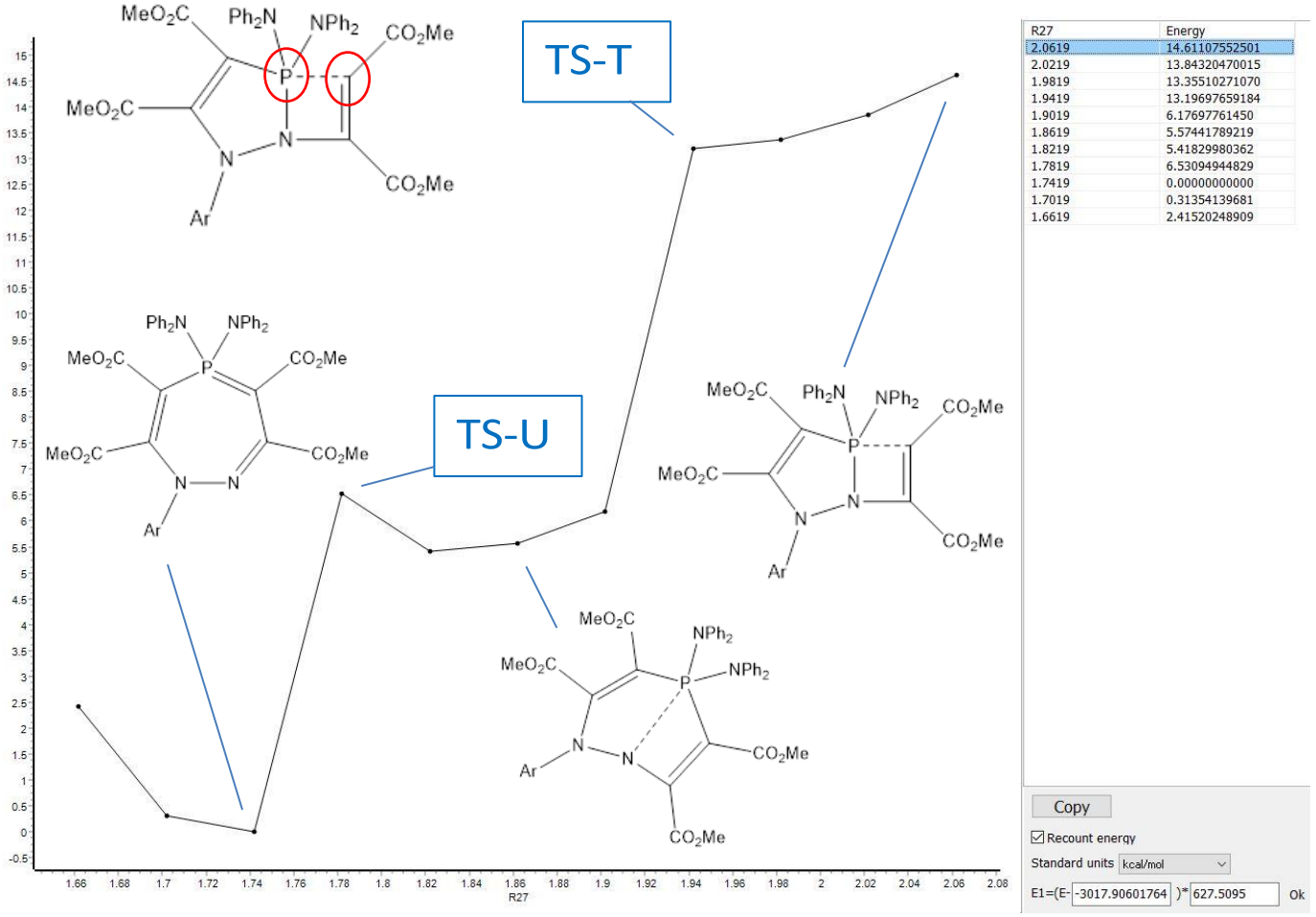

Subsequent transition state calculations

The negative frequency obtained in **TS-T** corresponded to dynamic rocking of the whole molecule (clearly not corresponding to a relevant transition state), with the overall structure resembling **I1**.

The negative frequency obtained in **TS-U** corresponded to twisting of a CH_3 group on one of the ester groups, with the overall structure resembling the product.

S5.4. Cartesian coordinates for optimised structures

*Table S9. Cartesian coordinates of the optimised structure of **1**.*

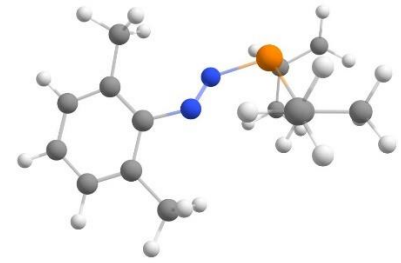

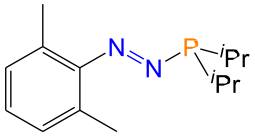

C	1.17214	-0.21298	0.29011
C	2.67326	-0.13102	0.34648
C	3.37909	1.05989	0.56857
N	2.75973	2.32348	0.77391
N	1.76352	2.56267	0.08131
P	0.91475	4.06381	0.32700
C	2.17508	5.18569	1.10000
C	1.84413	6.66065	0.87319
C	2.25048	4.88703	2.59955
C	0.84689	4.48031	-1.48345
C	-0.15592	5.59552	-1.77818
C	2.20061	4.72221	-2.14511
C	4.77653	1.07771	0.68222
C	5.50837	2.36319	0.95139
C	5.47162	-0.11035	0.51786
C	4.79564	-1.29589	0.28465
C	3.41439	-1.30104	0.21425
H	0.70192	0.42053	1.04232
H	0.85368	-1.24259	0.45588
H	0.79068	0.11663	-0.67592
H	3.14340	4.95238	0.64715

H	0.81941	6.89117	1.17628
H	1.96398	6.96171	-0.16682
H	2.51021	7.28320	1.47539
H	1.29673	5.10481	3.08630
H	3.01493	5.51422	3.06560
H	2.50396	3.84500	2.78791
H	0.43539	3.55083	-1.89090
H	0.18887	6.56258	-1.41000
H	-1.12535	5.39110	-1.32127
H	-0.30285	5.69089	-2.85647
H	2.67282	5.63448	-1.77617
H	2.07697	4.83299	-3.22527
H	2.88618	3.89199	-1.96956
H	5.10383	2.86693	1.82979
H	5.41129	3.06011	0.11624
H	6.56925	2.17187	1.11115
H	6.55288	-0.10635	0.58761
H	2.88994	-2.23638	0.05786
H	5.34500	-2.22216	0.17220

*Table S10. Cartesian coordinates of the optimised structure of **3**.*

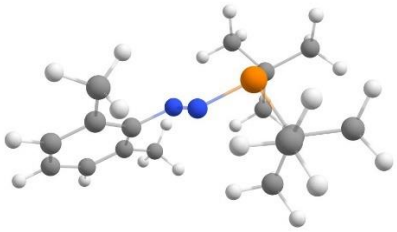

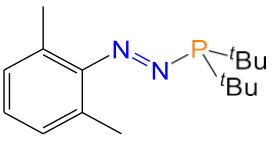

C	1.33979	-0.15410	0.81605
C	2.78960	-0.17156	0.41258
C	3.42425	0.89920	-0.22989

N	2.74516	2.10099	-0.58256
N	2.02407	2.57364	0.30396
P	1.01565	3.95162	0.05893
C	1.52924	4.79075	1.67011
C	3.02944	4.72691	1.97110
C	1.06795	6.24930	1.68009
C	0.77179	4.02868	2.76792
C	1.60544	4.90213	-1.45432
C	1.37244	3.95847	-2.64781
C	0.67642	6.10976	-1.64371
C	3.06290	5.35773	-1.43628
C	4.75906	0.82359	-0.64619
C	5.41052	1.98528	-1.34254
C	5.47536	-0.33094	-0.36895
C	4.87158	-1.39848	0.27411
C	3.54228	-1.31772	0.64733
H	1.19555	0.37415	1.75866
H	0.97722	-1.17531	0.93718
H	0.71576	0.34759	0.07672
H	3.62714	5.22466	1.20911
H	3.37316	3.69597	2.05539
H	3.22568	5.22524	2.92536
H	1.68243	6.87324	1.03071
H	1.16091	6.64613	2.69476
H	0.02399	6.35467	1.37706
H	1.03445	2.97008	2.77044
H	-0.30837	4.11442	2.63770
H	1.03298	4.44704	3.74431
H	0.35066	3.57166	-2.65722
H	2.06003	3.11607	-2.63232

H	1.52471	4.51722	-3.57591
H	-0.37444	5.81212	-1.62704
H	0.87772	6.56225	-2.61901
H	0.82261	6.88016	-0.88918
H	3.74132	4.52801	-1.23705
H	3.23312	6.13597	-0.69124
H	3.32520	5.77828	-2.41215
H	5.54348	2.82827	-0.66022
H	4.79743	2.34129	-2.17142
H	6.39124	1.70354	-1.72498
H	6.51429	-0.39616	-0.66973
H	3.06761	-2.16520	1.12786
H	5.43435	-2.30199	0.47240

Table S11. Cartesian coordinates of the optimised structure of $(C(CO2Et))_2$.

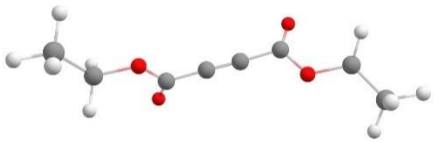

EtO_2C—≡—CO_2Et

C	-3.40373	1.05995	-0.16566
C	-2.25583	1.12844	0.17000
C	-4.78418	1.02772	-0.61739
O	-5.47722	0.10466	0.03941
C	-6.86711	-0.01242	-0.31500
C	-7.46177	-1.10839	0.53241
H	-6.93872	-0.23397	-1.38091
H	-7.35202	0.94921	-0.14019
H	-6.96627	-2.06056	0.34212
H	-8.52068	-1.21784	0.29544
H	-7.36814	-0.87470	1.59299
O	-5.21288	1.75098	-1.47199

C	-0.88197	1.25935	0.62374
O	-0.08178	0.43505	-0.04277
C	1.31093	0.47966	0.31652
C	2.02928	-0.55161	-0.51637
H	1.40310	0.27931	1.38495
H	1.68538	1.48779	0.13186
H	1.64161	-1.55089	-0.31774
H	3.09245	-0.53857	-0.27351
H	1.91586	-0.34070	-1.57982
O	-0.54432	2.01878	1.48771

*Table S12. Cartesian coordinates of the optimised structure of **TS1** (R = ^{i}Pr).*

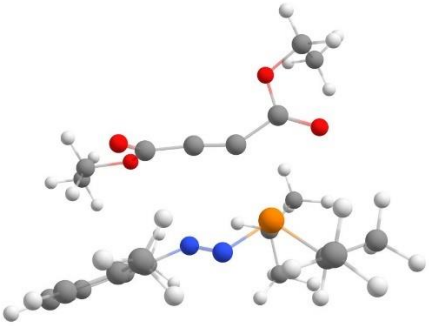

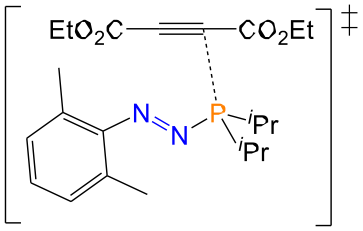

C	1.84545	-0.55322	-2.97346
C	3.29358	-0.35017	-3.34153
O	4.09369	-0.97598	-2.32722
C	5.41523	-0.84124	-2.48310
C	6.16767	-1.44829	-1.43512
C	6.93390	-1.79738	-0.54044
C	7.84907	-2.84079	-0.05544
O	7.70597	-3.94730	-0.77756
C	8.50044	-5.08064	-0.39283

C	7.86578	-5.82871	0.75904
O	8.61996	-2.72356	0.86248
P	7.13460	-0.19481	1.22472
C	8.48033	0.63502	2.17418
H	8.03312	1.49842	2.67511
C	9.08384	-0.30096	3.21931
C	9.54070	1.12620	1.18926
C	5.78040	-0.69567	2.37249
H	4.93197	-0.71052	1.68148
C	5.96067	-2.10182	2.94082
C	5.49630	0.34224	3.45603
N	6.51099	1.13986	0.36676
N	5.33189	0.98681	-0.01363
C	4.78308	1.95415	-0.88532
C	3.38639	2.06650	-0.77972
C	2.62851	1.25615	0.23425
C	2.72064	2.93953	-1.62344
C	3.41913	3.65847	-2.58025
C	4.78976	3.51527	-2.69153
C	5.50967	2.67417	-1.84772
C	6.99448	2.55471	-2.03636
O	5.93605	-0.27865	-3.41750
H	1.20972	-0.11090	-3.74174
H	1.61647	-0.07353	-2.02204
H	1.60706	-1.61458	-2.89566
H	3.55205	0.70905	-3.39224
H	3.53128	-0.80209	-4.30612
H	9.50655	-4.74454	-0.14307
H	8.53913	-5.69373	-1.29154
H	7.85276	-5.21466	1.65933

H	8.43907	-6.73299	0.96977
H	6.84424	-6.11930	0.51152
H	8.36512	-0.57245	3.99294
H	9.92430	0.19457	3.71026
H	9.44989	-1.21843	2.75719
H	9.11364	1.78674	0.43470
H	10.01242	0.28212	0.68145
H	10.31754	1.67545	1.72604
H	6.03683	-2.84790	2.15003
H	5.09725	-2.35866	3.55905
H	6.85302	-2.18421	3.56238
H	5.33901	1.33356	3.02901
H	6.31186	0.40675	4.17868
H	4.59295	0.06660	4.00552
H	2.83212	0.19243	0.10395
H	1.55653	1.42713	0.13210
H	2.91901	1.51368	1.25426
H	1.64588	3.04639	-1.53942
H	5.32491	4.06395	-3.45714
H	7.27986	3.00146	-2.98853
H	7.31373	1.51306	-2.03836
H	7.53476	3.05852	-1.23469
H	2.88997	4.32548	-3.24937

*Table S13. Cartesian coordinates of the optimised structure of **TS1** (R = ^{t}Bu).*

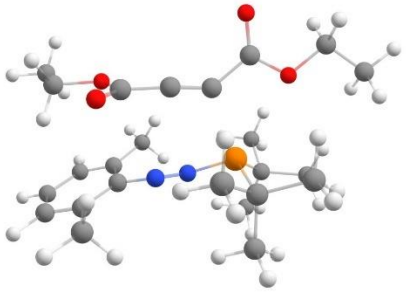

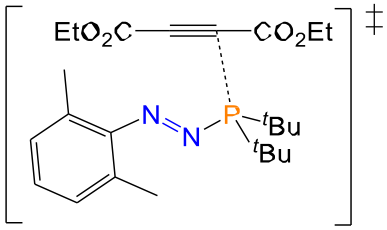

C	2.20759	-0.36981	-1.17897
C	2.91430	-0.48894	0.14148
C	2.97741	0.54420	1.09235
N	2.41128	1.83106	0.92399
N	2.35570	2.26914	-0.24621
P	1.46875	3.66730	-0.54092
C	1.83727	5.00621	0.72375
C	3.33773	5.30434	0.77695
C	1.05173	6.28153	0.38978
C	1.36523	4.52181	2.10414
C	2.13522	4.02702	-2.26140
C	1.34983	3.07859	-3.18050
C	1.87042	5.46848	-2.69309
C	3.63228	3.72682	-2.39904
C	3.54862	0.34182	2.35960
C	3.52820	1.42689	3.39896
C	4.12308	-0.88838	2.64131
C	4.09677	-1.90884	1.70649
C	3.48758	-1.70921	0.48086
H	1.23909	0.11764	-1.06271
H	2.04655	-1.36265	-1.60052
H	2.78417	0.22001	-1.89121
H	3.70272	5.73338	-0.15669
H	3.91569	4.40567	0.99727
H	3.53070	6.03146	1.57072
H	1.42218	6.78817	-0.49789

H	1.15055	6.97409	1.22972
H	-0.00941	6.07387	0.25055
H	1.83247	3.58558	2.39558
H	0.28587	4.38153	2.13897
H	1.62875	5.29101	2.83524
H	0.28417	3.31134	-3.17418
H	1.47662	2.03740	-2.88082
H	1.72025	3.18296	-4.20401
H	0.84018	5.76816	-2.51228
H	2.06233	5.55497	-3.76578
H	2.53358	6.17062	-2.18758
H	3.84957	2.68418	-2.17578
H	4.24155	4.35079	-1.74587
H	3.93500	3.92970	-3.43087
H	2.49822	1.67970	3.65593
H	4.01058	2.33796	3.04263
H	4.04194	1.09576	4.30120
H	4.58203	-1.05007	3.60893
H	3.44146	-2.52247	-0.23381
C	-0.56640	2.73124	0.10099
C	-1.67628	3.42467	-0.57143
O	-2.82142	3.09557	-0.43442
O	-1.29941	4.46108	-1.33597
C	-2.37861	5.18049	-1.95081
C	-1.79873	6.31930	-2.75093
H	-3.04877	5.53809	-1.16762

H	-2.94706	4.49336	-2.57903
H	-1.20608	6.98203	-2.11852
H	-2.61081	6.90139	-3.18818
H	-1.16880	5.95300	-3.56207
C	-0.40790	1.83222	0.93414
C	-0.14055	0.84894	1.92157
O	-0.11168	-0.38023	1.38111
O	0.02550	1.08169	3.09694
C	0.21075	-1.45477	2.27122
C	0.10949	-2.73824	1.48493
H	-0.48192	-1.43943	3.11406
H	1.22000	-1.30204	2.65895
H	-0.90064	-2.88236	1.10008
H	0.35991	-3.58210	2.12960
H	0.80634	-2.72990	0.64657
H	4.53956	-2.86944	1.93845

*Table S14. Cartesian coordinates of the optimised structure of **I1** (R = ^{i}Pr).*

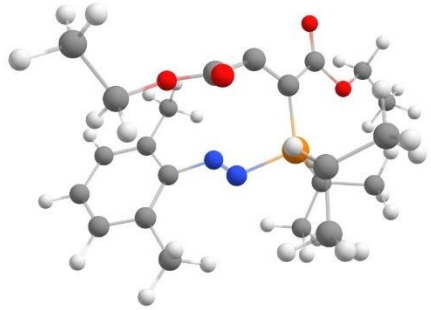

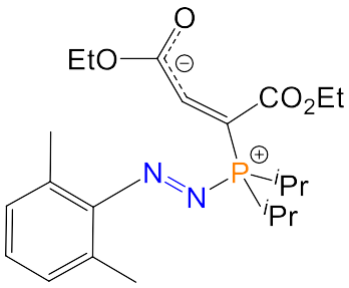

C	3.56055	1.28330	1.77921

C	3.51081	0.40153	0.56461
C	2.80699	0.71663	-0.61399
N	2.03847	1.87583	-0.81666
N	1.63169	2.48492	0.18242
P	0.63206	3.84510	-0.22544
C	-0.14969	4.16385	1.38314
C	0.84769	4.48834	2.49373
C	-1.30244	5.16354	1.30153
H	-0.59090	3.17967	1.58562
C	1.82523	5.15656	-0.72755
H	1.90210	5.00900	-1.80699
C	1.28834	6.56531	-0.46881
C	3.21485	4.98039	-0.10767
C	2.80024	-0.14089	-1.72976
C	2.01526	0.19773	-2.96331
C	3.48996	-1.34001	-1.64036
C	4.19115	-1.66499	-0.49230
C	4.20827	-0.79898	0.58779
H	3.76154	2.32379	1.52146
H	4.33851	0.93350	2.45785
H	2.60560	1.27555	2.30543
H	1.28799	5.47973	2.37447
H	1.65081	3.75232	2.54031
H	0.32660	4.47440	3.45232
H	-0.95575	6.18408	1.13748
H	-1.84822	5.14462	2.24592
H	-2.00392	4.89747	0.51090
H	0.28023	6.69715	-0.85307
H	1.93434	7.28904	-0.96903

H	1.29437	6.79865	0.59634
H	3.68600	4.04639	-0.40741
H	3.18223	5.01466	0.98163
H	3.85228	5.79967	-0.44617
H	2.30591	1.16814	-3.36543
H	0.95004	0.25522	-2.73535
H	2.17088	-0.56124	-3.72936
H	3.47736	-2.02410	-2.47957
H	4.76908	-1.06096	1.47672
C	-0.61848	3.27417	-1.38160
C	-1.19329	2.10582	-1.08581
C	-1.03205	1.19065	-0.02302
C	-1.03797	4.03709	-2.58681
O	-1.82244	3.66514	-3.40985
O	-0.41554	5.23920	-2.67450
C	-0.72490	6.01378	-3.83582
C	0.08199	7.28871	-3.78207
H	-1.79716	6.21489	-3.85591
H	-0.48696	5.42673	-4.72459
H	-0.19531	7.89831	-2.92131
H	-0.10045	7.87281	-4.68491
H	1.15044	7.07427	-3.72470
O	-1.55000	1.28186	1.08335
O	-0.30314	0.10375	-0.39722
C	-0.03673	-0.87072	0.60878
C	-1.14989	-1.89110	0.71725
H	0.12208	-0.37073	1.56566
H	0.89777	-1.34102	0.29709
H	-2.07249	-1.41122	1.04130

H	-0.87961	-2.65739	1.44690
H	-1.32142	-2.37508	-0.24515
H	4.73264	-2.60126	-0.43752

*Table S15. Cartesian coordinates of the optimised structure of **I1** (R = ^{t}Bu).*

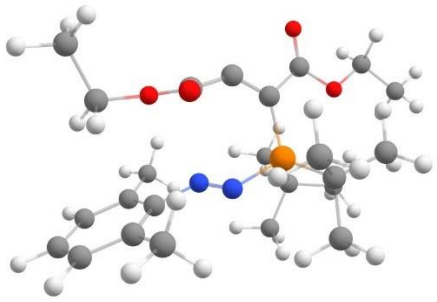

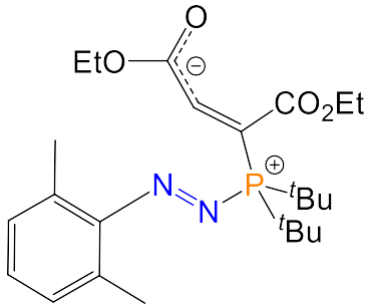

C	2.20451	0.74310	2.33225
C	2.87563	0.11599	1.14675
C	2.77037	0.59964	-0.17429
N	2.06579	1.74502	-0.57967
N	1.62302	2.51489	0.28681
P	0.78643	3.87617	-0.38383
C	0.37045	4.76885	1.18646
C	1.65167	5.13018	1.94809
C	-0.47041	6.02538	0.94066
C	-0.45942	3.79190	2.03516
C	2.06137	4.73478	-1.46775
C	1.88238	4.18464	-2.89019
C	1.89482	6.25718	-1.48284
C	3.48987	4.41676	-0.99104

C	3.34113	-0.09075	-1.26077
C	3.14635	0.38726	-2.67131
C	4.06527	-1.24433	-1.00976
C	4.20058	-1.71817	0.28352
C	3.60509	-1.05043	1.33917
H	2.58662	1.74448	2.52965
H	2.36643	0.12444	3.21484
H	1.13032	0.83961	2.15914
H	2.24452	5.88636	1.43391
H	2.27425	4.25270	2.12334
H	1.37000	5.54057	2.92043
H	0.04680	6.77322	0.34343
H	-0.69794	6.47102	1.91182
H	-1.41305	5.78775	0.45130
H	0.09251	2.88851	2.28368
H	-1.37498	3.48392	1.53217
H	-0.72879	4.30166	2.96315
H	0.94290	4.51140	-3.33265
H	1.91498	3.09585	-2.90734
H	2.69916	4.56330	-3.51006
H	0.88405	6.55262	-1.73973
H	2.57173	6.66121	-2.23969
H	2.16636	6.71016	-0.52971
H	3.75674	3.37664	-1.16339
H	3.64591	4.64009	0.06391
H	4.17682	5.03890	-1.56921
H	3.62342	1.35447	-2.83747
H	2.08470	0.50733	-2.88796
H	3.57324	-0.32747	-3.37412
H	4.51314	-1.78221	-1.83588

H	3.69593	-1.44876	2.34216
C	-0.69464	3.21850	-1.20968
C	-1.11390	1.97757	-0.98443
C	-0.74803	0.87627	-0.19927
C	-1.53222	4.11249	-2.05880
O	-2.49220	3.78073	-2.68987
O	-1.09996	5.40131	-2.04143
C	-1.93186	6.33082	-2.74563
C	-1.36447	7.71924	-2.57377
H	-2.94367	6.26111	-2.34326
H	-1.97982	6.04188	-3.79660
H	-1.25756	7.97011	-1.51733
H	-2.04184	8.44356	-3.02787
H	-0.39244	7.82020	-3.05782
O	-1.04354	0.72522	0.97999
O	-0.11590	-0.09389	-0.92250
C	0.07236	-1.35109	-0.27874
C	-1.13039	-2.25145	-0.46635
H	0.27173	-1.19437	0.78142
H	0.96372	-1.77635	-0.74296
H	-2.00851	-1.80884	0.00376
H	-0.94447	-3.22395	-0.00551
H	-1.33817	-2.40289	-1.52628
H	4.75925	-2.62698	0.47023

*Table S16. Cartesian coordinates of the optimised structure of **TS2** (R = ^{i}Pr).*

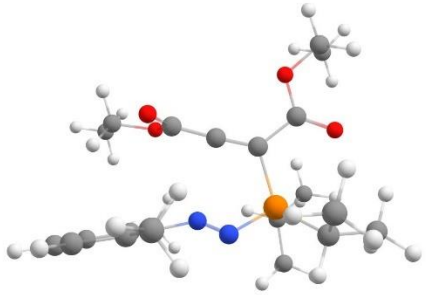

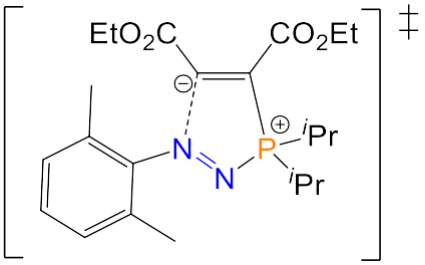

C	1.84046	-0.54289	-2.68906
C	3.30140	-0.34203	-3.01180
O	4.05707	-0.77214	-1.87918
C	5.39522	-0.55469	-1.96801
C	6.08151	-0.83655	-0.80034
C	6.86961	-1.07842	0.19315
C	7.64888	-2.29341	0.51071
O	7.52871	-3.25392	-0.39096
C	8.20156	-4.49151	-0.12317
C	7.36481	-5.38263	0.76897
O	8.32754	-2.38326	1.51366
P	7.04989	0.24524	1.52027
C	8.69352	0.75823	2.13755
H	8.50816	1.79682	2.43146
C	9.23338	-0.00851	3.34065
C	9.68068	0.75865	0.96790
C	5.82985	-0.08902	2.83646
H	4.90631	-0.06885	2.24788
C	5.95881	-1.46205	3.49134

C	5.77688	1.05479	3.84962
N	6.56809	1.60557	0.66458
N	5.38223	1.41663	0.25888
C	4.85638	2.28430	-0.71086
C	3.45154	2.36097	-0.68205
C	2.66410	1.60562	0.35036
C	2.80892	3.14315	-1.62545
C	3.53781	3.80377	-2.60178
C	4.91506	3.68761	-2.64235
C	5.61165	2.93343	-1.70443
C	7.09975	2.79771	-1.83875
O	5.93106	-0.11314	-2.97497
H	1.23026	-0.23958	-3.54150
H	1.54762	0.05802	-1.82700
H	1.62958	-1.59027	-2.46898
H	3.52163	0.70811	-3.21575
H	3.59950	-0.91965	-3.88930
H	9.17323	-4.28432	0.32468
H	8.34553	-4.93827	-1.10536
H	7.23454	-4.93002	1.75201
H	7.86170	-6.34549	0.89859
H	6.38448	-5.55689	0.32456
H	8.56884	0.05110	4.20221
H	10.18904	0.43090	3.63314
H	9.39217	-1.05688	3.09854
H	9.29025	1.30531	0.10911
H	9.90796	-0.26244	0.65921
H	10.61168	1.23474	1.28067
H	5.87162	-2.26446	2.76059
H	5.15639	-1.58247	4.22212

H	6.91017	-1.58370	4.00813
H	5.63198	2.01841	3.36021
H	6.68552	1.10889	4.45083
H	4.94111	0.89438	4.53325
H	2.88179	0.53870	0.28411
H	1.59549	1.75819	0.19750
H	2.91315	1.92750	1.36284
H	1.72885	3.22370	-1.60577
H	5.47081	4.18030	-3.43066
H	7.42138	3.21452	-2.79278
H	7.38914	1.74642	-1.81170
H	7.62400	3.30841	-1.03184
H	3.02595	4.40019	-3.34692

Table S17. Cartesian coordinates of the optimised structure of ***TS2*** *(R = ^{t}Bu).*

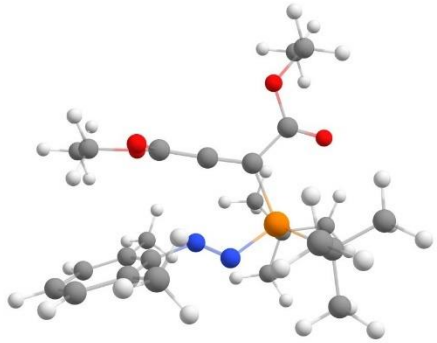

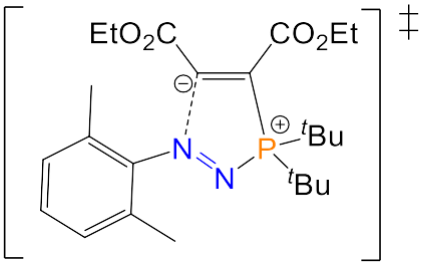

C	2.02514	-0.42631	-2.95892
C	3.50348	-0.20205	-3.16764
O	4.18018	-0.67002	-2.00149
C	5.52947	-0.49210	-2.00979
C	6.12805	-0.79434	-0.80187

C	6.81589	-1.07818	0.25279
C	7.36763	-2.38286	0.67089
O	7.32722	-3.30735	-0.27456
C	7.74895	-4.63033	0.08307
C	6.64554	-5.38679	0.79070
O	7.79334	-2.57837	1.79186
P	7.03584	0.24578	1.58802
C	8.78260	0.74847	1.97712
C	8.75511	2.02518	2.82858
C	9.62263	-0.32110	2.68072
C	9.43495	1.05499	0.61841
C	5.92156	-0.07585	3.05816
C	4.77903	-0.99098	2.59729
C	6.66654	-0.74688	4.21593
C	5.33324	1.25700	3.54474
N	6.49706	1.60168	0.74141
N	5.33444	1.36944	0.29838
C	4.78768	2.26411	-0.63949
C	3.38086	2.27900	-0.64461
C	2.59393	1.41624	0.29985
C	2.72694	3.09326	-1.55328
C	3.44708	3.84324	-2.46886
C	4.82804	3.78136	-2.48527
C	5.53411	2.99917	-1.57799
C	7.02721	2.92445	-1.69405
O	6.13636	-0.07067	-2.98530
H	1.47540	-0.10135	-3.84384
H	1.66218	0.14314	-2.10241
H	1.81191	-1.48239	-2.78806
H	3.72549	0.85764	-3.31534
H	3.86957	-0.74184	-4.04294

H	8.64511	-4.56869	0.70084
H	8.00004	-5.09626	-0.86805
H	6.41664	-4.92547	1.75096
H	6.96282	-6.41520	0.97124
H	5.74202	-5.40659	0.18052
H	8.37519	1.83580	3.83321
H	8.15289	2.80666	2.36466
H	9.77714	2.39872	2.93023
H	9.22990	-0.59614	3.65593
H	10.62305	0.09335	2.82880
H	9.70990	-1.22868	2.08962
H	8.94090	1.87888	0.10851
H	9.42314	0.18674	-0.04227
H	10.47713	1.33063	0.79502
H	5.14017	-1.99172	2.36271
H	4.27005	-0.58808	1.72363
H	4.05788	-1.07451	3.41432
H	7.16905	-1.65895	3.90055
H	5.93089	-1.00511	4.98160
H	7.39175	-0.07577	4.67655
H	4.70299	1.72146	2.78896
H	6.10350	1.97136	3.83450
H	4.71648	1.05550	4.42406
H	2.83093	0.36492	0.13016
H	1.52510	1.56306	0.14353
H	2.81782	1.63786	1.34384
H	1.64423	3.12541	-1.55684
H	5.38105	4.34087	-3.22971
H	7.34616	3.37997	-2.63104
H	7.35859	1.88546	-1.69036
H	7.51729	3.43682	-0.86625

H	2.92658	4.46466	-3.18702

*Table S18. Cartesian coordinates of the optimised structure of **4**.*

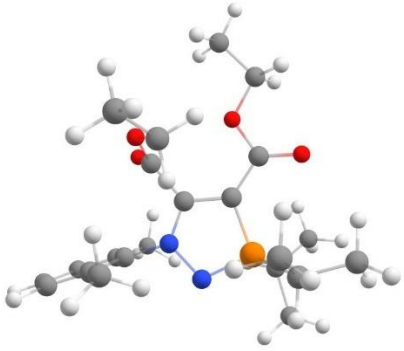

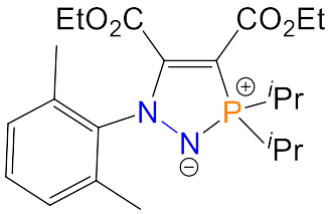

C	1.82004	2.04898	-1.02383
C	2.85877	1.16081	-0.38531
O	3.51501	1.92496	0.63350
C	4.70177	1.57116	1.12433
C	5.44270	0.46544	0.41343
C	5.25983	-0.91024	0.59258
C	4.28303	-1.56938	1.41520
O	3.54678	-0.70256	2.13604
C	2.53522	-1.24753	2.98454
C	1.82427	-0.08650	3.63605
O	4.11153	-2.77078	1.46827
P	6.44037	-1.66596	-0.46366
C	5.74868	-2.74193	-1.77614
C	5.40264	-4.16838	-1.34952
C	4.54160	-2.03759	-2.39403
C	7.77602	-2.57465	0.40747
C	7.32480	-3.59633	1.44858
C	8.79522	-3.13238	-0.58636

N	7.01742	-0.28742	-1.10898
N	6.37484	0.76870	-0.47177
C	6.90476	2.07611	-0.71930
C	6.47549	2.79053	-1.83300
C	5.45828	2.22669	-2.78283
C	7.02653	4.04908	-2.04581
C	7.97629	4.56152	-1.18046
C	8.40548	3.81674	-0.09490
C	7.88416	2.55439	0.15097
C	8.35712	1.72431	1.30730
O	5.16759	2.14126	2.06554
H	1.28696	1.49253	-1.79609
H	2.28475	2.92226	-1.48317
H	1.09810	2.39393	-0.28370
H	3.58320	0.81096	-1.12180
H	2.40162	0.28854	0.08474
H	3.00385	-1.90141	3.72232
H	1.85742	-1.85919	2.38564
H	2.52180	0.51875	4.21515
H	1.04693	-0.45778	4.30530
H	1.35906	0.55535	2.88681
H	6.55268	-2.76771	-2.52076
H	4.72019	-4.16857	-0.49892
H	6.28729	-4.74380	-1.08071
H	4.91823	-4.68433	-2.18123
H	3.71221	-2.00923	-1.68385
H	4.21028	-2.57770	-3.28267
H	4.78160	-1.01447	-2.68507
H	8.24827	-1.74156	0.93886
H	6.86065	-4.47092	0.99580

H	6.60639	-3.17082	2.14782
H	8.19521	-3.93552	2.01505
H	8.39144	-3.98075	-1.14177
H	9.67984	-3.48224	-0.05088
H	9.11349	-2.37087	-1.30057
H	5.59099	1.15148	-2.90108
H	5.55004	2.69566	-3.76192
H	4.44303	2.41155	-2.42493
H	6.70939	4.62565	-2.90653
H	9.16173	4.21425	0.57078
H	9.24789	2.16240	1.75551
H	8.59636	0.71194	0.97635
H	7.58158	1.65737	2.07221
H	8.39619	5.54327	-1.36007

*Table S19. Cartesian coordinates of the optimised structure of **6**.*

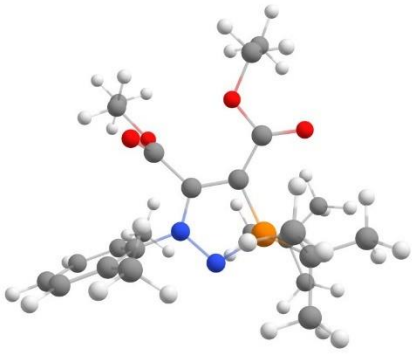

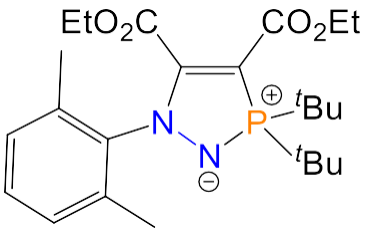

C	2.22851	-2.40967	-2.59727
C	3.57939	-1.77740	-2.81916
O	3.99565	-1.19998	-1.57363
C	5.17048	-0.58270	-1.57531

C	5.51007	-0.06073	-0.20993
C	6.14650	-0.76761	0.81317
C	6.65716	-2.10826	0.75660
O	6.33400	-2.74279	-0.38978
C	6.78397	-4.08858	-0.54559
C	5.79004	-5.06806	0.04108
O	7.32603	-2.63297	1.62578
P	6.37432	0.41114	2.10233
C	8.16077	0.77102	2.50405
C	8.27274	2.22938	2.96927
C	8.77553	-0.17405	3.53789
C	8.92283	0.61872	1.18076
C	5.38901	-0.00729	3.63105
C	3.92374	0.01604	3.17812
C	5.70953	-1.40300	4.17340
C	5.57700	1.05838	4.71480
N	5.71156	1.67261	1.30837
N	5.27464	1.20433	0.07485
C	4.67514	2.14622	-0.82026
C	3.28637	2.25070	-0.86449
C	2.41164	1.42379	0.03181
C	2.73619	3.16412	-1.75665
C	3.54548	3.94730	-2.56054
C	4.92307	3.83194	-2.48613
C	5.51321	2.92766	-1.61353
C	7.00240	2.78192	-1.52523
O	5.87417	-0.43528	-2.53365
H	1.87892	-2.86438	-3.52493
H	1.49776	-1.66349	-2.28377
H	2.28323	-3.18429	-1.83196
H	3.54479	-0.99265	-3.57619

H	4.32860	-2.50902	-3.12652
H	7.76199	-4.19808	-0.07802
H	6.88619	-4.22511	-1.62192
H	5.69946	-4.92009	1.11717
H	6.12506	-6.09121	-0.13853
H	4.80768	-4.94121	-0.41643
H	7.80845	2.39341	3.94074
H	7.81273	2.90890	2.25127
H	9.33150	2.48439	3.06146
H	8.35399	-0.02837	4.53209
H	9.84649	0.03531	3.60735
H	8.65056	-1.21763	3.24874
H	8.47722	1.21655	0.38588
H	8.95468	-0.42082	0.85477
H	9.95038	0.96109	1.32695
H	3.74458	-0.67450	2.35180
H	3.63394	1.01631	2.86059
H	3.28909	-0.28368	4.01567
H	5.56948	-2.17054	3.41342
H	5.02911	-1.61644	5.00259
H	6.72706	-1.49162	4.54572
H	5.41755	2.06306	4.31816
H	6.56492	1.01463	5.17202
H	4.84161	0.89196	5.50633
H	2.59341	0.35684	-0.10171
H	1.35963	1.62114	-0.17104
H	2.60887	1.65899	1.07780
H	1.65897	3.26412	-1.81365
H	5.55378	4.44706	-3.11616
H	7.50086	3.46848	-2.20791

H	7.30232	1.76330	-1.78041
H	7.34185	2.98647	-0.50855
H	3.09997	4.65461	-3.24893

*Table S20. Cartesian coordinates of the optimised structure of **TS3** (R = ^{i}Pr).*

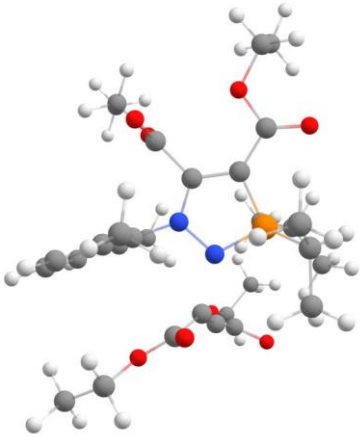

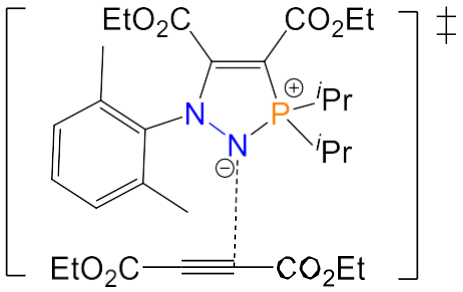

C	1.42793	-1.60400	-1.09698
C	2.78956	-1.45012	-1.72551
O	3.60276	-0.69470	-0.81278
C	4.83573	-0.41777	-1.21198
C	5.55530	0.37470	-0.15555
C	6.37236	-0.13238	0.83988
C	6.69343	-1.50421	1.13718
O	6.07732	-2.37834	0.32435
C	6.30760	-3.77064	0.56029
C	5.35002	-4.31451	1.59811
O	7.44297	-1.83778	2.03242
P	6.88088	1.23186	1.82175
C	8.67526	1.52004	1.93809

C	8.97994	2.99809	2.20626
H	9.00302	0.90742	2.78381
C	9.37019	1.03845	0.66653
C	6.24224	0.99511	3.52024
C	4.71521	1.00688	3.49027
H	6.58081	-0.03085	3.71341
C	6.81282	1.90524	4.60434
N	6.13946	2.34334	0.86730
N	5.41532	1.68690	-0.13541
C	4.68006	2.45743	-1.09032
C	3.37675	2.84086	-0.77418
C	2.74581	2.46246	0.53175
C	2.68592	3.59146	-1.71700
C	3.27698	3.93483	-2.92042
C	4.56975	3.53317	-3.20888
C	5.30171	2.78232	-2.29711
C	6.70098	2.33430	-2.59891
O	5.31794	-0.73057	-2.26142
H	0.78534	-2.18963	-1.75534
H	0.96263	-0.63103	-0.93679
H	1.49893	-2.11801	-0.13809
H	2.74518	-0.91669	-2.67598
H	3.27353	-2.41252	-1.89946
H	7.34293	-3.91506	0.86731
H	6.15327	-4.24251	-0.40928
H	5.52002	-3.83610	2.56249
H	5.50316	-5.38847	1.71676
H	4.31523	-4.14493	1.29692
H	8.45947	3.39271	3.07772
H	8.70176	3.60081	1.34141

H	10.05217	3.11413	2.37377
H	8.99843	1.58188	-0.20420
H	9.22184	-0.02840	0.50233
H	10.44185	1.22846	0.74778
H	4.32037	0.31485	2.74446
H	4.33394	2.00311	3.26465
H	4.32627	0.70986	4.46559
H	6.57870	2.95589	4.43421
H	7.89322	1.79644	4.70002
H	6.37250	1.62818	5.56439
H	3.18680	3.03037	1.35248
H	2.88791	1.40221	0.74449
H	1.67694	2.67134	0.51417
H	1.67260	3.90667	-1.50135
H	5.02336	3.80118	-4.15521
H	7.06506	2.81113	-3.50790
H	6.73766	1.25254	-2.74094
H	7.37387	2.60038	-1.78369
C	5.77993	4.18242	1.22046
C	5.24197	4.53280	2.27901
C	6.37397	4.81318	0.02552
O	5.55533	5.74338	-0.45870
C	6.02109	6.45807	-1.60798
C	4.89399	7.34419	-2.07510
H	6.31278	5.73737	-2.37388
H	6.90806	7.03254	-1.33304
H	4.02234	6.74338	-2.33719
H	5.20857	7.90503	-2.95654
H	4.60660	8.05277	-1.29816
O	7.45672	4.56579	-0.43942

C	4.67882	4.67131	3.55857
O	3.33186	4.51880	3.53200
O	5.29929	4.90841	4.57509
C	2.65878	4.64128	4.78718
C	2.69868	3.34822	5.57477
H	1.63556	4.90966	4.52559
H	3.10651	5.45562	5.35664
H	2.25507	2.53159	5.00302
H	2.13833	3.46365	6.50442
H	3.72752	3.08826	5.82325
H	2.72180	4.52003	-3.64325

*Table S21. Cartesian coordinates of the optimised structure of **TS3** (R = ^{t}Bu).*

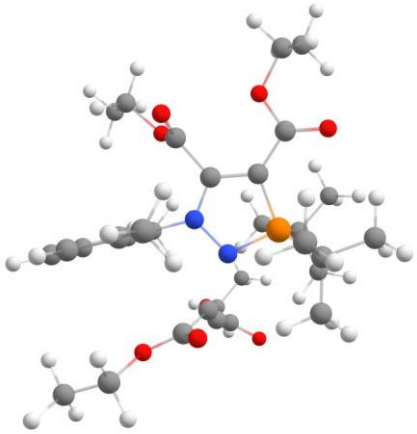

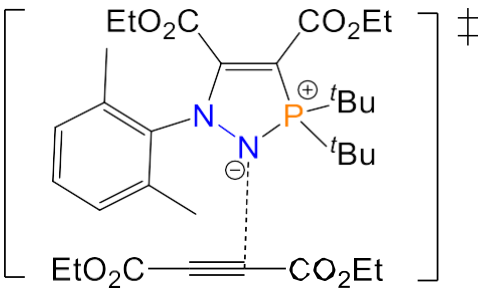

C	1.19214	-1.02910	-0.98681
C	2.59394	-1.22127	-1.50774
O	3.48560	-0.59560	-0.57085
C	4.74893	-0.46405	-0.94756
C	5.50132	0.36599	0.05745

C	6.41470	-0.08437	0.99418
C	6.84303	-1.45157	1.18528
O	6.01199	-2.33290	0.60402
C	6.36422	-3.71764	0.68010
C	5.86610	-4.33906	1.96678
O	7.83387	-1.78555	1.79825
P	6.93685	1.33818	1.90181
C	8.74773	1.72237	1.83283
C	8.98030	3.21318	2.11394
C	9.56468	0.85932	2.79925
C	9.17817	1.41904	0.39175
C	6.27524	1.23052	3.64101
C	4.74990	1.32084	3.50622
C	6.61956	-0.12797	4.26763
C	6.78199	2.35921	4.54141
N	6.10069	2.39282	0.94840
N	5.31226	1.67341	0.03966
C	4.55221	2.36769	-0.95783
C	3.24649	2.75526	-0.65387
C	2.63224	2.48096	0.68451
C	2.52497	3.41253	-1.64289
C	3.08437	3.66117	-2.88324
C	4.37634	3.25295	-3.16250
C	5.14003	2.59444	-2.20613
C	6.54379	2.16453	-2.51473
O	5.22681	-0.89248	-1.95749
H	0.47848	-1.47442	-1.68092
H	0.96432	0.03299	-0.89034
H	1.06797	-1.50215	-0.01246
H	2.73519	-0.75312	-2.48276
H	2.86270	-2.27533	-1.59457

H	7.44525	-3.81820	0.58772
H	5.88883	-4.16842	-0.19014
H	6.36339	-3.88985	2.82612
H	6.07905	-5.40948	1.96721
H	4.78866	-4.20277	2.06938
H	8.70891	3.49937	3.12785
H	8.44121	3.84141	1.40719
H	10.04732	3.41261	1.98701
H	9.36510	1.10396	3.84191
H	10.62325	1.05975	2.61659
H	9.38554	-0.20387	2.64182
H	8.61236	2.01894	-0.31987
H	9.05770	0.36287	0.14909
H	10.23438	1.67607	0.28518
H	4.35943	0.54005	2.85019
H	4.43176	2.28584	3.11812
H	4.30304	1.18367	4.49319
H	6.16162	-0.95402	3.72492
H	6.21821	-0.13739	5.28414
H	7.68920	-0.31531	4.32615
H	6.62338	3.34801	4.11527
H	7.83847	2.24296	4.78080
H	6.22902	2.32698	5.48321
H	2.86396	1.47306	1.02717
H	1.54924	2.58982	0.63369
H	3.00345	3.18482	1.43081
H	1.50977	3.72609	-1.43346
H	4.80523	3.43946	-4.13932
H	7.24948	2.72219	-1.89902
H	6.77457	2.35981	-3.56104

H	6.68944	1.09969	-2.33246
C	5.68392	4.23129	1.16357
C	5.12813	4.66861	2.18207
C	6.24243	4.79732	-0.08046
O	5.38921	5.66704	-0.61386
C	5.81940	6.32487	-1.80958
C	4.65794	7.14376	-2.31408
H	6.12745	5.56999	-2.53526
H	6.68938	6.94340	-1.57966
H	3.80688	6.49838	-2.53452
H	4.94502	7.66653	-3.22765
H	4.35123	7.88237	-1.57340
O	7.32859	4.55675	-0.54299
C	4.55380	4.90671	3.44172
O	3.20864	4.72785	3.41780
O	5.16032	5.24205	4.43814
C	2.52630	4.90637	4.66019
C	2.58129	3.65433	5.51072
H	1.50060	5.14556	4.38041
H	2.95866	5.75507	5.18970
H	2.15848	2.80320	4.97459
H	2.01073	3.80320	6.42930
H	3.61254	3.42597	5.77999
H	2.50517	4.17159	-3.64297

*Table S22. Cartesian coordinates of the optimised structure of **I2** (R = ^{i}Pr).*

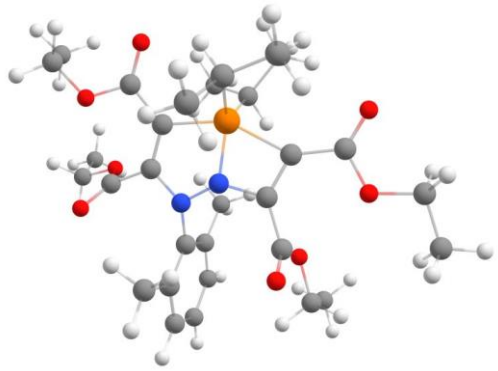

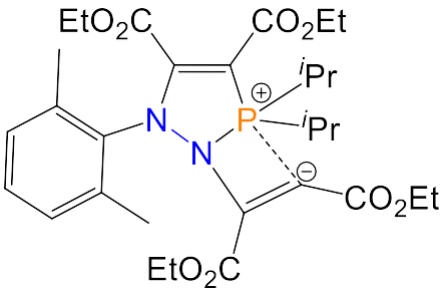

C	2.79491	-2.94639	-1.91509
C	4.00849	-2.19193	-2.39697
O	4.43519	-1.33454	-1.33046
C	5.49223	-0.56786	-1.57816
C	5.87588	0.20644	-0.35044
C	6.37209	-0.27153	0.82278
C	6.80208	-1.64501	1.00153
O	6.93458	-2.31230	-0.16536
C	7.28033	-3.69561	-0.09581
C	6.05673	-4.55781	0.13030
O	7.06957	-2.15775	2.06776
P	6.35485	1.06240	2.16051
C	8.05932	0.80701	2.81128
C	8.43523	1.61181	4.04974
H	8.07576	-0.26023	3.04566
C	9.06835	1.07662	1.69047
C	4.92776	0.44621	3.21136
H	4.18913	1.23579	3.04550

C	4.28993	-0.88327	2.81937
C	5.28149	0.44077	4.69867
N	6.17537	2.10461	0.75915
N	5.70950	1.54725	-0.42185
C	4.83760	2.27103	-1.28984
C	3.46855	2.30320	-1.01750
C	2.89988	1.62555	0.19405
C	2.65441	3.02454	-1.88162
C	3.19521	3.69538	-2.96539
C	4.55852	3.66059	-3.20427
C	5.40823	2.94649	-2.36919
C	6.88747	2.90408	-2.60070
O	6.04197	-0.46860	-2.63799
H	2.45127	-3.62683	-2.69499
H	1.98295	-2.25994	-1.67333
H	3.02945	-3.53077	-1.02466
H	3.79085	-1.58413	-3.27649
H	4.83368	-2.86162	-2.64864
H	8.01446	-3.84267	0.69607
H	7.74432	-3.91098	-1.05769
H	5.59763	-4.32832	1.09175
H	6.33808	-5.61230	0.12662
H	5.32045	-4.39718	-0.65898
H	7.70417	1.54545	4.84960
H	8.56149	2.66772	3.80773
H	9.39021	1.24251	4.43036
H	9.03384	2.12426	1.38212
H	8.89186	0.45920	0.81090
H	10.07445	0.86816	2.05895
H	4.03931	-0.93835	1.76094

H	3.36520	-1.00161	3.38912
H	4.94434	-1.72044	3.05624
H	5.60676	1.41666	5.05316
H	6.05703	-0.29940	4.90710
H	4.39609	0.15670	5.27177
H	3.27060	0.60606	0.30194
H	1.81280	1.58817	0.14034
H	3.17057	2.17637	1.09876
H	1.58729	3.06082	-1.69843
H	4.97436	4.19123	-4.05151
H	7.15437	3.48188	-3.48438
H	7.22298	1.87533	-2.73817
H	7.41748	3.32314	-1.74359
C	5.81617	3.27056	1.41708
C	6.01296	2.96810	2.70950
C	5.49134	4.53014	0.67973
O	4.21559	4.85891	0.82429
C	3.77495	6.01587	0.09873
C	2.29106	6.15135	0.32665
H	4.01272	5.87265	-0.95658
H	4.32774	6.88495	0.45979
H	1.76733	5.26697	-0.03785
H	1.91457	7.02249	-0.21084
H	2.06930	6.27738	1.38687
O	6.29614	5.12922	0.02283
C	5.96667	3.91854	3.81305
O	5.79380	5.18423	3.37722
O	6.05092	3.65269	4.98908
C	5.65645	6.20270	4.36603
C	5.26244	7.47209	3.64895

H	6.60509	6.31620	4.89515
H	4.90504	5.89801	5.09622
H	6.01277	7.74704	2.90689
H	5.16777	8.28918	4.36547
H	4.30396	7.34483	3.14315
H	2.54732	4.25511	-3.62863

*Table S23. Cartesian coordinates of the optimised structure of **I2** (R = ^{t}Bu).*

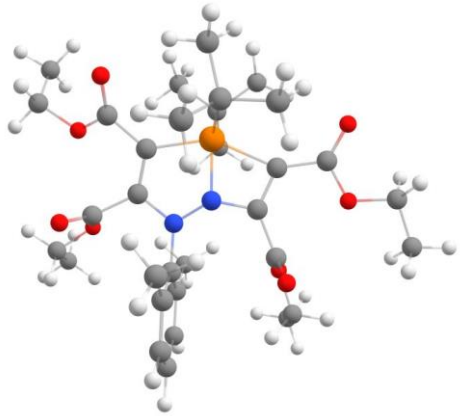

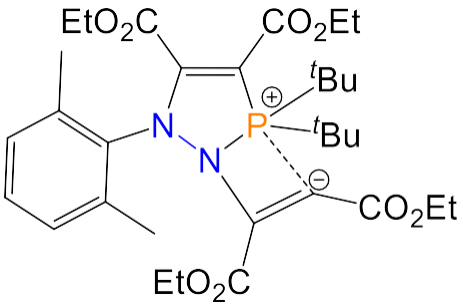

C	2.06533	-1.52967	-2.68509
C	3.56924	-1.44317	-2.75257
O	4.02341	-0.88764	-1.50985
C	5.31880	-0.61370	-1.42430
C	5.64403	0.11187	-0.14707
C	6.38245	-0.33853	0.89605
C	6.85221	-1.72753	0.86801
O	5.99361	-2.53927	0.21572
C	6.38285	-3.90472	0.04564

C	5.98622	-4.73616	1.24659
O	7.87858	-2.14489	1.34862
P	6.52583	1.00379	2.24779
C	8.39096	1.10704	2.53360
C	8.78442	2.43704	3.17804
C	8.87064	-0.02883	3.44504
C	9.09166	1.00260	1.17361
C	5.45242	0.11874	3.54569
C	4.00076	0.47559	3.17962
C	5.57129	-1.40939	3.51705
C	5.75984	0.57508	4.97363
N	5.96121	2.02802	0.92774
N	5.24446	1.41017	-0.09900
C	4.79725	2.18801	-1.21136
C	3.41804	2.37074	-1.34742
C	2.45576	1.78486	-0.35547
C	2.96762	3.12979	-2.41958
C	3.86414	3.69508	-3.31201
C	5.22490	3.51050	-3.14771
C	5.71998	2.75160	-2.09385
C	7.19455	2.57362	-1.89698
O	6.13047	-0.84056	-2.27615
H	1.67979	-1.95474	-3.61252
H	1.62754	-0.53960	-2.55240
H	1.74825	-2.16472	-1.85739
H	3.90556	-0.79632	-3.56426
H	4.03222	-2.42215	-2.88724
H	7.45680	-3.95451	-0.13037
H	5.85912	-4.23014	-0.85291
H	6.52618	-4.40752	2.13416

H	6.22413	-5.78590	1.06635
H	4.91464	-4.65327	1.43382
H	8.32047	2.57868	4.15250
H	8.52938	3.28770	2.54473
H	9.86867	2.43815	3.31635
H	8.45799	0.05975	4.44868
H	9.95746	0.04854	3.53356
H	8.64289	-1.00768	3.03267
H	8.73769	1.76692	0.48147
H	8.96087	0.02502	0.71573
H	10.16148	1.16052	1.33082
H	3.77113	0.22164	2.14148
H	3.78705	1.53168	3.33569
H	3.33031	-0.10648	3.81683
H	5.13928	-1.84553	2.61796
H	5.00441	-1.80094	4.36545
H	6.59839	-1.75425	3.62149
H	5.89996	1.64596	5.07910
H	6.64984	0.08069	5.36205
H	4.92611	0.28101	5.61738
H	2.56242	0.70242	-0.29335
H	1.42813	2.01609	-0.63672
H	2.63550	2.19288	0.64055
H	1.90318	3.28269	-2.55130
H	5.92087	3.95719	-3.84682
H	7.73874	2.87184	-2.79177
H	7.44704	1.53680	-1.67193

H	7.53502	3.19239	-1.06421
C	5.55081	3.13107	1.66312
C	5.95153	2.87025	2.90965
C	5.06046	4.36462	0.97162
O	3.74625	4.50312	1.08122
C	3.16865	5.60777	0.37031
C	1.67101	5.49490	0.49949
H	3.49221	5.55557	-0.67076
H	3.55057	6.53482	0.80158
H	1.31511	4.56647	0.05132
H	1.19469	6.33075	-0.01442
H	1.36685	5.51470	1.54649
O	5.78699	5.09979	0.36348
C	5.97851	3.88165	3.96877
O	5.36446	5.01946	3.58718
O	6.46520	3.75966	5.06818
C	5.35004	6.09987	4.51861
C	4.64448	7.25474	3.84884
H	6.37751	6.35369	4.78615
H	4.83886	5.78353	5.42989
H	5.15854	7.53630	2.92891
H	4.62912	8.11795	4.51567
H	3.61415	6.99038	3.60561
H	3.49751	4.28655	-4.14180

*Table S24. Cartesian coordinates of the optimised structure of **I3** (R = ^{i}Pr).*

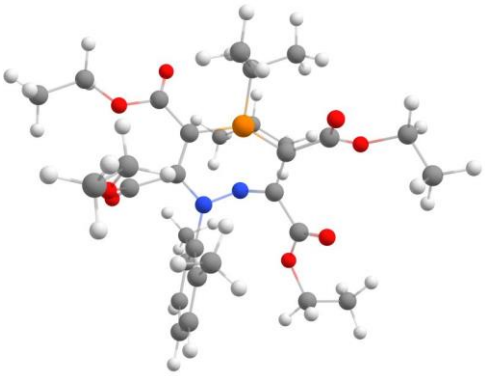

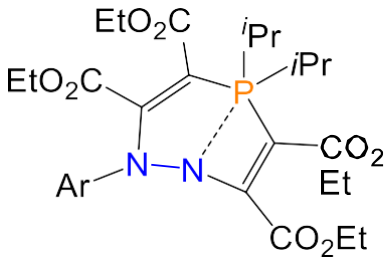

C	2.72398	1.85055	-2.30147
C	3.58588	0.98416	-1.41826
O	3.83045	1.71641	-0.20708
C	4.72947	1.31776	0.68400
C	5.77710	0.30377	0.25342
C	5.60508	-1.06669	0.28410
C	4.47227	-1.66748	0.97812
O	3.40324	-0.85240	1.02368
C	2.33532	-1.20957	1.90624
C	1.34823	-0.06786	1.89186
O	4.46382	-2.75595	1.50772
P	6.99226	-2.07368	-0.27537
C	6.12621	-3.63618	-0.80337
H	5.67317	-4.00525	0.11672
C	5.00889	-3.38489	-1.81742
C	8.07988	-2.73353	1.07218
H	7.79054	-3.78234	1.16294
C	9.56291	-2.66581	0.71536
N	7.97386	-0.17155	-0.14263

N	6.97010	0.80808	-0.04676
C	7.32837	2.19604	-0.04103
C	7.13885	2.96542	-1.18636
C	6.56081	2.42211	-2.46317
C	7.53515	4.30059	-1.14873
C	8.11196	4.83850	-0.01687
C	8.31295	4.04587	1.10307
C	7.92981	2.71459	1.11061
C	8.16044	1.84962	2.31099
O	4.77465	1.79742	1.77865
H	2.52386	1.33066	-3.23910
H	3.21967	2.79510	-2.52788
H	1.77332	2.07040	-1.81554
H	4.52809	0.73660	-1.90542
H	3.08151	0.05482	-1.15647
H	2.74587	-1.37765	2.90308
H	1.88959	-2.14514	1.56469
H	1.82993	0.85952	2.20236
H	0.52759	-0.28310	2.57748
H	0.93163	0.07582	0.89380
H	4.22883	-2.73717	-1.41726
H	4.53887	-4.33322	-2.08845
H	5.39478	-2.93340	-2.73286
H	9.78878	-3.17110	-0.22469
H	10.14377	-3.14413	1.50676
H	9.89013	-1.62883	0.63233
H	6.52173	1.33512	-2.48235
H	7.16205	2.74131	-3.31513
H	5.54831	2.79954	-2.61840
H	7.39231	4.91444	-2.03028

H	8.76901	4.46829	1.99000
H	8.56405	2.43414	3.13648
H	8.86337	1.05166	2.06571
H	7.22753	1.38805	2.63860
C	8.34266	-0.42593	-1.45967
C	9.19769	0.46271	-2.30850
C	7.89909	-1.63436	-1.81691
O	9.87897	1.32560	-1.56865
C	10.67799	2.29885	-2.25505
C	12.05067	1.75293	-2.57946
H	10.72924	3.13625	-1.56114
H	10.15315	2.61163	-3.15811
H	12.54761	1.40075	-1.67505
H	12.66165	2.54013	-3.02409
H	11.97997	0.93009	-3.29033
O	9.24355	0.38796	-3.50926
C	8.22895	-2.35279	-3.07710
O	7.45389	-2.52713	-3.97780
O	9.49364	-2.77753	-3.06830
C	9.98024	-3.39783	-4.26971
C	10.49773	-2.35927	-5.23923
H	9.17909	-3.98998	-4.71143
H	10.77350	-4.06262	-3.93114
H	9.70020	-1.68022	-5.53765
H	10.89165	-2.85309	-6.12917
H	11.29670	-1.77309	-4.78451
C	7.08591	-4.71395	-1.32243
H	6.59105	-5.68638	-1.27899
H	8.00624	-4.79472	-0.74202
H	7.35747	-4.54744	-2.36410
C	7.78677	-2.05303	2.40574

H	7.99434	-0.98632	2.34778
H	8.42801	-2.48603	3.17689
H	6.74977	-2.19420	2.70878
H	8.41179	5.87898	-0.00400

*Table S25. Cartesian coordinates of the optimised structure of **7**.*

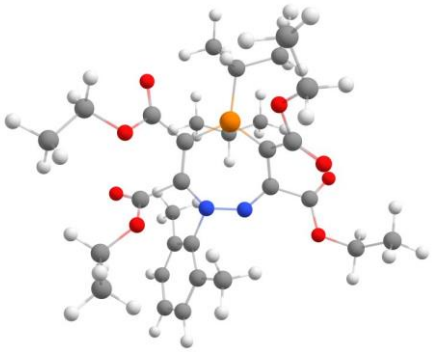

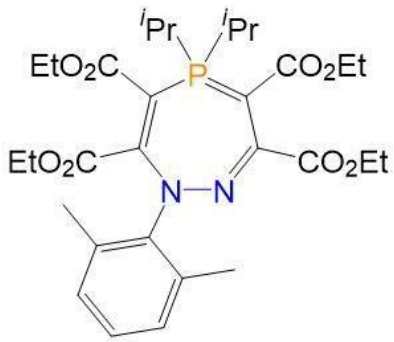

C	0.96951	-0.20658	2.53758
C	2.05487	0.03271	1.47862
C	2.81385	1.31467	1.83237
P	3.11944	-1.45420	1.26383
C	4.43134	-1.50273	2.55392
C	5.54845	-0.47951	2.34699
C	3.87554	-1.49161	3.97719
C	2.23718	-2.93920	1.34754
C	0.90921	-3.17621	0.88006
O	0.36818	-2.09836	0.24618
C	-0.96611	-2.24274	-0.22925
C	-1.39667	-0.90330	-0.77921

O	0.30764	-4.22961	0.96397
C	3.02135	-4.09603	1.66232
C	2.48386	-5.04750	2.71568
O	2.53307	-6.31144	2.31878
C	1.94636	-7.28545	3.19311
C	0.45353	-7.37924	2.96520
O	2.07678	-4.66701	3.77998
N	4.17439	-4.44475	1.22625
N	4.83388	-3.85041	0.15002
C	5.88572	-4.76902	-0.23629
C	7.19459	-4.50177	0.15436
C	7.52911	-3.31046	1.00424
C	8.18385	-5.39683	-0.24018
C	7.86616	-6.52502	-0.97343
C	6.54756	-6.79100	-1.30644
C	5.52953	-5.92389	-0.93506
C	4.09672	-6.22998	-1.25340
C	4.69400	-2.68759	-0.56006
C	5.59467	-2.70286	-1.79805
O	5.12281	-3.52183	-2.72008
C	6.01976	-3.86356	-3.78796
C	5.32353	-4.88151	-4.65372
O	6.61407	-2.07722	-1.87068
C	4.01191	-1.52891	-0.29358
C	3.98899	-0.40707	-1.23587
O	4.07530	-0.79034	-2.51556
C	4.19529	0.24991	-3.49117
C	4.62798	-0.38802	-4.78810
O	3.85917	0.75239	-0.91883
H	0.32220	0.67282	2.55579

H	1.40138	-0.31855	3.53104
H	0.35508	-1.07577	2.33270
H	2.11318	2.14879	1.76284
H	3.63981	1.51437	1.15849
H	3.17383	1.28092	2.86116
H	5.24587	0.52367	2.64016
H	5.88740	-0.44325	1.31131
H	6.40133	-0.76300	2.96686
H	3.49773	-0.50575	4.25095
H	4.67889	-1.73768	4.67409
H	3.08110	-2.22754	4.10746
H	-1.61168	-2.56753	0.58917
H	-0.99417	-3.02008	-0.99537
H	-1.38636	-0.14116	0.00161
H	-2.40959	-0.97271	-1.17826
H	-0.73217	-0.58272	-1.58305
H	2.45009	-8.21772	2.94140
H	-0.02883	-6.42900	3.19035
H	0.03223	-8.15103	3.61208
H	0.23892	-7.63369	1.92729
H	6.96935	-3.34218	1.94163
H	7.29032	-2.37424	0.49856
H	8.59122	-3.29972	1.24467
H	9.21187	-5.20539	0.04166
H	6.29953	-7.69022	-1.85765
H	4.02754	-7.07173	-1.94208
H	3.59779	-5.37185	-1.70385
H	3.55206	-6.48019	-0.34078
H	6.93267	-4.26474	-3.34267
H	6.27541	-2.95915	-4.34060

H	5.07632	-5.77208	-4.07542
H	5.98113	-5.17379	-5.47328
H	4.40536	-4.47206	-5.07579
H	4.92009	0.98537	-3.14155
H	3.22950	0.74980	-3.58626
H	5.61608	-0.83581	-4.68006
H	4.67863	0.36972	-5.57091
H	3.92259	-1.15950	-5.09884
H	4.87148	-2.48745	2.39036
H	1.57710	0.15381	0.50556
H	2.17447	-7.02187	4.22580
H	8.64724	-7.21206	-1.27402

Table S26. Cartesian coordinates of the optimised structure of seven-membered ring with R = ^{t}Bu phosphorus substituents.

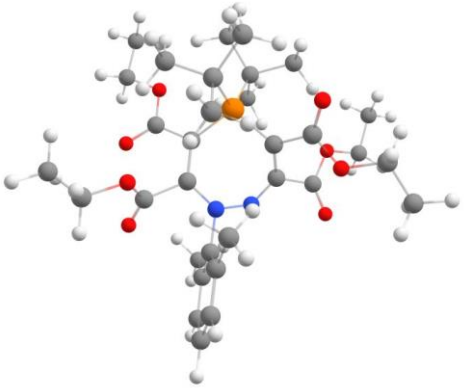

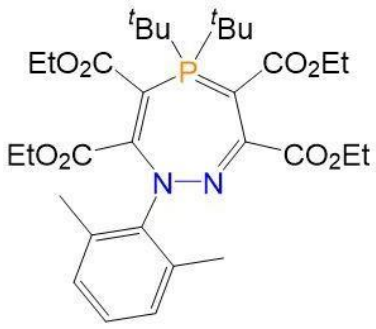

C	2.52379	0.45641	-0.64209
C	1.77836	-0.76137	-0.07397
C	1.33868	-1.63632	-1.25260

P	2.94529	-1.80699	0.98163
C	3.12477	-1.09875	2.72330
C	1.95243	-1.60802	3.57748
C	4.43368	-1.66279	3.29125
C	2.42214	-3.47625	1.13661
C	1.06004	-3.83657	1.40205
O	0.93136	-5.18573	1.50422
C	-0.33171	-5.68394	1.93472
C	-0.20407	-7.18337	2.05958
O	0.08522	-3.11416	1.49641
C	3.41111	-4.50407	1.34723
C	3.31494	-5.44966	2.54824
O	2.91721	-4.79737	3.64371
C	2.74697	-5.58535	4.82525
C	2.29319	-4.65944	5.92663
O	3.59141	-6.61134	2.52052
N	4.43064	-4.81913	0.64137
N	4.59610	-4.22826	-0.59978
C	4.80265	-5.25688	-1.59844
C	6.02581	-5.92824	-1.61647
C	7.12711	-5.57310	-0.66514
C	6.18994	-6.92407	-2.56669
C	5.17339	-7.23957	-3.45401
C	3.96628	-6.57102	-3.39459
C	3.75195	-5.56831	-2.45348
C	2.42740	-4.86434	-2.38373
C	4.74349	-2.93890	-0.82801
C	5.33114	-2.64236	-2.21618
O	4.44082	-1.93844	-2.91234
C	4.81463	-1.57283	-4.25144

C	5.67756	-0.33155	-4.26021
O	6.36140	-3.07488	-2.63562
C	4.48472	-1.88179	0.06649
C	5.38737	-0.75632	-0.14692
O	5.28583	0.24110	0.74642
C	6.20270	1.32703	0.55809
C	5.97820	2.34341	1.65122
O	6.22141	-0.70837	-1.02767
H	-1.09739	-5.40048	1.21051
H	-0.59437	-5.21928	2.88818
H	0.04362	-7.63312	1.09787
H	-1.14655	-7.60789	2.40881
H	0.58206	-7.44974	2.76715
H	3.69224	-6.07498	5.06469
H	2.01137	-6.36598	4.62036
H	3.03118	-3.87537	6.10043
H	2.16361	-5.22192	6.85201
H	1.34298	-4.18784	5.67372
H	6.81854	-5.75643	0.36454
H	7.38150	-4.51642	-0.76057
H	8.01935	-6.16027	-0.87746
H	7.13340	-7.45360	-2.61411
H	3.16619	-6.83360	-4.07597
H	1.65267	-5.47048	-2.85158
H	2.46599	-3.90829	-2.90957
H	2.13201	-4.65817	-1.35521
H	3.86465	-1.40645	-4.75698
H	5.32533	-2.41738	-4.71401
H	5.16155	0.50157	-3.78201
H	5.90094	-0.05689	-5.29269

H	6.61209	-0.50822	-3.73094
H	6.04099	1.75979	-0.43046
H	7.21906	0.93258	0.58161
H	4.98556	2.79066	1.58628
H	6.71536	3.14123	1.55245
H	6.09293	1.89195	2.63733
C	0.53221	-0.25336	0.66383
H	2.93162	1.10012	0.13492
H	1.80319	1.04324	-1.21627
H	0.73362	-2.48019	-0.92732
H	2.19439	-1.99875	-1.81907
C	3.13394	0.42955	2.84257
H	5.30421	-1.23387	2.79785
H	4.48230	-2.74787	3.20675
H	1.96454	-2.68857	3.67858
H	0.98603	-1.30923	3.17684
H	2.05782	-1.17045	4.57366
H	3.84666	0.89897	2.18064
H	3.41377	0.67858	3.86964
H	2.14985	0.85888	2.67018
H	-0.11430	0.22336	-0.07768
H	0.77312	0.50253	1.40748
H	-0.02107	-1.06214	1.12929
H	0.73334	-1.02186	-1.92394
H	3.32400	0.16743	-1.32278
H	4.48338	-1.41530	4.35478
H	5.32289	-8.01916	-4.19048

*Table S27. Cartesian coordinates of the optimised structure of **11**.*

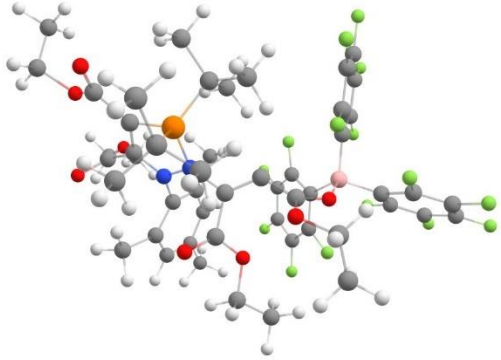

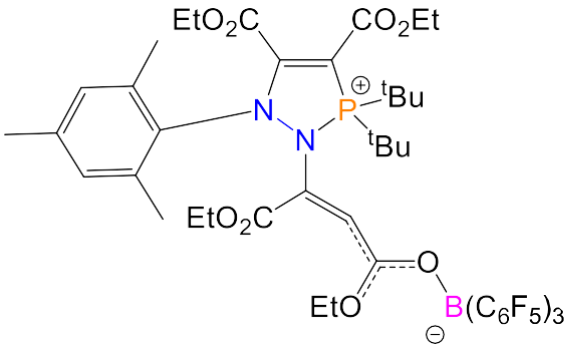

C	0.98887	-1.07894	0.02361
C	2.33741	-1.19787	-0.64604
O	3.34573	-1.01030	0.35763
C	4.49271	-0.46308	-0.00065
C	5.30309	-0.12865	1.23204
C	6.39014	-0.82643	1.72933
C	6.99304	-1.98985	1.08782
O	6.16384	-2.54560	0.19783
C	6.65509	-3.63257	-0.59064
C	6.45866	-4.95859	0.11467
O	8.10498	-2.41406	1.31449
P	7.00288	0.03247	3.15932
C	8.66860	0.83121	2.86342
C	8.90969	2.00798	3.82166
C	9.78346	-0.21829	2.99993
C	8.62169	1.36107	1.42119
C	6.88823	-1.01925	4.70655
C	5.40425	-1.10804	5.08607

C	7.41041	-2.42781	4.37119
C	7.67719	-0.42584	5.87649
N	5.76619	1.19154	3.02734
N	4.95894	0.97066	1.88945
C	3.80079	1.77400	1.63403
C	2.64646	1.50472	2.39099
C	2.63837	0.37703	3.37787
C	1.52307	2.29122	2.16301
C	1.53429	3.33492	1.22848
C	2.68016	3.52484	0.45751
C	3.82929	2.74178	0.61978
C	4.99298	2.93485	-0.31235
O	4.84138	-0.18850	-1.11257
H	0.19157	-1.22337	-0.71928
H	0.87088	-0.08270	0.47454
H	0.86967	-1.83633	0.81135
H	2.47972	-0.44053	-1.42994
H	2.49275	-2.18856	-1.10010
H	7.71671	-3.45865	-0.81505
H	6.08031	-3.58023	-1.52482
H	7.05461	-4.99704	1.03725
H	6.78446	-5.78070	-0.53917
H	5.39979	-5.11592	0.36609
H	8.83816	1.73246	4.88012
H	8.21537	2.83507	3.63704
H	9.92917	2.38265	3.63875
H	9.92216	-0.54979	4.03773
H	10.72641	0.25143	2.67962
H	9.60202	-1.09470	2.36329
H	7.80936	2.09116	1.29330
H	8.51567	0.55003	0.68705

H	9.56999	1.88135	1.21681
H	4.78398	-1.45615	4.24703
H	5.02773	-0.13912	5.44420
H	5.30323	-1.83909	5.90295
H	6.76689	-2.94215	3.64409
H	7.39367	-3.01399	5.30275
H	8.43693	-2.43489	3.98411
H	7.34818	0.59448	6.10619
H	8.76161	-0.43462	5.70574
H	7.48517	-1.03944	6.76857
H	2.96685	-0.55578	2.89514
H	1.63869	0.21792	3.79488
H	3.32299	0.58325	4.21222
H	0.60959	2.08474	2.72318
C	0.34029	4.23850	1.08861
H	2.68697	4.30392	-0.30974
H	4.72628	2.56774	-1.31481
H	5.88815	2.39754	0.01542
H	5.25209	3.99910	-0.38732
C	5.59228	2.36298	3.83023
C	5.68290	2.30868	5.15625
C	5.65245	3.64666	3.05680
O	4.92153	4.61485	3.58793
C	5.00634	5.88860	2.93807
C	4.25009	6.90659	3.75313
H	4.58610	5.78045	1.92510
H	6.06792	6.15518	2.82432
H	3.19694	6.62383	3.87204
H	4.29360	7.88122	3.24609
H	4.68874	7.01489	4.75355
O	6.35891	3.79656	2.08547

C	5.97370	3.36911	6.01439
O	7.13498	3.97093	5.80370
O	5.33393	3.75025	7.04515
C	7.62676	4.90879	6.77522
C	6.99221	6.27284	6.59960
H	8.70805	4.94201	6.58872
H	7.44679	4.50973	7.78078
H	7.43921	6.98301	7.31060
H	5.91204	6.22419	6.79281
H	7.15807	6.65422	5.58098
F	7.19191	-0.60887	9.14957
F	1.15423	5.88641	4.81219
F	5.12399	-1.95768	10.28539
C	5.96294	-0.10212	9.10411
C	4.91158	-0.79346	9.69190
F	3.26314	5.52799	6.41814
C	1.43651	4.67510	5.28371
F	-0.47224	3.78941	4.22155
F	6.81161	1.73554	7.99959
C	5.72439	1.12160	8.47839
C	3.63681	-0.23485	9.66841
F	2.62799	-0.86333	10.25375
C	2.54819	4.45116	6.08779
C	0.60283	3.60887	4.97818
C	3.44727	0.99052	9.03837
C	4.45666	1.69013	8.37467
C	2.88703	3.20401	6.61503
C	0.91433	2.34326	5.45373
F	2.21828	1.50275	9.09232
B	4.10525	3.15468	7.71721
C	2.06851	2.15293	6.21017

F	0.13184	1.31665	5.12646
F	2.34021	0.88990	6.53917
F	6.10159	4.02507	9.62044
C	3.81559	4.15613	8.99914
C	4.87316	4.50473	9.84167
C	2.57205	4.65784	9.38409
F	1.46532	4.37298	8.69851
C	4.73912	5.33158	10.95375
F	5.78930	5.63353	11.70560
C	2.39038	5.48410	10.49354
C	3.48139	5.82555	11.28389
F	1.18507	5.94125	10.80192
F	3.32569	6.60793	12.33971
H	0.35946	4.79455	0.14135
H	0.32437	4.96770	1.91351
H	-0.60031	3.67265	1.14555

S6. References

S1. E.J. Jordan, E.D.E. Calder, H.V. Adcock, L. Male, M. Nieger, J.C. Slootweg, and A.R. Jupp, *Chem. Eur. J.*, **2024**, e202401358.

S2. CrysAlisPro, Rigaku Oxford Diffraction, 2021.

S3. O. V. Dolomanov, L. J. Bourhis, R. J. Gildea, J. A. K. Howard and H. Puschmann, *J. Appl. Crystallogr*., 2009, **42**, 339-341.

S4. G. M. Sheldrick, *Acta Crystallogr*., 2015, **A71**, 3-8

S5. G. M. Sheldrick, *Acta Crystallogr*., 2015, **C71**, 3-8.

S6. C.A. Busacca, T. Bartholomeyzik, S. Cheekori, R. Raju, M. Eriksson, S. Kapadia, A. Saha, X. Zeng, and C.H. Senanayake, *Synlett*, 2009, **2**, 287-291.

S7. A. Naghipour, S. Javad Sabounchei, D. Morales-Morales, S. Hernandez-Ortega, and C.M. Jensen, *J. Organomet. Chem*., 2004, **15**, 2494-2502.

S8. D. R. Allan, H. Nowell, S.A. Barnett, M.R. Warren, A. Wilcox, J. Christensen, L.K. Saunders, A. Peach, M.T. Hooper, L. Zaja, S. Patel, L. Cahill, R. Marshall, S. Trimnell, A.J. Foster, T. Bates, S.Lay, M.A. Wiliams, P.V. Hathaway, G. Winter, M. Gerstel, and R.W. Wooley, *Crystals* **2017**, *7*(11), 336.

S8. G. Winter, *J. Appl. Crystallogr.*, 2010, **43**, 186-190.

S10. G. Winter, D.G. Waterman, J.M. Parkhurst, A.S. Brewster, R.J. Gildea, M. Gerstel, L. Fuentes-Montero, M. Vollmar, T. Michels-Clark, I.D. Young, N.K. Sauter, and G. Evans, *Acta Crystallogr*., 2018, **D74**, 85-97.

S11. Gaussian 09, Revision D.01, M. J. Frisch, G. W. Trucks, H. B. Schlegel, G. E. Scuseria, M. A. Robb, J. R. Cheeseman, G. Scalmani, V. Barone, G. A. Petersson, H. Nakatsuji, X. Li, M. Caricato, A. Marenich, J. Bloino, B. G. Janesko, R. Gomperts, B. Mennucci, H. P. Hratchian, J. V. Ortiz, A. F. Izmaylov, J. L. Sonnenberg, D. Williams-Young, F. Ding, F. Lipparini, F. Egidi, J. Goings, B. Peng, A. Petrone, T. Henderson, D. Ranasinghe, V. G. Zakrzewski, J. Gao, N. Rega, G. Zheng, W. Liang, M. Hada, M. Ehara, K. Toyota, R. Fukuda, J. Hasegawa, M. Ishida, T. Nakajima, Y. Honda, O. Kitao, H. Nakai, T. Vreven, K. Throssell, J. A. Montgomery, Jr., J. E. Peralta, F. Ogliaro, M. Bearpark, J. J. Heyd, E. Brothers, K. N. Kudin, V. N. Staroverov, T. Keith, R. Kobayashi, J. Normand, K. Raghavachari, A. Rendell, J. C. Burant, S. S. Iyengar, J. Tomasi, M. Cossi, J. M. Millam, M. Klene, C. Adamo, R. Cammi, J. W. Ochterski, R. L. Martin, K. Morokuma, O. Farkas, J. B. Foresman, and D. J. Fox, Gaussian, Inc., Wallingford CT, 2016.

S12. J-D. Chai and M. Head-Gordon, *Phys. Chem. Chem. Phys.*, 2008, **10**, 6615-6620.

S13. F. Weigend and R. Ahlrichs, *Phys. Chem. Chem. Phys.***,** 2005, **7**, 3297-3305.

S14. M. Nottoli and F. Lipparini, *J. Chem. Phys*., 2020, **153**, 224108.

S15. NBO Version 3.1, E. D. Glendening, A. E. Reed, J. E. Carpenter, and F. Weinhold.